UNIVERSITÀ
DEGLI STUDI
DI PADOVA

Università degli Studi di Padova

Dipartimento di Ingegneria Civile e Ambientale

CORSO DI DOTTORATO DI RICERCA IN: Scienze dell'ingegneria civile e ambientale
CICLO XXX

STUDY OF THE FRACTURES IN SLOWLY DRIVEN DOMINATED THRESHOLD SYSTEMS

Coordinatore: Ch.mo Prof. Stefano Lanzoni
Supervisore: Ch.mo Prof. Francesco Pesavento
Co-Supervisore: Ch.mo Prof. Gunnar Pruessner

Dottorando : Pietro Favia

Dedicated to my lovely parents, Diana, Giuseppe and Silvia

DECLARATION

I hereby declare that except where specific reference is made to the work of others, the contents of this dissertation are original and have not been submitted in whole or in part for consideration for any other degree or qualification in this, or any other university. This dissertation is my own work and contains nothing which is the outcome of work done in collaboration with others, except as specified in the text and Acknowledgements.

Pietro Favia

May 2017

Acknowledgements

Ci sono molte persone che hanno contribuito a farmi arrivare alla fine del lungo percorso di dottorato, “a journey alone” come mi confidò una volta una persona durante il mio periodo di Visiting Student a Londra.

In ogni viaggio che si compie tuttavia è sempre possibile incontrare dei compagni ai quali non può che andare la più grande gratitudine per il solo fatto di aver condiviso un momento della loro vita con te. Ed è a loro che questa breve paginetta è dedicata: l’ordine in cui compaiono non è importante. Ognuno di loro mi ha lasciato qualcosa da un punto di vista professionale e/o umano.

Tra queste non posso che ringraziare Carlo il quale mi ha dato una enorme mano con le simulazioni numeriche. Mi mancherà il modo di lavorare che avevo instaurato con lui: diretto, vivace, spiritoso. Sempre a contatto e sempre a sfruttare ogni decimo di secondo per produrre e per interpretare la fisica del problema! Da ciò è nato anche un forte legame e gli auguro di trovare la sua strada nel futuro.

Devo moltissimo a Giuseppe e Silvia: senza di loro probabilmente non sarei partito per Londra e non avrei avuto la molla che mi ha spinto poi ad andare avanti nel mio progetto di dottorato. Per non parlare poi di tutto il resto: degli stimoli da loro ricevuti. Amici di una vita, di quegli amici che ti porti per tutta la vita e di cui anche a distanza non riesci a farne a meno.

Ringrazio Diana, che mi ha sopportato in questi mesi di “produzione” e di stesura: senza il suo affetto, il suo appoggio, la sua pazienza, il suo attaccamento e il suo continuo stimolarmi in un anno e mezzo, tale lavoro non sarebbe stato possibile in nessun modo. Ci si rende conto solo in certi momenti di quanto si sia fortunati a incontrare certe persone nel proprio cammino apprezzando la casualità con cui ciò avvenga e chiamandola “*suerte*”.

Non posso non citare Gunnar, il cui appuntamento del giovedi alle 15 del pomeriggio presso il Complexity Science Centre mi ha permesso di vederci chiaro nello studio del Fiber Bundle Model da un punto di visto termodinamico e del Prof. Pesavento per l’appoggio datomi in questi tre anni.

Al gruppo dell’aula Simo, Mattia, Claudio e soprattutto Pietro: grazie per aver allietato con vostra leggerezza e positività il mio secondo anno di dottorato, a Sergio un abbraccio per avermi ospitato nel mese di maggio, cruciale per la stesura della tesi ed essere stato mio compagno nel percorso di PhD e a Enrico un grosso ringraziamento per la sua disponibilità sin dal primo giorno in cui ho iniziato.

A Davide, Alice, Giovanni, Sara, Ilaria: grazie per il tempo passato con me in questi anni e per avermi accompagnato nelle serate di spritz padovani.

E infine un ringraziamento ai miei genitori, ai miei zii e Cristina che hanno sempre creduto in me motivandomi e dandomi la forza di andare avanti.

Questo lavoro è dedicato a tutti voi.

Luton, 31 Ottobre 2017

Abstract

Fracture mechanics plays an important role in the material science, structure design and industrial production due to the failure of materials and structures are paid high attention in human activities.

For this reason, the fracture mechanics can be considered today one of the most important research fields in engineering. The attempts to predict the failure of a material are able to link different disciplines: in this dissertation, a very deep use of the statistical physics will be done in order to try to introduce the disorder of the medium into the breaking and to a give a new point of view to the fracture mechanics.

In the following, we will introduce a new kind of model to evaluate the genesis of the crack: *the statistical central force model*. As we will see, this model tries to compute the genesis of the fracture in a medium by taking into account the presence of defects of the material that are the main cause of the differences between the critical theoretical strength of a material and the real one. This innovation introduced by this model which is difficult to find in other kinds of techniques existing today united to the fact that we try to predict the behaviour of a macro system by knowing exactly the statistical behaviour of the micro-components of the system itself (the trusses) like in complex systems happens, is the main innovation of the statistical central force model. The model consists of a truss structure in which each truss is representative of a little portion of the material. Since this model was already applied in static for a porous medium in literature, we will study it from a mathematical viewpoint and we will apply it to the study of the dynamic of a dry medium before (the applications could be for the study of the fracture in metals and composites with loads changing in time) and of a porous medium later (in order to study the fracking into soils and the fracture of the concrete). Further developments could bring us to develop the same method for the study of the spalling in the concrete because of the application of a thermal load. In the dissertation we will introduce the mathematical tools to understand this model and some simulation on generic media will be realized.

This dissertation consists basically of five chapters.

In chapter 1 a brief description of the state of the art will be given: we will leave from the birth of the classical elastic fracture mechanics and we will shortly talk about the fracture mechanics in a plastic field. After this we will describe two important techniques used today for the evaluation of the crack: the XFem and the Peridynamics; the first one is a numerical technique allowing the FEM to take into account the possibility to create a breaking into the material. This is done, as we will see, by adding further degrees of freedom to the finite elements. In this way a single finite element will have the possibility to “open” itself and to simulate a discontinuous field of displacements, which is the main problem concerning with FEM in calculating the fracture. The second one is a theory that postulates that each medium can be divided in particles and that each particle interacts with its own neighbours within a given horizon. From which we get the word “*peri*”. By this assumption it is possible to get some integro-equations that can be defined on the surfaces of the tips and of the cracks as well.

In chapter 2 we will talk about the so called Fiber Bundle Model which is the basis of our statistical model. We will talk about the dry FBM that was already studied at the beginning of ’90s from a mathematical viewpoint : it consists of a bundle of fibers clamped at one edge and free to move to the other one. The model is one dimensional and it is probably one of the most naïve models to begin to study the fracture; however, despite to its simplicity, it contains an important tool: the possibility to take into account the defects of the medium by introducing the concept of variable thresholds in stress. As we will see, these thresholds will be picked up by a probability density function. Then we will apply the theory of the statistical ensembles to study one of the extensions of the FBM: the continuous fiber bundle model. This is necessary to have an idea of how the micro-components of our model, the trusses, behave in a truss structure subject to an external load.

In chapter 3 we will report briefly the theory of the porous medium according to the mixture theories of De Boer. So an overview about the equations will be given and then we will discretize these equations according to the finite element technique. After this, we will briefly describe in which part of the algorithm the concept of imperfection/threshold in stress enters. We will do this for a dry medium and for a porous medium in dynamics.

In chapter 4 we will report the numerical results. Some simulations in dynamics will be done both for a dry medium and for a porous medium. Furthermore we will introduce in the end a new damage law that will have a precise statistical meaning: it will be the average among all the possible realizations of the constitutive laws of our truss structure and for a big number of trusses, it will become the constitutive behaviour of our structure from which to get the damage law. And this result will take into account the disorder of the medium.

In chapter 5 we will talk about a controversial argument: the Self Organized Criticality (SOC) that was sticked in previous papers to the statistical central model. We will try to understand what SOC is and if our system with our algorithm to compute the fracture gets the necessary and sufficient conditions to enter into the set of the SOC systems.

At the end of our journey we will have hopefully done a first step into the description of a new numerical tool to evaluate the crack into a generic medium without needing an initial discontinuity to develop the crack itself. The next steps will be to validate this technique for existing materials and to compare it to other numerical tools like XFem or Peridynamics. After this, the future will be to extend the technique passing from trusses to 2D elements.

Table of contents

Chapter 1

Getting started: a basic review about Fracture Mechanics and the state of the art

" The Romans supposedly tested each new bridge by requiring the design engineer to stand underneath while chariots drove over it. Such a practice would not only provide an incentive for developing good designs, but would also result in the social equivalent of Darwinian natural selection, where the worst engineers were removed from the profession."

T.L. Anderson, Fracture Mechanic

1.1 Fracture Mechanics

1.1.1 Why Fracture Mechanics?

How was this branch of the structural mechanics born? In the past, the strength of the materials was evaluated according two different approaches: a material was said to fracture if the maximum tensile stress or maximum dimension in a body exceeded a certain threshold value. So the strength was considered basically dependent on the material properties and the effect of the fracture on the strength of a material was not taken into account. The consequence of this last idea was to achieve some theoretical strength values which were very high; but actually the strength of the material was lower than the actual. Among the earliest brittle fracture accidents, we remember the Montrose Bridge in 1830 and the Tay Rail bridge in 1879. The costs brought by these accidents and the fail in term of human lives, brought people to think of strength fracture in materials. During the years 1930 and 1950 the failure of welded ships and commercial airplanes, made this situation more serious. Up to that Griffith and Irwin's works led to a foundation of a new branch of the structural mechanics, known as fracture mechanics; and in the following years the studies in this branch growth till today, where a lot of numerical techniques can be used to compute the nucleation of the fracture.

Failures have occurred for many reasons, including uncertainties in the loading or environment, defects in the materials, inadequacies in design, and deficiencies in construction or maintenance. Design against fracture has a technology of its own, and this is a very active area of current research.

As we know, the strength of structural metals – particularly steel – can be increased to very high levels by manipulating the microstructure so as to inhibit dislocation motion. Unfortunately, this renders the material increasingly brittle, so that cracks can form and propagate catastrophically with very little warning.

An unfortunate number of engineering disasters are related directly to this phenomenon, and engineers involved in structural design must be aware of the procedures now available to safeguard against brittle fracture.
In the following pages, we will deal with some theoretical concepts in the elastic and elasto-plastic fracture mechanics.

1.1.2 The Energy-Balance approach

When A.A. Griffith (1893–1963) began his pioneering studies of fracture in glass in the years just prior to 1920, he was aware of Inglis' work in calculating the stress concentrations around elliptical holes, and naturally considered how it might be used in developing a fundamental approach to predicting fracture strengths. However, the Inglis solution poses a mathematical difficulty: in the limit of a perfectly sharp crack, the stresses approach infinity at the crack tip. This is obviously nonphysical (actually the material generally undergoes some local yielding to blunt the crack tip), and using such a result would predict that materials would have near zero strength: even for very small applied loads, the stresses near crack tips would become infinite, and the bonds there would rupture. Rather than focusing on the crack-tip stresses directly, Griffith employed an energy balance approach that has become one of the most famous developments in material science.
The strain energy per unit volume of stressed material is

$$U^* = \frac{1}{V}\int f\,dx = \int \frac{f}{A}\frac{dx}{L} = \int \sigma dx$$

(1.1)

If the material is linear, $\sigma = E\varepsilon$, then the strain energy per unit volume is

$$U^* = \frac{E\varepsilon^2}{2} = \frac{\sigma^2}{2E}$$

(1.2)

When a crack has grown into a solid to a depth a, a region of material adjacent to the free surfaces is unloaded, and its strain energy released. Using the Inglis' solution, Griffith was able to compute just how much energy this is.

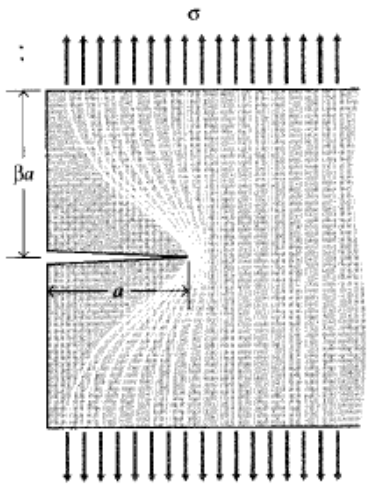

*Figure 1.1: development of the crack on a rectangular plate (*Roylance, D,2001*)*

A simple way of visualizing this energy release, illustrated in Fig. 1.1, is to regard two triangular regions near the crack flanks, of width a and height β_a, as being completely unloaded, while the remaining material continues to feel the full stress σ. The parameter β can be selected so as to agree with the Inglis' solution, and it turns out that for plane stress loading $\beta = \pi$. The total strain energy U released is then the strain energy per unit volume times the volume in both triangular regions:

$$U = \frac{-\sigma^2}{2E}\pi a^2$$

(1.3)

Here the dimension normal to the $x - y$ plane is taken to be unity, so U is the strain energy released per unit thickness of specimen. This strain energy is liberated by crack growth. But in forming the crack, bonds must be broken, and the requisite bond energy is in effect absorbed by the material. The surface energy S associated with a crack of length a (and unit depth) is:

$$S = 2\gamma a$$

(1.4)

where γ is the surface energy (e.g., Joules/meter) and the factor 2 is needed since two free surfaces have been formed. As shown in Fig. 1.2, the total energy associated with the crack is then the sum of the (positive) energy absorbed to create the new surfaces, plus the (negative) strain energy liberated by allowing the regions near the crack flanks to become unloaded.

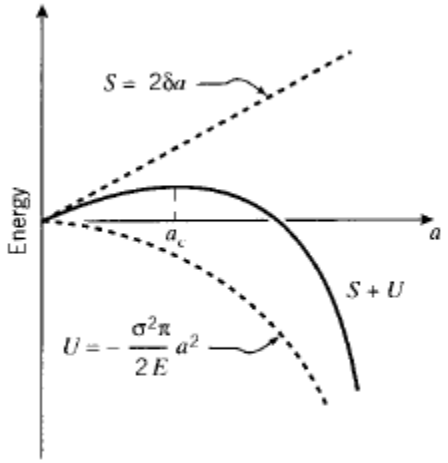

Figure 1.2: Plot of the curve $(S + U)$*-a*

As the crack grows longer (a increases), the quadratic dependence of strain energy on a eventually dominates the surface energy, and beyond a critical crack length a_c the system can lower its energy by letting the crack grow still longer. Up to the point where $a = a_c$, the crack will grow only if the stress is increased. Beyond that point, crack growth is spontaneous and catastrophic.
The value of the critical crack length can be found by setting the derivative of the total energy $S + U$ to zero:

$$\frac{\partial(S+U)}{\partial a} = 2\gamma - \frac{\sigma_f^2}{E}\pi a \tag{1.5}$$

Since fast fracture is imminent when this condition is satisfied, we write the stress as σ_f. Solving,

$$\sigma_f = \sqrt{\frac{2E\gamma}{\pi a}} \tag{1.6}$$

Griffith's original work dealt with very brittle materials, specifically glass rods. When the material exhibits more ductility, consideration of the surface energy alone fails to provide an accurate model for fracture. This deficiency was later remedied, at least in part, independently by Irwin and Orowan. They suggested that in a ductile material a good deal – in fact the vast majority – of the released strain energy was absorbed not by creating new surfaces, but by energy dissipation due to plastic flow in the material near the crack tip. They suggested that catastrophic fracture occurs when the strain energy is released at a rate sufficient to satisfy the needs of all these energy "sinks," and denoted this critical strain energy release rate by the parameter G_c; the Griffith equation can then be rewritten in the form:

$$\sigma_f = \sqrt{\frac{EG_c}{\pi a}}$$

(1.7)

This expression describes, in a very succinct way, the interrelation between three important aspects of the fracture process: the material, as evidenced in the critical strain energy release rate G_c; the stress level σ_f; and the size a of the flaw. In a design situation, one might choose a value of a based on the smallest crack that could be easily detected. Then for a given material with its associated value of G_c,the safe level of stress σ_f could be determined. The structure would then be sized so as to keep the working stress comfortably below this critical value.
It is important to realize that the critical crack length is an absolute number, not depending on the size of the structure containing it. Each time the crack jumps ahead, say by a small increment δa, an additional quantity of strain energy is released from the newly-unloaded material near the crack. Again using our simplistic picture of a triangular-shaped region that is at zero stress while the rest of the structure continues to feel the overall applied stress, it is easy to see in Fig. 1.3 that much more energy is released due to the jump at position 2 than at position 1. This is yet another reason why small things tend to be stronger: they simply aren't large enough to contain a critical-length crack.

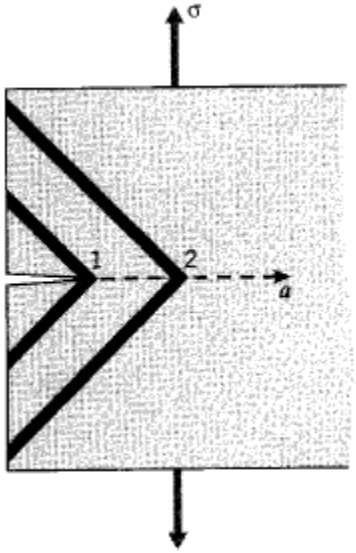

*Figure 1.3: development of the crack on a rectangular plate showing two different position of the crack tip ((*Roylance, D,2001*)*

1.1.3 Compliance calibration

A number of means are available by which the material property G_c can be measured. One of these is known as *compliance calibration*, which employs the concept of compliance as a ratio of

deformation to applied load: $C = \delta/P$. The total strain energy U can be written in terms of this compliance as:

$$U = \frac{1}{2}P\delta = \frac{1}{2}\,CP^2$$

(1.8)

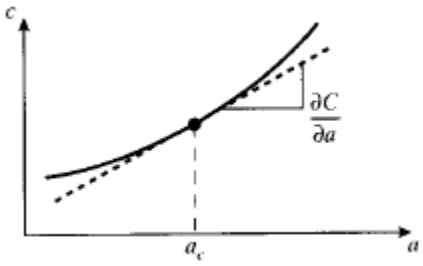

Figure 1.4: Plot of the Curve critical length vs Compliance

The compliance of a suitable specimen, for instance a cantilevered beam, could be measured experimentally as a function of the length a of a crack that is grown into the specimen (see Fig. 1.4.) The strain energy release rate can then be determined by differentiating the curve of compliance versus length:

$$G = \frac{\partial U}{\partial a} = \frac{1}{2}P^2\frac{\partial C}{\partial a}$$

(1.9)

The critical value of G, G_c, is then found by measuring the critical load P_c needed to fracture a specimen containing a crack of length a_c, and using the slope of the compliance curve at this same value of a:

$$G_c = \frac{1}{2}P^2\frac{\partial C}{\partial a}$$

(1.10)

to be calculated for $a = a_c$

1.1.4 The stress intensity approach

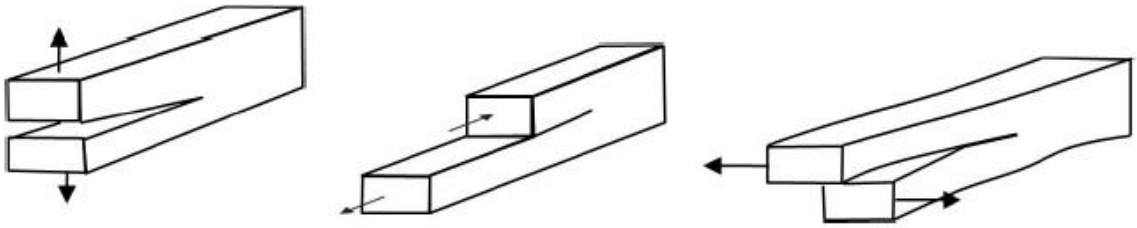

Figure 1.5: Mode I,II,III representing the opening ways of a material

While the energy-balance approach provides a great deal of insight to the fracture process, an alternative method that examines the stress state near the tip of a sharp crack directly has proven more useful in engineering practice. The literature treats three types of cracks, termed mode I, II, and III as illustrated in Fig.1.5 Mode I is a normal-opening mode and is the one we shall emphasize here, while modes II and III are shear sliding modes.
The semi-inverse method developed by Westergaard shows the opening-mode stresses to be:

$$\sigma_x = \frac{K_I}{\sqrt{2\pi r}}\cos\frac{\theta}{2}\,(1-\sin\frac{\theta}{2}\sin\frac{3\theta}{2}) + \cdots$$

$$\sigma_y = \frac{K_I}{\sqrt{2\pi r}}\cos\frac{\theta}{2}\,(1+\sin\frac{\theta}{2}\sin\frac{3\theta}{2}) + \cdots$$

$$\tau_{xy} = \frac{K_I}{\sqrt{2\pi r}}\cos\frac{\theta}{2}\,\cos\frac{3\theta}{2}\sin\frac{\theta}{2} + \cdots$$

(1.11)

For distances close to the crack tip ($r \leq 0.1a$), the second and higher order terms indicated by dots may be neglected. At large distances from the crack tip, these relations cease to apply and the stresses approach their far-field values that would obtain were the crack not present.
The K_I in (1.11) is a very important parameter known as the *stress intensity factor*. The I subscript is used to denote the crack opening mode, but similar relations apply in modes II and III. The equations show three factors that taken together depict the stress state near the crack tip: the denominator factor $\sqrt{2\pi r}$ shows the singular nature of the stress distribution; σ approaches infinity as the crack tip is approached, with a $r^{-1/2}$ dependency. The angular dependence is separable as another factor; e.g. $f_x = \cos\theta/2 \cdot \left(1 - sin\frac{\theta}{2}\sin 3\theta/2\right)$ … The factor K_I contains the dependence on applied stress σ_∞, the crack length a, and the specimen geometry. The K_I factor gives the overall intensity of the stress distribution, hence its name.
For the specific case of a central crack of width $2a$ or an edge crack of length $2a$ in a large sheet, $K_I = \sigma_\infty\sqrt{\pi a}$ and $K_I = 1.12\sigma_\infty\sqrt{\pi a}$ for an edge crack of length a in the edge of a large sheet. (The factor π could obviously be cancelled with the π in the denominator of Eq. 1.11, but is commonly retained for consistency with earlier work.) Expressions for K_I for some additional geometries are given in Table 1. The literature contains expressions for K for a large number of crack and loading geometries, and both numerical and experimental procedures exist for determining the stress intensity factor is specific actual geometries.

Type of crack	**Stress Intensity factor K_I**
Center crack, length $2a$, in an infinite plate	$\sigma_\infty\sqrt{\pi a}$
Edge crack, length a, in a semi-infinite plate	$1.12\ \sigma_\infty\sqrt{\pi a}$
Central penny shaped cracked, radius a, in an infinite body	$2\ \sigma_\infty\sqrt{\frac{\pi}{a}}$
Central crack, length $2a$, in a plate of width W	$\sigma_\infty\sqrt{W\tan(\pi a/W)}$
2 symmetrical edge cracks, each length a, in a plate of total width W	$\sigma_\infty\sqrt{W\tan\left(\frac{\pi a}{W}\right)+0.1\sin(\frac{2\pi a}{W})}$

Table 1: Values of the stress intensity factor computed for different geometries

These stress intensity factors are used in design and analysis by arguing that the material can withstand crack tip stresses up to a critical value of stress intensity, termed K_{Ic}, beyond which the crack propagates rapidly. This critical stress intensity factor is then a measure of material toughness. The failure stress σ_f is then related to the crack length a and the fracture toughness by

$$\sigma_f = \frac{K_{IC}}{\alpha\sqrt{\pi a}}$$

(1.12)

where α is a geometrical parameter equal to 1 for edge cracks and generally on the order of unity for other situations. Expressions for α are tabulated for a wide variety of specimen and crack geometries, and specialty finite element methods are available to compute it for new situations. The stress intensity and energy viewpoints are interrelated, as can be seen by comparing Eqs. 1.1 and 1.12 (with $\alpha = 1$):

$$\sigma_f = \sqrt{\frac{EG_c}{\pi a}} = \frac{K_{IC}}{\sqrt{\pi a}} \longrightarrow {K_{IC}}^2 = EG_c$$

(1.13)

This relation applies in plane stress; it is slightly different in plane strain:

$${K_{IC}}^2 = EG_c(1-\upsilon^2)$$

(1.14)

For metals with $\nu = 0.3, (1-\nu_2) = 0.91$. This is not a big change; however, the numerical values of G_c or K_{Ic} are very different in plane stress or plane strain situations, as will be described below.

Typical values of G_{Ic} and K_{Ic} for various materials are listed in Table 2, and it is seen that they vary over a very wide range from material to material. Some polymers can be very tough, especially when rated on a per-pound bases, but steel alloys are hard to beat in terms of absolute resistance to crack propagation.

MATERIAL	$G_{IC}\ (KJ\ m^{-2})$	$K_{IC}\ (MN\ m^{2})$	$E(GPa)$
Aluminium alloy	107	150	210
wood	0.12	0.5	2.1
glass	0.007	0.7	70
rubber	13	----------	0.001
PMMA	0.5	1.1	2.5
Polystirene	0.4	1.1	3
Steel-mild	12	50	210

Table 2: Critical values of G_I, K_I, E for different materials

The toughness, or resistance to crack growth, of a material is governed by the energy absorbed as the crack moves forward. In an extremely brittle material such as window glass, this energy is primarily just that of rupturing the chemical bonds along the crack plane. But as already mentioned, in tougher materials bond rupture plays a relatively small role in resisting crack growth, with by far the largest part of the fracture energy being associated with plastic flow near the crack tip. A "plastic zone" is present near the crack tip within which the stresses as predicted by Eqn. 4 would be above the material's yield stress σ_Y . Since the stress cannot rise above σ_Y , the stress in this zone is σ_Y rather than that given by Eqn. 1.11. To a first approximation, the distance r_p this zone extends along the x-axis can be found by using Eqn. 1.11 with θ = 0 to find the distance at which the crack tip stress reduces to σ_Y :

$$\sigma_{y=}\sigma_Y = \frac{K_I}{\sqrt{2\pi r_p}}$$

(1.15)

$$r_p = \frac{K_I^2}{2\pi\sigma_Y^2}$$

(1.16)

This relation is illustrated in Fig. 1.6.

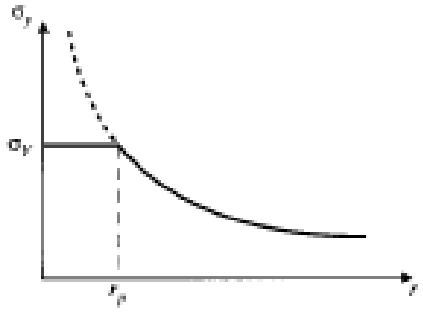

*Figure 1.6: Stress limited by yield within zone r_p(*Roylance, D,2001*)*

As the stress intensity in increased either by raising the imposed stress or by crack lengthening, the plastic zone size will increase as well. But the extent of plastic flow is ultimately limited by the material's molecular or microstructural mobility, and the zone can become only so large. When

the zone can grow no larger, the crack can no longer be constrained and unstable propagation ensues. The value of K_I at which this occurs can then be considered a materials property, named K_{Ic}.
In order for the measured value of K_{Ic} to be valid, the plastic zone size should not be so large as to interact with the specimen's free boundaries or to destroy the basic nature of the singular stress distribution. The ASTM specification for fracture toughness testing specifies the specimen geometry to insure that the specimen is large compared to the crack length and the plastic zone size (see Fig. 1.7):

$$a, b, (W - a) \geq 2.5 \left(\frac{K_I}{\sigma_Y}\right)^2 \quad (1.17)$$

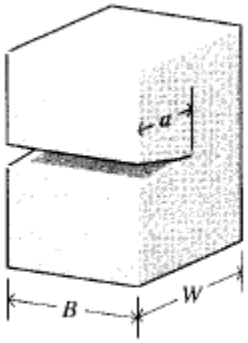

Figure 1.7: Definition of the previous quantities (Royalance, 2001)

A great deal of attention has been paid to the important case in which enough ductility exists to make it impossible to satisfy the above criteria. In these cases the stress intensity view must be abandoned and alternative techniques such as the J-integral or the crack tip opening displacement method used instead.

1.1.5 J Integral

Previously we analysed problems in which the plastic zone was very small if compared with the dimensions of the specimen dimensions.
Now we will present a technique to analyse situations in which there can be a large scale yielding and we will determine expressions for the stress components inside the plastic zone; let's begin with the J integral; The J integral is a line integral (path-independent) around the crack tip. It has enormous significance in elastic-plastic fracture mechanics. (J. R. Rice, Journal of Applied Mechanichs, 1968).
Consider the path around the crack tip shown below:

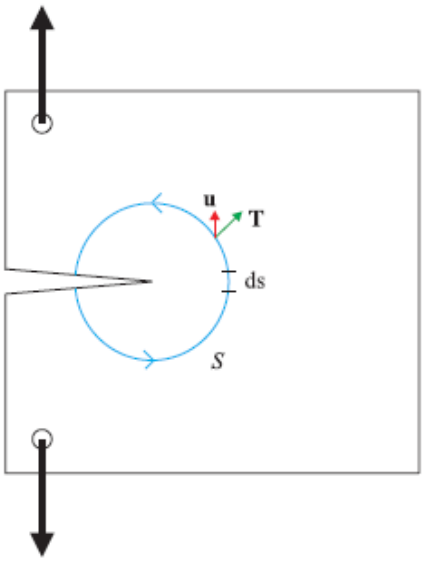

Figure 1.8: development of the crack on a rectangular plate

In the following, we will use the variables:

a= crack lenghth

S= a curve that links the lower and the upper surface

$\overrightarrow{d\Gamma}$= an infinitesimal arc of this curve

$\vec{T}$= traction vector defined in relation to an outward normal unit vector $\vec{T} = \vec{n} \cdot \vec{\sigma}$

$\vec{u}$= vector of the displacements

So, now let us consider a strain constant experiment neglecting deformation induced blunting of the crack tip.

The total mechanical potential energy of the crack body is

$$u_M = u_e + u_{app}$$

(1.18)

where the first term is the stored strain potential energy while the second one is the potential energy of the loads applied; so if we call w the strain energy density, and we know that

$$\sigma_{ij} = \frac{\partial w}{\partial \varepsilon_{ij}}$$

(1.19)

dA is an element of cross section A within S.

Let's take now the derivative of the mechanical energy with respect the crack length

$$-\frac{du_M}{da} = \int_S (w\,dy - \vec{T}\cdot\frac{\partial u}{\partial x})\overrightarrow{d\Gamma} \equiv J$$

(1.20)

J represents the rate of change of net potential energy with respect to crack advance (per unit thickness of crack front) for a non-linear elastic solid. J also can be thought of as the energy flow into the crack tip. Thus, J is a measure of the singularity strength at the crack tip for the case of elastic-plastic material response.
For the special case of a **linear elastic** solid, it's possible to show that

$$J = G = -\frac{d(PE)}{da} = -\frac{dU_M}{da} = \frac{K^2}{E}(1-\upsilon^2)$$

(1.21)

This relationship can be used to infer an equivalent K_{Ic} value from J_{Ic} measurements in high toughness, ductile solids in which valid K_{Ic} testing will require unreasonably large test specimens. This integral is independent on the path we choose around the tip. In fact it's possible to show that if we chose two different paths

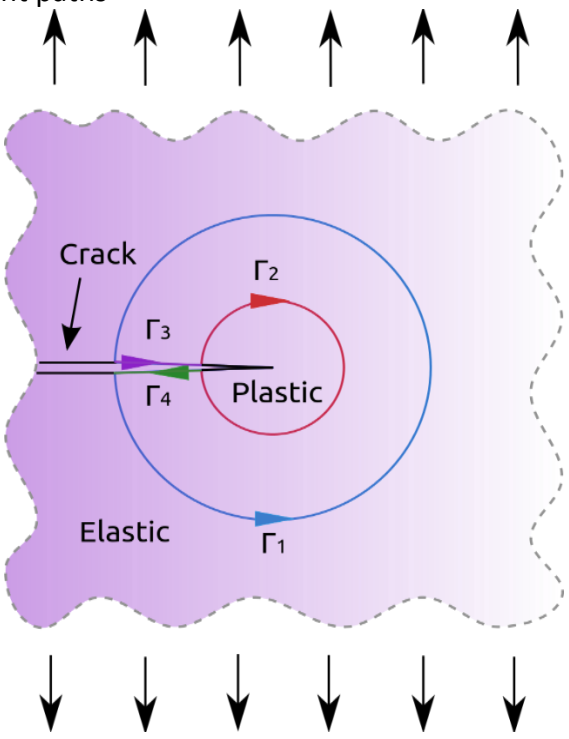

Figure 1.9: development of the crack on a rectangular plate, considering the elastic and plastic regions

The value of J along Γ_2 must be the same along Γ_1:
Hutchinson, Rice and Rosengren subsequently showed that J characterizes the singular stress and strain fields at the tip of a crack in nonlinear (power law hardening) elastic-plastic materials where the size of the plastic zone is small compared with the crack length. Hutchinson used a material constitutive law of the form suggested by Ramberg and Osgood

$$\frac{\varepsilon}{\varepsilon_y} = \frac{\sigma}{\sigma_y} + \alpha\left(\frac{\sigma}{\sigma_y}\right)^n$$

(1.22)

where σ is the stress in uniaxial tension, σ_y is a yield stress, ε is the strain, and $\varepsilon_y = \sigma_y/E$ is the corresponding yield strain. The quantity E is the elastic Young's modulus of the material. The model is parametrized by α, a dimensionless constant characteristic of the material, and n, the coefficient of work hardening. This model is applicable only to situations where the stress increases monotonically, the stress components remain approximately in the same ratios as loading progresses (proportional loading), and there is no unloading.

If a far-field tensile stress σ_{far} is applied to the body shown in the adjacent figure, the J-integral around the path Γ_1 (chosen to be completely inside the elastic zone) is given by

$$J_{\Gamma 1} = \pi(\sigma_{far})^2$$

(1.23)

Since the total integral around the crack vanishes and the contributions along the surface of the crack are zero, we have

$$J_{\Gamma 1} = -J_{\Gamma 2}$$

(1.24)

If the path Γ_2 is chosen such that it is inside the fully plastic domain, Hutchinson showed that

$$J_{\Gamma 2} = -\alpha K^{n+1} r^{(n+1)(s-2)+1} I$$

(1.25)

where K is a stress amplitude, (r,ϑ) is a polar coordinate system with origin at the crack tip, s is a constant determined from an asymptotic expansion of the stress field around the crack, and I is a dimensionless integral. The relation between the J-integrals around Γ_1 and Γ_2 leads to the constraint

$$s = \frac{2n+1}{n+1}$$

(1.26)

and an expression for K in terms of the far-field stress

$$K = \left(\frac{\beta\pi}{\alpha I}\right)^{1/(n+1)} (\sigma_{far})^{2/(n+2)}$$

(1.27)

where $\beta = 1$ for plane stress and $\beta = 1 - \nu^2$ for plane strain (ν is the Poisson's ratio).

The asymptotic expansion of the stress field and the above ideas can be used to determine the stress and strain fields in terms of the J-integral:

$$\sigma_{ij} = \sigma_Y \left(\frac{EJ}{r\alpha\sigma_Y^2 I} \right)^{1/(n+1)} \widetilde{\sigma_{ij}}\ (n,\theta)$$

(1.28)

$$\varepsilon_{ij} = \frac{\alpha\varepsilon_Y}{E} \left(\frac{EJ}{r\alpha\sigma_Y^2 I} \right)^{n/(n+1)} \widetilde{\varepsilon_{ij}}\ (n,\theta)$$

(1.29)

where $\widetilde{\sigma_{ij}}\ (n,\theta)$ and $\widetilde{\varepsilon_{ij}}\ (n,\theta)$ are dimensionless functions.

These expressions indicate that *J* can be interpreted as a plastic analog to the stress intensity factor (*K*) that is used in linear elastic fracture mechanics, i.e., we can use a criterion such as $J > J_{Ic}$ as a crack growth criterion.

Obviously these are the theoretical fundaments of the elasticity and plasticity fracture mechanics.

However when we begin to analyse more complicated geometries, the calculations begin quite complicated. For this reason, in the years different numerical techniques have been developed in order to obtain numerical results from quite complicated objects.

The FEM allowed us to achieve this purpose and today it is fully used by companies and for research. However the FEM is not able to simulate a discontinuous field; and this happens in fracture mechanics when we observe a crack that begins to propagate. So in order to overcome the limitations of FEM and in order to have an instrument that allow us to follow the nucleation or the development of the fracture in a material, point by point not to pass through the calculation of the fracture mechanics (that can become very complicated for complicated surfaces), different numerical techniques were developed: we will analyse two of them: XFEM and Peridynamics.

1.2 XFEM

1.2.1 XFEM: Generalities

We will give an overview about the method XFEM (extended Finite Element Method). This new method is already implemented in some commercial software, for example ANSYS. For this reason our description will be based in introducing few concepts about it from a mathematical viewpoint and then we will perform a little numerical simulation in ANSYS in order to understand the basic steps.

The XFEM is a numerical technique used to model the cracks (for this reason it is used very much in Fracture Mechanics) and other kind of discontinuities. What's on the basis of this method? The main idea is to enrich the degrees of freedom in some regions of the model with additional displacements functions with respect the classical method (FEM). This is necessary in order to simulate the jump/discontinuity in displacements at the interface of the crack. In fact, given a crack, when this is going to open because of the load conditions on the structure, we will always

notice a jump in displacements. So, In XFEM, it is possible to simulate this particular jump by introducing these additional degree of freedom.

Among the principal features of this method, we remind the possibility to model the cracks without explicitly meshing the crack surfaces. In other codes, able to simulate the nucleation of the cracks in fact, it is necessary to introduce some parameters in the simulation that determine a particular mesh, necessary for the calculation of some quantities like the “stress intensity factor” or the J integral (that we recover from the classical fracture mechanics).

Another feature is that by this method it is possible a random growing of the crack inside the mesh. It is not necessary to know a priori the path of propagation of the crack as for example we do when we study phenomenon like delamination: in this case in fact it is important to define an interface of separation between two laminas of a composite or between two layers of materials: we already know that the separation, if it will happen, will develop on the interface we defined a priori. By XFEM we do not have the necessity to know this information; the direction of propagation of the crack is calculated into the code.

Furthermore it is not necessary to remesh or to morphing the system for each substep in which the crack grows as happens in other codes that use different numerical techniques.

1.2.2 Mathematical formalism

We will introduce now a brief mathematical formalism in order to describe better this method

The generalized FEM is a Partition Unity Method with the partition of unity provided by Lagrangian FE shape functions. The same method is also known as eXtended FEM.

Let’s begin with some definitions; let’s consider a body B, and let’s perform a mesh over it in which we will find different nodes.

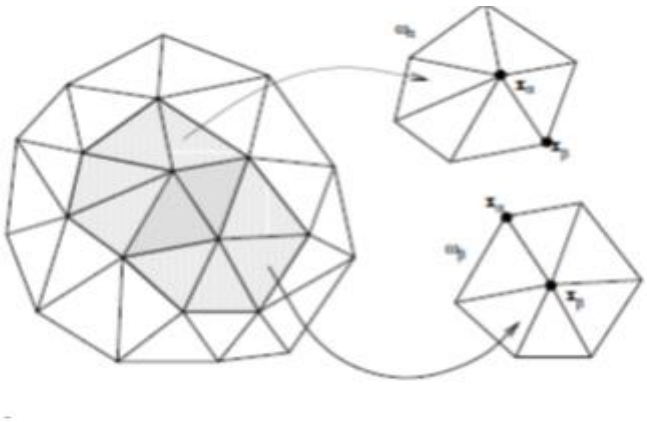

*Figure 1.10: Open Cover associated with a Finite Element Mesh (*Ahmed, A., 2009*)*

A “cloud” or a “patch” ω_α is given by the union of Finite Elements sharing a particular node α of the Finite Element mesh covering the domain of interest, that we call Ω.

The set $\tau_N = \{\omega_\alpha\}_{\alpha=1}^N$ in a Finite Element Mesh with N nodes is an open cover of Ω, i.e:

$$\Omega = U_{\alpha=1}^N \omega_\alpha$$

(1.30)

Now, we know that the Lagrangian shape functions φ_α with $\alpha = 1, .., N$ must satisfy the Partion of Unity:

$$\sum_{\alpha=1}^{N} \varphi_\alpha(\vec{x}) = 1 \qquad \forall\, \vec{x} \epsilon \Omega$$

(1.31)

and this must be true for each $\vec{x}$ into the domain Ω.

This propriety can be better understood by the following figure:

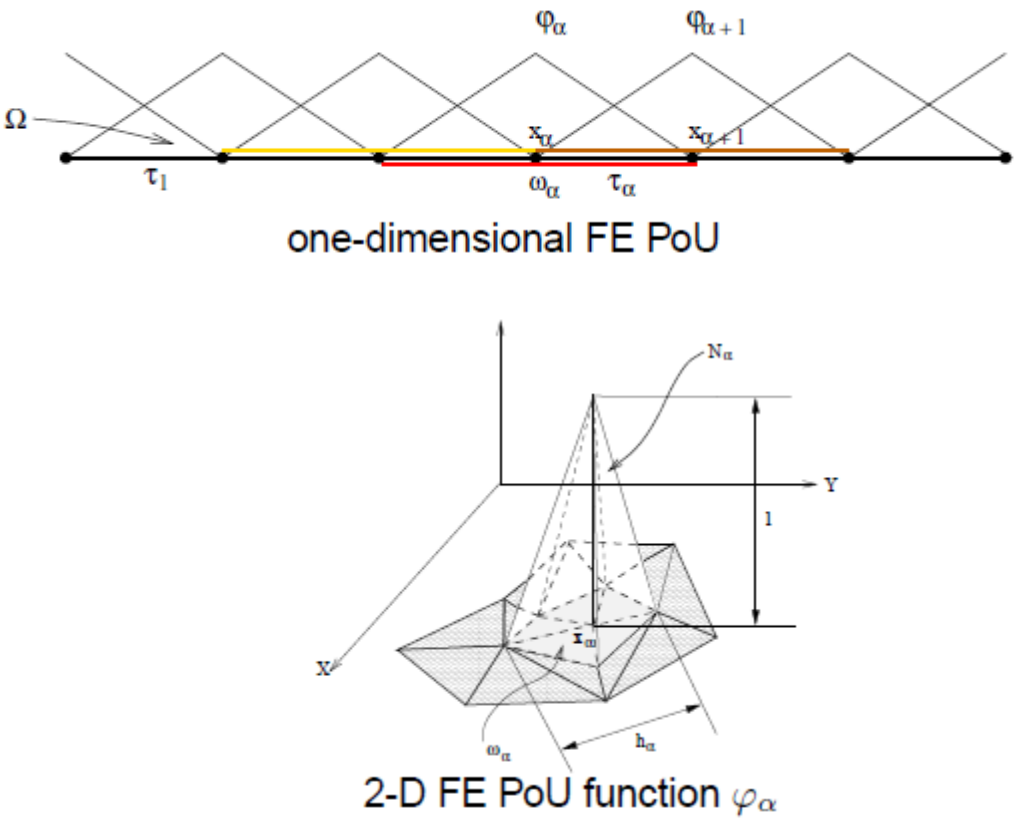

*Figure 1.11: One dimensional FE PoU (above) and 2D FE PoU functionsφ_α (below) (*Ahmed, A., 2009)

that show basically that our shape functions are at compact support.

Now, let's introduce the Cloud Space Approximation: to each cloud of our system ω_α, we associate a $D_L(\alpha)$ dimensional space $\Theta_\alpha$of functions which are defined on ω_α

$$\Theta_\alpha = span\{L_{\alpha j}, 1 < j < D_L, L_{\alpha j} \in H\}$$

(1.32)

where j are the degree of freedom and H the usual space of the shape functions of the Finite Element Method. The basis functions $L_{\alpha j}$ are known as enrichment functions.

For a precise definition of the spaces H and of the topology of the problem, we quote Belytschko et al., 2014.

A cloud approximation $\overrightarrow{u_\alpha^{hp}}(\vec{x}) \in \Theta_\alpha$ (which is the restriction to Θ_α of the function $\vec{u}$ defined on Ω) is:

$$\overrightarrow{u_\alpha^{hp}}(\vec{x}) = \sum_{j=1}^{D_L} \overrightarrow{u_{\alpha j}} L_{\alpha j}$$

(1.33)

Now we are ready to define the GFEM space: the trial space for GFEM, is given by:

$$X(\Omega) = span\{\varphi_{\alpha j} = \varphi_\alpha L_{\alpha j}, 1 < j < D_L, 1 < \alpha < N\}$$

(1.34)

Now the function

$$\varphi_{\alpha j}(\vec{x}) = \varphi_\alpha(\vec{x}) L_{\alpha j}(\vec{x})$$

(1.35)

where α is a node of the model, is called GFEM shape function.

A GFEM approximation is given by

$$\vec{u}^{hp}(\vec{x}) = \sum_{\alpha=1}^{N} \sum_{j=1}^{D_L} \overrightarrow{u_{\alpha j}} \varphi_\alpha(\vec{x}) L_{\alpha j}(\vec{x}) = \sum_{\alpha=1}^{N} \varphi_\alpha(\vec{x}) \overrightarrow{u_\alpha^{hp}}(\vec{x})$$

(1.36)

So, from a physical viewpoint, it's worth to notice that the displacement field over a given cloud ω_α is obtained by using the classical shape functions $\varphi_\alpha(\vec{x})$ already defined, multiplied by these enrichment functions $L_{\alpha j}(\vec{x})$; The product between the $L_{\alpha j}(\vec{x})$ and the original degree of freedom gives us some new degrees of freedom $\overrightarrow{u_\alpha^{hp}}(\vec{x})$ that now will be able to be used in order to take into account the jump that we could meet into the solution; the possibility to simulate discontinuities in the solution depends on the particular kind of functions $L_{\alpha j}(\vec{x})$ that we chose.

1.2.3 Simulation in ANSYS: Generalities

As we told first the XFEM is already implemented in some trade codes, for example ANSYS. So let's give a numerical example to better understand how this technique works. The technique used in ANSYS is called Phantom Node Method: by this we can con consider the jump in displacements through the surfaces of the cracks. Here the crack terminates on the face or on the corner of a finite element as we see in the figure:

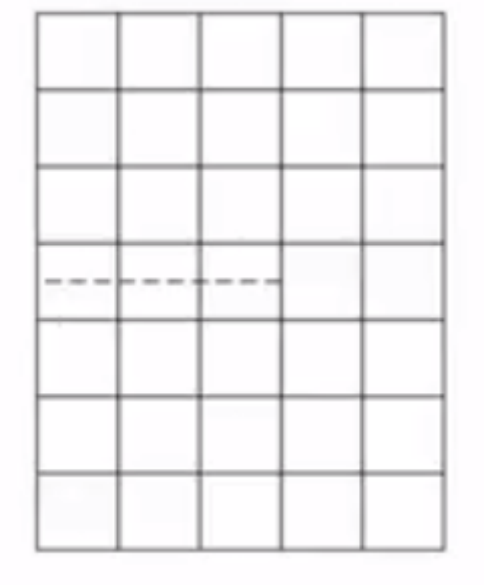

Figure 1.12: Plate considered in the simulation containing the initial crack

This must be valid when we define the crack: as we notice from the figure, the extension of the crack must be introduced for the crack to cover the elements in their length. If we want a crack defined for three elements, a mesh has to be chosen in order to adapte the lenghth of the crack to mesh itself.

Now, if we decide to use the enrichment functions in the region of the crack, we will have this kind of situation:

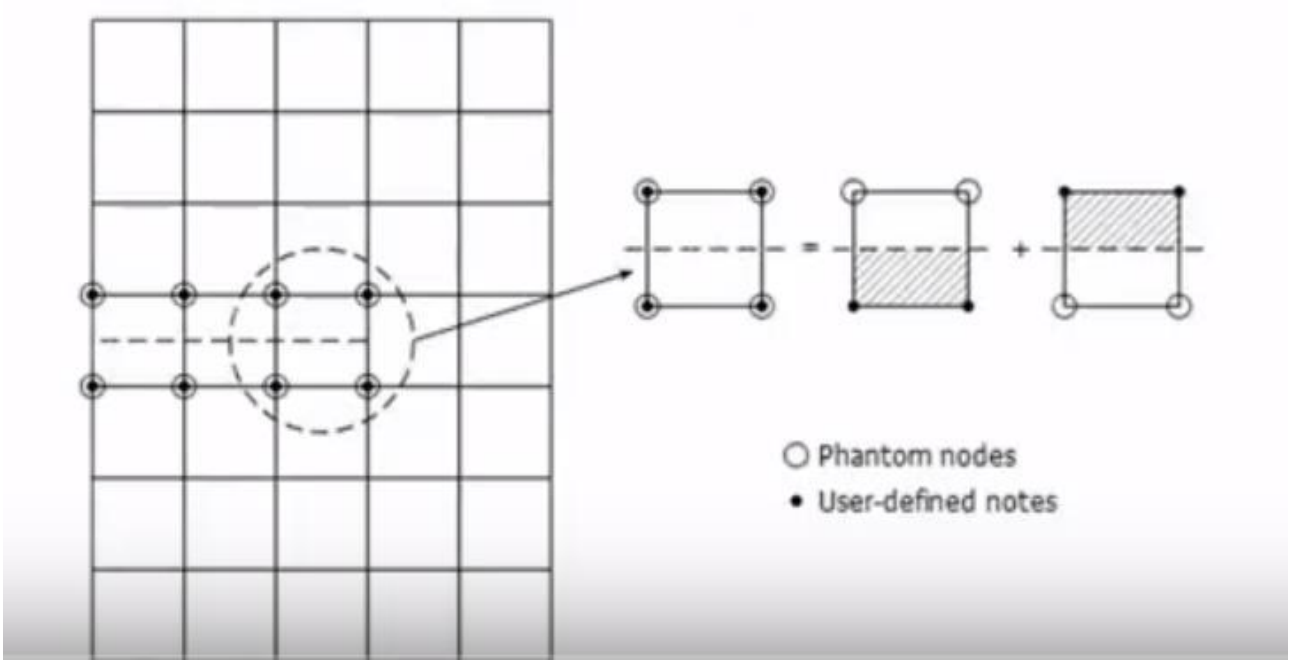

Figure 1.13: Phantom nodes in the mesh of the model

By the Phantom Node Method, some additional degrees of freedom are overlapped to the existing nodes, defined in the mesh. As we notice from the figure, in black the traditional degrees of freedom are represented and in white are represented the phantom nodes. The consequence of this introduction leads us to divide in two parts the original element. In dash we notice the interface of the crack and all that we must do is to simulate the jump of the displacements at the interface of the crack. So the code introduces the phantom nodes and this results into the split of the element in two different phantom elements. In this way, from a physical viewpoint, we will have a field of displacements above and another field of displacements below and generally these two displacement fields can be different in order to simulate the discontinuity.

Thanks to the phantom nodes superimposed, the displacements of the nodes of our elements can be rewritten, using the theory, like

$$\vec{u}(x,t) = \overrightarrow{u_l^1}(t)N_l(x)H(-f(x)) + \overrightarrow{u_l^2}(t)N_l(x)H(f(x)) \quad (1)$$

Here,

$\overrightarrow{u_l^1}$ is the displacement vector in the subelement 1, i.e. in the first phantom element.

$\overrightarrow{u_l^2}$ is the displacement vector in the subelement 2, i.e. in the second phantom element.

$f(x)$ defines the surface of the crack; in the case 1D, in our example, the crack is obviously a line; in 2D instead, this will be a surface. The equation

$$f(x) = 0$$

(1.37)

defines the surface of the crack.

Then we have the Heaviside function that represent $L_{\alpha j}(\vec{x})$. We decide to introduce it to define the discontinuities: as we know, in fact

$$H(x) = \begin{cases} 1 \; if \; x \geq 0 \\ 0 \; if \; x \leq 0 \end{cases}$$

(1.38)

In this figure we can observe what the introduction of the Heaviside functions implicate:

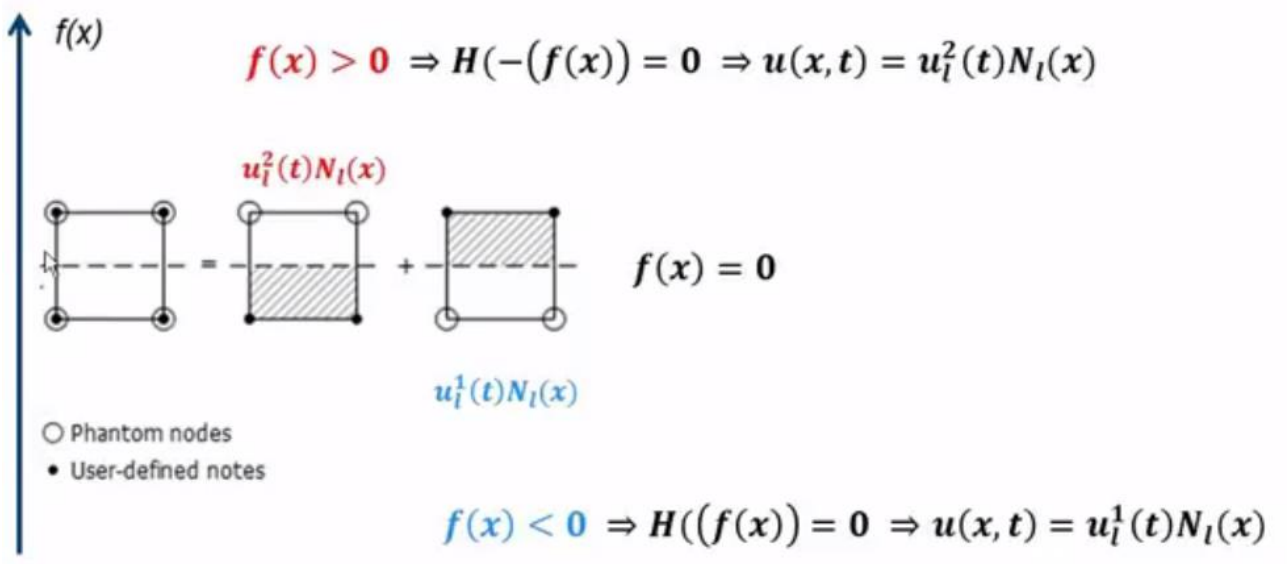

Figure 1.14: definition of the crack region

In dashed we notice the surface of the initial crack

$$f(x) = 0$$

So, if we move above,

$$f(x) > 0$$

and so the Heaviside function $H(-f(x)) = 0$. So the first term in (1) will be equal to 0. Only the contribute of the subelement 2 will remain, and this will have its own field of displacement. Instead, if we move below, the second term in (1) will be equal to 0 and the first term will give its displacements to our finite element. So by this way we have two different displacements field that can be discontinuous above and below the crack. This means basically that the main trick in enriching the degrees of freedom of our element, i.e in the equation

$$\vec{u}^{hp}(\vec{x}) = \sum_{\alpha=1}^{N} \sum_{j=1}^{D_L} \overrightarrow{u_{\alpha j}} \, \varphi_\alpha(\vec{x}) L_{\alpha j}(\vec{x}) = \sum_{\alpha=1}^{N} \varphi_\alpha(\vec{x}) \overrightarrow{u_\alpha^{hp}}(\vec{x})$$

(1.39)

is basically to allow the element to split in two different subelements in order to describe the crack. From a math viewpoint this is a consequence of the introduction of the enrichment functions: the element has more degree of freedom and so it is able to split itself.

During the simulation, the study of propagation of the crack is assumed to be quasi static; so the inertial effects are negligible.

The main steps to do this simulation are the following ones;

1) To create the mesh by the classical FEM. So we must give position, inclination and geometry of the crack/s inside the mesh.
2) To define the crack growth criterion of the crack;

obviously if we consider a structure characterized by a certain external load, the crack can or cannot propagate according to the stresses reached locally around the crack. So this phenomenon is considered into the code by introducing such criterion. This criterion consists in calculating a main tension in the circumferential direction; If this stress is bigger than a fixed value, the crack propagates.

   If necessary, we must define the decay of stresses in the new crack segments created. In fact if the original crack grows, new crack segments are created and each of them will recover the length of one or different elements. These new interfaces created (the new crack segments) are modelled by a cohesive law. This means that for them we will have a certain degree of strength to the separation. So, we will see that if we choose a certain criterion, it is necessary to introduce this decay law of stresses to simulate the values of the stresses when the main crack opens.
3) For each substep, the solver will evaluate the crack growth criterion, and so it will decide if the crack must grow or not.
4) Perform the crack growth calculation

The initial position of the crack is chosen by the so called *level set method*. In order to define the position and the original inclination of the crack, we must give the distances from the plane of the crack to the nodes

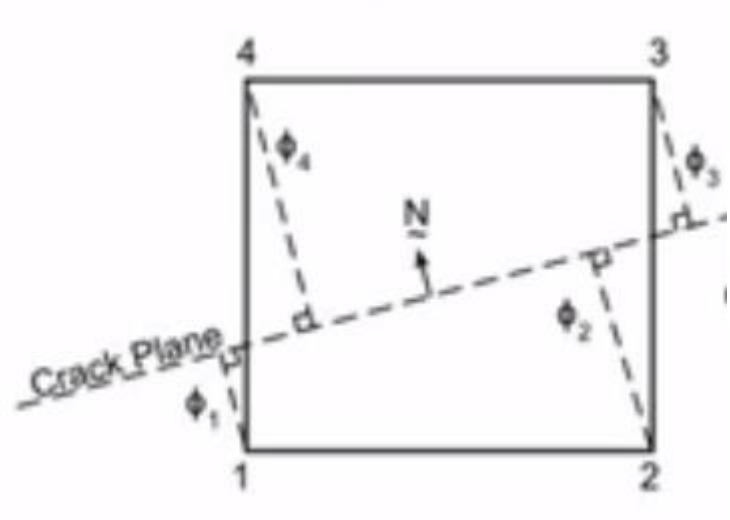

Figure 1.15: definition of the crack plane inside one element

In this figure we notice the crack inside the element and then the four distances $\varphi_1\varphi_2\varphi_3\varphi_4$ between the crack line and the nodes of the element. By playing with this distances we can decide to introduce the crack around an oblique direction as well.

So we will know a priori what is the distance between the crack and the node. For this reason by playing with these distances, we can insert the crack into the element as we wish. This is done in the code by some commands.

1.2.4 Criterion of crack

Now let's specify the criterion of growth of the crack. When the critical value of this criterion is reached, the crack propagates into the elements. The crack segments are such that they fully cut elements ahead of the crack. This means that for each progress, the crack covers the dimension of an element. Furthermore the distances fi cannot be 0. This means that a crack cannot cut the mesh passing through the nodes, but it must cut the element. The crack propagates at the rate of only one element at time. For this reason we must use a good number of substeps.

In order to define the criterion we must the material and the type of criterion:

1) Maximum stress criterion: it is based on evaluating the maximum value of the circumferential $\sigma_{\theta\theta}$ stress in some sampling points, indicated in the figure when sweeping around the crack tip. We can specify the positions at which it will be evaluated, by specifying both the distance ahead and of the crack tip and the angles to be scanned, as we can see by the figure. Where the stress is maximum, a new crack will be opened.
2) Circumferential stress criterion based on $\sigma_{r\theta} = 0$; This criterion looks for the direction in this circumferential region in which this cut stress is 0. Here the cirumferential stress will be maximum and the crack will propagate in traction according to the mode 1.

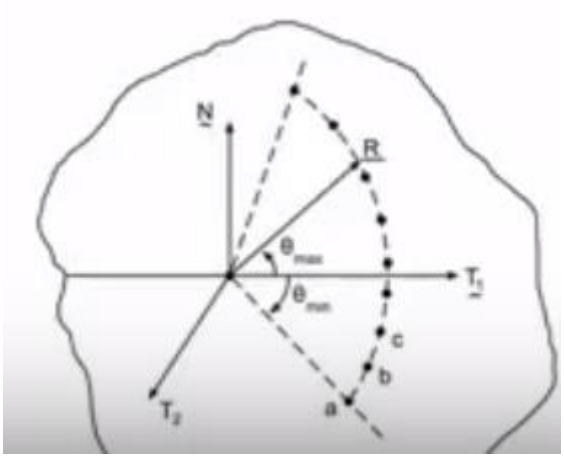

Figure 1.16: development of the crack on a rectangular plate

RESULTS

So let's apply these concepts to a test case in ANSYS, in order to understand how the XFEM works. We will consider basically a plate characterized by the loads in the figure:

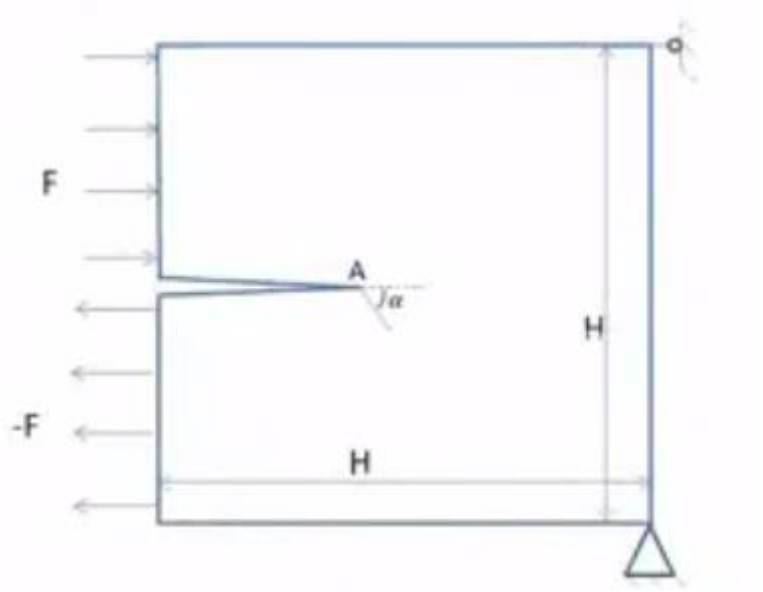

Figure 1.17: development of the crack on a rectangular plate

In this structure we have an initial crack and the loads applied are such that we have a pure shear stress. It is interesting to study also the initial value of the propagation of the crack and to compare analytically with results that we already know. If we model the structure with plane strain elements we have

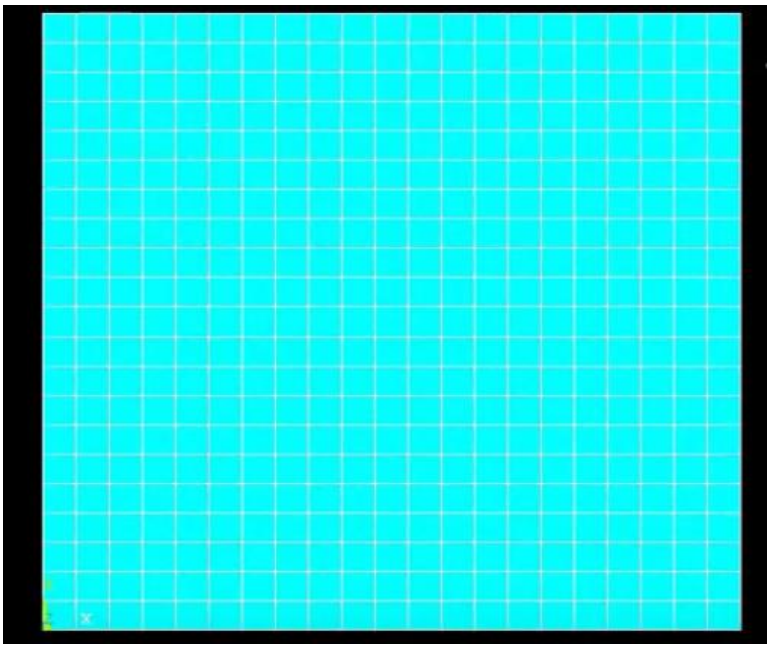

Figure 1.18: Mesh of the plate in ANSYS

We expect in this case the crack propagates in the lower zone; so we should try to define the enrichment of the degree of freedom of the elements in the part below. This could be a limit for XFEM, i.e. to know in which part of the system the crack will grow.

The next step is to introduce the crack into the element we are interested:

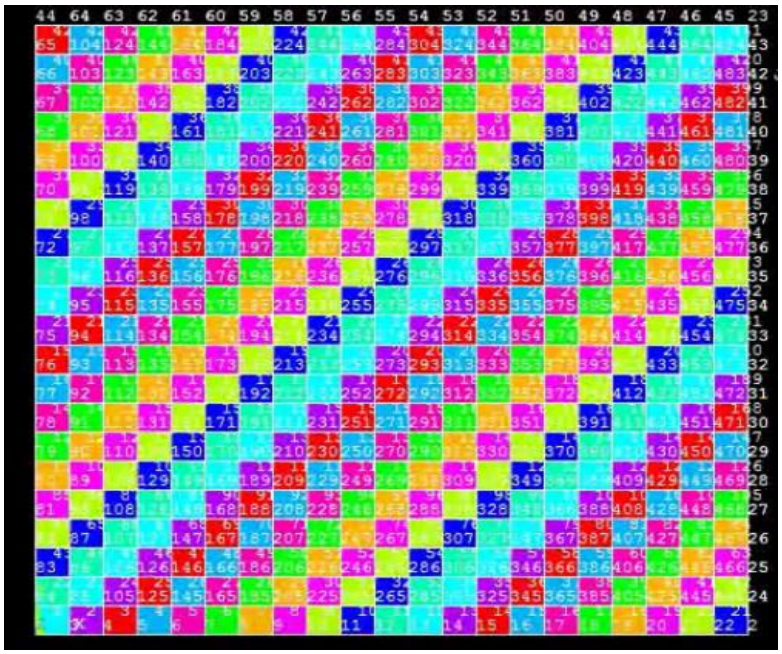

Figure 1.19: Numeration of the elements of the mesh

By inserting the crack into the an element on the left and on the middle, we have

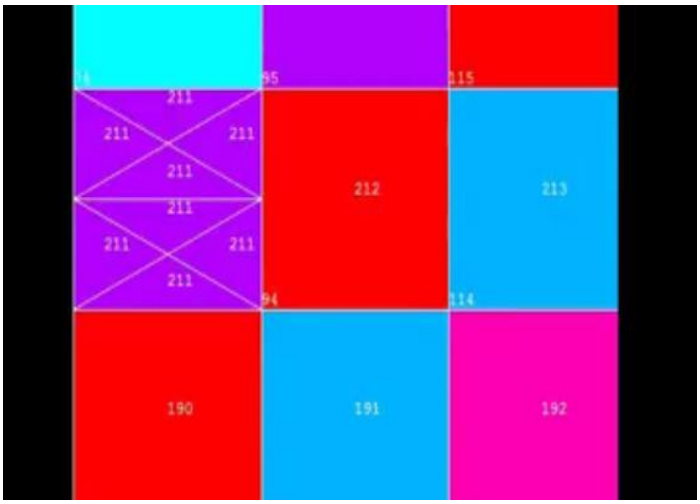

Figure 1.20: inserting the crack inside one element

As we notice, the software has divided in 2 parts the elements in order to create the 2 phantom element to study propagation of crack. In this example the example extends till the half of the structure but this is only a picture to understand how the software creates it.

The results is:

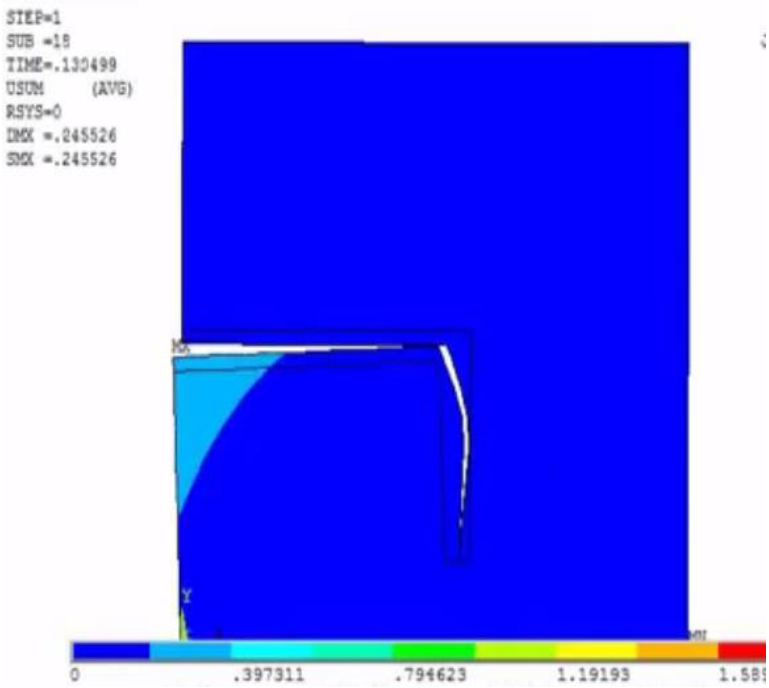

Figure 1.21: development of the crack on a rectangular plate

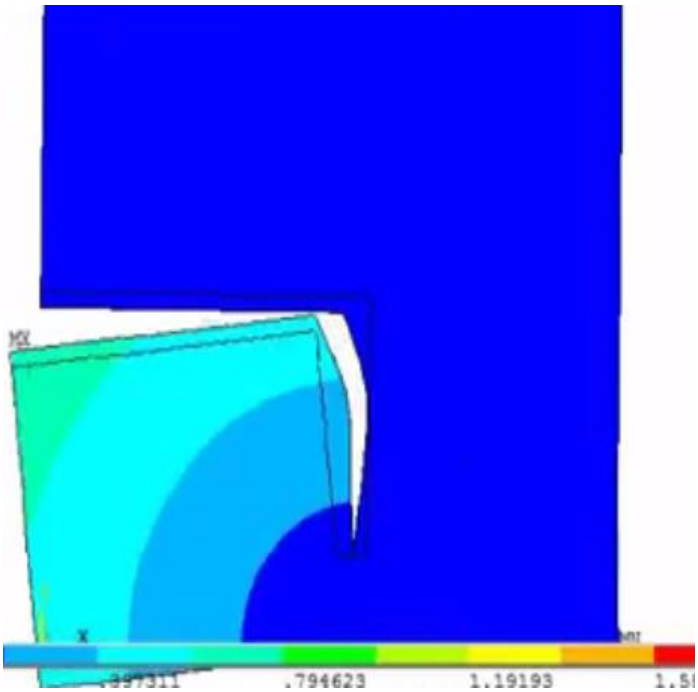

Figure 1.22: development of the crack on a rectangular plate

In which we notice that crack growths in the region below. So we do not need to know the direction of propagation of the crack because this is computed automatically. If we zoom inside the elements, we can notice what happens into the elements.

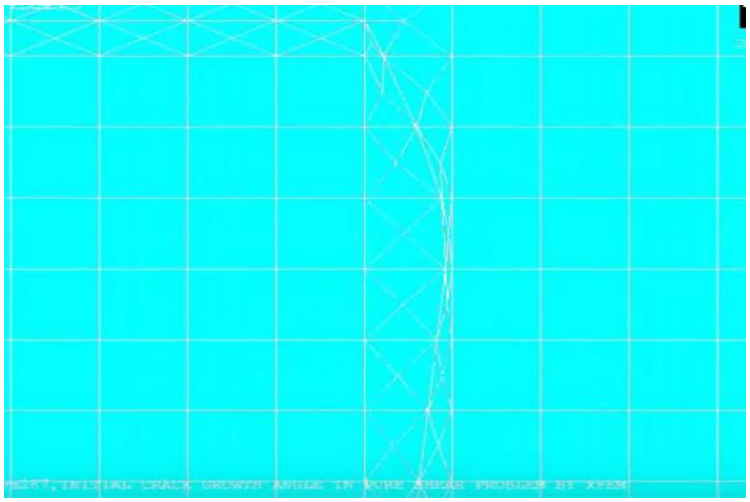

Figure 1.23: zoom inside the elements

As we notice, the initial crack is represented in white on the above part of the figure. Then the software has calculated the evolution and we can observe the new crack segments that will have some values of fi, that are the 4 distances from the nodes of an element that will be computed automatically.

We applied this method to compute the development of the crack into the system if a pre existing crack was already in the structure. Anyway some recent developments in this field have allowed to

calculate the nucleation of the fracture itself (Ernst). We remind to the bibliography to have these concepts clearer.

1.3 Peridynamics

1.3.1 Peridynamics: Basic concepts

In the next pages we will deal with an alternative technique developed in the last few years, which is called Peridynamics. We have decided to talk about this theory because there are some important points in common with the statistic theory we will develop in the next chapters.

The Peridynamics theory of Mechanics attempts to unite the mathematical modelling of continuous media, cracks and particles into a single framework. It does this by replacing the partial differential equations of the classic theory of mechanics of solid with integro-differential equations. This is a very important point for Peridynamics: in fact the derivatives appearing in these equations are not defined on the surfaces of the tips and their surfaces. These equations are based on a model of internal forces within a body in which material points interact with each other directly over finite distances. To these points we associate some cubic cells that can interact one another. In the following pages we will describe briefly the *bond based theory* taking into account the various texts and articles in the bibliography. In doing this we will consider the introduction of Matteo Garelli's thesis which offers a very clear path to the understanding of the theory.

In Peridynamics, the particles represented in cubic cells, suffer an acceleration: in particular it is possible to show (Peridynamics: Theory and its applications, Madenci) that the acceleration in the direction x at the time t is

$$\rho\ddot{\vec{u}}(\vec{x},t) = \int_{H_x} \vec{f}\left(\vec{u}(\overrightarrow{x'},t) - \vec{u}(\vec{x},t), \overrightarrow{x'} - \vec{x}\right) dV_{x'} + \vec{b}(\vec{x},t)$$

(1.37)

where

H_x is the set of points close to x

$\vec{u}$ is the displacement

$\vec{b}(\vec{x},t)$ the vector of the external forces

ρ the density of the body

$\vec{f}$ the pairwise function whose value (per unit volume to the power of 2) is equal to the force that the particle x' applies on the particle x. Obviously, it is possible to describe the relative position among the two particles in the reference configuration, by considering the Eulerian viewpoint: this is given by $\vec{\xi}$. So, indicating with $\overrightarrow{x'}$ and $\vec{x}$ the positions of the two particles with respect an origin, their relative position is

$$\vec{\xi} = \overrightarrow{x'} - \vec{x}$$

(1.38)

while we consider

$$\vec{\eta} = \overrightarrow{u'} - \vec{u}$$

(1.39)

as regards the relative displacements.

Now, a very important point in peridynamics is about the description of the physical interaction between two particles: we call this interaction *bond* and this, in a first kind of approach, can be described by an elastic spring. This concept is one of the main differences between the peridynamics and the classical theory: in fact the classical theory is based on the so called contact forces in the sense that a particle is able to act only with the particles with whom is in contact; in peridynamics instead a particle can interact with them but also with particles that are not in contact with it. However the bonds have a particular length that must be chosen a priori: a bond associated to a given particle cannot be bigger than a given length which is called *horizon* of that particle.

It is possible to show that the equations of the linear momentum and the angular momentum are respected because the forces of the bonds are equal and changed of sign and directed along a vector. This vector links in the actual position, two interacting particles.

So, if we indicate the horizon with δ, we have

$|\vec{\xi}| > \delta$ means that $\vec{f}(\vec{\eta}, \vec{\xi}) = 0 \ \forall \vec{\eta}, \vec{\xi}$

So this rule means that the particle which is located in $\vec{x}$ is not able to have interactions with particles that are beyond the horizon.

By analysing the equations of the linear and angular momentum (Peridynamics and its applications), we get two important rules that the pairwise function must satisfy:

$\vec{f}(-\vec{\eta}, -\vec{\xi}) = -\vec{f}(\vec{\eta}, \vec{\xi}) \ \forall \vec{\eta}, \vec{\xi}$ for the conservation of the linear momentum

$\vec{\xi} + \vec{\eta} \ x \ \vec{f}(-\vec{\eta}, -\vec{\xi}) = 0 \ \forall \vec{\eta}, \vec{\xi}$ for the conservation of the angular momentum

We resume all the concepts introduced in the following picture:

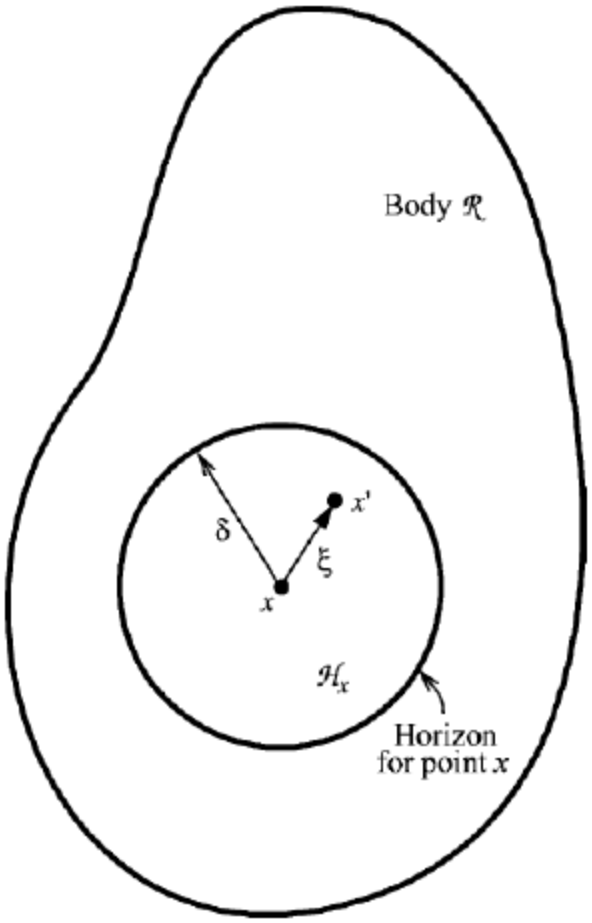

Figure 1.12: the concept of horizon in Perydynamics

We understand now the meaning of the word Peridynamics: it comes from the Greek *peri* which means “horizon”.

1.3.2 The elastic potential and fracture in Perydynamics

Now, this as regards the basic concepts; now we will introduce a potential that will be linked to the force.

A material is called *microelastic* if the pairwise force function can be derived from a scaling micropotential w:

$$\vec{f}(\vec{\eta},\vec{\xi}) = \frac{\partial w}{\partial \vec{\eta}}(\vec{\eta},\vec{\xi}) \qquad \forall \vec{\eta},\vec{\xi} \tag{1.40}$$

The micropotential is the energy of each single bond, and it is dimensionally an energy per square volume unit. The energy per unit volume is then given by the summation of all the energies of the bonds into the horizon H_x:

$$W = 1/2 \int_{H_x} w\left(\vec{\eta}, \vec{\xi}\right) dV_\xi$$

(1.41)

The factor ½ is due to the fact that the bond holds only half the bond energy. If the body is made by a microelastic material, the work carried out by the external forces is "stored" by the component and it is recoverable by modifying its shape like in the theory of classical mechanics (Theory of Elasticity). It can also be shown that the micropotential depends on the displacement $\vec{\eta}$ between the two points; however only to the scalar distance between the deformed points enters into the functional form:

$$\widetilde{w}\left(y,\ \vec{\xi}\right) = \ w\left(\vec{\eta}, \vec{\xi}\right) \qquad \forall \vec{\eta}, \vec{\xi}$$

(1.42)

where

$$y \ = \ |\vec{\eta} \ + \ \vec{\xi}\ |$$

(1.43)

If we consider equations (1.6) and (1.8) and we differentiate the second with respect $\overrightarrow{\eta}$, we get:

$$\vec{f}\left(\vec{\eta}\ , \vec{\xi}\right) = \frac{\vec{\xi} + \vec{\eta}}{|\ \vec{\xi} + \vec{\eta}\ |}\ \vec{f}\ (|\ \vec{\xi}\ + \ \vec{\eta}\ |, \vec{\xi}) \qquad \forall \vec{\xi}, \overrightarrow{\eta}$$

(1.44)

with $\vec{f}$ defined by: $\vec{f}\left(y, \vec{\xi}\right) = \frac{\partial \widetilde{w}}{\partial y}\ (y, \vec{\xi}) \qquad \forall y, \vec{\xi}$

(1.45)

This satisfies the equations (1.4) and (1.5):

$$\widetilde{w}\ (y, -\xi) = \ \widetilde{w}\ (y, \xi) \qquad \forall y, \vec{\xi}$$

(1.46)

The relationships formed by the equation (1.1) and the equation (1.9) contain the parameters we need to build a model of non-linear microelastic material with peridinamic theory.

The problem of rigid rotation is not taken into account because y is invariant with respect to body rotations.

A linearized version of the theory of microelastic materials allows us to get:

$$\vec{f}\left(\vec{\eta},\vec{\xi}\right) = C(\vec{\xi})\,\vec{\eta} \qquad \forall\vec{\eta},\vec{\xi}$$

(1.47)

where C, which is a second order tensor, is called *micro module function* of the material; this is defined as

$$C\left(\vec{\xi}\right) = \frac{\partial\vec{f}}{\partial\vec{\eta}}\left(\vec{0},\vec{\xi}\right) \qquad \forall\,\vec{\xi}$$

(1.48)

with

$$C\left(-\vec{\xi}\right) = C\left(\vec{\xi}\right) \qquad \forall\,\vec{\xi}$$

Now, if we would like to describe a spontaneous fracture, the concept of breaking limit for non-linear microelastic material should be introduced. It is assumed that $\vec{f}$ depends solely on the bond stretch, defined as:

$$s = \frac{|\vec{\xi} + \vec{\eta}| - |\vec{\xi}|}{|\vec{\xi}|} = \frac{y - |\vec{\xi}|}{|\vec{\xi}|}$$

(1.49)

With this particular kind of notation, the elongation "s" with respect to the initial configuration is positive when there is an increase in length as regards the bond, and it is negative if there is a shortening. If the material is isotropic there is no dependence on $\vec{f}$ from the direction of $\vec{\xi}$. The most direct way to introduce the concept of breaking limit is to assume that the bond (modelled as a spring) breaks if it suffers an elongation s bigger than a threshold elongation s_L. When the bond breaks, it must not return as it was before the breaking: obviously this happens because the breaking process is an irreversible one. This means that the bond must get broken for the whole simulation.

Now let us consider a Prototype Microelastic Brittle material-PMB whose pairwise function is defined as:

$$f\left(y\left(t\right),\vec{\xi}\right) = g\left(s\left(t,\vec{\xi}\right)\right)\mu\left(t,\vec{\xi}\right)$$

(1.50)

where g which is a linear function at scalar values given by

$g\,(s) = cs \quad \forall s$

(1.51)

So, we get $c = constant$ and μ a scalar function dependent on the previous history that can only assume unitary value or it can be equal to 0:

$$\mu\,(t,\vec{\xi}) \;=\; \begin{cases} 1 & if\ s\left(t',\vec{\xi}\right) < s_0 \quad \forall 0 \le t' \le t \\ 0 & in\ other\ cases \end{cases}$$

(1.52)

$\mu = 0$ means that the bond is irremediably broken and $\mu = 1$ indicates that it is integer and its length depends on the load that has been applied to it.

The critical load of the bond, s_0, is assumed constant (Figure 1-213). If the material is initially isotropic when the bonds break, the isotropic condition is lost and in the subsequent calculation step, the material is generally anisotropic.

By inserting the breaking condition into the equation of the bond material (1.16), a unique local damage condition is defined: in fact it is possible to derive a “damage equation” or “index” indicating the ratio between the number of broken bonds and the total bonds in a portion of material. The variable damage is defined as

$$\Phi\,(\vec{x},t) \;=\; 1 - \frac{\int_{H_x} \mu\,(\vec{x},t,\vec{\xi}) dV_\xi}{\int_{H_x} dV_\xi}$$

(1.53)

where $\vec{x}$ is included as the argument of μ. φ as we said before, represents the damage and its values are into the range $0 \le \varphi \le 1$. The value zero represents the state of the initial isotropic material in which all the bonds are present, while the value 1 represents the state in which the node we are considering is completely disconnected from the nodes with which it was initially connected. If the bonds are broken they no longer support any load; for this reason they create a localized material weakening; the load in fact does not vary and it is applied to the bonds that are still intact. The latter ones are now subject to an increased stress because the same load is now subdivided into a lower number of bonds. The remaining bonds are now more likely to reach the condition of breaking. A single broken bond creates the conditions for other bonds to break and this creates an avalanche effect, well visible in the simulations, allowing the fracture to advance in the body.

The two parameters that govern this mechanism from a physical viewpoint are the constant of the spring of the bond (spring constant) indicated by the letter "c" and the critical bond (critical bond stretch) indicated with "s_0". Now let us consider a homogeneous and isotropic body with constant s for each ξ and with $\vec{\eta} = s\vec{\xi}$. If we assume $\xi = |\xi|$ and $\eta = |\eta|,\ \eta = s\xi$ and by the equation of the micropotential (1.6) we get

$$f = cs \;=\; c\,\eta/\xi$$

from which

$$w \;=\; c\eta^2 \,/\, 2\xi \;=\; cs^2\xi \,/\, 2$$

and from the equation (1.7) we have:

$$W = \frac{1}{2}\int w\, dV_\xi = \frac{1}{2}\int_0^\delta \left(\frac{cs^2\xi}{2}\right) 4\,\pi\xi^2 d\xi = \frac{\pi c s^2 \delta^4}{4}$$

(1.54)

Taking into account that the strain we got is the same of the classical theory of elasticity, according to which $W = 9\,ks^2/2$, It is possible to obtain the spring spring constant for a PMB material that is:

$$c = 18\frac{k}{\pi\,\delta^4}$$

(1.55)

The critical load for breaking the bonds s_0 can be considered as a measurable amount that interacts with a flat large internal fracture surface of a sufficiently large homogeneous body. If we would like to have a complete body separation in two halves, it is necessary that the fracture surface extends between two opposite extremities of the body and that all bonds of the body nodes crossing that surface break. The work needed to break a single bond is indicated by $w_0(\vec{x})$ and is given by:

$w_0(\xi) = \int_0^{s_0} g(s)\,\xi\, ds \qquad with\ \xi = |\vec{\xi}|$

and

$d\eta = \xi\, ds$

In the case of PMB material, $w_0(\vec{\xi}) = cs_0^2\xi/2$. Thus, the work (energy) necessary to break all bonds per unit area (of the area of the fracture surface) is defined:

$$G_0 = \int_0^\delta \int_0^{2\pi} \int_z^\delta \int_0^{\cos^{-1}z/\xi} \left(\frac{cs_0^2\xi}{2}\right) \xi^2\, sen\varphi\, d\varphi\, d\xi\, d\theta\, dz$$

(1.56)

When we solve this multiple integral) and we get G_0, we are able to obtain the numerical value of the energy per unit surface (of the fracture surface) necessary to have the complete separation of the body in two halves, which is

$$G_0 = \pi\, c\, s_0^2 \frac{\delta^5}{10}$$

(1.57)

Since for PMB materials the amount of energy is measurable, from equation (1.24) it is possible to obtain G_0 for the complete separation with the assumption of absence of other dissipative mechanisms. So we get

$$s_0 = \sqrt{10\frac{G_0}{\pi\, c\, \delta^5}} = \sqrt{5\frac{G_0}{9k\delta}}$$

(1.58)

For many materials, PMB hypotheses are not so closed to the reality and it is wrong or not so accurate to consider that the conditions of the bonds are independent of the ones of other bonds. Therefore, some corrective coefficients and relationships that link bonds affected by fracture with the bond states of the rest of the body are introduced. In a micro plastic material, the bond forces become:

$$f\,(s,\xi,t) = \begin{cases} c\left(s - s\,\overline{(t)}\right) & if\ \ |\xi| \le \delta \\ 0 & in\ other\ cases \end{cases}$$

(1.59)

$$\bar{s}(0) = 0$$

$$\dot{\bar{s}} = \begin{cases} \dot{\bar{s}} & if\ \ |s - \bar{s}| \le s_Y \\ 0 & in\ other\ cases \end{cases}$$

(1.60)

At the bond level the material has elastic characteristics combined with features of perfect plasticity. At a macroscopic level the material suffers hardening and the bonds do not all slip instantly or to the same deformation.

The “micro” properties of the bonds must not be in contrast with macroscopic property. For a micro-fragile material, the bond yields are tied to the maximum engineering strength (in stress σ_{ult}) to which all bonds yield if it is reached. From (1.25) we obtain:

$$\sigma_{ult} = \int_0^{\delta}\int_0^{2\pi}\int_z^{\delta}\int_0^{cos^{-1}z/\xi} f_Y\, \xi^2\, cos\varphi\, sen\varphi\, d\varphi\, d\xi\, d\theta\, dz = \frac{\pi f_Y \delta^4}{6}$$

(1.61)

with f_Y bond yield strength

$$fy = cs_Y$$

(1.62)

The equation (1.28) is approximated as it is calculated on the undeformed geometry instead of the deformed geometry. From the equations (1.21), (1.28) and (1.29) we get the (1.30) that links the bond yielding stress with the conventional convention continuum theory:

$$s_Y \approx \frac{\sigma_{ult}}{3k}$$

(1.63)

1.3.3 Perydynamics and Central Force Model

In the last pages we described briefly two techniques used currently to consider the genesis of the fracture in a medium. The XFem is basically a numerical method and it can be considered like an extension of the FEM: as we already said it is based on the assignation of further degrees of freedom to the finite elements in order to take into account the fact that they would be able to open and to break.

Basically it is a numerical technique that solves the system of partial differential equations of the continuum mechanics and it contains a forcing in order to give us the possibility to break and to compute the fracture.

The peridynamics instead uses a different approach in the sense that it does not solve the partial differential equation system that we are normally get used to observe but it leaves from a different point of view: the body is made of different particles and each particle is able to interact only with the particles that we find within an "horizon" by a mutual micropotential. By using this assumption it is possible to get the equations of the motion for each particle: these equations are integral and so this makes possible to solve them in correspondence of the surfaces of the halves or tips. Furthermore if we represent each particle by a cubic cell, it is possible to transform the right term of the equation () in its discretized form

$$\rho\ddot{\vec{u}}(\vec{x},t) = \sum_p \vec{f}\left(\overrightarrow{u_p^n} - \overrightarrow{u_i^n}, \overrightarrow{x_p} - \overrightarrow{x_i}\right) V_p + \overrightarrow{b_i^n}$$

(1.64)

where $\vec{f}$ comes from the equation (1.9), V_p is the volume of the cubic cell representing the point p into the horizon of the point i, n is the time step while the subscript indicates the number of the node according to:

$$\overrightarrow{u_i^n} = \vec{u}(\vec{x}_i, t)$$

(1.65)

As regards the left hand term, for the calculation of the acceleration, we basically use a finite difference formula:

$$\ddot{\vec{u}}(\vec{x},t) = \ddot{\overrightarrow{u_i^n}} = \frac{\overrightarrow{u_i^{n+1}} - 2\overrightarrow{u_i^n} + \overrightarrow{u_i^{n-1}}}{\Delta t^2}$$

(1.66)

So according to this kind of discretization, we do not need to mesh the whole system and in fact this technique enters into the so called meshless methods.

We can notice however, either XFem and Peridynamics are able to consider the possibility that the material cracks but they do not contain inside into their equation the fact that the material is not "pure". As we already said at the beginning of the chapter, each material contains some impurities or local defects that create a "local" weakening. And that is the main source of breaking or fracture for each material in nature.

Our purpose in the next pages, will be to develop a theory that could take into account these defects into the material. Obviously it is not possible to know exactly where these defects are and for this reason we will be forced to consider them into our material from a statistical viewpoint.

A first way to think about the defects of a material is to introduce the concept of variability into the material itself. This can be done by introducing a probability density function according to which to get the elastic properties of the medium (like Young modulus E, Poisson's coefficient ν and Lame's coefficient G). A second way to take into account the disorder of the medium is to introduce the concept of "threshold" as the Peridynamics did for PBM. However in Peridynamics, the threshold was constant and fixed in strain to s_0. We would like to vary this threshold in order to take into account the defects of the medium that obviously can affect the "breaking limit" of a portion of material, and we would vary it according to a probability density function.

So this is our starting point. As we will see, at the beginning of the 90's, a simple mono-dimensional model called Fiber Bundle Model (FBM) was further studied to take into account the possibility to study in a very simple way the breaking of a material through thresholds in stress. This model consists in a bundle of parallel fibers clamped at one edge and free to move on the other edge.

In the next chapter we will study extensively this model from a mathematical viewpoint: we will introduce an extension of the FBM, the so called Continous Fiber Bundle Model (CFBM) that will allow us to begin to study the fracture at a bigger length scale and we will study its properties in a strain constant experiment by the Theory of the statistical ensembles. Then we will try to extend our knowledge the 2D in order to study the development of the fracture of a porous medium taking into account the disorder.

Before beginning with Chapter 2 it is important to introduce a difference between the Peridynamics and our new statistical model:

as we noted, the Peridynamics supposes the body made by "particles" and that each particle communicates with the other ones inside its own horizon. In fact in some Peridynamics simulations the system of equations given by (1.67) for each particle, is transformed into a "finite element equation system" by considering each bond like a truss with a limit breaking stretch. However the interactions we are studying from a physical viewpoint is always among the particles: this kind of point of view in fact allows us to get a meshless method and integro equations that do not create problems close to the surfaces of the cracks.

The statistical central force model instead, is son of the FBM: so as we will see in chapter 2, we will suppose to divide the material into little portions that will be described by trusses in contact only

with its neighbours depending on the geometrical form of the structure we will use to describe the continuum. There will not be a horizon; however each truss will be free to “talk” with all the trusses of our system by the occurrence of *avalanches*. This difference (i.e. to discretize the material into micro components in contact with its own neighbours with the possibility to exchange information through the occurrence of avalanches with the elements of the whole system instead of particles communicating with its neighbours inside a horizon) offers a further different point of view with respect the peridynamics. Furthermore, the possibility to take account of the disorder into the medium for the genesis of the breaking makes the technique of the statistical central force model one of the most innovative and original methods to evaluate the fracture in a medium.

Chapter 2

Thermodynamic analysis of the Fiber Bundle Model

"Who ... is not familiar with Maxwell's memoirs on his dynamical theory of gases? ... from one side enter the equations of state; from the other side, the equations of motion in a central field. Ever higher soars the chaos of formulae. Suddenly we hear, as from kettle drums, the four beats 'put n = 5.' The evil spirit v vanishes; and ... that which had seemed insuperable has been overcome as if by a stroke of magic ... One result after another follows in quick succession till at last ... we arrive at the conditions for thermal equilibrium together with expressions for the transport coefficients."

Ludwig Boltzmann

2.1 Introduction

We will provide now a brief introduction about the model which is our starting point for the building of our technique to study the fracture: the Fiber Bundle Model.

The FBM is one of the most important tools used by the scientists to study the problem of the fracture in disordered media. From an historical viewpoint this model is very ancient: its first version is dated 1927 and it is due to Peires to understand the strength of cotton yarns. Daniels in 1947 introduced for the first time the probabilistic problem inside it. And in the last two decades this problem was widely studied and extended to capture more complicated behaviours in media.

So, the development of the FBMs founded two different challenges:

a) One of the most important needs of the damage mechanics, is to realize failure models of materials that are able to introduce a detailed description of the microstructure of the material and of the local stress fields. Such model are optimal to identify the effect of the

microstructural parameters assigned to the model on the macrostructural behaviour of the system itself (emergent behaviour).
For this reason the FBMs were during the years the starting point for the study of micromechanicals models that found their application in fiber renforced composites, widely used in the aeronautical and automotive sector.

b) The damage and the fracture of disordered media is a new challenge for the statistical physics. That's why it was possible to notice that materials embedded in a disordered environment look to show phase transitions or critical phenomena like other kinds of systems like gases (in which the disorder is given by the thermal motion).

For (a) good numerical models were developed to study the behaviour of the fibrous materials towards the fracture on a big scale length. For (b) instead the FBMs give us the possibility to have a good analytical testing ground to study from a physical viewpoint the behaviour of these systems in presence of a critical point.

In the following pages we will give some snapshots to better understand the dynamics of the FBMs and we will discuss its extensions and the reasons for which it was necessary to introduce some extensions into the classical FBM.

2.2 Up to the construction of a Fiber Bundle Model

The construction of a FBM must get through different steps, that are basically the initial hypothesis necessary to build these kinds of models.

1) *Discretisation:* the solid is represented by N different fibers. Obviously these fibers are not realistic in the sense that they do not exist in the reality into the solid itself. They are only a method to discretize the structure into "micro components", in which the disorder will be introduced, as we will see. The fibers can only support *longitudinal deformation or loads.* So this model allows us to study only loadings parallel to the fibers. This is a big limitation of the FBMs that we will try to overcome by a 2D version of the FBM (the central force model)

2) *Failure law:* when a bundle is subject to an increasing external load, the fibers are assumed to have a perfectly brittle behaviour. The law that links the stress they feel to the strength is basically the Hooke's law,

$$\sigma = E\varepsilon$$

To each fiber a threshold in stress, σ_{ic} is assigned. The thresholds are picked up from a probability density function as we will see later. When the stress on a fiber reaches its strength threshold, the fiber breaks suddenly and irreversibly, so that the stress curve goes immediately to 0. Obviously the broken fibers are not restored. In the picture we can have a look to the topology of the model and to the constitutive behaviour of a single fiber

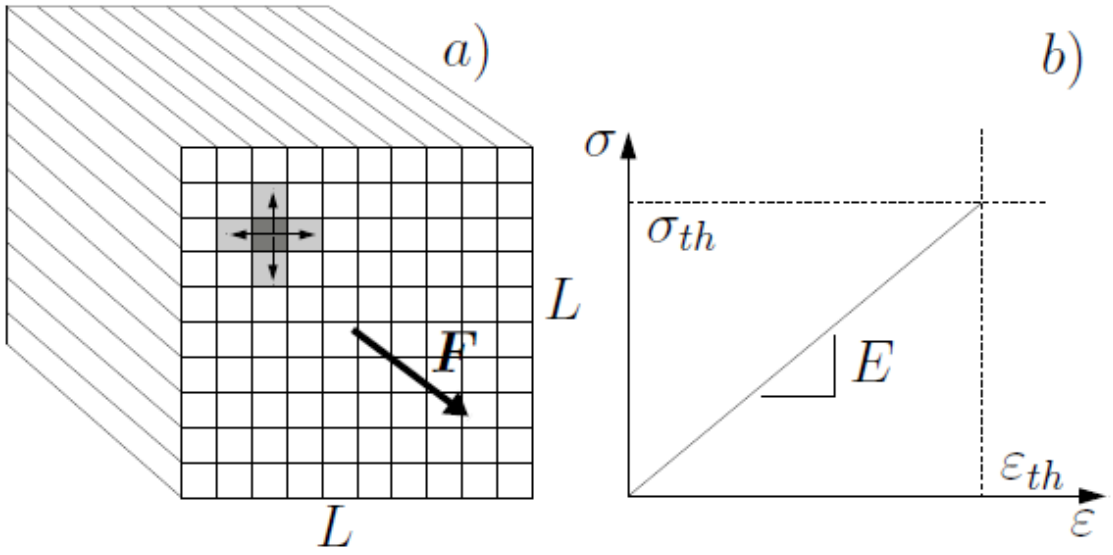

*Figure 2.1: representation of a fiber bundle model whose elements behave elastically (on the left) and constitutive elastic behaviour of the th- fiber (*Kun et al., 2007)

3) *Load sharing rule:* it's possible to perform in this model two kinds of experiments: strain or stress controlled. In the second case, because of our boundary condition, when a fiber fails, the load which was sustained by it, must be taken by the surviving fibers. This creates an avalanche behaviour as we will investigate in the following pages. However, the range or form of interaction of the fibers, which is called load sharing rule LSR, has a great importance on the micro and macro behaviour of the system. There are basically two important LSR: in the first one, called equal load sharing, the stress which was carried by one fiber is equally taken by the surviving fibers: so this load will be divided among them and the distance between a generic fiber and the failed fiber is not important. This "approximation" that introduces large distance correlation (or an approach of infinite horizon if we want to use the terminology of the Peridynamics) corresponds to a Mean Field approximation of the FBM where the topology of the bundle becomes irrelevant. Are there any real situations in which the Mean Field approach is not an approximation? The answer is yes, and we are talking about systems in which parallel fibers are loaded among perfectly rigid supports (wire cable of a lift). Except for this case, the Equal Load Sharing (LSR) is only an approximation; but it is a very important approximation because it allows to obtain some important results in closed form from an analytic viewpoint. The second LSR corresponds to more realistic physical situations: in this case the load of the broken fiber is redistributed among the closest lived fibers, which are chosen depending on the distance from the failed fiber. This leads to a stress concentration along the failed regions and so by these considerations, we can understand that the macroscopic behaviour of the model can be different by this sharing rule. However, because of non trivial spatial correlations, this model can be very complicated to study from an analytical viewpoint. Numerical simulations are necessary to catch the emergent behaviour of the bundle.

4) *Distribution of failure thresholds:* As we already said, the thresholds in stress are picked up by a probability density function (p.d.f.). In fact, assigning thresholds in stress to some kinds of fibers means from a physical viewpoint to introduce some tips or imperfections (in the way in which they were described in fracture mechanics) in discretised sub-structure of our model (the fibers). The fact that the thresholds are variable from a fiber to another one is a direct consequence of the way in which these imperfections are spread into the substructures/fibers. Which kind of p.d.f. can we use to give thresholds in stress? Basically there are two functions widely used in literature: the uniform distribution and the Weibull distribution. If we know these probability density functions that we call $p(\sigma)$, we can build a cumulative distribution according to $P(\sigma) = \int_0^\sigma p(\sigma')d\sigma'$ where σ is the stress that our fiber suffers (Abaimov).
   If we use these considerations as starting point, the FBM can also be used to understand the difference between the fracture mechanics and the damage mechanics: as we know the classical mechanics is formed by two separate disciplines: theoretical and statistical mechanics. In the same way there are two different disciplines that describe the destruction of a solid: fracture mechanics and damage mechanics; the first one is a deterministic discipline studying the behaviour of separate (a few) defects into the solid like theoretical mechanics studies the behaviour of a few degrees of freedom into a deterministic system. On the contrary, damage mechanics describes the behaviour of very many microdefects stochastically distributed into the system. For this reason the damage mechanics fits the statistical physics, studying stochastically the behaviour of many degrees of freedom, that in our case are represented by the microdefects we can find inside a solid.

5) *Time dependence:* According to the time dependence of the fiber strength, two classes of FBMs can be taken into account: in static FBMs the thresholds are constant in time during the entire history of the loading. So if we would like to model the creep rupture and fatigue behaviour of the materials, time dependent strength must be introduced. The literature is full of examples in which different modified models were introduced to take into account this behaviour. So we quote the literature for the interested reader. [7, 65, 34, 35, 42]

2.3 The Dry Fiber Bundle model

2.3.1 Strain and stress controlled experiments

We will describe now very briefly the first model of Fiber Bundle Model; the so called Dry Fiber Bundle Model (DFBM). As we already said, this has been the starting point for realizing extensions, in order to capture particular behaviours of some materials.

Basically, the DFBM is made of a set of parallel fibers (fig.2.1) clamped at one edge and free to move on the other one. The system is very simple: each fiber has the same Young Modulus and the same length.

To each fiber we assign a threshold in stress which is taken by a probability density function, typically the Weibull or the uniform distribution.

The fibers can damage only one time: this happens when the stress reaches or gets bigger than the threshold; when this situation realizes the fiber breaks.

So now, it is possible to perform two kind of experiments: the strain constant or the stress constant experiment. The behaviour of the model is different in the two cases: let's consider a FBM with a number N of fibers;

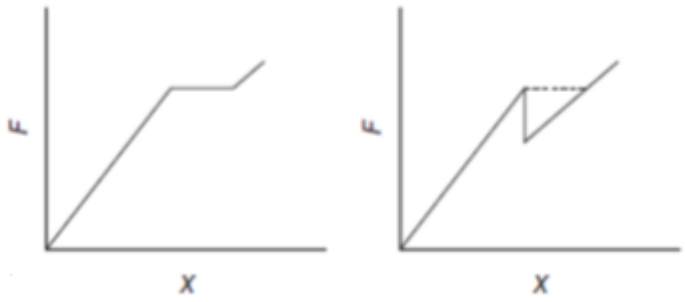

*Figure 2.2: Plot of the curve displacement vs force in a strain controlled experiment (on the left) and stress controlled experiment (on the right) (*Hansen et al, 2015)

Strain controlled experiment: in this case the avalanche behaviour does not exist. Each fiber suffers the same value of strain (this depends on the way in which the experimental apparatus is built) and the same value of stress as well (this is instead a consequence of fact that the fibers have the same Young modulus E and are able to damage only one time). So, let's suppose to perform a strain controlled experiment in which the external strain, which is our control parameter, is changed very slowly (quasi-static conditions). For a given value of strain, the fibers will suffer the same stress, $\sigma = E\varepsilon$; if we think to order the thresholds of the fibers, so that

$$\sigma_{1c} < \sigma_{2c} < \cdots < \sigma_{Nc}$$

we will meet the situation for which

$$\sigma_{i-1c} < \sigma < \sigma_{i+1c}$$

so the i-th fiber will fail; obviously the other ones will keep on taking the same load σ, but because of the failure the total stress on the bundle at that given strain will suffer a drop. That's the reason of the curve into the figure 2.2 on the left.

So if we plot the total stress as a function of the displacement we will have different infinite constitutive behaviours as shown in the figure 2.3 above, generated by the disorder. However it is possible to show that for N big, all these different curves collapse into one unique curve (Abaimov), and it is possible to notice all the plateau of the constitutive curve because we are in a strain constant experiment.

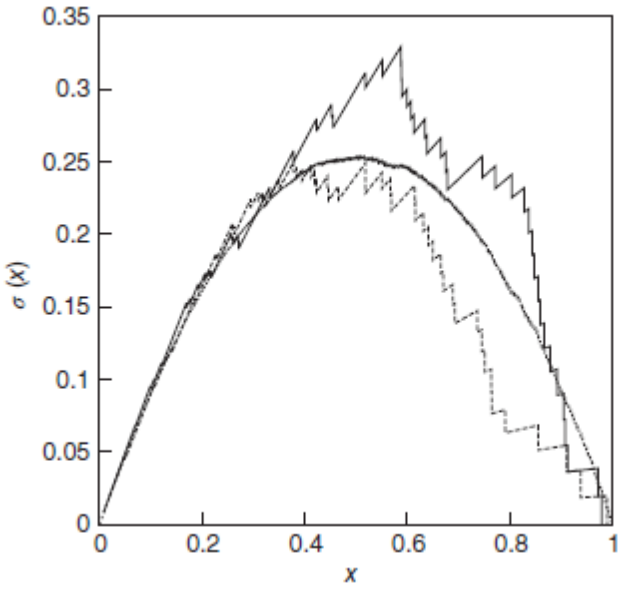

Figure 2.3: plot of the constitutive behaviour of a DFBM in a strain constant experiment; as it is possible to notice, the disorder generates infinite different constitutive behaviour but if we increase the number of fibers, these "fluctuations" go to zero and all the curve collapse into a unique curve. The three plots are obtained by numerical simulations: on the top and on the bottom we show two different realization for $N = 50$*, while in the middle* $N = 5000$*. The numerical results show that for* $N = 5000$ *two different realizations have almost the same constitutive behaviour. This was proved from a math viewpoint for the DFBM. We will prove that such a behaviour is present for the so called continuous fiber bundle model (*Hansen et al, 2015)

We will prove for the CFBM, the considerations a), b) and c) from a statistical viewpoint. In fact these conclusions will come out as results from the theory of the ensembles applied to the CFBM.

Stress controlled experiment: In this experiment the curve must be different; let's always suppose to consider a quasi static experiment, by changing in a very slow way the external force F (and so the overall stress applied on the bundle).

Again, the thresholds are ordered so that

$$\sigma_{1c} < \sigma_{2c} < \cdots < \sigma_{Nc}$$

and again, each fiber suffers the same strain (like a consequence of the experimental apparatus) and the same stress. The fact the stress is the equal for each alive fiber is true only according to a Mean Field approximation: in fact if the external stress σ_{tot} is such that for a given fiber, for example the i-th

$$\sigma_{fiber} < \sigma_{ic}$$

this one breaks.

However the external force applied on the model must remain constant (now it is the new boundary condition). From a physical viewpoint the only way to do this is that the other fibers alive take the load of the broken fibers. So the strain of these fibers grow (because we are loading them by a surplus of stress) while the external force remains constant. That's the reason for which we notice the horizontal length.

Obviously, because of the nature of the experiment we will not be able to observe anymore all the plateau of the curve but only half of it.

The same considerations about the curve force-displacement we talked about in the strain constant experiment can be applied here: i.e. the disorder generates infinite constitutive behaviour that collapse all together in a unique curve for N big (Abaimov).

2.3.2 Constitutive behaviours

We could try now to obtain the constitutive behaviour of the FBM; obviously, the curve depends on the kind of experiment we perform.

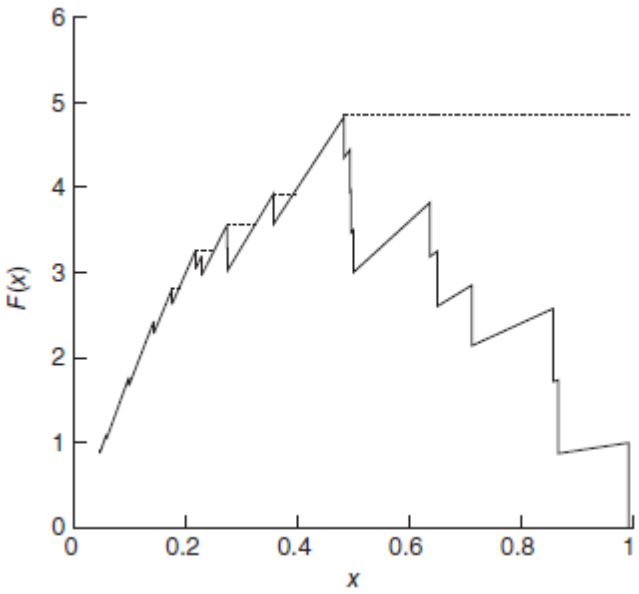

*Figure 2.4: the constitutive behaviour in the strain controlled experiment (solid curve) and the LMF function in the stress controlled experiment (*Hansen et al, 2015)

In the figure 2.4 we reported how the force on the bundle varies as a function of the strain, that in this case we call x. In a strain controlled experiment the solid curve is followed. After a fiber fails in a force controlled experiment instead, the system follows a horizontal constant force line, with increasing x until a new stable situation is reached or the whole bundle collapses. In the figure this "route" is replaced by a horizontal dashed line. So the resulting graph for the force controlled experiment, can be characterized by the least monotonic function of x that nowhere is less than the elastic function $F(x)$. The function which must be considered in a force controlled experiment is therefore

$$F_f(x) = LMF\ F(x)$$

with $LMF\ F(x) \geq F(x)$.

So, to know the constitutive curve of the bundle in a strain constant experiment allows us to get the same curve in a force constant experiment by the least function.

The same considerations can be applied for the CFBM we will introduce later. What we will talk now is the so called avalanche behaviour, which is a very interesting property of the DFBM. We will give some snapshots about the theory of Hemmer and Hansen in the case of a global load sharing.

2.3.3 Avalanche behaviour in DFBM

To achieve the avalanche behaviour from an analytical viewpoint is very complicated. This can be done however for a simple mono dimensional system like the FBM; so we briefly report the calculations realized by the two authors, Hemmer and Hensen.

Again, let us consider fiber characterized by a length l and let us assign them a threshold in stress that we call t_i. The FBM is a very simple model as we already discussed: when a fiber reaches its own threshold in stress, it breaks. So the force response for one fiber will be:

$$f_i = \begin{cases} kx & if \quad kx < t_i \\ 0 & if \; kx \geq t_i \end{cases}$$

(2.1)

Here k is the elastic constant of each fiber and t_i the threshold value in stress, which is picked up by a p.d.f $p(t)$ associated to a cumulative probability $P(t)$, defined like

$$prob\ (t_i < t) = P(t) = \int_0^f p(u)du$$

(2.2)

Since the elastic constant is the same for each fiber, we can fix the thresholds in strain as well. Nothing changes in this case. Let us call x_k the ordered sequence of failure thresholds in strain (they would be the thresholds in displacements supposing that $k = 1$), so that

$$x_1 < x_2 < \cdots . < x_N$$

where N is the total number of fibers. The external load F on the whole bundle in the point in which the k-th fiber is about to fail, can then be expressed as

$$F_k = k\ (N + 1 - K)x$$

(2.3)

where we add the number one because $K - 1$ fibers already failed and the $K - th$ is going to fail. It is important to do an observation before going ahead: we note that the sequence $\{F_k\}$ of forces on the bundle cannot be like a monotonic function because it is the product of a monotonically increasing function x_k and a monotonically decreasing factor $(N + 1 - K)$. This will be the force expressed by the bundle, which is different from the external force. Obviously at the equilibrium

the two forces must be the same, like the equilibrium between internal and external forces in structural mechanics. Now we have all the ingredients. For a burst of dimension Δ begins when the k-th fiber is going to fail, two conditions must be satisfied; the first one is the so called forward condition for which

$$F_{k+j} < F_k \quad \text{for } j = 1,2,3, \dots, \Delta - 1$$

(2.4 a)

$$F_{k+\Delta} > F_k$$

(2.4 b)

that represents the *attempt* of the bundle in reaching the equilibrium with an external force, whose value is exactly F_k: in fact as it is possible to notice from (2.4 a), the force F_{k+j} on the left is always less than F_k for $j = 1,2,3, \dots, \Delta - 1$; so after the failure of the first fiber, that represents our trigger, other $\Delta - 1$ fibers will fail in the attempt of reaching the equilibrium with the external force, represented by the right term of the (2.4 a). After these failures, if 2.4 b is satisfied, then the external force is less than the internal force the bundle can express: this guarantees mechanical equilibrium at an external force equal to F_k, even if this mechanical equilibrium is paid at the price of to get Δ fibers to fail. This is the physical meaning of the forward condition.

This is not sufficient however. We must ensure that F_k exceeds the previous values so that

$$F_j < F_k$$

(2.5)

which may be called the backward condition. Otherwise the burst may occur *inside* a larger burst and consequently it will not be recorded in experiments with increasing external load.
These two conditions can be translated as conditions on the threshold values x_k. So, from the Eq (2.3),

$$F_{k+j} >< F_k$$

(2.6)

is equivalent to

$$x_{k+j} >< x_k \frac{N+1-K}{N+1-K-j} = x_k[1 + \frac{j}{N+1-K-j}]$$

(2.7)

So, with

$$\delta_k = \frac{x_k}{N+1-K-j} \sim \frac{x_k}{N-K}$$

(2.8)

Assuming that $j \ll N - K$.
So we transformed the equation

$$F_{k+j} >< F_k$$

(2.9)

in

$$x_{k+j} >< x_k + \delta_k$$

(2.10)

where $><$ indicates bigger or less than something.

Let us determine at first the probability for the forward condition, that we call $\varphi(\Delta, x_k, k)$, for a burst of length Δ starting with the $k-th$ fiber at the threshold value x_k is fulfilled. By the equation (2.10) we see that the $\Delta - 1$ threshold values $x_{k+1}, \dots, x_{k+\Delta-1}$ must fall into the interval $(x_k, x_k + (\Delta - 1)\delta_k)$ and $x_{k+\Delta}$ must be bigger than $x_k + \Delta\delta_k$. The probability for this event to occur is

$$\varphi(\Delta, x_k, k) = \binom{N-K}{\Delta-1}\left(\frac{P(x_k + (\Delta-1)\delta_k) - P(x_k)}{1 - P(x_k)}\right)^{\Delta-1}\left(\frac{1 - P(x_k + \Delta\delta_k)}{1 - P(x_k)}\right)^{N-K-\Delta-1}$$

(2.11)

Here, we suppose that $\Delta \ll N - k$, so we can expand $\Delta\delta_k$. To the first order, we have

$$\varphi(\Delta, x_k, k) = \binom{N-K}{\Delta-1}\left(\frac{p(x_k)(\Delta-1)\delta_k)}{1 - P(x_k)}\right)^{\Delta-1}\left(1 - \frac{p(x_k)\Delta\delta_k}{1 - P(x_k)}\right)^{N-K-\Delta-1}$$

(2.12)

The last factor of (2.12) for large $N - K$ is basically

$$exp\ (-\Delta x_k p(x_k)\ \ /1 - P(x_k)\ )$$

(2.13)

using $\delta_k = \frac{x_k}{N-K}$.

Then another useful approximation regards the binomial coefficient:

$$\binom{N-K}{\Delta-1} \sim \frac{(N-K)^{\Delta-1}}{(\Delta-1)!}$$

(2.14)

So in the end, the (2.12) becomes

$$\varphi(\Delta, x_k, k) = \frac{1}{(\Delta-1)!}\left(\frac{p(x_k)x_k(\Delta-1)}{1-P(x_k)}\right)^{\Delta-1} exp\ (-\Delta x_k p(x_k)\ \ /1-P(x_k)\ )$$

(2.15)

It remains to secure that all the $\Delta-1$ inequalities (2.4 a) are fulfilled, i.e., that $x_{k+1} < x_k + \delta_k < x_k + 2\delta_k$, etc., given that all the $\Delta-1$ threshold values fall in the interval $(x_k, x_k + (\Delta-1)\delta_k)$. Since the probability density can be considered constant in the small interval $(\Delta-1)\delta_k$, this is equivalent to the following combinatorial problem: $\Delta-1$ elements are to be randomly distributed among $\Delta-1$ numbered slots, and we require the probability $\epsilon_{\Delta-1}$ that the first slot contains at least one element, the two first slots contain at least two elements, and so on. It is possible to show that

$$\epsilon_{\Delta-1} = \frac{\Delta^{\Delta-2}}{(\Delta-1)^{\Delta-1}}$$

(2.16)

So, our desired probability will be the product of $\tilde{\varphi}(\Delta, x_k, k)$ and $\epsilon_{\Delta-1}$:

$$\varphi(\Delta, x_k, k) = \tilde{\varphi}(\Delta, x_k, k)\epsilon_{\Delta-1} = \frac{\Delta^{\Delta-1}}{\Delta!}\left(\frac{p(x_k)x_k}{1-P(x_k)}\right)^{\Delta-1}\exp\left(-\frac{\Delta x_k p(x_k)}{1-P(x_k)}\right)$$

(2.17)

These are the calculations regarding the forward condition.

Now we are ready to compute the backward probability:
The backward condition is simply that F_k should be the largest breaking force that has appeared until the k-th fiber (threshold value x_k) fails. For an *average* force $\bar{F}(x)$ which is an increasing function of the elongation *x,* it is clear that in general it is the first few *neighbouring* force values, F_{k-1}, F_{k-2} ….that are most likely to exceed F_k due to fluctuations. Let us therefore calculate $\mathrm{X}(d, x_k, k)$, the probability that none of the values F_{k-1} , F_{k-2}, … , F_{k-d} exceed F_k, for $d \ll N$.
For the simplest case $d = 1$ we have by eq 2.17

$$\mathrm{X}(1, x_k, k) = \exp -\frac{\Delta x_k p(x_k)}{1-P(x_k)}$$

(2.18)
Since the probability that , F_{k-1} does not exceed F_k equals the probability that the forward condition for a burst of size $\Delta = 1$ to occur, is fulfilled. To determine $\mathrm{X}(d, x_k, k)$ for $d \neq 1$ we need according eq 2.10 the conditions

$$\begin{gathered} x_{k-1} < x_k - \delta_k \\ x_{k-2} < x_k - 2\delta_k \\ . \\ . \\ . \\ x_{k-d} < x_k - d\delta_k \end{gathered}$$

(2.19)

This implies that a number h not exceeding $d-1$ of threshold values may stay in the small interval $(x_k - d\delta_k, x_k - \delta_k)$ while all the $k-1-h$ remaining threshold values, below x_k must be smaller than $x_k - d\delta_k$. The probability for this event to occur is

$$\binom{k-1}{h}\left(\frac{(d-1)\delta_k p(x_k))}{P(x_k)}\right)^h\left(1-\frac{d\delta_k\, p(x_k)}{P(x_k)}\right)^{k-1-h}$$

(2.20)

Since k is of order N and $\delta_k = \frac{x_k}{N-K}$ of order $1/N$ the last factor in the formula is essentially

$$\exp(-\frac{d\delta_k p(x_k)k}{P(x_k)})$$

(2.21)

and the factorial for $k \gg h$ can be approximated to

$$\binom{k-1}{h} \sim \frac{k^h}{h!}$$

(2.22)

It remains to secure that the *h* values in the interval fulfil Eq. (2.19). This is again a combinatorial problem with *d* — 1 slots, so that at most one value should be found in the slot to the right, at most two values in the two rightmost slots, etc.
This problem can be solved, and the probability for all conditions to be fulfilled is

$$\epsilon_{h,\Delta-1} = (d-h)\frac{d^{h-1}}{(d-1)^h}$$

(2.23)
Multiplying together Eq. (2.20) and Eq. (2.23), introducing the simplifications (2.21) and (2.22), and summing over the allowed values of *h* we have

$$\mathrm{X}(d, x_k, k) = e^{-yd}\sum_{h=0}^{d-1}\frac{d-h}{h!\,d}\, yd^h$$

(2.24)

with

$$y(x_k) = \frac{x_k p(x_k)}{1-P(x_k)}$$

(2.25)
So the eq 2.24 can be written like

$$\mathrm{X}(d, x_k, k) = (1-y)e^{-yd}\sum_{h=0}^{d-1}\frac{yd^h}{h!} + e^{-yd}\frac{yd^d}{d!}$$

(2.26)

Using $y^d e^{-yd} < e^{\sim}d$, the last term on the right-hand side of Eq. (2.26) is seen to vanish when *d* increases. Furthermore, the first term approaches the value it would have had if the sum had continued to ∞, viz. $(1 - y)$. In conclusion,

$$\mathrm{X}(d, x_k, k) \to m(x_k) = 1 - \frac{x_k p(x_k)}{1 - P(x_k)}$$

(2.27)

when *d* increases. This is therefore the probability that the backward condition is fulfilled when the *k-th* fiber fails.

Now, the probability of a burst of size Δ starting at fiber *k* with tolerance value x_k is given by the product of the forward and the backward probabilities Eq. (2.17) and Eq. (2.27),

$$\frac{\Delta^{\Delta-1}}{\Delta!}\left(1 - \frac{x_k p(x_k)}{1 - P(x_k)}\right)\left(\frac{p(x_k)x_k}{1 - P(x_k)}\right)^{\Delta-1} \exp - \frac{\Delta x_k p(x_k)}{1 - P(x_k)}$$

(2.28)

Finally, we must sum over *k,* since a burst of size Δ may occur at any point before complete failure of the whole bundle. Since Eq. (2.28) depends only on x_k, we may instead integrate over the threshold values that there are using $Np(x_k)dx_k$ *k*-values in a small threshold interval dx_k .Thus,

$$\frac{D(\Delta)}{N} = \frac{\Delta^{\Delta-1}}{\Delta!}\int_0^{x_0} dx\, p(x)\left(1 - \frac{xp(x)}{1 - P(x)}\right)\left(\frac{p(x)x}{1 - P(x)}\right)^{\Delta-1} \exp - \frac{\Delta xp(x)}{1 - P(x)}$$

(2.29)

If we call the average number of fibers that break as result of the load, like

$$a = a(x) = Np(x)dx = \frac{xp(x)}{1 - P(x)}$$

(2.30)

the previous formula (2.29) can be written like

$$\frac{D(\Delta)}{N} = \frac{\Delta^{\Delta-1}}{\Delta!}\int_0^{x_0} \left[a(x)e^{-a(x)}\right]^{\Delta} a(x)^{-1}[1 - a(x)]\, p(x)dx$$

(2.31)

This function is strongly peaked at the upper limit of integration f_c, since $a(x)e^{-a(x)}$ is maximal for $a(x) = 1$. Since $a(x_0) = 1$, we have this maximum at $x = (x_0)$. So for large Δ, an expansion of the integral around (f_c) can give us the dominant contribute;
The delta-dependent factor around $a = 1$ can be write like

$$ae^{-a} = \exp\left[-a + \ln\left(1 - (1 - a)\right)\right] = exp\left[-1 - \frac{1}{2}\,(1 - a)^2\right]$$

(2.32)

followed by an expansion of $a(f)$ around f_c. So, at the linear order, this gives

$$a(x) = 1 + a'(x_0)(x - x_0)$$

(2.33)

with $a'(x_0) = \frac{2p(x_0)+x_0p'(x_0)}{f_c p(x_0)}$

Inserting these expressions into the integral and by using Stirling's approximation

$$\Delta! = \Delta^{\Delta} e^{-\Delta}\sqrt{2\pi\Delta}$$

valid for big Δ, i.e. for big avalanches, we have

$$\frac{D(\Delta)}{N} \sim (2\pi)^{-\frac{1}{2}}\Delta^{-\frac{3}{2}}p(x_0)a'(x_0)\int_0^{f_c} \mathrm{e}^{-\frac{a'(x_0)^2(x-x_0)^2\Delta}{2}}(x_0 - x)dx =$$
$$= (2\pi)^{-\frac{1}{2}}\Delta^{-\frac{5}{2}}p(x_0)a'(x_0)^{-1}\left[\mathrm{e}^{-\frac{a'(x_x)^2(x-x_0)^2\Delta}{2}}\right]_0^{x_0}$$

(2.34)

The lower limit vanishes for large Δ. So the asymptotic behavior of the avalanche size distribution is

$$\frac{D(\Delta)}{N} \sim C\Delta^{-\frac{5}{2}}$$

(2.35)

where

$$C = (2\pi)^{-\frac{1}{2}}p(x_0)a'(x_0)^{-1}\left[\mathrm{e}^{-\frac{a'(x_0)^2(x-x_0)^2\Delta}{2}}\right]_0^{x_0}$$

(2.36)

So we obtained a general result which is independent on the p.d.f we chose for our thresholds in stress. The only assumptions to do are that the p.d.f. is a continuous function and the average force $< F(f) >$ *has a single parabolic maximum.*

Here for large Δ the maximum contribution to the integral comes from the neighborhood of the upper limit, since $a(x)e^{-a(x)}$ is maximal for $x = x_0$. The expansion around the saddle point yields the asymptotic behaviour $\frac{D(\Delta)}{N} \propto \Delta^{-5/2}$.

2.4 Extensions of the Fiber Bundle Model

What we described now is the so called dry fiber bundle model; as we already said, this model has suffered different extensions about we will talk in the next pages. We will quote the paper "Extensions of Fiber Bundle Model" by Kun, Raischel, Hidalgo and Hermann to give a bigger picture about the topic.

So why are the extensions necessary? They are necessary to describe the fail behaviour of some materials, that, otherwise with the dry FBM we would not be able to describe.

A very important class of materials that can be studied by the FBM are the so called fiber reinforced composites (FRC). These materials have two basic ingredients: the fibers (made in carbon or glass) and a carrier material called matrix in which the fibers are embedded according to a certain geometry. In the last years these materials where extensively used in the automotive and aerospace sector: in fact the FRC provide a very high strength at a relatively low mass and they are able to maintain their properties in different environment conditions, for example at high temperatures or pressure. The mechanical properties of the FRC can be controlled by varying the properties of the fibers, of the matrix and of the geometrical interface between the fibers and the matrix. This a very important point for FRC: this flexibility in changing their properties makes possible the use of such materials in different fields of applications

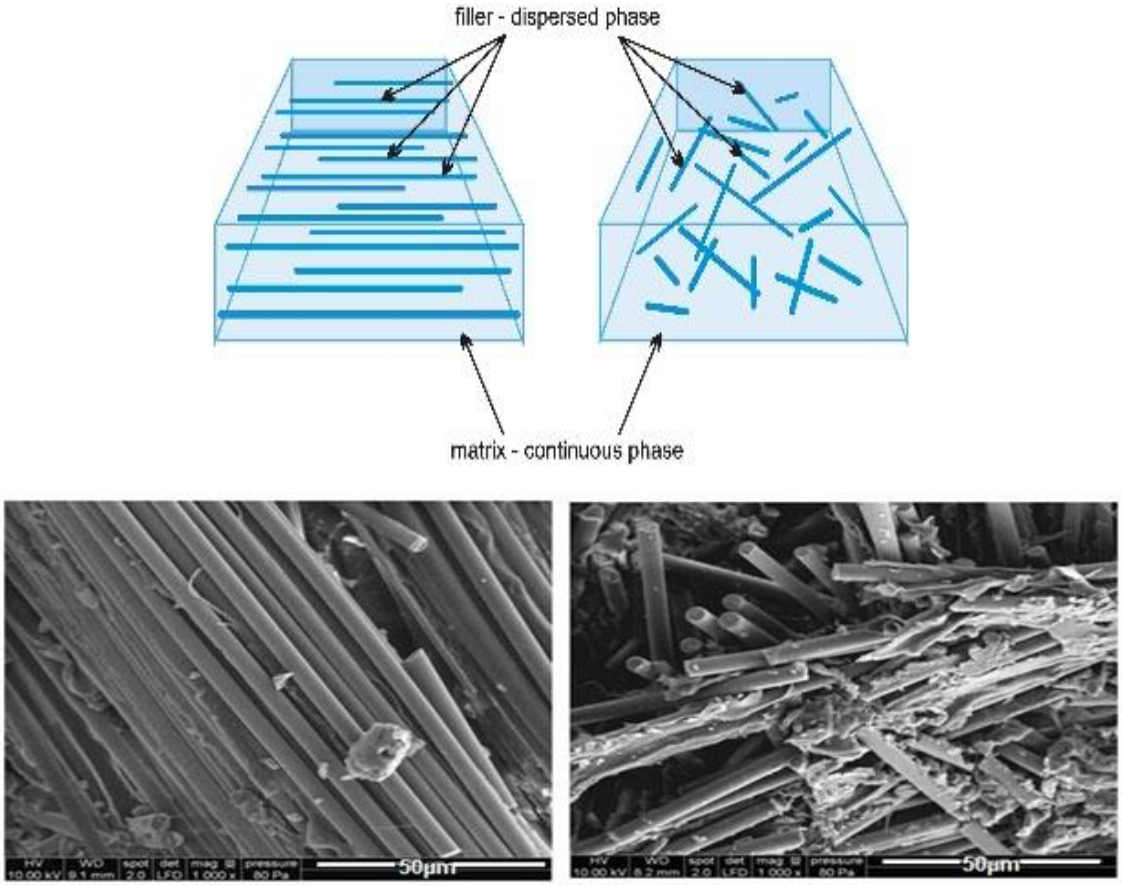

*Figure 2.5: Representation of a matrix with fibers oriented according to different directions (above) and visualization of fibers (below) at the microscope (*Kun et al*, 2007)*

The figure (2.5 a) shows the geometry of a FRC: as it is possible to notice, the fibers inside the matrix, that are in a dispersed phase, can be characterized by different geometries: they can be parallel or simply “dispersed into the matrix” with random directions. Obviously this change in orientation can modify the properties of the whole system from a structural viewpoint, that appears in the constitutive law of the FRC.

The figure (2.5 b) instead shows some carbon fibers into the matrix. In this case the fibers are ordered in an unique bundle and they are always embedded into the matrix. The characteristic length of these fibers is about 10-15 μm, as regards the diameter.

So the theoretical study of the fracture of the composites must basically undertake two important challenges:

on one hand what we would like to obtain applying these materials to construction components is the development of analytical and numerical models, able to give in output the damage history of the material by the knowledge of the micro parameters of the constituents. This is the bigger challenge that the physicists in the last years tried to solve.

On the other hand these models must recover the basic properties of the fracture in a composite that are independent on the “micro properties” of the system. So we should develop a model that should recover the basic properties of the fracture of a composite taking into account that these macroscopic properties can be dependent on the “micro properties” of the system. The importance of the these micro properties lays in the fact that by introducing them in our model and by considering their existence, it is possible to design monitoring techniques to predict the failure (we are now talking about the sound emissions from a sample that is suffering a damage; if we use the FBM we can find a direct explanations about these emissions: this is a direct consequence of the avalanche behaviour in our model in a stress controlled experiment, that depends on the thresholds assigned to the fibers in our model, that are micro properties of the systems, describing stochastically the presence of flaws or vacuums).

So let’s describe briefly the behaviour of a FRC during the fracture; in this way we will understand why the extensions are necessary.

When a FRC is subject to a load parallel to the fibers, most of the load is taken by the fibers. The matrix material and the properties of the fiber-matrix interface instead determine the interaction among the fibers (we are talking about the sharing load rule). For this reason we can already understand that the FBM represents a good tool to study the fracture into a FRC. What happens inside a FRC during the development of the damage? In the applications long fiber composites loaded parallel to the direction of the fibers often undergo a gradual degradation process; for this reason the constitutive behaviour $\sigma(\varepsilon)$ develops a plateau regime and the global failure is preceded by hardening. So this effect becomes particularly important when the bundle of the fibers inside the composite has a hierarchical organization, so that the failure of a little component can activate failures in substructures at a bigger scale length. When the fibers are embedded into the matrix material, after the breaking of a fiber, the matrix debonds in the vicinity of the crack. However because of the frictional contact at the interface the broken fiber is able to contribute to

the overall load on the structure, even if it suffered a partial damage. For this reason an extension of the dry FBM is necessary to simulate this phenomenon; in this first extension the fibers are allowed to fail prescribed numbers of time; this model is called Continuous Fiber Bundle Model (CFBM) and in the chapter we will give a further description of it by using the theory of the statistical ensembles used by Abaimov, Pride and Touissant for the dry FBM.

A second possible extension is about the time deformation: under high steady stresses, materials may undergo time dependent deformations resulting in failure called creep rupture. This complex time behaviour emerges like a consequence of the time dependent deformation of the single constituents and because of the gradual accumulation of damage.

The third extension is about the solid blocks that are often joined together by welding or gluing the interfaces, that should sustain different kinds of external loads. Interfacial failure also occurs in FRC, where the debonding of the fiber matrix interface can be the dominating mechanism of damage when the composite is sheared. So when the interface of our solid is subject to a shear, the interface elements do not suffer only longitudinal loads; for this reason this behaviour cannot be captured by the simple fiber bundle model, but a more complex model made by beams must be introduced (in the figure below)

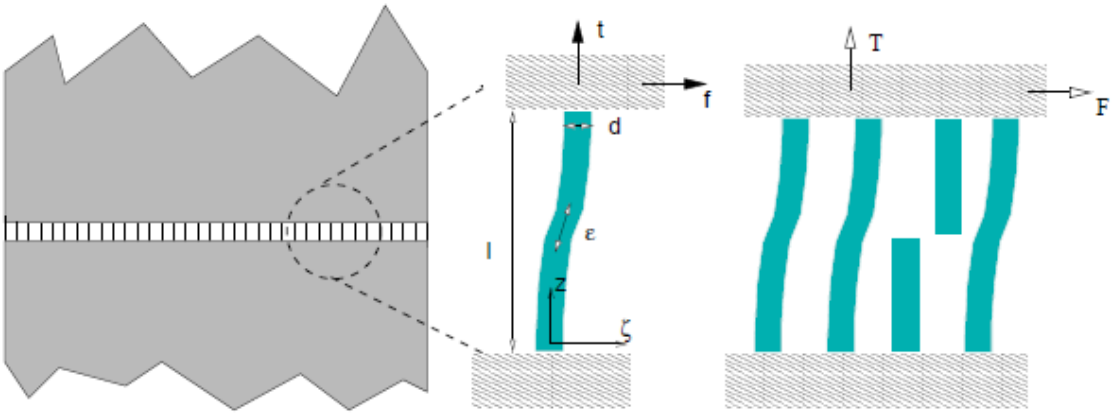

*Figure 2.6: Third extension of the DFBM (*Kun et al.*, 2007)*

The last extension is about the sharing load rule into the model; as we know, this rule plays a very important game because in the case of a stress constant experiment, it is the rule that allows us to redistribute the load on the "surviving" fibers. So in order to introduce a local distribution of the load, we must consider a stress transfer function,

$$F(r_{ij}, \gamma) = Z r_{ij}^{-\gamma}$$

where r_{ij} is the distance between the j-failed fiber and the I fiber:

$$r_{ij} = \sqrt{(x_i - x_j)^2 + (y_i - y_j)^2}$$

and Z the normalization function:

$$Z = \sum_{i \in I} \left({r_{ij}}^{-\gamma} \right)^{-1}$$

where the sum runs over the intact elements. So by doing a fine tuning of the parameter γ, it is possible to spread the load of the failed fiber among the neighbours, depending on their distance. Obviously the analytical approach is quite complicated, so numerical treatments are necessary.

So it is possible now to resume the extensions of the dry FBM in this figure:

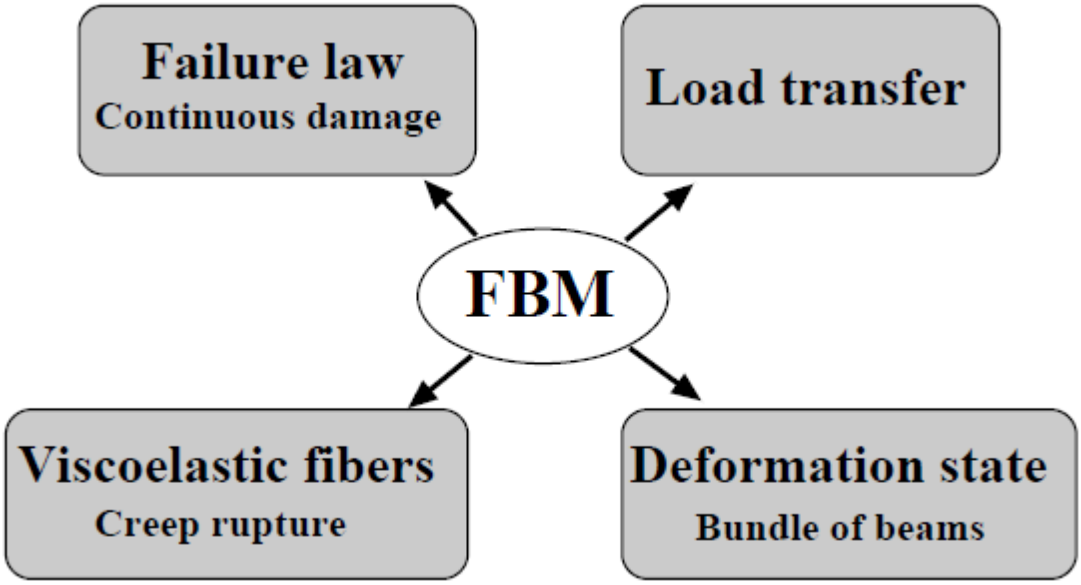

*Figure 2.7:extensions of the DFBM (*Kun et al, *2007)*

In the following pages we will study the CFBM, and we will arrive to its own constitutive behaviour in a different way with respect Kun, Hermann and Hidalgo, i.e. by applying the theory of the statistical ensembles used by Abaimov, Pride and Touissant for the dry FBM.

2.5 About the Continuous Fiber Bundle Model

2.5.1 Introduction

As we already said, we will study a modified version of our fiber bundle model: instead of considering a single fiber as broken/no broken, we will suppose that each of them could suffer different levels of damage. This extension is necessary for better studying the central force model (in which as we know, each truss can damage many times before breaking) and it's possible to use this simple model to study materials suffering a progressive damage during their load conditions like reinforced composite materials.

A collection of N fibers is considered; these N fibers are strechted between two rigid supports; one support is held fixed while the other one is free to move

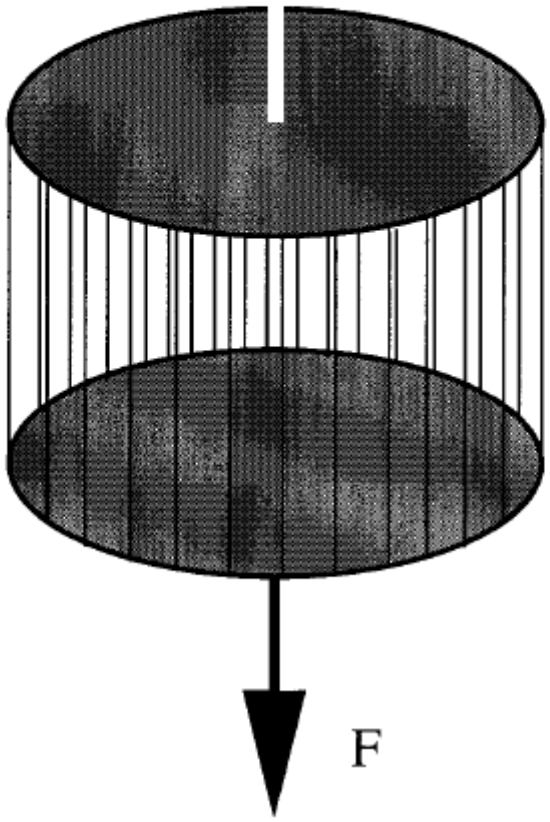

*figure 2.8: image of the experimental equipment for the fiber bundle model (*Kloster et al, *1997)*

In the figure above an external load, a force F_N is applied on the bottom. Our CFBM will be like a black box in which we only know the external load applied. By these assumptions, we are able to introduce the overall tension/stress, defined like

$$\tau = \frac{F_N}{A_f N}$$

(2.37)

where A_f is the longitudinal area of one fiber and N the total number of the fibers themselves.

It's possible to define the strain ε applied to each fiber. When $\tau = 0$, the length of each fiber is L_0. Otherwise the fibers will experiment a variation in their length going to L; so the strain is defined like

$$\varepsilon = \frac{L}{L_0} - 1$$

(2.38)

How does the model work? "The rules of the game" will be the following ones:

1) Each fiber will experiment the same strain ε . That's a consequence of the way in which is built our experimental apparatus (figure 2.8).

2) Each fiber, at the beginning, will have the same Young modulus E and different strenghts in stress $(\sigma_{1c}, \dots., \sigma_{nc})$.

These strengths are taken by a probability density function (p.d.f.) $p(\sigma)$, for which we can define a cumulative distribution $P(\sigma) = \int_0^\sigma p(\sigma)\, d\sigma$. Obviously the sthrenghts are given according to the quenched or the annealed disorder. Why do we impose a pdf over the strenghts and we do not do the same for the elastic properties? That's why the distribution of the elastic properties of individual fibers narrows down much faster with the length of the fibers than does the distribution of the strength of single fibers, since the elastic properties are like an average along the fiber while the strength is determined by its weakest point.

3) If $f_i \geq \sigma_{ic}$

where f_i is the force acting on the i-fiber and σ_{ic} its threshold, then the fiber breaks.

A fiber can break k_{max} times and every time its Young modulus is reduced by a factor a becoming $a^k E$ with $0 \leq a < 1$. A fiber with a Young Modulus equal to $a^{kmax} E$ will be considered as broken.

4) It's possible to realize two different experiments: to apply a strain ε from the external environment or a force F. In both cases, because of the structure of our experimental apparatus, the strain suffered by the fibers will be always the same (rule 1). If we perform a force controlled experiment, when a fiber suffers a damage, its Young modulus decreases and its load is taken by other fibers. This can create an avalanche behaviour that does not happen in the case of strain controlled experiment (Kun et al, 2000).

However, the important thing to notice is that, even if ε is the same for each fiber, in the case of strain or stress controlled experiment, there will be a distribution of the forces that each fiber will suffer inside the model. That's why the Young modulus of each fiber is given by $K_i = Ea^k$ and this can be different from a fiber to another one, because it depends on the history of the fiber, i.e. from how many times the fiber has damaged before arriving to suffer a given strain.

4) The quantity of fundamental importance is the probability $P_i(\varepsilon)$ that during the load of a specimen, from 0 to ε, a fiber can damage k times with $i = 0,1, \ldots, k_{max}$. We will define these probabilities in the following according to the annealed and quenched disorder. These probabilities can be built by the pdf that we introduced previously and they respect the normalization condition

$$\sum_{i=0}^{kmax} P_i = 1$$

(2.39)

So,

$$P_0(\varepsilon) = prob\ that\ at\ given\ \varepsilon\ a\ fiberis\ not\ damaged$$

$$P_1(\varepsilon) = prob\ that\ at\ given\ \varepsilon\ a\ fiber\ is\ \ damaged\ 1\ time$$

.

.

.

$$P_{kmax}(\varepsilon) = prob\ that\ at\ given\ \varepsilon\ a\ fiber\ is\ damaged\ kmax\ times$$

These probability density functions were already obtained in literature (Kun et al., 2000). So in the following we will introduce their analytical expressions; if we suppose to set the Young modulus of the fibers equal to the unity, basically there are two sets of functions $P_i(\varepsilon)$, depending on the kind of disorder we chose:

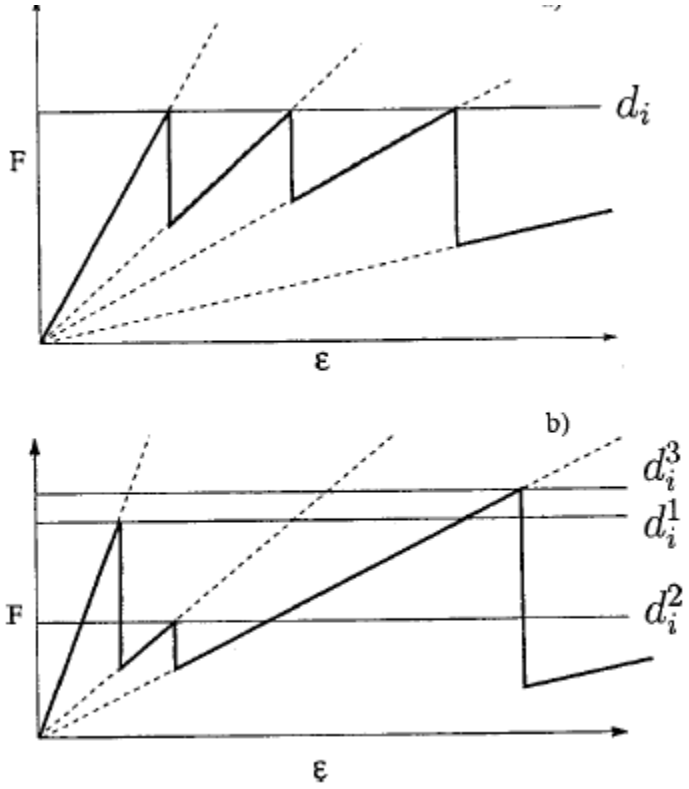

*Figure 2.9: stress strain law for the quenched (a) and annealed disorder (*Hidalgo, R. C., Kun, F. & Herrmann*, 2001)*

In the "quenched" disorder the threshold in stress is fixed during the whole life of the fiber (fig.2.9) and in the figure the threshold is called d_i. It's possible to show that the probability $P_i(\varepsilon)$ can be cast in the form:

$$P_0(\varepsilon) = 1 - P(\varepsilon)$$

and

$$P_i(\varepsilon) = P\left(a^{i-1}\varepsilon\right) - P\left(a^i\varepsilon\right) for\ i > 0$$

(2.40)

For the "annealed" disorder instead, the threshold is not fixed; if a fiber has got the possibility to fail k_{max} times, after the fail number i, a new threshold in stress from the same probability density function is chosen. From a physical wievpoint this is due to the fact that in the CFBM, a fiber represents a portion of a material (for example in the example of the composites, it can represent the carbonium fiber and a portion of the matrix around it); for this reason it is possible that after the damage, there could be like a reorganization of the structure from a mesoscopic viewpoint that can lead to a new threshold, taken obviously by the same p.d.f. This can also happen in the quenched disorder, with the difference that the new thresholds taken are so close to the previous ones that can be considered the same. So the probability functions for the annealed disorder can be written

$$P_i(\varepsilon) = \left[1 - P(a^i\varepsilon)\right] \prod_{j=0}^{i-1} P(a^j\varepsilon) \quad for\ 0 \le i \le k_{max} - 1$$

and

$$P_{kmax}(\varepsilon) = \prod_{j=0}^{kmax-1} P(a^j\varepsilon) \quad for\ i = k_{max}$$

(2.41)

5) It's important to define the variable damage D; in the simple Fiber Bundle Model, we have

$$D_{FBM} = 1 - \frac{\sum_{i=1}^{N} E_i/100MPa}{N}$$

(2.42)

where $E_i/100Mpa$ is the Young Modulus of a single truss, normalized to 1. The term $\frac{\sum_{i=1}^{N} E_i/100MPa}{N}$ in this context, could be considered like an order parameter (Vespignani, Zapperi) for our model. In fact, by defining the fraction of "alived" trusses like

$$\varphi = \frac{\sum_{i=1}^{N} E_i/100MPa}{N}$$

(2.43)

it's obvious that this parameter φ reflects the simmetry of the system between the two phases (the non broken and the broken one).

So

$$D_{FBM} = 1 - \varphi$$

(2.44)

In the DFBM, by analogy with the FBM, we could define the damage like

$$D_{DFBM\ tot} = 1 - \frac{\sum_{i=1}^{N} \frac{\sum_{j=0}^{Kmax} E_{ij}}{100MPa}}{N}$$

(2.45)

where N is always the total number of trusses in our system while $Kmax$ represents the maximum number of times for which one truss can suffer a damage. However, it makes no sense to define D_{DFBM} because for a given value of $D_{DFBM\ tot}$ we could have different combinations of simple damages into the model, i.e. D_0, D_1… D_{Kmax}, which are the fractions of fibers damaged 0 times, the fraction of fibers damaged 1 time and so on. That's why there will be different fractions of fibers characterized by a different level of damage. If we defined the damage in analogy with the FBM, i.e. like (2.45), in the summation we would lose the way in which the damage is spread into the model. For this reason, for the CFBM, it's important to redefine the damage and to consider a *"state"* of damage made by

$$D_{DFBM} = \{D_0, D_1, \ldots\ldots, D_{kmax}\}$$

(2.46)

So, the knowledge of the variable *total damage* (2.45) , does not allow us to know how the simple damages are spread into the model; while the knowledge of the simple damages,

$$\{D_0, D_1, \ldots\ldots, D_{kmax}\}$$

(2.47)

that build the state of damage (2.46) allows us to build the variable "total damage" that is the (2.45). In this way we are able to know how many terms $a^0E, a^1E, \ldots\ldots, a^{kmax}E$ there are (i.e. the Young modulus of all the fibers) and to build (2.45).

Obviously, both the single damages $D_0, D_1, \ldots\ldots, D_{kmax}$ and so, the total damage $D_{DFBM\ tot}$, are random variables and the way in which they will appear into the model for a given strain/stress, will depend on the way in which the thresholds of our fibers are spread for a given realization. This means exactly that, it's possible to choose the thresholds to assign to the fibers, picking them up from a p.d.f. So, if we perform for the first time an experiment in which we pull our sample, we will obtain a state of damage

$$D_{DFBM} = \{D_0, D_1, \ldots\ldots, D_{kmax}\}$$

(2.48)

and by knowing these fractions of fibers, we know as well how many terms $a^0E, a^1E, \ldots\ldots, a^{kmax}E$ there are.So the total damage will be

$$D_{DFBM\ tot} = 1 - \frac{\sum_{i=1}^{N} \sum_{j=0}^{Kmax} E_{ij} / 100MPa}{N}$$

(2.49)

If we perform a second time the same experiment, the thresholds given to the fibers will always belong to the same p.d.f but they will be different. And for this reason they will give us a new state of damage

$$D_{DFBM}{}' = \{D_0', D_1', \ldots\ldots, D_{kmax}'\}$$

(2.50)

and a total damage will be now different, because the fractions of fibers with $a^0E, a^1E, \ldots\ldots, a^{kmax}E$ will change:

$$D_{DFBM\ tot}{}' = 1 - \frac{\sum_{i=1}^{N} \sum_{j=0}^{Kmax} E_{ij} / 100MPa}{N}$$

(2.51)

By these considerations, we understand from a physical viewpoint that the variable "damage" is

a) A set of Fractions of fibers that are damaged $0,1, \ldots, kmax$ times

So

$$D_{DFBM} = \{D_0, D_1, \ldots\ldots, D_{kmax}\} = \{\frac{n_0}{N}, \ldots\ldots, \frac{n_{kmax}}{N}\}$$

(2.52)

b) They are random variables because their apparitions are a direct consequence of the thresholds assigned to the fibers (that are random variables themselves).

2.5.2 Microstates and macrostates

We are ready now to define the microstates and macrostates of our model. Let's suppose to perform a strain constant experiment (from this point we will be working into the ε ensemble).

The concept of microstate and macrostate arises in the way of looking to the same system in two different modes; in the first one we are looking to our system from a microscopical viewpoint; for example, for a gas, this point of wiev gives us the possibility to know the position and the velocity of the particles in each time by leaving from initial conditions; the knowledge of these "microvariables" allows us to calculate the macrovariables of the system like pressure, temperature. These macrovariables describe the system from a macroscopic viewpoint, using a bigger scale lenght. So if we leave from the knowledge of a microstate, we are able to build the macrostate of the system in each time like a b correspondence; but if we

think on the reverse, i.e., we leave from the knowledge of the macrostate and its variables, for sure different microstates will correspond to the realization of the same macrostate (for gases a given macrostate with pressure and temperature will correspond to different combinations of velocity and position of the particles). The bijective correspondence does not exist anymore. So the conclusion to which we arrive is that a macrostate can display in different microstates of the system. Of course if we think of a gas inside a box, we can understand that the number of particles it contains is huge, very close to 10^{23}. The argument used by the statistical physics to study such a system, is to imagine that an infinite number of mental copies of the same system is generated because of the uncertainty generated by thermal agitation. Obviously each mental copy of the system in this model, with its set of positions and velocities is a microstate.

Let's apply now this argument to our model.

The fact that we are assigning thresholds in stress to our fibers, creates the same kind of uncertainty we observed for a gas: for this reason, even for the FBM we can imagine that infinite mental copies of the system are generated because of the extraction of the thresholds from the probability density function. And it is obvious that at a given strain, each mental copy will have a different state of damage, depending on chosen thresholds.

What we must define now, is the concept of microstates and macrostates for the FBM. It will be easier to understand the point by analysing the model by Abaimov for FBM. In the FBM, the microstates are the configurations of intact and broken fibers. For example, if $N = 3$, all the possible kind of microstates in which the mental copies of the system fall, are

$$\{|||\}\ \{||*\}\ \{|*|\}\ \ \{*||\}\{|**\}\{*|*\}\{**|\}\ \{***\}$$

where * is for broken and | is for intact. In other words, by prescribing that each fiber is broken or alive, we make a particular microstate. As we said at first, by knowing a microstate of the system, we are able to know exactly the microscopical properties of the system itself: for a gas they were position and velocity of the particles; for our FBM, they are the knowledge of **WHICH KIND OF FIBERS ARE INTACT AND BROKEN** (the first one intact, the second one broken and so on..). By knowing one microstate of the system, we are able to know the correspondent macrostate that will be described by a macrovariable : the damage D (for gases it was the pressure or the temperature). In fact this variable D can be considered like a macrovariable because it only gives us the different fractions of broken fibers and it does not say us *which* fibers are broken or not. It's a variable that introduces the notion of damage from a bigger scale length.

So a fluctuation $\{\{D\}\}$ is a macrostate when its damage is D. For the system $N = 3,$ the three microstates $\{||*\}\ \{|*|\}\{*||\}$ define a fluctuation $D = 1/3$.

Obviously, as we said above, a macrostate can display in different microstates because the bijective correspondence does not exist anymore. We can try to count them but we cannot say a priori which of them will correspond to our macrostate like in gas happens. In a gas to a given pressure or temperature, different states of position/velocity of the particles will correspond; and we cannot say which of them is the one in which the macrostate displays.

So the damage is fixed ($D = 1/3$); to define a macrostate we are counting the possible ways in which this damage can appear,i.e. three.

The same arguments apply for CFBM; a microstate is a general configuration in which we can observe generic states of damage $\{D_0, D_1, \ldots\ldots, D_{kmax}\}$ and in which we know exactly *which* fibers are damaged $0,1,..,kmax$ times. A macrostate instead in which we observe a given damage

$$\mathcal{D} = \{D_0, D_1, \ldots\ldots, D_{kmax}\}$$

is the set of all the microstates that have a state of damage $\mathcal{D} = \{D_0, D_1, \ldots\ldots, D_{kmax}\}$ and in which the macrostate itself can displays with equal probability. It is described by the macrovariable $\mathcal{D}$ in which we lose the knowledge of which fibers are damaged. We only know the fractions of them. Even now, in order to count the microstates associated to our macrostate, we fix the state of damage $\mathcal{D}$ and the single simple damages are exchanged among the fibers (like in the example for simple FBM); let's calculate it analytically.

From a physical viewpoint, what's the probability p_D to observe a microstate? p_D is the probability to have a particular microstate in which we observe a particular state of damage $\mathcal{D} = \{D_0, D_1, \ldots\ldots, D_{kmax}\}$.

So

$$p_D = P_0^{ND_0} P_1^{ND_1} P_2^{ND_2} \ldots\ldots P_{kmax}^{ND_{kmax}}$$

where a generic $ND_i = n_i$, i.e. the number of fibers damaged i-times.

This probability p_D however, from a physical wievpoint can be written like

$$p_D = \frac{\#\ of\ mental\ copies\ of\ the\ \ system\ that\ have\ fractions\ of\ fibers\ spread\ in\ D_0, D_1.., D_{kmax}}{\#\ of\ total\ mental\ copies\ of\ the\ system}$$

In other words, we can compute the number of all copies of our system (because the disorder into the threshold generates infinite systems) and we choose only the number of systems whose thresholds, at a given ε, allow to have $\{n_0\ n_1\ \ldots\ldots n_k\}$ fibers damaged $0,1,..,kmax$ times.These two numbers are impossible to calculate but we can know their ratio; that's why we are able to compute the probability to have a configuration in which we observe $\{n_0\ n_1\ \ldots\ldots n_k\}$ fibers damaged $0,1,..,kmax$ times. From a mathematical wievpoint, the fact that we are choosing some systems into the set of all the possible mental copies of the system given by the disorder, appears in the functions $P_0\ P_1\ \ldots. P_{Kmax}$, that are built by the p.d.f. that generates the disorder itself.

So, now, we can imagine a big set in which we can insert all the mental copies of the systems (which differ one another because of their thresholds, that however are picked by the same p.d.f) and at a given ε, each system falls into different subsets in which we have different states of damage D, D', D'', D''' and so on.

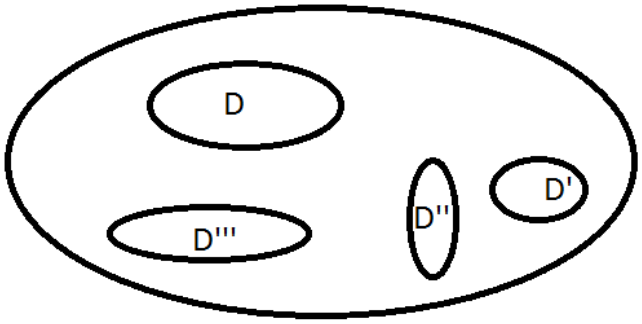

Figure 2.10: the ensemble of strain: each system drops in a subset depending on its state of damage D

Each system into a particular subset is different from the other ones into the same subset (in fact they have different thresholds but at a given strain they will have the same state of damage D). However in each D, we can have also systems that have the same damage D and in which the thresholds of the fibers are manteined and exchanged among the fibers themselves.The number of ways in which we can perform this exchange is given by the multinomial coefficient:

$$\binom{N}{n_0\, n_1 \ldots . (N - n_0 - \cdots . - n_{kmax}}$$

that gives the number of ways in which it's possible to put N objects in $kmax$ boxes, stating that n_0 are in the first one, n_1 in the second one and so on.

This means that the total fraction of systems we can find in each subset D, D', …, taking into account the exchange of the single damages among the fiber, provided by the multinomial coefficient, is the probability to have a macrostate or fluctuation $\{\{D\}\}$ or state of damage D according to the definition given above.

So the probability to have a macrostate or in general, a state of damage D is:

$$P_D = \binom{N}{n_0\, n_1 \ldots . (N - n_0 - \cdots . - n_{kmax}} P_0^{ND_0} P_1^{ND_1} P_2^{ND_2} \ldots . P_{kmax}^{ND_{kmax}}$$

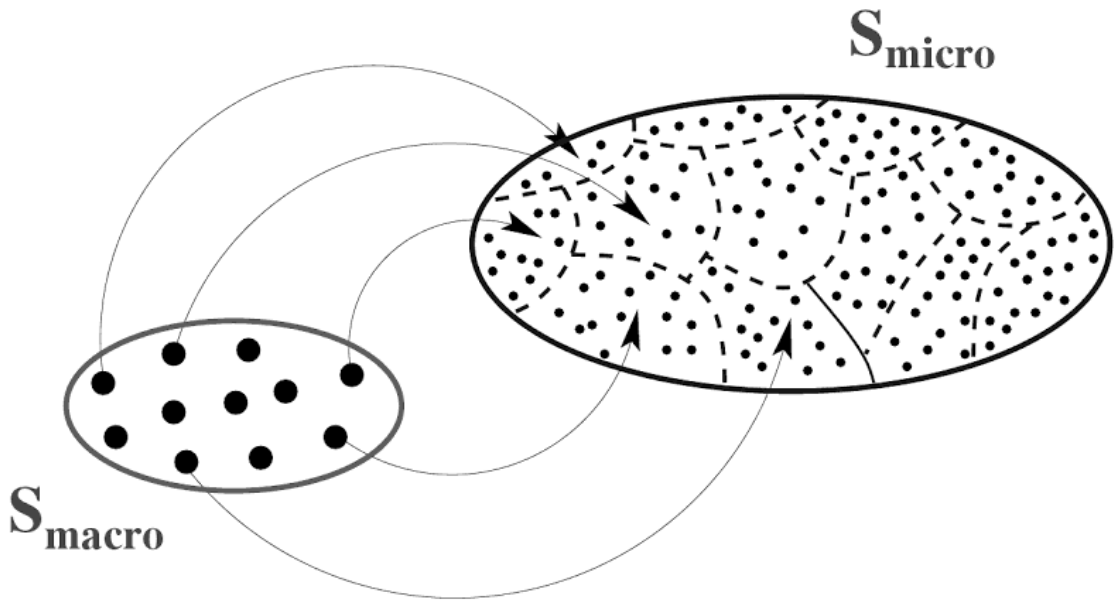

Figure 2.11: differences between microstates and macrostates

2.5.3 Thermodynamics and Entropy

We can now introduce the entropy like a Shannon's measure of the disorder:

$$S = -\sum_{D} p_D log\ p_D$$

Now let's consider the definition of entropy (the previous claim is correct for a non degenerate system): this physical quantity we introduced into the system can be considered like a measure of the disorder. It comes out like a summation over the states of damage and for this reason it is not defined only for one copy of the system; so it makes no sense to say that one mental copy of the system has got a given entropy; it is an ensemble quantity like the internal energy (as we will see). It measures the disorder (that in theory of the information is linked to the knowledge of how are deployed the mental copies of the system into the subsets of the ensemble). If it is small, we know for certain that almost all the mental copies are in a given subset of damage. For example $S = 0$ means that all the systems are into the state D in which $\frac{n_0}{N} = 1$ or into the state in which $\frac{n_{kmax}}{N} = 1$. When it is large instead, it means that a given strain the various mental copies of the system are spread into the subsets of damage of the ensemble. So, from a physical viewpoint, it is linked to the total fluctuation of the fractions of fibers and we expect to find the same point of maximum for these two physical quantities.

Basically the entropy is "an average ensemble" of the function $\log\ p_D$.

It is linked to the mean value of the probability to have one microstate with damage D (one small black point into the previous figure), i.e p_D. In this probability p_D, as we already said there is the fraction of systems with different thresholds that have this particular state of damage. However, in our system, for a given state of damage D, there exist "degenerate states", whose number is given by the multinomial coefficient, fixed the state of damage D; the probability that takes into account these degenerate states is the probability to have a macrostate and in order to perform the averages in the ensemble, we must consider it; in fact from a physical viewpoint, if we picked up from the box of the damage D some mental copies of our system, we could have, among the all possible results, two identical systems with exchanged and identical thresholds; for this reason we must consider the level of degeneracy in the ensemble averages; from a physical viewpoint the degenerate states take part to the mean values, because they can come out from our extraction.

So in the ensemble averages, the probability of a microstate p_D with whom we compute in thermodynamic the averages like

$$< A > = \sum_i p_i A_i$$

will have to take inside the corrective factor (multinomial coefficient); so

$$< A > = \sum_i P_i A_i$$

and this concept is true also for the mean value of log p_D that will be for a degenerate system like:

$$S = -\sum_D P_D log\ p_D$$

If we follow this assumption, we can obtain the same result by Pride Toiussant for the calculation of the entropy for the system broken/no broken.

So now let's apply the concept of entropy to our system.

How does this concept apply to our model? We remind that we are in the strain-ensemble. So when we move from ε to $\varepsilon + d\varepsilon$ there will be a work carried out in reversibly way by stretching the fibers plus an additional work carried out due to the irreversible fibers breakings. (Pride et al., 2002)

Let's consider for example three subsets of the ensemble, $D, D''\ and\ D'''$. In these two subsets we will find different systems at a given strain ε represented by dots. Due to the breaking or damage, some members of the subset D''' in the ensemble (in fig 4) will be led out of their current state of damage to a new state of damage at $\varepsilon + d\varepsilon$, while the ones that were previosly at ε into other subsets, will enter into the state of damage D. This "flux" of systems is represented by the arrows in the figure below.

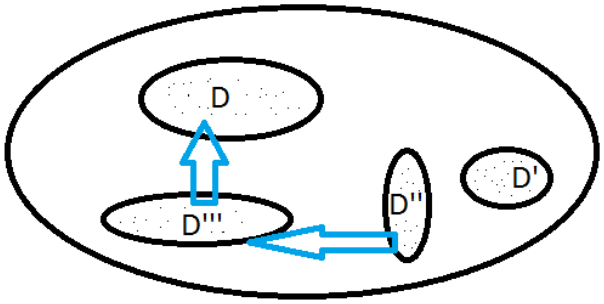

Figure 2.12: flux of the mental copies of the system because of an infinitesimal change of strain

From a mathematical viewpoint, if some systems experience a change in their state of damage in moving from ε to $\varepsilon + d\varepsilon$, the number of systems into the subests of damage D''' changes, so the fractions of systems will change as well, being like dp_D. This affects the term $p_D log\ p_D$ into the summation that defines the entropy and so the entropy itself. And the same happens for other subsets D, D'', D and so on that experience like a variation in number of their members because of the flux of system we described at first. So each term of the summation of the entropy experiences an infinitesimal change in going from ε to $\varepsilon + d\varepsilon$: however this last sentence is true for a given subset D''' only and only if at the infinitesimal change of strain there will be a variation of mental copies of the systems into the subset D'''. If yes, in fact this means some mental copies of the system have broken in changing the load condition; and it's fair that the entropy grows! If not, no systems in D''' experience a breaking and so the disorder should remain the same. So the single term $p_D log\ p_D$ does not change at all. (The other terms in the summation $p_D, log\ p'_D \quad p_{D,,} log\ p_{D''}$ etc could vary and so they however could affect the variation of the summation and so of the entropy).

It's possible to introduce the average energy density:

$$U = \sum_D P_D E_D$$

(2.53)

where E_D is the energy required to create a single state of damage D when the strain is ε. Furthermore this energy must be averaged over all the members that have been led into the state D. In fact, as it will be clearer later, the energy we need to create a single state of damage depends on the strenghts of the particular mental copy of the system. So it's possible to find different systems into a a state of damage D (everyone of them with different thresholds): at a given ε they all will have the same damage D. But by having different thresholds, the energy required to make them arrive at this damage D at this strain ε, can be different! We will need to perform an average over the thresholds to sustain that each element into the subset (that have the same damage D) will require the same energy E_D to be created.

Now if we move from ε to $\varepsilon + d\varepsilon$, the internal energy changes like:

$$dU = \sum_D E_D dP_D + \sum_D P_D dE_D$$

(2.54)

Here, the first term is the energy we use to change the disorder. So, let us look at the figure (2.12)

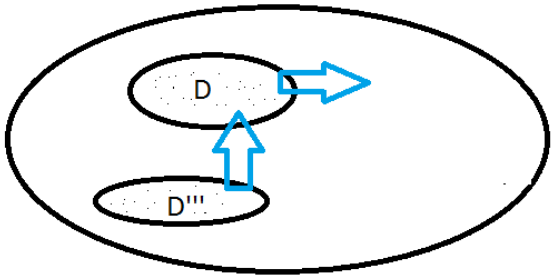

if we always consider the state of damage D, we are putting out some systems and introducing other systems into the set D (that thanks to our average became the set E_D as well). It means that some systems are breaking or damaging; in fact we can observe an infinitesimal variation of the fraction of systems dP_D.

Because of this breaking, we should observe a change infinitesimal in the disorder and so in entropy. So it's fair to assume that

$$TdS \equiv \sum_D E_D dP_D$$

(2.55)

What about the second term? Each p_D is fixed here; only E_D changes; so it means that we are increasing the energy of each system without damaging it but only by stretching it. So

$$fd\varepsilon \equiv \sum_D P_D dE_D$$

(2.56)

Be careful in Eq. (2.56), we have also the irreversible changes due to the breakings that do not change the occupation numbers P_D (Pride et al., 2002); for example, by increasing E_D, it will be possible that n systems will go out from the subset D and n systems will enter to D, so that P_D remains constant.

NB: We have to notice that it's correct to use P_D instead of p_D in describing the flux of the mental copies of the system; Obviosly if one mental copy of the system suffers a change in damage, its degenerate states (which are identical from a physical wievpoint) will do; so it's correct to find dP_D into (2.55) and (2.56).

The proportional constants are defined like:

$$T = \left(\frac{\partial U}{\partial S}\right)_{\varepsilon}$$

(2.57)

$$f = \left(\frac{\partial U}{\partial \varepsilon}\right)_{S}$$

(2.58)

That's why $U = U(S, \varepsilon)$.

So in the end, we obtain

$$dU = TdS + fd\varepsilon$$

(2.59)

What can we say about dU? We know that this term here is the average elastic energy. So on average this term here must be related to $\tau d\varepsilon$, where τ is the overall tension averaged into the ε ensemble. A purpose of us will be to compute this quantity. The overall tension τ is something different from the state function f.

For this reason, Eq. (2.59) becomes

$$(\tau - f)d\varepsilon = TdS$$

(2.60)

A positive increment in $d\varepsilon$ leads us to $dS > 0$ only if $(\tau \neq f)$. And this means that when $\tau \neq f$, some systems into our ensemble have suffered damage.

2.5.4 Hamiltonian of the system

Let's compute now the energy E_D associated to the state of damage D. As we know this is the energy required to create this state of damage and as we can imagine, this physical quantity will depend on the particular threshold we assign to the system. So as we said at first for a given state of damage D, there will be different energies associated to it, depending on the thresholds given to our fibers.

Let's try to show this from a mathematical viewpoint:

we are dealing with a system that has got n_0 fibers alived, n_1 fibers damaged one times, n_2 fibers damaged two times and so on. So the question we are addressing is: what's the energy required to create a state in which the fibers have the state of damage $\{\frac{n_0}{N}, \dots, \frac{n_{kmax}}{N}\}$?

If we suppose to apply a constant strain ε and we want to arrive to this state of damage, the total stress on the whole bundle will be:

$$\frac{F_{ext}}{NA} = E\ \varepsilon\ (\frac{n_0}{N} + .. + a^{kmax-1}\frac{n_{kmax-1}}{N})$$

(2.61)

where N is the number of fibers in the model while A, the longitudinal section of one fiber. In (2.61) we do not have the last term, i.e. $a^{kmax}\frac{n_{kmax}}{N}$, because we are supposing that the n_{kmax} fibers have failed and cannot support any load. If we liked to recover the "work hardening" behavior, we would have to insert this last term; that's why the fibers are not allowed to fail and so from a given strain applied, everyone of them will have failed k_{max} times but will be able to sustain a load. So, for the work hardening we expect to recover like an elastic behavior.We will see later.

In order to understand easy the mathematical tools we will use, let's think of the FBM for a moment. Using the work of Touissant and Pride, we have already the energy required to create a damage D, where m fibers are broken; by calling the thresholds (in strains) $\varepsilon_1\ \varepsilon_2\ \dots\ \varepsilon_n$ ordered from the smallest one to the bigger one (we know each of them), the energy will be:

$$E_D = \int_0^{\varepsilon} \tau(x)dx = \sum_{m=0}^{n} \int_{\varepsilon_m}^{\varepsilon_{m+1}} \tau_m(x)dx = \sum_{m=0}^{n} \left(1 - \frac{m}{N}\right)\left(\frac{\varepsilon_{m+1}^2}{2} - \frac{\varepsilon_m^2}{2}\right)$$

(2.62)

where obviously $\tau_m(x) = x\ (1 - \frac{m}{N})$ and $\varepsilon_{m+1} = \varepsilon$.

A direct recursion relation gives us

$$E_D = (1 - n/N)\frac{\varepsilon^2}{2} + \sum_{m=1}^{n} \frac{\varepsilon_m^2}{2N}$$

(2.63)

where we recognize in the first term the energy that can be recovered by decreasing the strain, elastically, while the second one represents the energy irreversibly lost because of the breaking process.

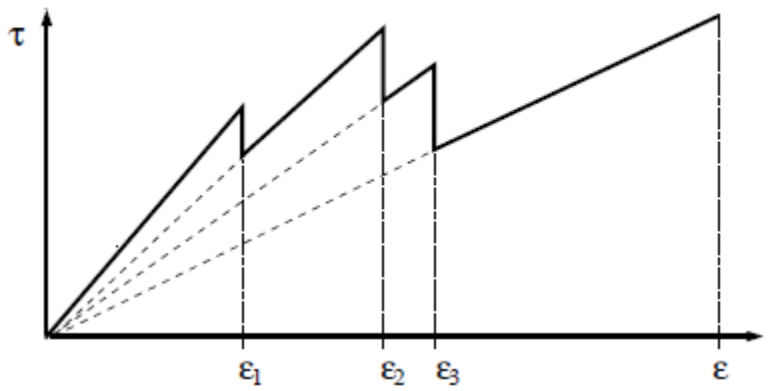

Fig 2.13: The constitutive law stress- strain for the FBM in a strain controlled experiment: the solid line is the load path followed during the experiment while the dashed one is the trajectory path the system would follow if the strain was decreased during the experiment. When a fiber breaks at a given strain, the load on the fiber must be reduced; this generates a drop into the constitutive law (Pride et al., 2002)

It's possible to recover this relation by looking at the figure 2.13, from a physical viewpoint. The thresholds are given in strain for the simple FBM (we will see later the consequences from a physical viewpoint) and are ordered. The experiment is a strain constant one; this means, as we explained in the introduction that when a threshold is reached, the constitutive behaviour has got a vertical drop. In the end we arrive to the final damage ε with three fibers broken. So in the end, the total stiffness of the system has changed from $Y(E) = E$ to $Y(E) = \frac{N-3}{N}E$. So, with this residual stifness, the system will have an energy that can be recovered from an elastic viewpoint, going back to 0 which is:

$$E_{rec} = (1 - 3/N)\frac{\varepsilon^2}{2}$$

This is the energy in the figure 2.13. However, because of the breakdown, we spent a further amount of energy, that is represented by the area 1, 2, 3. This energy was used to create the state of damage $D = 3/N$ but it cannot be recovered anymore because of the breakdown. Let's compute for example the second piece of area; let's define the area of the triangle

$$A_{i2} = \frac{\tau_2 \varepsilon_2}{2}$$

and

$$A_{f2} = \frac{\tau_2{}^* \varepsilon_2}{2}$$

where τ_2 is the value of stress into the bundle before reaching the second threshold ε_2 and $\tau_2{}^*$ its value after the drop. The amplitude of the drop is given by

$$\Delta(\tau) = \tau_2 - \tau_2^{\,*} = \left(1 - \frac{1}{N}\right)\varepsilon_2 - \left(1 - \frac{2}{N}\right)\varepsilon_2$$

So the area we need to calculate (which enters into the plastic energy that cannot be used anymore) is:

$$A_{i2} - A_{f2} = \frac{\Delta(\tau)\varepsilon_2}{2} = \frac{\varepsilon_2^2}{2N}$$

To the same result we can arrive for the first area

$$A_{i1} - A_{f1} = \frac{\Delta(\tau)\varepsilon_1}{2} = \frac{\varepsilon_1^2}{2N}$$

and for the third one; in general the summation of all these areas above the straight line that is swept by the system if we relax it, is:

$$E_{pl} = \sum_{m=1}^{n} \frac{\varepsilon_m^2}{2N}$$

This energy is summed to the elastic energy that we have already computed and that can be recovered; so the total energy to create a state of damage D is (2.63), i.e.

$$E_D = (1 - n/N)\frac{\varepsilon^2}{2} + \sum_{m=1}^{n} \frac{\varepsilon_m^2}{2N}$$

(2.64)

So, that's the energy we spend to create a microstate with damage n/N. And as it's possible to see, this energy (which is the area below the curve) depends on the disorder. In this picture it's easy to see that the state of damage we are calculating is $D = \frac{3}{N}$. From last Eq above we notice that if the three thresholds change, we always obtain a state of damage 3 but in this case the energy required to create the state changes. This is obvious by looking at the area below the curve: to change the thresholds, means to change the area below the curve and so the energy itself. So if we are interested in having one average energy to create a microstate D with damage n/N, we need to average the term depending on the thresholds over the disorder; so

$$h(\varepsilon) \equiv < \frac{\varepsilon_m^2}{2} >_{dis} = \frac{1}{P(\varepsilon)} \int_0^{\varepsilon} \frac{x^2 p(x)}{2} dx$$

where $p(x)$ is the p.d.f. and $P(\varepsilon)$ the cumulative distribution in strain.

So the Hamiltonian of the system will be like:

$$H = (1 - n_D/N)\frac{\varepsilon^2}{2} + \frac{n_D}{N}\, h(\varepsilon)$$

that will be the average work density required to create a state with damage D.

Now let's apply the same arguments to our CFBM, so the threshold in stress (fixed or variable) can be thought as associated a k_{max} thresholds in strain.

So, by this kind of picture, we can leave from the smallest one and going towards the bigger one (it's possible that two consecutive strain thresholds will belong to the same fiber. This means that in increasing the external strain by an infinitesimal quantity, the same fiber will break two consecutive times. Then it will be the turn of another one and so on. However, we can imagine that when one threshold is reached, we will see a drop into the curve of the strain constant experiment.) So let's calculate the energy which is lost (no more recovered) because of the damage of one fiber; let's consider the $m-th$ fiber and let's suppose this has reached its $i+1-th$ threshold, with $i+1<kmax$ in strain, ε_i. This means as well that our threshold has already damaged i times;

The stress before the drop will be

$$\tau_{in}=(\frac{n_o}{N}+..+a^{i-1}\frac{n_{i-1}}{N}+a^i\frac{n_i}{N}+..+a^{kmax-1}\frac{n_{kmax-1}}{N})E\varepsilon_i$$

while after the drop,

$$\tau_{fin}=(\frac{n_o}{N}+..+a^{i-1}\frac{n_i-1}{N}+a^i\frac{n_i+1}{N}+..+a^{kmax-1}\frac{n_{kmax-1}}{N})E\varepsilon_i$$

The energy lost because of the damage is:

$$A_{i2}-A_{f2}=\frac{\Delta(\tau)\varepsilon_i}{2}=\frac{\varepsilon_i^2}{2N}(a^{i-1}-a^i)$$

So this lost of energy will appear for each threshold of our fiber. This means that the total energy lost because of the breakdown of our m-th fiber is

$$\sum_{i=1}^{kmax}\frac{E\varepsilon_i^2}{2N}(a^{i-1}-a^i)$$

(2.65)

while the energy lost because of the breakdown of each fiber is

$$\sum_{n=1}^{N}\sum_{i=0}^{kmax}\frac{E\varepsilon_i^2}{2N}(a^{i-1}-a^i)$$

(2.66)

which is obviously the total elastic energy that the system has. Now,

$$\sum_{i=1}^{kmax} \frac{E\varepsilon_i^2}{2N}(a^{i-1} - a^i)$$

(2.67)

does not depend on the history of the other fibers; in fact in this equation the quantities like the equivalent Young modulus of the bundle or the fractions of the fibers into the model are not present and the reason from a math viewpoint is that this expression comes out from a difference in stresses $\frac{\Delta(\tau)\varepsilon_i}{2}$ in which all the other contributes to the Young modulus disappear. For that given external strain ε strain, we meet the $i-\ th$ threshold of the $m-\ th$ fiber which is ε_i and the $m-th$ fiber damages 1 time without affecting the other ones. If the fibers do not feel the history of the bundle we can calculate the energy lost because of the damages for a system with n_0 $n_1 \ldots . n_{kmax}$ fibers, simply by summing together the quantities

$$\sum_{n=1}^{n_r}\sum_{i=0}^{r} \frac{E\varepsilon_i^2}{2N}(a^{i-1} - a^i)$$

(2.68)

This is

$$E_{pl} = \sum_{j=1}^{n_1}\sum_{i=1}^{1} \frac{\varepsilon_{ji}^2}{2N}(a^{i-1} - a^i) + \sum_{j=1}^{n_2}\sum_{i=1}^{2} \frac{\varepsilon_{ji}^2}{2N}\left(a^{i-1} - a^i\right) + \cdots + \sum_{j=1}^{n_{kmax}}\sum_{i=1}^{kmax} \frac{\varepsilon_{ji}^2}{2N}(a^{i-1} - a^i)$$

(2.69)

This is valid in general. Now we must introduce in (2.67) the difference between quenched and annealed disorder.

a) ***Annealed disorder:*** in this situation for a fixed j-fiber, we have r different thresholds in stress:

$$\sigma_{j-cr,1}, \sigma_{j-cr,2}, \sigma_{j-cr,3}, \ldots . , \sigma_{j-cr,r}$$

So the strains in which we will observe the failures will be:

$$\varepsilon_{j1} = \frac{\sigma_{j-cr,1}}{E};\ \varepsilon_{j2} = \frac{\sigma_{j-cr,2}}{aE}; \varepsilon_{j3} = \frac{\sigma_{j-cr,3}}{a^2E}; \ldots .;\ \varepsilon_{j,r} = \frac{\sigma_{j-cr,r}}{a^{r-1}E}$$

while the plastic energy will be

$$E_{pl-r} = \sum_{j=1}^{n_r}\left(\frac{\sigma_{j-cr,1}}{E2N}(1-0) + \frac{\sigma_{j-cr,2}}{Ea2N}(a-1) + \cdots + \frac{\sigma_{j-cr,r}}{Ea^{r-1}2N}(a^{r-1} - a^r)\right)$$

Now, as we already know, these thresholds in stress are chosen by a p.d.f. independently and in sequence (only when the fiber has failed I times, the $i+1-th$ fiber is chosen (Milanese)). In the last formula we have a summation of r terms, in which the thresholds in stress appear; so this energy depends on the particular value of these thresholds. For this reason, we need to perform an average as we did for FBM to have a bijective correspondence between state of damage and energy. Let's consider one threshold, for example $\sigma_{j-cr,i}$ with $1 < i < r$. When we perform the average of this stress threshold, we must take into account all the possible values that can be taken by $\sigma_{j-cr,i}$ in all the possible "constitutive curves" of our fiber that damage r-times (the set of all the constitutive curves is the set of all the possible ways in which our fiber can damage r times). So when we take the average, we have:

$$g(a^{i-1}E\varepsilon) \equiv < \frac{\sigma_{j-cr,i}^2}{2} >_{dis} = \frac{1}{P(a^{i-1}E\varepsilon)} \int_0^{a^{i-1}E\varepsilon} \frac{x^2}{2} p(x)dx$$

in which what we know and what we control is the control parameter ε.

In taking the average, ε is fixed; the average is done between 0 (limit situation for which all the r thresholds coincide one another and are equal to 0) and $a^{i-1}E\varepsilon$(which is another limit situation in which all the stress thresholds are such that the strain thresholds coincide one another. In this case we notice a continuous drop in ε). Obviosly between 0 and $a^{i-1}E\varepsilon$ there are all the possible values that the i-threshold of the r-s, associated to the Young modulus $a^{i-1}E$ can assume among all the possible ways that our fiber has to damage itself r times. And by varying the strain between 0 and ε , we visit all these values in stress; and by dividing by $P(a^{i-1}E\varepsilon)$ we calculate the mean value among these values.

For the other values in thresholds, we apply the same concepts:

$$g(E\varepsilon) \equiv < \frac{\sigma_{j-cr,1}^2}{2} >_{dis} = \frac{1}{P(E\varepsilon)} \int_0^{E\varepsilon} \frac{x^2}{2} p(x)dx$$

$$g(aE\varepsilon) \equiv < \frac{\sigma_{j-cr,2}^2}{2} >_{dis} = \frac{1}{P(E\varepsilon)} \int_0^{aE\varepsilon} \frac{x^2}{2} p(x)dx$$

.

.

.

$$g(a^{r-1}E\varepsilon) \equiv < \frac{\sigma_{j-cr}^2}{2} >_{dis} = \frac{1}{P(E\varepsilon)} \int_0^{Ea^{r-1}\varepsilon} \frac{x^2}{2} p(x)dx$$

In this way we include all the possible values of stress threshold (and so of strain threshold) for the first, second,.., r-th failure of the fiber, chosen among all the constitutive behaviour curves, and we take the average, varying the strain among 0 and ε. This must be done for all the r-drops of our fiber, because for the quenched disorder, they are independent.

The r-th term of the plastic energy becomes:

$$E_{pl-r} = \sum_{j=1}^{n_r} \sum_{i=1}^{r} \frac{g\left(a^{i-1}E\varepsilon\right)}{NEa^{2(i-1)}}\left(a^{i-1} - a^{i}\right) = \frac{n_r}{N} \sum_{i=1}^{r} \frac{g\left(a^{i-1}E\varepsilon\right)\left(a^{i-1} - a^{i}\right)}{Ea^{2(i-1)}}$$

b) ***Quenched disorder***: let's consider the r-term of the summation

$$E_{pl-r} = \sum_{j=1}^{n_r} \sum_{i=1}^{r} \frac{E\varepsilon_{ji}^2}{2N}(a^{i-1} - a^{i})$$

Let's take for example the first fiber among the n_r; in the last expression, the energy is written as a function of the strain in which we observe the drop; in the quenched disorder the threshold in stress is fixed for each fiber; so for our first fiber among the n_r, this will be σ_{1c}; so the values of the strains in which we will have the drops, are:

$$\varepsilon_{j1} = \frac{\sigma_{j-cr,}}{E};\ \varepsilon_{j2} = \frac{\sigma_{j-cr,}}{aE}; \varepsilon_{j3} = \frac{\sigma_{j-cr,}}{a^2E}; \ldots.;\ \varepsilon_{j,r} = \frac{\sigma_{j-cr}}{a^{r-1}E}$$

So the previous expression becomes

$$E_{pl-r} = \sum_{j=1}^{n_r} \sum_{i=0}^{r} \frac{\sigma_{j-cr,1}^2}{2NEa^{2(i-1)}}(a^{i-1} - a^{i})$$

and as it's possible to notice, it depends on the values of the r-thresholds of the n_r fibers. For this reason, as it was done in the FBM, we must perform an average of $\sigma_{j-cr,1}^2$. How can we do this?

The problem we must solve is now different from the quenched because we have only one threshold in stress for our fiber, which is $\sigma_{j-cr,1}^2$. This is chosen in the beginning and it remains always the same. In order to perform a mean value, we must average $\sigma_{j-cr,1}^2$ among all the possible constitutive curves/realizations of our curve, *taking into account that the fiber can damage r times.* A priori we could realize the mean value of $\sigma_{j-cr,1}^2$ in different ways: we know in fact that $\sigma_{j-cr,1}^2$ is the threshold to which the fiber damages the first time; so we could approximate the threshold by

$$g(E\varepsilon) \equiv < \frac{\sigma_{j-cr,1}^2}{2} >_{dis} = \frac{1}{P(E\varepsilon)} \int_0^{E\varepsilon} \frac{x^2}{2} p(x)dx$$

and we could repeat the same reason for the second drop, the third drop and so on. So what number of drop in strain have we to chose to take the correct mean value of $\sigma_{j-cr,1}^2$? $g(E\varepsilon), g(aE\varepsilon), \ldots$ or $g(a^{r-1}E\varepsilon)$?

The answer is the r-th, the last one. In fact if we performed the average in the i-th drop of the constitutive curve, with $1 < i < r$, we would have this result from the average of the stress threshold

$$g(a^i E\varepsilon) \equiv < \frac{\sigma^2_{j-cr,1}}{2} >_{dis} = \frac{1}{P(a^i E\varepsilon)} \int_0^{a^i E\varepsilon} \frac{x^2}{2} p(x)dx$$

In performing the average we could say that our fiber can damage i times from 0 (limit situation in which the stress threshold is 0) to $a^i E\varepsilon$. But in this last situation, with the i-th drop coinciding in ε, the other $r-i$ strain thresholds would be bigger than the strain ε we have fixed from the external world. This is not possible and this means that we are not considering the right constitutive curves/possible ways of breaking of our fiber, that *must damage r times between 0 and* ε. This consideration leads us to conclude that the right way to take the mean value of $\sigma^2_{j-cr,1}$ is

$$g(a^{r-1} E\varepsilon) \equiv < \frac{\sigma^2_{j-cr,1}}{2} >_{dis} = \frac{1}{P(a^{r-1} E\varepsilon)} \int_0^{a^{r-1} E\varepsilon} \frac{x^2}{2} p(x)dx$$

In this way in fact we take the mean value of the stress threshold by exploring all the possible stress thresholds from 0 (limit situation) to $a^{r-1}E\varepsilon$ when the last r-th drop is recorded at our ε fixed from the external environment. Doing this, we are imposing that the fiber has damaged r-times (from a math viewpoint this appears in the integral thanks to the upper limit $a^{r-1}E\varepsilon$). And by performing the average of the stress threshold in correspondence of the last drop, we automatically set for each realization, the position of the other drops, by

$$\varepsilon_{r-1} = a\varepsilon_r;\ \varepsilon_{r-2} = a^2\varepsilon_r;\ \ \varepsilon_1 = a^{r-1}\varepsilon_r$$

that will be smaller than ε.

So the plastic energy is:

$$E_{pl-r} = \sum_{j=1}^{n_r} \sum_{i=0}^{r} \frac{g(a^{r-1}E\varepsilon)}{NEa^{2(i-1)}} \left(a^{i-1} - a^i\right) = \frac{n_r g(a^{r-1}E\varepsilon)}{N} \sum_{i=1}^{r} \frac{\left(a^{i-1} - a^i\right)}{Ea^{2(i-1)}}$$

Resuming, in general:

$$E_{pl-annealed} = \left(\frac{n_1}{N} g(E\varepsilon) \sum_{i=1}^{r=1} \frac{\left(a^{i-1} - a^i\right)}{Ea^{2(i-1)}} + \right.$$
$$+ \frac{n_2}{N} g(aE\varepsilon) \sum_{i=1}^{r=2} \frac{\left(a^{i-1} - a^i\right)}{Ea^{2(i-1)}} \ldots . + \frac{n_{kmax}}{N}\ g(a^{kmax-1}E\varepsilon) \left. \sum_{i=1}^{r=kmax} \frac{\left(a^{i-1} - a^i\right)}{Ea^{2(i-1)}} \right) =$$
$$= \left(\frac{n_1}{N}\ A_1(\varepsilon) + \frac{n_2}{N}\ A_2(\varepsilon) + \cdots + \frac{n_{kmax}}{N}\ A_{kmax}(\varepsilon) \right)$$
$$E_{pl-quenched} = \frac{n_1}{N} \sum_{i=1}^{r=1} \frac{g\left(a^{i-1}E\varepsilon\right)\left(a^{i-1} - a^i\right)}{Ea^{2(i-1)}} + \frac{n_2}{N} \sum_{i=1}^{r=2} \frac{g\left(a^{i-1}E\varepsilon\right)\left(a^{i-1} - a^i\right)}{Ea^{2(i-1)}} + \cdots$$
$$+ \frac{n_{kmax}}{N} \sum_{i=1}^{r=kmax} \frac{g\left(a^{i-1}E\varepsilon\right)\left(a^{i-1} - a^i\right)}{Ea^{2(i-1)}} =$$

$$= \left(\frac{n_1}{N}\, Q_1(\varepsilon) + \frac{n_2}{N}\, Q_2(\varepsilon) + \cdots + \frac{n_{kmax}}{N}\, Q_{kmax}(\varepsilon)\right)$$

By these two expressions, we notice that the plastic energy for the quenched disorder is smaller than the one for the annealed. In fact for the coefficients of the two formulas

$Q_i(\varepsilon) \leq A_i(\varepsilon)$ for $1 < i < kmax$.

Both the expressions recover the classical FBM if $kmax = 1$ and $a = 0$, if in this case the thresholds were given in stresses;

2.5.5 Most likely state and average state

As we said at first, the probability to have a macrostate which is also the probability to have a state of damage is:

$$P_D = \binom{N}{n_0\, n_1 \ldots . (N - n_0 - \cdots . - n_{kmax}} P_0^{n_0} P_1^{n_1} P_2^{n_2} \ldots . . P_{kmax}^{n_{kmax}}$$

A good check to verify if this is true is to try to understand if this probability satisfies the normalization condition:

$$\sum_D P_D = 1$$

(2.70)

Now, the summation over all the possible state of damage D can be realized like:

$$\sum_D P_D = \sum_{n_0=0}^{N} \sum_{n_1=0}^{N-n_0} \ldots \ldots \sum_{n_{kmax-1}=0}^{N-n_0-n_1-..-n_{kmax-2}} P_D$$

This is expression is very similar to the summations we find into the so called Multinomial Theorem according to, given $x_1, x_2 \ldots . , x_n$ variables

$$(x_1 + x_2 + .. + x_n)^N = \sum_{b_1+b_2+..+b_n=N} \binom{N}{b_1, b_2, .., b_n} \prod_{j=1}^{n} x_j^{b_j}$$

(2.71)

So we can perform the summation by using the multinomial theorem

$$\sum_{n_0}^{N}\sum_{n_1}^{N-n_0}\ldots\ldots\sum_{nk_{max-1}}^{N-n_0-n_1-..-n_{kmax-2}}\binom{N}{n_0,n_1,..,n_{kmax}}P_0^{n_0}P_1^{n_1}P_2^{n_2}\ldots..P_{kmax}^{N-n_0-n_1-..-n_{kmax-1}}$$

(2.72)

By this summation we are able to explore basically all the state of damage into the ensemble: in fact by fixing a combination of number of fibers n_0, n_1, n_2, n_3 ……(and this is done in the summations), we fix the state of damage and then we calculate the probability of that particular state, that is

$$P_D=\binom{N}{n_0,n_1,..,n_{kmax}}P_0^{n_0}P_1^{n_1}P_2^{n_2}\ldots..P_{kmax}^{N-n_0-n_1-..}$$

However, by the multinomial Theorem, it's possible to show that (2.72) is equal to:

$$(P_0+P_1+P_2+\cdots.)^N=1$$

So the normalization condition is satisfied.

Now, given P_D,which is a likelihood function, we could try to catch its maximum. In fact, P_D is a function of k_{max} variables, which are n_0, n_1, n_2, n_3 or $ND_0, ND_1, .., ND_{kmax}$. However, if we want to be more precise, this likelihood function depends on $k_{max}-1$ variables because if we know $ND_0, ND_1, .., ND_{kmax-1}$, we already know ND_{kmax} which is

$$ND_{kmax}=N-ND_0-ND_1-,..,-ND_{kmax-1}$$

So, we should reach for the values $D_o^*, D_{1,\ldots}^* D_{kmax-1,\ldots}^*$ that maximizes this probability/likelihood function.

We can perform the calculation on the variables n_0, n_1, n_2, n_3; nothing changes from D_0, D_1, D_{kmax-1} but a moltiplicative factor N.

Taking into account the last two considerations, i.e

$n_k=N-\sum_{i=0}^{k-1}n_i$ (conservation of the mass)

(2.73a)

$P_k=1-\sum_{i=0}^{k-1}P_i$ (condition of normalization on probabilities P_i)

(2.73b)

we have:

$$P_D=\binom{N}{n_0,n_1,..,(N-n_0-n_1-..-n_{kmax})}P_0^{n_0}P_1^{n_1}P_2^{n_2}\ldots..(1-P_0-..-P_{kmax-1})^{N-n_0-..-n_{kmax-1}}$$

Let's do the calculation for one variable n_i. In order to compute the derivative in an easier way, we can take the logaritm of the function P_D; this operation enables us to transform a product in summation. Indeed, because of its monotonic behavior, the maximum of the function $\log P_D$ coincides with the maximum of the function P_D. So,

$$\log P_D = \log N! - \log n_0! - \cdots - \log(N - n_0 - n_1 - \cdots - n_{k-1})! + n_0 \log P_0 + n_1 \log P_1 + \cdots + (N - n_0 - \cdots - n_{k-1}) \log(1 - P_0 - P_1 - \cdots - P_{k-1})$$

For big N, we apply the Stirling approximation for the factorial

$$N! = N \log N - N$$

retaining only the terms we need to do the derivative,

$$\cong -n_0 \log n_0 + n_0 + n_0 \log P_0 + (N - n_0 - \cdots - n_{k-1}) \log(1 - P_0 - \cdots - P_{k-1}) - (N - n_0 - \cdots - n_{k-1}) \log(N - n_0 - \cdots - n_{k-1}) + (N - n_0 - \cdots - n_{k-1})$$

So,

$$\frac{\partial \log P_D}{\partial n_0} = -\log n_0 - 1 + 1 + \log P_0 - \log(1 - P_0 - P_1 - \cdots - P_{k-1}) + \log(N - n_0 - \cdots - n_{k-1}) - (N - n_0 - \cdots - n_{k-1}) \frac{(-1)}{N - n_0 - \cdots - n_{k-1}} - 1 = 0$$

In the end, mutandis mutandum,

$$\log\left(\frac{P_0}{1 - P_0 - \cdots - P_{k-1}}\right) = \log\left(\frac{n_0}{1 - n_0 - \cdots - n_{k-1}}\right)$$

from which we have

$$\frac{P_0}{P_k} = \frac{n_0^*}{n_k^*} = \frac{n_0^*/N}{n_k^*/N}$$

In general we have:

$$\frac{P_i}{P_k} = \frac{n_i^*}{n_k^*} = \frac{n_i^*/N}{n_k^*/N}$$

for $i < kmax$.

What can we say about n_k^*?

We know that $n_i^* = n_k^* \frac{P_i}{P_k}$, ando so the various n_i^* for $i < kmax$ are fixed because they are functions of the probabilities $\frac{P_i}{P_k}$, that we already know, and of n_k^*.

So, let's try to find n_k^*; from (2.73)

$$n_o^* + \cdots + n_{kmax-1}^* = N - n_{kmax}^* = \frac{n_k^*}{P_k}\sum_{i=0}^{k-1} P_i = \frac{n_k^*}{P_k}(1 - P_k)$$

By which we have

$$\frac{n_k^*}{N} = P_k$$

This result allows us to write the previous conditions in a better way, obtaining the following equations of state:

$$\begin{cases} P_0 = n_0/N \\ P_1 = n_1/N \\ \dots = .. \end{cases}$$
$$\dots = \cdots$$
$$\begin{cases} P_{kmax-1} = n_{kmax-1}/N \\ P_{kmax} = n_{kmax}/N \end{cases}$$

So, for a given strain ε, the most likely state of damage is given by:

$D^* = \{P_0(\varepsilon), P_1(\varepsilon), \dots, P_{kmax}(\varepsilon)\}$

(2.74)

Now, let's try to find the average value of the state of damage for a given strain ε.

Let's consider for example the fraction of fibers damaged i-times $D_i \equiv \frac{n_i}{N}$.

If we liked to calculate its ensemble average for example, we would have to calculate the value of $D_1 \equiv \frac{n_1}{N}$ in each subset of the ensemble of the figure (3) and to multiply it by its probability to appear, according to the definition of mean value. So,

$$< D_1 >= \sum_D P_D D_1$$

which is

$$< D_1 > = \sum_{n_0+..+n_{k=N}} \{\binom{N}{n_0, n_1, .., (N - n_0 - n_1 - .. - n_{kmax-1})} P_0^{n_0} P_1^{n_1} .. (1 - P_0 - .. - P_{kmax-1})^{N-n_0-..-n_{kmax}-1}\} D_1$$

Now, the Multinomial theorem states that:

$(x_1 + x_2 + .. + x_n)^N = \sum_{i+j+k+..=N} C^N_{i,j,\dots}\ {x_1}^i {x_2}^j \dots {x_n}^{N-i-j-..}$

(2.75)

where we have n terms$x_1, x_2, .., x_n$, and where $i, j, k \dots \geq 0$; $C^N_{i,j,\dots} = \binom{N}{i,j,..,w)}$ is the multinomial coefficient (that gives us the number of ways in which we can put N objects in n boxes, in which we find i objects in the first box, j ones in second and so on) and

let's differentiate this equation with respect the i-term, for example the second one (if we want to compute $\frac{n_1}{N}$) and we have:

$$N(x_1 + x_2 + .. + x_n)^{N-1} = \sum_{i+j+k+\dots=N} C^N_{i,j,\dots}\ {x_1}^i j {x_2}^{j-1} \dots {x_n}^{N-i-j-..}$$

$$= \sum_{i=0}^{N} \sum_{j=0}^{N-i} \sum_{k=0}^{N-i-j} \dots C^N_{i,j,\dots}\ {x_1}^i j {x_2}^{j-1} \dots {x_n}^{N-i-j-..}$$

Let's multiply now by x_2/N:

$$x_2(x_1 + x_2 + .. + x_n)^{N-1} = \sum_{i+j+k+..=N} C^N_{i,j,\dots}\ {x_1}^i (j/N) {x_2}^j \dots {x_n}^{N-i-j-..}$$

So, if we call ${x_1}^i = {P_0}^{n_0}$, ${x_2}^j = {P_1}^{n_1}$ … , ${x_n}^{N-i-j-..} = {P_k}^{N-n_0-n_1-\dots}$,and $\frac{j}{N} = \frac{n_1}{N}$,

we have

$$P_1(P_0 + P_1 + P_2 + .. + P_k)^{N-1} = \sum_{i+j+k+..=N} C^N_{n_0 n_1 \dots}\ {P_0}^{n_0} \frac{n_1}{N} {P_1}^{n_1 - 1} \dots {P_k}^{N-n_0-n_1-..} \equiv < \frac{n_1}{N} >$$

and using the normalization condition over the probabilities $P_0 + P_1 + P_2 + .. + P_k = 1$, we have

$$P_1 = < \frac{n_1}{N} >$$

We can apply the same result to the other fractions of fibers;

So the average state of damage at the strain ε is given by

$\overline{D} = \{P_0(\varepsilon), P_1(\varepsilon), \dots, P_{kmax}(\varepsilon)\}$

(2.76)

And coincides with the most likely state of damage.

So we shown that for a given strain ε,

$$D^* = \overline{D} = \{P_0(\varepsilon), P_1(\varepsilon), \dots, P_{kmax}(\varepsilon)\}$$

(2.77)

2.5.6 Fluctuations

We have just shown that for each strain, the most likely state coincides with the average ensemble of the state of damage. But what can we say about the fluctuations? For example, if we choose a given fraction of fibers, $\frac{n_i}{N}$, how this fraction change from one subset to another one for a given strain?

To answer this question we must compute the variance of $\frac{n_i}{N}$, i.e:

$$\Delta\left(\frac{n_i}{N}\right) = \sqrt{< (\frac{n_i}{N})^2 > - < \frac{n_i}{N} >^2}$$

So, what we need now, is to compute the term $< (\frac{n_i}{N})^2 >$ and in order to do this, we use always the multinomial theorem; we know by (24) that

$$(x_0 + x_1 + .. + x_k)^N = \sum_{n_0+n_1+..=N} C^N_{n_0 n_1 \dots}\, x_0^{n_0} x_1^{n_1} \dots x_{kmax}^{n_{kmax}}$$

with $C^N_{n_0 n_1 \dots}$ the multinomial coefficient

Let's calculate the derivative with respect x_i:

$$N(x_0 + x_1 + .. + x_k)^{N-1} = \sum_{n_0+n_1+..=N} C^N_{n_0 n_1 \dots}\, x_0^{n_0} x_1^{n_1} .. n_i x_i^{n_i - 1} \dots P_{kmax}^{n_{kmax}}$$

Let's multiply by $\frac{x_i}{N}$:

$$x_i(x_0 + x_1 + .. + x_k)^{N-1} = \sum_{n_0+n_1+..=N} C^N_{n_0 n_1 \dots}\, x_0^{n_0} x_1^{n_1} .. \frac{n_i}{N} x_i^{n_i} \dots x_{kmax}^{n_{kmax}}$$

Let's calculate again the derivative $\frac{d}{dx_i}$:

$$\left(\sum_{i=0}^{kmax} x_i\right)^{N-1} + (N-1)x_i\left(\sum_{i=0}^{kmax} x_i\right)^{N-2} = \sum_{n_0+n_1+..=N} C^N_{n_0 n_1 \dots}\, x_0^{n_0} x_1^{n_1} .. \frac{{n_i}^2}{N} x_i^{n_i - 1} \dots x_{kmax}^{n_{kmax}}$$

Let's multiply again by $\frac{x_i}{N}$:

$$\frac{x_i}{N}\left(\sum_{i=0}^{kmax} x_i\right)^{N-1} + \frac{(N-1)}{N}x_i^2\left(\sum_{i=0}^{kmax} x_i\right)^{N-2} = \sum_{n_0+n_1+..=N} C^N_{n_0 n_1 \ldots}\, x_0^{n_0} x_1^{n_1} .. \frac{{n_i}^2}{N^2} x_i^{n_i-1} \ldots x_{kmax}^{n_{kmax}}$$

$$\equiv < \frac{{n_i}^2}{N^2} >$$

So again, if $x_i = P_i$ we are able to calculate $< \frac{{n_i}^2}{N^2} >$ by simply knowing the probabilities on the left; and we have, by using the normalization condition,

$$< \frac{{n_i}^2}{N^2} >= P_i^2 + \frac{P_i(1-P_i)}{N}$$

So the variance

$$\Delta\left(\frac{n_i}{N}\right) = \sqrt{< (\frac{n_i}{N})^2 > - < \frac{n_i}{N} >^2}$$

is

$$\Delta\left(\frac{n_i}{N}\right) = \sqrt{\frac{P_i(1-P_i)}{N}}$$

and this result can be applied on each fraction of fibers $\left(\frac{n_i}{N}\right)$ with $0 < i < k_{max}$.

We are able now to derive a very important result by this last equation; as we notice, the fluctuations of a given fraction of fibers damaged i times, goes to 0 with $1/\sqrt{N}$. This means that in the thermodynamic limit, for $N \longrightarrow \infty$, goes to 0.

From a physical viewpoint we can catch the following conclusion: in the ε ensemble, there is always a state of damage more likely than the other ones; this is

$$D^* = \{P_0(\varepsilon), P_1(\varepsilon), \ldots, P_{kmax}(\varepsilon)\}$$

and this state of damage coincides with the ensemble average of the state of damage

$$\overline{D} = \{P_0(\varepsilon), P_1(\varepsilon), \ldots, P_{kmax}(\varepsilon)\}$$

Indeed for $N \longrightarrow \infty$, the fluctuations around each fraction of fibers $\frac{n_i}{N}$ goes to 0 and so this particular state of damage

$$D = \{P_0(\varepsilon), P_1(\varepsilon), \ldots, P_{kmax}(\varepsilon)\}$$

is also the only one.

The claim to whom we arrive by these calculations is:

For a large number of fiber we are able to know the state of damage D with great precision.

2.5.7 Average quantities

Now we have all the tools to calculate the average quantities of our system;

Let' s begin from the overall tension; as we have already said, the overall tension is defined like:

$$\tau = \frac{F_N}{A_f N}$$

where N is the total number of fibers, A_f is the longitudinal area of one fiber while F_N is the equivalent force the whole bundle suffers because of our strain experiment.

For one single realization the overall tension τ is given by:

$$\tau = E\left(\frac{n_0}{N} + a\frac{n_1}{N} + \cdots + a^{kmax-1}\frac{n_{kmax-1}}{N}\right)\varepsilon$$

(2.78)

From a physical viewpoint (2.78) is straightforward; the CFBM, is a mono dimensional system in which the fibers are connected in parallel. So the fraction not damaged will have a Young modulus

$$E\frac{n_0}{N}$$

the fraction of fibers that have failed one time will have a Young modulus $aE\frac{n_1}{N}$

and so on till to arrive to the fraction of fibers failed $k_{max} - 1$ times, that have a Young modulus

$$a^{kmax-1}E\frac{n_{kmax-1}}{N}$$

All these fractions of fibers contribute in an equal way to the total stiffness of the bundle and obviously, if they are characterized by the same strain (strain constant experiment), they will suffer different stresses f_i. In fact, (2.78) could be written like

$$\tau = f_1 + f_2 + .. + f_{kmax-1}$$

This fact depends on the different stiffness the fibers have because of the failures.

In (2.78) we did not consider the last term:

$$a^{kmax} E \frac{n_{kmax}}{N}$$

That's why the fibers that have failed $kmax$ times are considered broken. If we added this last term into (2.78), it would mean that the fibers failed $kmax$ times can take some of the total load on the bundle. So they would not be considered as broken. Furthermore as we can imagine from a physical viewpoint, in a strain constant experiment, the system evolves from the state of damage

$$D = \{1,0,0, \dots ,0\}$$

where all the fibers are not damaged, to the final state of damage, in which

$$D = \{0,0,0, . . ,1\}$$

where $1 = \frac{n_{kmax}}{N}$ and in which all the fibers have Young modulus $a^{kmax} E$. If we do not consider them as broken, they will take the load on the structure. So, from a physical viewpoint, this means that the bundle, will experiment like a transient in which "the" state of damage change with the strain (supposing that N is large; so it's possible to talk about unique state of damage), and in which the equivalent Young modulus will be

$$Y(E) = E \left(\frac{n_0}{N} + a \frac{n_1}{N} + \cdots + a^{kmax-1} \frac{n_{kmax-1}}{N} \right)$$

(2.79 a)

After this state of transient we expect that the equivalent Young modulus is

$$Y(E) = E \left(a^{kmax} \frac{n_{kmax}}{N} \right)$$

So the bundle would have like a residual constant stiffness and we expect to recover the so called "work hardening".

So, now, let's calculate the average overall tension, in the case that the term $E \left(a^{kmax} \frac{n_{kmax}}{N} \right)$ does not exist. The ensemble average among all the overall tensions in the ensemble is:

$$< \tau > = \sum_D P_D Y(E) \varepsilon$$

This ensemble average is easy to calculate after the calculations in the previous section: so we have

$$< \tau > = E\{P_0(\varepsilon) + aP_1(\varepsilon) + \cdots + a^{kmax-1} P_{kmax-1}(\varepsilon)\} \varepsilon$$

(2.79 b)

in which we recognize as well the expectation value of the Young Modulus in the strain ensemble:

$$< Y(E) > = E\{P_0(\varepsilon) + aP_1(\varepsilon) + \cdots + a^{kmax-1}P_{kmax-1}(\varepsilon)\}$$

A question we could ask is: what about the mistake of τ?

By definition,

$$Var\ (\tau(\varepsilon)) =< \tau(\varepsilon) >^2 -< \tau(\varepsilon)^2 >$$

(2.80)

So,

$$< \tau(\varepsilon) >^2 = \left(\sum_{i=0}^{k-1} a^i E\ P_i(\varepsilon)\varepsilon\right)^2$$

and

$$< \tau(\varepsilon)^2 > = < \left(\frac{n_0}{N}\right)^2 E^2\varepsilon^2 + \cdots + \left(\frac{n_{k-1}}{N}\right)^2 a^{2(k-1)}E^2\varepsilon^2 + 2\sum_{i=0}^{k-1}\sum_{j\neq i}^{-}\left(\frac{n_i}{N}\ \frac{n_j}{N}\right)a^{i+j}E^2\varepsilon^2 >$$

A quick calculation allows us to say, by the multinomial theorem, that

$$\mathbb{E}\left[\frac{n_i}{N}\frac{n_j}{N}\right] = P_iP_j\ \frac{\mathrm{N}-1}{N}$$

and as we have already showed

$$\mathbb{E}\left[\left(\frac{n_i}{N}\right)^2\right] = P_i^2 + \frac{P_i(1-P_i)}{N}$$

where with the symbol $\mathbb{E}$ we have indicated the mean expectation value.

A very brief algebraic calculation shows that this variance (2.80), with the quantities above introduced, goes exactly to 0 for $N \to \infty$:

$$Var\ (\tau(\varepsilon)) = (E\varepsilon)^2\left\{\left(\sum_{i=0}^{k-1} a^i\ P_i(\varepsilon)\right)^2 - \sum_{i=0}^{k-1} a^{2i}\left[P_i^2 + \frac{P_i(1-P_i)}{N}\right] - 2\sum_{i=0}^{k-1}\sum_{j\neq i}^{-} a^{i+j}P_iP_j\ \frac{\mathrm{N}-1}{N}\right\}$$

For $N \to \infty$, $Var\ (\tau(\varepsilon)) \to 0$. Obviously, it is banal to say that if we consider the total tension on the bundle, $\tau(\varepsilon)' = \sum_{i=1}^{N}\tau(\varepsilon)_i$ and we consider the properties

a) $< \tau(\varepsilon)' > = < N\ \tau(\varepsilon) > = N\ < \tau(\varepsilon) >$ for the expectation value
b) $Var\ (\tau(\varepsilon)') = Var\left(N\ \tau(\varepsilon)\right) = N^2\ Var\ (\tau(\varepsilon))$ that is the theorem of the variance in which the covariances are always equal to 0 because in the strain ensemble the fibers are not correlated.

So we have for $N \to \infty$

$$< \tau(\varepsilon)' > = N\left(E\varepsilon \sum_{i=0}^{k-1} a^i P_i(\varepsilon) \right)$$

and by De l'Hopital

$$Var\ (\tau(\varepsilon)') = 0$$

The thing makes sense because we showed in the thermodynamic limit that there exists only one state of damage; so each fiber will have only one kind of damage and for this reason the mean value of each fiber will be in this limit equal with uncertainty equal to 0. And this leads us to state with absolutely precision that

$$< \tau(\varepsilon)' > = N\left(E\varepsilon \sum_{i=0}^{k-1} a^i P_i(\varepsilon) \right)$$

with a mistake equal to 0. For N different from 0 the mean value of each fiber will be always the same, $\tau(\varepsilon)$, but there will be an uncertainity associated to it. And this will affect the expectation value $< \tau(\varepsilon)' >$ because of the summation of the variances.

The effect of seeing one only state in the thermodynamic limit, from a physical viewpoint, can be thought as a function of the passage between the discrete and the continuum. In fact for $N \to \infty$ the bundle becomes a piece of material with a given Young modulus through a direction (the one of the fiber). So this material must have a unique state of damage. This is confirmed in some different damage laws obtained for the concrete (Mazars). We will see this collapse of all the possible state into a unique one in chapter 4 for the statistical central force model as well; there will be in fact a unique constitutive curve in the thermodynamic limit and so a unique state of damage.

So in the thermodynamic limit the fluctuations around $< \tau >$ previously computed go to 0 as we could expect by the results got in the previous paragraph: in fact if in the thermodynamic limit there exist only one state of damage, there must exist only one constitutive behaviour curve as well from a physical viewpoint.

In the same way we can compute the entropy of the system; the entropy is defined according to the measure of Shannon:

$$S = -\sum_{D} P_D log\ p_D \equiv < \log p_D >$$

where p_D is the probability of a single microstate; the entropy is an ensemble mean value of the logaritm of the microstates by the definition of Boltzmann.Here we can decide to define the entropy simply by defining the way in which we count the states. Following the approach of Pride and Touissant, we are interested in which fibers and not in how many fibers are damaged. This means that the definition of entropy will be given above, taking the mean value of $\log p_D$.However, the total number of microstates into a state of damage D is given by P_D; so in order to realize the ensemble average of the function $\log p_D$, we must count all the microstates in D; this means that we must multiply p_D by the multinomial coefficient and in this way we obtain

the fraction of all the possible systems with damage D. Then we multiply this term by the function $\log p_D$. And by varying D, we perform the mean value.

So we need to compute the average value of $\log p_D$.

Now, $p_D = P_0^{n_0} P_1^{n_1} \dots P_{kmax}^{n_{kmax}}$. So

$$\log p_D = n_0 \log P_0 + n_1 \log P_1 + \dots . + n_{kmax} \log P_{kmax}$$

So,

$$S = -\sum_{n_0+n_1+..=N} \binom{N}{n_0, n_1, .., (N - n_0 - n_1 - .. - n_{kmax-1})} P_0^{n_0} \dots P_{kmax}^{n_{kmax}} \sum_{i=0}^{kmax} n_i \log P_i$$

Which can be written like:

$$S = -< \log P_0 > \; - < \log P_1 > \; - \cdots - < \log P_k >$$

So this means that we have to perform $kmax$ ensemble averages. Let's take the i-term:

$$C_{n_0 n_1 \dots}^{N} \; P_0^{n_0} \; \dots \; P_{kmax}^{n_{kmax}} n_i \log P_i$$

From the multinomial theorem we have:

$$(x_0 + x_1 + .. + x_k)^N = \sum_{n_0+n_1+..=N} C_{n_0 n_1 \dots}^{N} \; x_0^{n_0} x_1^{n_1} \; x_i^{n_i} \; \dots x_{kmax}^{n_{kmax}}$$

We derive with respect x_i:

$$N(x_0 + x_1 + .. + x_k)^{N-1} = \sum_{n_0+n_1+..=N} C_{n_0 n_1 \dots}^{N} \; x_0^{n_0} x_1^{n_1} \; n_i x_i^{n_i - 1} \; \dots x_{kmax}^{n_{kmax}}$$

Let's multiply by $\log x_i$:

$$N \; \log x_i \; (x_0 + x_1 + .. + x_k)^{N-1} = \sum_{n_0+n_1+..=N} C_{n_0 n_1 \dots}^{N} \; x_0^{n_0} x_1^{n_1} \; n_i \log x_i \; x_i^{n_i - 1} \; \dots x_{kmax}^{n_{kmax}}$$

Then we multiply by x_i:

$$N \; x_i \log x_i \; (x_0 + x_1 + .. + x_k)^{N-1} = \sum_{n_0+n_1+..=N} C_{n_0 n_1 \dots}^{N} \; x_0^{n_0} x_1^{n_1} \; n_i \log x_i \; x_i^{n_i} \; \dots x_{kmax}^{n_{kmax}}$$

that gives

$$N \; x_i \log x_i = < n_i \log x_i >$$

So, as usual if we take $x_0 = P_0 \dots . . x_{kmax} = P_{kmax}$,

$$N\ P_i \log P_i = < n_i \log P_i >$$

So if in S we find the summation of all these $kmax$ terms here, we get

$$S = -N\ (\sum_{i=0}^{kmax} P_i\ (\varepsilon) \log P_i(\varepsilon))$$

What about the internal energy?

As we know, it is defined like :

$$U = \sum_D P_D E_D$$

where $E_D$is given by the mean value for each subset:

$$\overline{E_D} = \left(\frac{n_0}{N} + \cdots + a^{kmax-1}\frac{n_{kmax-1}}{N}\right)\frac{E\varepsilon^2}{2} + \frac{n_1}{N}h_1(\varepsilon) + \cdots + \frac{n_{kmax}}{N}h_{kmax}(\varepsilon)$$

Here, we have decided to indicate with $h_1(\varepsilon)$ …. $h_{kmax}(\varepsilon)$ the coefficients

$$A_1(\varepsilon), A_2(\varepsilon), \dots, A_{kmax}(\varepsilon)$$

for the annealed, and

$$Q_1(\varepsilon), Q_2(\varepsilon), \dots, Q_{kmax}(\varepsilon)$$

for the quenched.
So, it's easy now to calculate the average value:

$$U = (P_0 + \cdots + a^{kmax-1}P_{kmax-1})\frac{E\varepsilon^2}{2} + P_1(\varepsilon)h_1(\varepsilon) + \cdots + P_{kmax}(\varepsilon)h_{kmax}(\varepsilon)$$

Then, as regards the state function f, we must calculate at first

$$\frac{dE_D}{d\varepsilon} = \sum_{i=0}^{kmax-1} E\varepsilon a^i \frac{n_i}{N} + \sum_{j=1}^{kmax}\frac{n_i}{N}[h(\varepsilon)]'_i$$

by which:

$$f = \sum_D P_D \frac{dE_D}{d\varepsilon} = E\varepsilon(P_0 + aP_1 + .. + a^{kmax-1}P_{kmax}) + \sum_{j=1}^{kmax} P_i(\varepsilon)[h(\varepsilon)]'_i$$

2.5.8 Plots

We can now introduce some plots, to better describe all the theoretical quantities we have introduced in this last chapter. So, let's suppose to use the Weibull distribution where the parameters of the distribution are set like

$$d_c = 0.5; m = 2$$

The Young modulus is put to the unity, 1.

We will show the shape of the probabilities functions $P_0, P_1, \dots, P_{kmax}$,average constituive behaviours (divided by N), the entropies and the fluctuations;

The number of fibers is $N = 10000$ and $a = 0.8$.

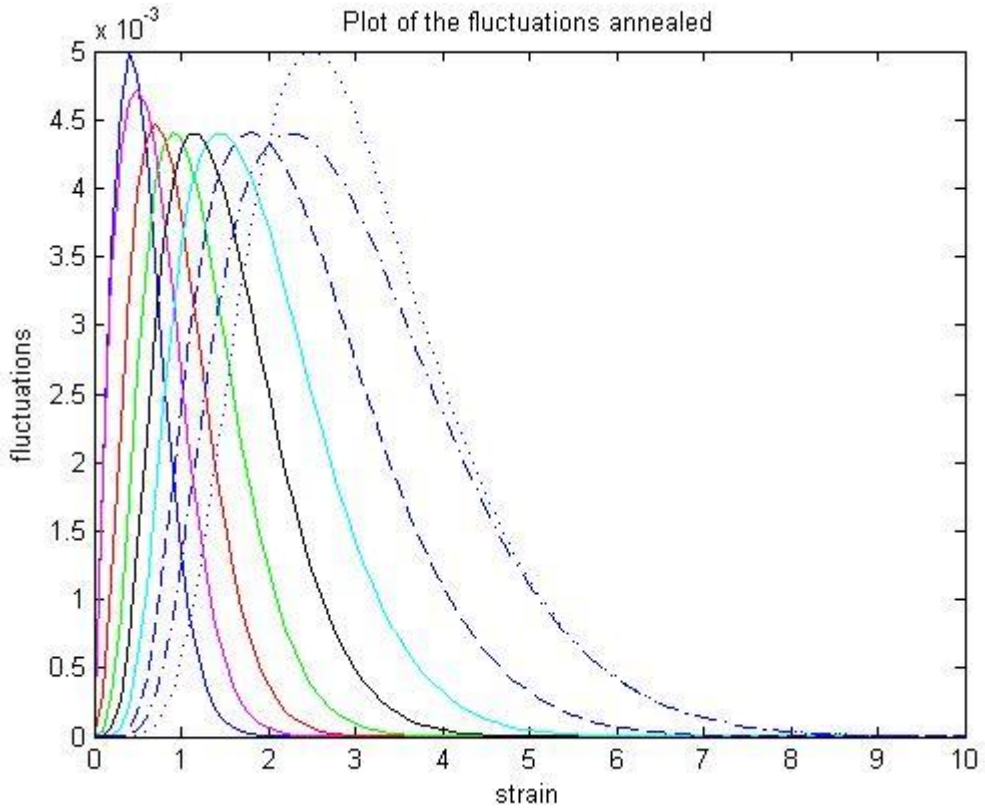

Figure 2.14.a: plot of the fluctuations for annealed disorder; $N = 10000$, $a = 0.8$ $kmax = 9$

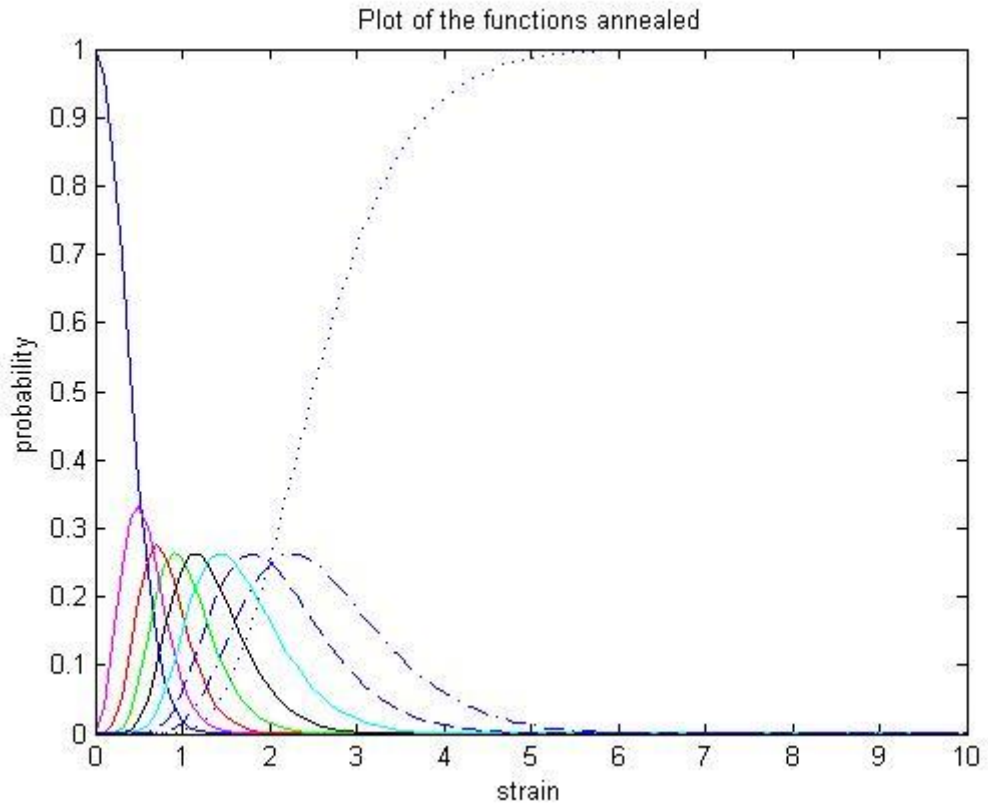

Figure 2.14.b: plot of the probabilty functions for annealed disorder; $N = 10000$, $a = 0.8 \quad kmax = 9$

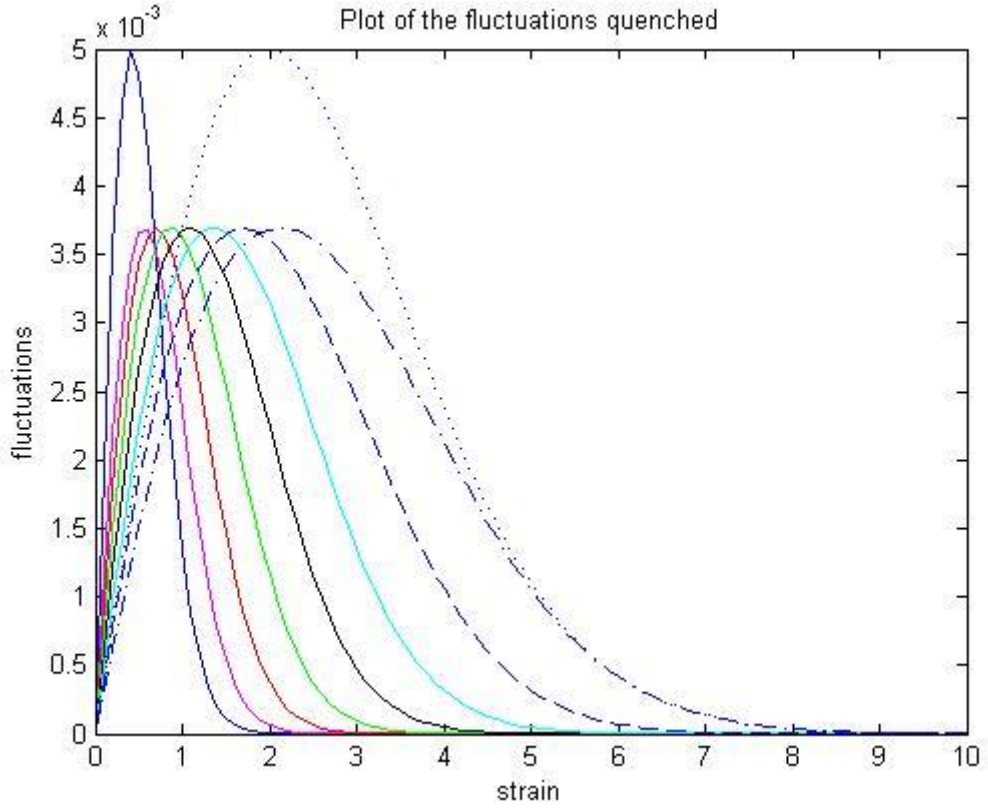

Figure 2.14.c: plot of the fluctuations for quenched disorder; $N = 10000$, $a = 0.8$ $kmax = 9$

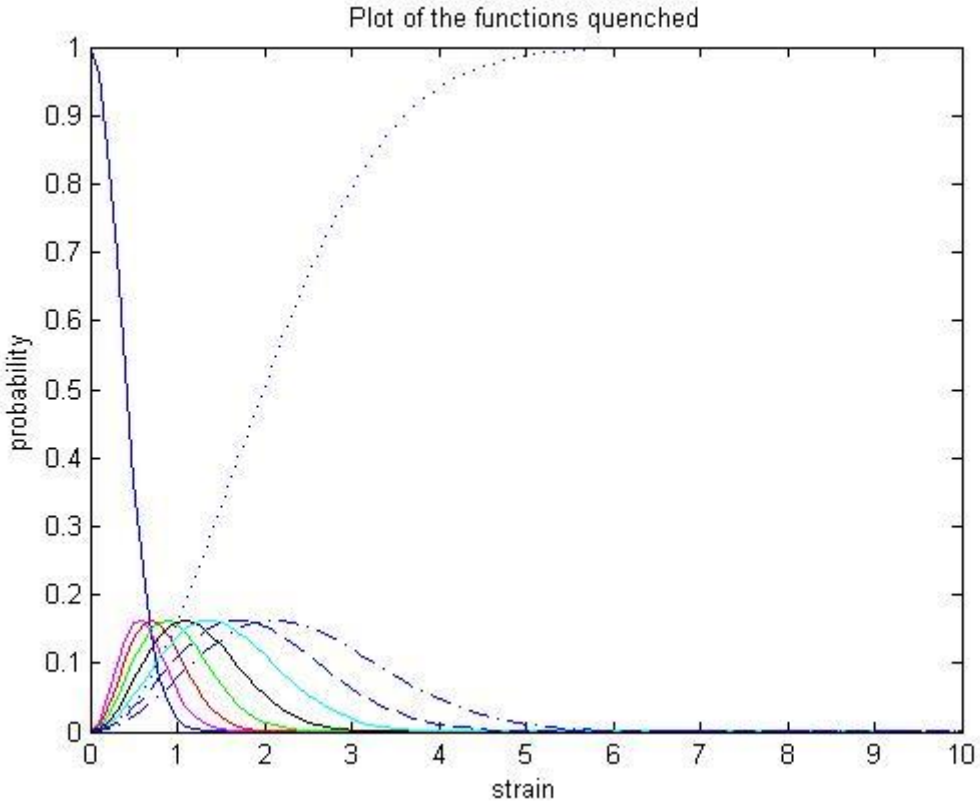

Figure 2.14.d: plot of the probability functions for quenched disorder; $N = 10000$, $a = 0.8$ $kmax = 9$

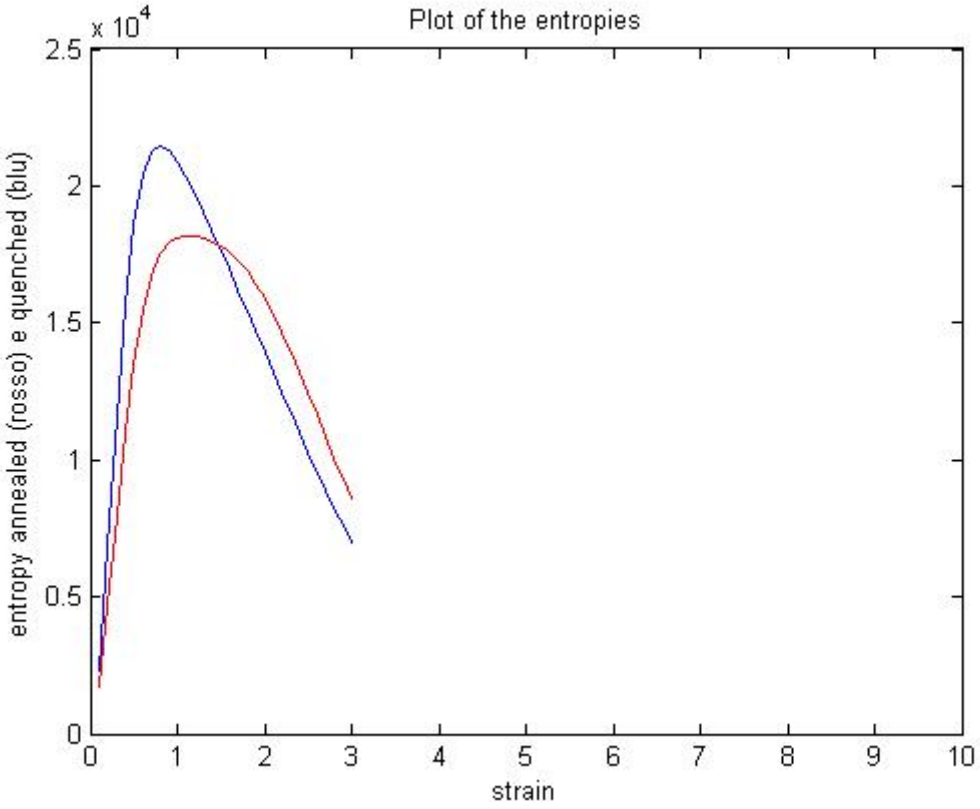

Figure 2.14.e: plot of the entropies for quenched and annealed disorder; $N = 10000$, $a = 0.8$ $kmax = 9$

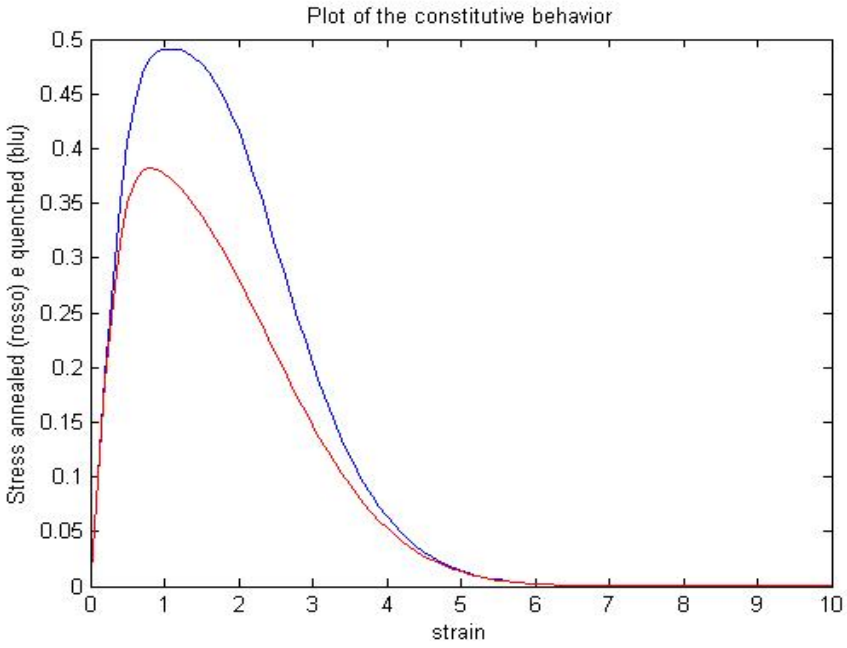

Figure 2.14.f: plot of the constitutive laws for quenched and annealed disorder; $N = 10000$, $a = 0.8$ $kmax = 9$

As it is possible to notice, the constitutive behaviours are different for quenched and annealed disorder: for the annealed the stress is always smaller than the quenched; this is a further confirmation about the computation of the plastic energy, which is always less for the annealed than the quenched one, as theory showed.

As regards the functions $P_0, P_1, \dots, P_{kmax}$, obviously they have a different shape for quenched and annealed disorder. These probability functions are characterized by a bell shape and as it is possible to notice, their maximum grows with the strain. This means that the function P_0 will have a maximum $P_0 = 1$ in $\varepsilon = 0$ (how we should obtain because in $\varepsilon = 0$ all the trusses are alived) P_1 will have its maximum at a bigger strain,, P_2 at a further bigger strain and so on till arriving to P_{kmax} which has its own maximum $P_{kmax} = 1$ at the strain in which all the fibers are broken. As we should expect the maximum of the function $P_1, P_2, \dots, P_{kmax-1}$ is not one; it cannot be one because at the strain in which we reach a given maximum for a function P_i the other probability density functions are different from 0. And this must happen because for a given strain there will be different fractions of fibers damaged 0 times, damaged one time and so on. It is also correct that the maximums of the these functions move to the right in increasing the index P_i: from a physical wievpoint the fraction of fibers that can damage more times, reach its maximum value later.

As regards the fluctuations, we obtain again bell shape functions; and these bell functions become more and more narrow when the number of total fibers grow.

Then we have the entropies which are different for quenched and annealed and that show a maximum close to region in which we observe the maximum of the constitutive curve.

We repeat now the same plots for a uniform distribution, in which

$$p(\sigma) = 1 \quad for\ 1 < \sigma < 2$$

and

$$p(\sigma) = 0 \quad for\ \sigma < 1 \ \ and\ p(\sigma) = 1 \quad \sigma > 2$$

We remind that we have considered the Young modulus of the fibers equal to the unit: so $E = 1$.

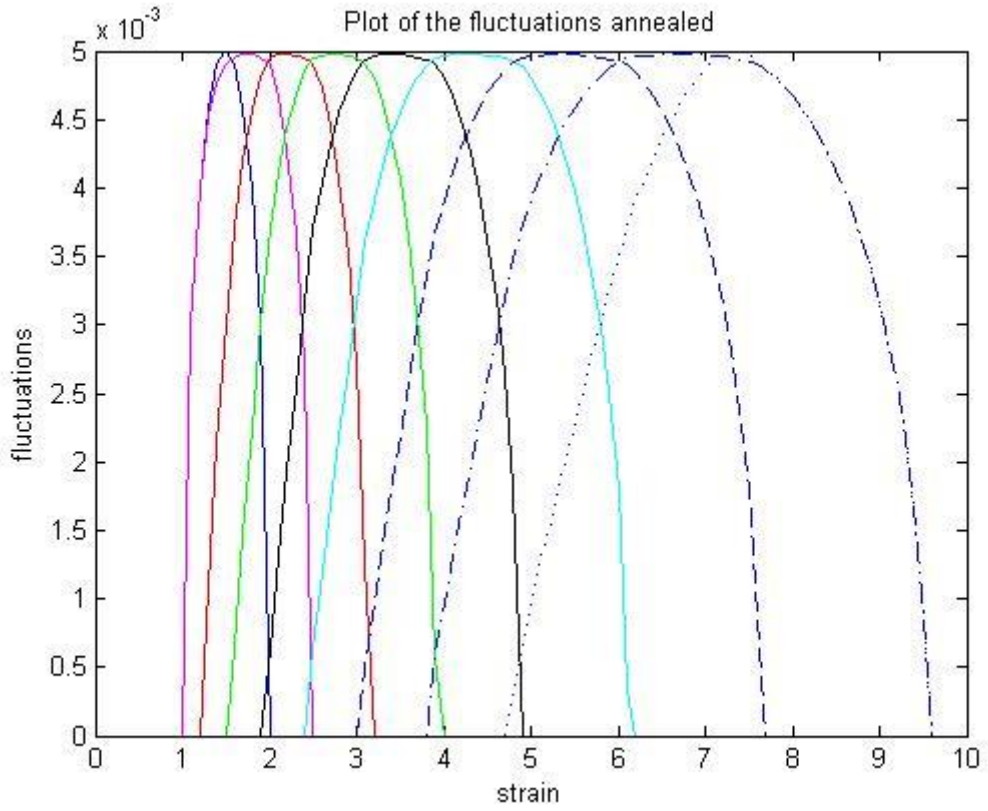

Figure 2.15.a: plot of the fluctuations for annealed disorder; $N = 10000$, $a = 0.8$ $kmax = 9$

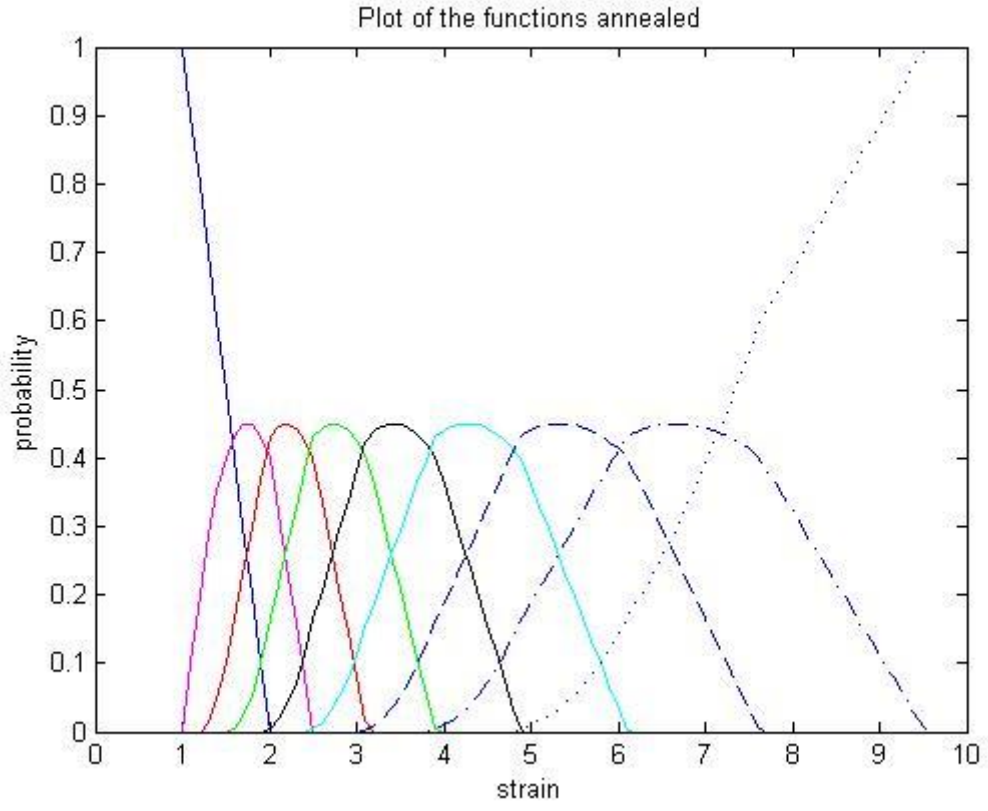

Figure 2.15.b: plot of the probability functions for annealed disorder; $N = 10000$, $a = 0.8$ $kmax = 9$

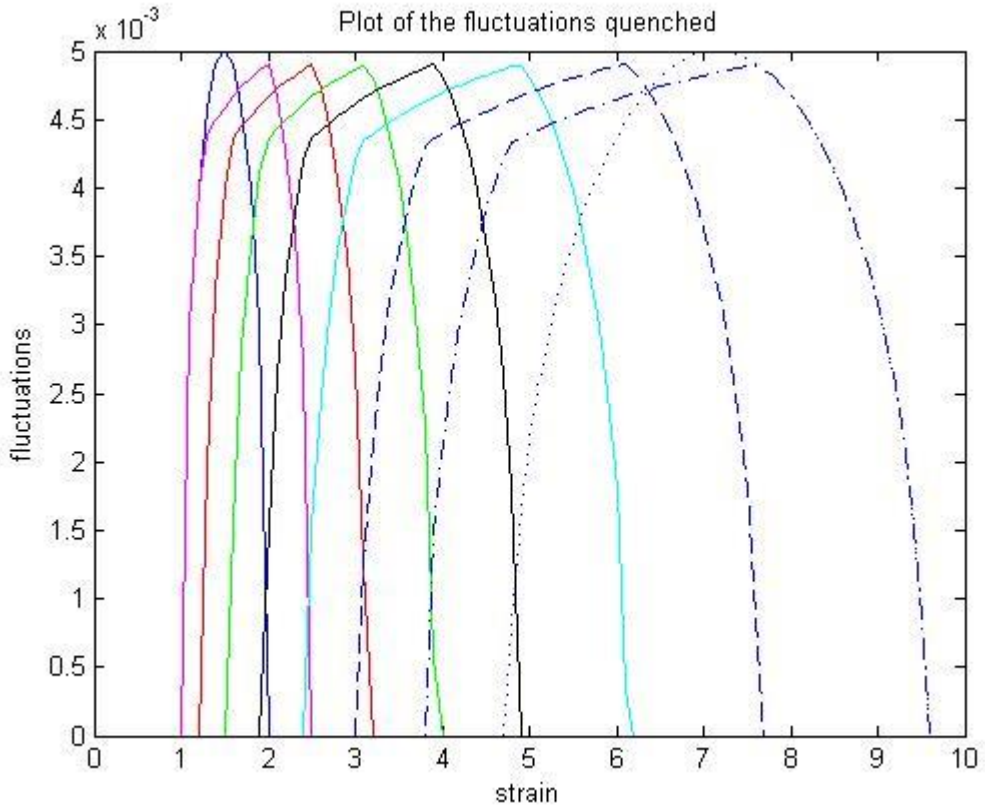

Figure 2.15.c: plot of the fluctuations for quenched disorder; $N = 10000$, $a = 0.8$ $kmax = 9$

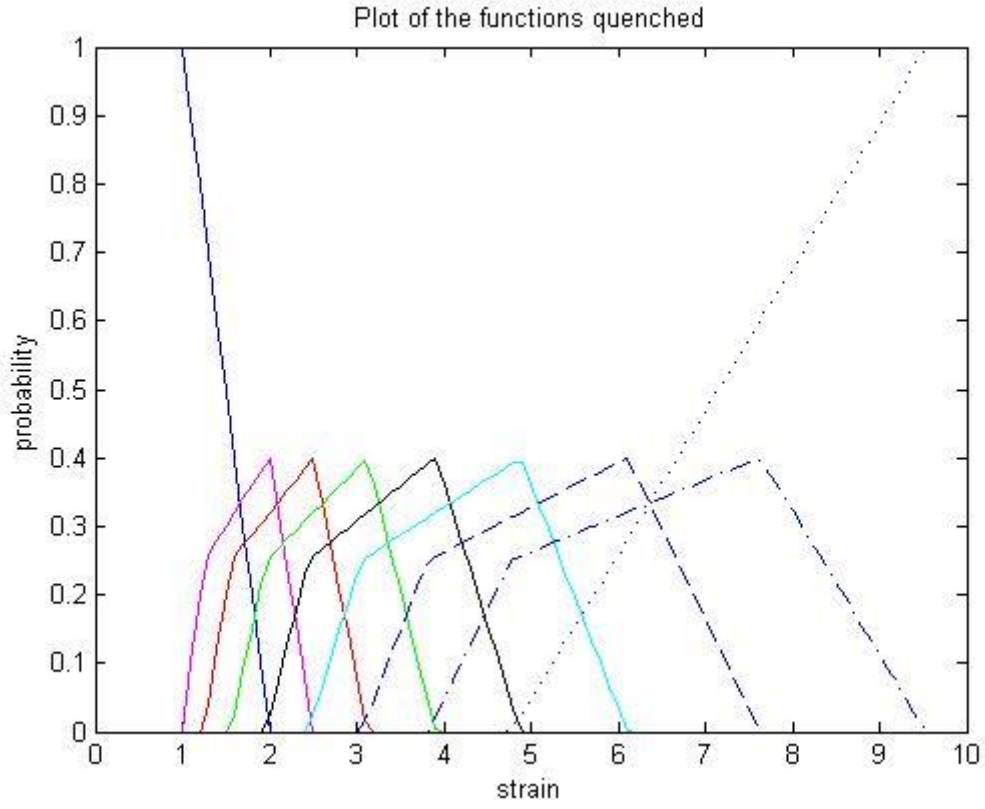

Figure 2.15.d: plot of the probabilty functions for quenched disorder; $N = 10000$, $a = 0.8$ $kmax = 9$

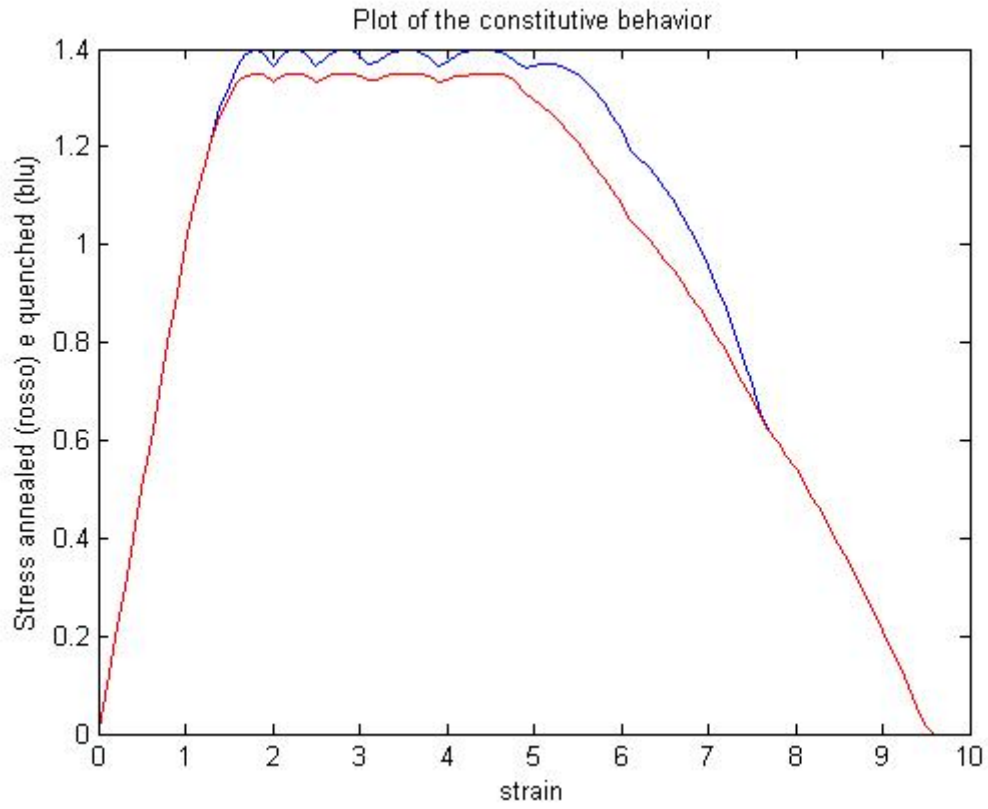

Figure 2.15.e: plot of the constitutive laws for quenched and annealed disorder; $N = 10000$, $a = 0.8$ $kmax = 9$

2.5.9 The Boltzmann's Distribution

In the previous pages we considered the probability to have a microstate with $n_0\ n_1 \dots n_{kmax}$ realizations like

$$p_D = P_0^{n_0} P_1^{n_1} .. P_{kmax}^{n_{kmax}}$$

This probability must be multiplied by multinomial coefficient to recover the probability to have a macrostate in order to take into account the fact the fibers are distinguishable.

So, we could now try to get the probability to have a particular state with $n_0\ n_1 \dots n_{kmax}$ fibers simply by maximazing the entropy we have introduced.

We know that the entropy, for the way in which we chose to count the states was defined like

$$S = \sum_D C^N_{n_0 n_1 .. n_{kmax}}\, p_D \log p_D$$

(2.81)

Here we do not consider the – sign to make the calculation easier. We will introduce it in the end of the calculations.

According to the sentence above, we must find the maximum of this function taking into account some constraints:

$$\begin{cases} U = \sum_D C^N_{n_0 n_1 .. n_{kmax}} p_D \overline{E_D} \\ 1 = \sum_D C^N_{n_0 n_1 .. n_{kmax}} p_D \\ \varepsilon = \varepsilon_D \end{cases}$$

(2.82)

The only way to catch this maximum taking into account the constraints is to use the Lagrange's multipliers; so we write the following function:

$$S = \sum_D C^N_{n_0 n_1 .. n_{kmax}} p_D \log p_D + \alpha \left(\sum_D C^N_{n_0 n_1 .. n_{kmax}} p_D - 1 \right) + \beta \left(\sum_D C^N_{n_0 n_1 .. n_{kmax}} p_D \overline{E_D} - U \right) + \gamma \sum_D (\varepsilon_D - \varepsilon)$$

(2.83)

In which the constants α, β, γ are the Lagrange multipliers. If we erase the last term (it does not contain the probability p_D so it is not important for tha calculation of the derivative), this expression can be written like

$$S = \sum_D C^N_{n_0 n_1 .. n_{kmax}} p_D (\log p_D + \alpha + \beta \overline{E_D}) - \alpha - \beta U$$

(2.84)

So if we take the derivative with respect p_D,

$$\frac{\partial S}{\partial p_D} = C^N_{n_0 n_1 .. n_{kmax}} (\log p_D + \alpha + \beta \overline{E_D}) + C^N_{n_0 n_1 .. n_{kmax}} = 0$$

(2.85)

So

$$\log p_D = -\alpha - 1 - \beta \overline{E_D}$$

(2.86)

and taking the exponential

$$p_D = e^{-\beta \overline{E_D}} e^{-(1+\alpha)}$$

(2.87)

Obviously

$$P_D = C^N_{n_0 n_1 .. n_{kmax}} e^{-\beta \overline{E_D}} e^{-(1+\alpha)}$$

$$1 = \sum_D C^N_{n_0 n_1 .. n_{kmax}} p_D = e^{-(1+\alpha)} \sum_D C^N_{n_0 n_1 .. n_{kmax}} e^{-\beta \overline{E_D}}$$

(2.88)

So

$$e^{(1+\alpha)} = \sum_D C^N_{n_0 n_1 .. n_{kmax}} e^{-\beta \overline{E_D}} \equiv \mathcal{Q}$$

(2.89)

which is the *partition function* of the strain ensemble.

Now

$$\frac{\partial \mathcal{Q}}{\partial \beta} = -\sum_D C^N_{n_0 n_1 .. n_{kmax}} E_D e^{-\beta \overline{E_D}} = -\mathcal{Q}U$$

If we know that

$$U = \sum_D C^N_{n_0 n_1 .. n_{kmax}} p_D \, \overline{E_D}$$

(2.90)

and that

$$\overline{E_D} = (-\log p_D - (\alpha + 1))/\beta$$

(2.91)

$$U = -\frac{1}{\beta} \sum_D C^N_{n_0 n_1 .. n_{kmax}} p_D \big(\log p_D + (\alpha + 1)\big) = -\frac{1}{\beta}(S + 1 + \alpha)$$

(2.92)

So, from the previous expression

$$-\beta U = S + 1 + \alpha$$

(2.93)

and now, if we change the sign of the entropy (because we defined it with the sign +) we have

$$\frac{\partial U}{\partial S} = 1/\beta$$

(2.94)

But

$$\frac{\partial U}{\partial S} = T$$

(2.95)

from the thermodynamics and so

$$\beta = 1/T$$

(2.96)

The parameter β that comes out from the probability density function obtained by the maximization of the entropy is basically the reverse of the temperature. Now, how is it possible to identify this parameter and so the equivalent temperature? To answer this question we can follow Pride and Toissant; the thermodynamics we defined previously leads us to say that

$$a\frac{d\beta}{d\varepsilon} + b\varepsilon + c = 0$$

(2.97)

where

$$a = \sum_D C^N_{n_0 n_1 .. n_{kmax}} p_D \, E_D (U - E_D)$$

$$b = \sum_D C^N_{n_0 n_1 .. n_{kmax}} p_D \, E_D (f - \frac{dE_D}{d\varepsilon})$$

$$c = \sum_D C^N_{n_0 n_1 .. n_{kmax}} p_D \, (\frac{dE_D}{d\varepsilon} - \tau_D)$$

(2.98)

which is a differential equation, non linear and so difficult to solve. It was shown for the simple FBM that a function $\beta(\varepsilon)$ could be obtained by

$$\beta(\varepsilon) = -\frac{N}{\varepsilon^2 - h(\varepsilon)} \log\left(\frac{1 - P(\varepsilon)}{P(\varepsilon)}\right)$$

(2.99)

As we noticed now, for the CFBM, it is more complicated to get this function and we must pass necessary for the above differential equation.

2.5.9 Stress Ensemble

The behaviour of the system in the sigma-ensemble is quite different. In this ensemble there is obviously a difference with respect the epsilon ensemble: in fact we are now performing a stress constant experiment on the system. So even in this case, the disorder generates an infinite number of mental copies of the system; and each system is characterized by different thresholds

taken by the same p.d.f. So from a theoretical viewpoint the mathematical formalism is identical to the one analysed previously for the strain-ensemble. At a given value of our new control parameter (the stress), each mental copy of the system will fall into a subset of our ensemble, which represents a given state of damage D. In going from σ to $\sigma + d\sigma$, there will be a "flux" of systems from subsets to other ones as it happened in the strain-ensemble.

However the development of the same mathematical formalism analysed in the previous section is too hard for this ensemble. The reason is that now, from a math viewpoint we are not able anymore the main tool we considered in the strain ensemble: the multinomial theorem; that's why the probability functions $P_0(\varepsilon) \dots P_{kmax}(\varepsilon)$ will be not anymore constant but they will change from one subset to another one because the strains that the various mental copies of the system will be different even if the stress will be the same. For this reason, the only way to analyse the CFBM in the case of a stress constant experiment is from a numerical viewpoint. By this sentence we are forced to certify that we will not able anymore to have all the amount of information we had with the strain ensemble. Furthermore for a numerical simulation, it is possible to analyse the behaviour of the system only for one realization at time (i.e. for a choice of a set of thresholds from our p.d.f.).

We remind that in this kind of system there is an avalanche behaviour; and that this is a consequence of the fact that the external force must remain constant in a stress controlled experiment even if one or more fibers can damage or fail because they reach their thresholds. This brings us to a redistribution of the load among the alive fibers that can damage again and so on. So in order to simulate the behaviour of the model when it suffers this boundary condition, we can apply the following rule (Kun, Hermann, Hidalgo):

We know that the external force F, is

$$F = \sum_{i=1}^{N} f_i = \varepsilon \sum_{i=1}^{N} a^{k(i)}$$

(2.100)

So by this simple law that expresses the relation between the external force and the single forces applied on the fibers, we can calculate the strain

$$\varepsilon = \frac{F}{\sum_{i=1}^{N} a^{k(i)}}$$

(2.101)

and the forces on the single fibers

$$f_i = \frac{F a^{k(i)}}{\sum_{i=1}^{N} a^{k(i)}}$$

(2.102)

So, in a given stable state of the system, we compute the forces on the single fibers, f_i, and, by knowing the thresholds d_i, we already know which fiber will break: it can be found by the ratio:

$$r = \frac{d_i{}^*}{f_i{}^*} = min \frac{d_i}{f_i} \quad r > 1$$

(2.103)

This means that the fiber that breaks is the one with the minimum value of this ratio. So, for example in increasing the load on the bundle from

$$F \to rF$$

(2.104)

a given fiber, with index i^*, will damage; so its damage index will increase from $k(i^*) \to k(i^*) + 1$. After this damage, the load on the other fibers must be recalculated by the Eq. (2.102) that provides the Local Sharing Rule into the model. A new value of the strain is also calculated.

If there will be other fibers that will reach their own thresholds, they will suffer a further damage and the process goes ahead, creating an avalanche whose size number s is exactly the number of total damages we notice in increasing the force from

$$F \to rF$$

in a quasi static way. The process will stop when for the value of the external force rF, and for a given state of damage $D = \{D_0, D_1, \dots, D_{kmax}\}$ and a given strain ε (which is the same for each fiber), there will not be further damages anymore. How does the algorithm work? In increasing the force from $F \to rF$, two new quantities will be introduced: the avalanche size s we talked about first and the number of iteration i.So at the beginning, it is possible that for $F_{ext} = rF$, for example m fibers will damage because they reach their threshold, according to the quenched or annealed disorder. So $i = 1$ and $s = m$. The Young modulus of the damaged fibers is reduced by the factor a and the equilibrium for $F_{ext} = rF$ is computed again; here $i = 2$ and for example n fibers damage, so $s = n$ and so on. The process will stop when after i iterations, and after a number of total avalanches $S = \sum_{j=1}^{i} s_i$, for a force $F_{ext} = rF$ and at the iteration $i + 1$, the number of avalanche $s(i + 1) = 0$, i.e. from a physical wievpoint we reach the equilibrium without noticing further damages. After this, the external force is increased to $F_{ext} = (r + r)F$ and the process goes ahead. Basically in the algorithm, we introduce some "substeps" in order to take into account the attempts of the system to reach the equilibrium suffering a particular value of the external force. In the constitutive curve stress-strain, these substeps appear into the

process like the horizontal lines we noticed in the figure (2), in which obviously the external force remains constant because it is the engine that drives the system towards the equilibrium and the strain ε of all the fibers growths (because from a physical viewpoint the strain of the fibers is the only physical quantity that the system can vary to reach the equilibrium).

So by these considerations, like in the FBM happened, in the CFBM we will have an avalanche behaviour which will be lead by a power law or by an exponential law. The behaviour of the system was extensively studied by Hidalgo,Kun, Kovacs, Pagonabarraga (Avalanche dynamics of the continuous fiber bundle model) and by Hidalgo Kun and Hermann (Bursts in a FBM with continuous damage).

In the study of the authors, it was possible to show that the avalanche behaviour depends basically on the damage reduction parameter a and on the number of allowed failures per fiber k_{max}. A complex phase diagram was introduced to resume this behaviour, in which we recognize three phases and a characteristic curve $a = a(kmax)$ which separates the phase 2 from the phase 3, and whose characteristic points $a(kmax = 1), a(kmax = 2)$ … can be calculated by knowing the p.d.f. from which we recover our thresholds:

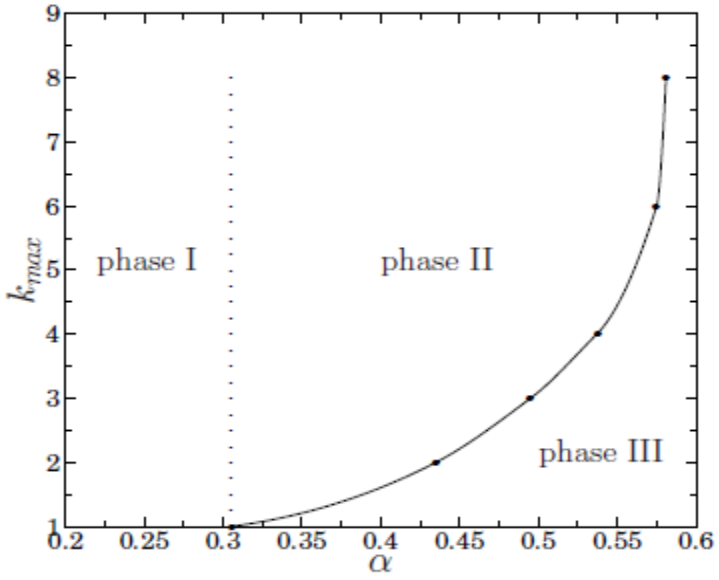

*Figure 2.16: state diagram of the CFBM (*Hidalgo et al., 2008*)*

Furthermore, we noticed in the strain ensemble, plotting the function (2.78 b) that by considering different values of a and $kmax$, the constitutive behaviour of the system was a function of the same two state parameters. This result was also obtained by Kun Hidalgo and Hermann and it was used as starting point by Hidalgo et al to calculate the avalanche dynamics in the CFBM. So, in the strain ensemble it was possible to notice that after the initial elastic response, the constitutive curve of the CFBM displayed a plateau regime which could be non-monotonic. We showed that by varying the two state parameters, it is possible to control the appearance of these maxima or inflection points. In the work by Hidalgo et al, it is possible to show that the presence of these local extreme values can affect the microscopic dynamics of the damage and the analytic form of the power law: in a particular way there could be situation in which, in the work hardening, an inflection point can appear (fig 2.17) and the

order of this inflection point can affect the avalanche dynamics. In their work, it is possible to show that the avalanche size distribution is

$$D(\Delta) \sim \Delta^{\frac{-4n+1}{2n}}$$

where n is the order of the inflection point. For an infinite plateau (this condition is reached if $k_{max} \to \infty$) $n \to \infty$, so

$$D(\Delta) \sim \Delta^{-2}$$

So, in the following, we will analyse this constitutive diagram including a brief resume of the work by Hidalgo and taking into account the so called work hardening, in which a fiber can fail k_{max} times but after these failures, it stores a residual stiffness

Phase 1:

When the fibers can fail only once, obviously $k_{max} = 1$, and for $a = 0$, we recover exactly the behaviour of the dry FBM (which is not present into the figure). Increasing the stress, we will arrive to the maximum value into the constitutive curve strain stress, and after it the model will fail. If we fix $k_{max} = 1$ and we change a up to a critical value $a_c(1) = 0.3$, we are considering the situation in which the fibers can fail only once, but they never lose their stiffness; so we would expect after an initial transient to recover a residual stiffness for the whole bundle: this situation will arise when every fiber will not fail. After this transient the behaviour will be elastic and we will have work hardening instead of a critical failure of the bundle.

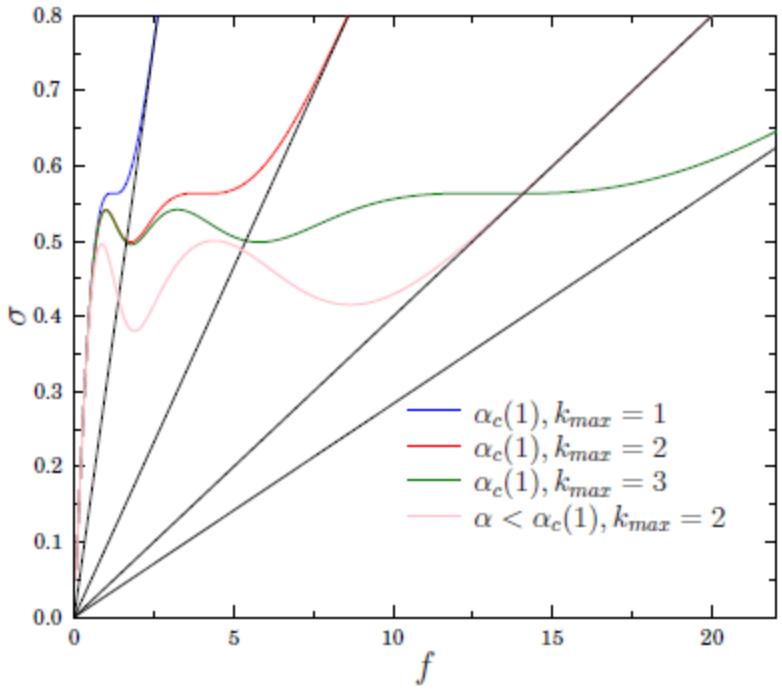

*Figure 2.17: constitutive behaviour of the CFBM for different choices of the damage parameters (*Hidalgo et al., 2008)

Now what happens for $k_{max} > 1$? It can be shown from an analytical wievpoint that in the case of the work hardening, the constitutive curve has k_{max} local maxima and at the critical value $a = a_c$ the last maximum turns into an inflection point in the figure above. Either the maxima and the inflection points are reached into the stress constant experiment for work hardening and for the failure. So we can state that for $a < a_c$ and for each k_{max}, the avalanche dynamics is characterized by a power law with exponent $-5/2$. This happens in the phase 1, in which we have

$$D(\Delta) \sim s^{-5/2}$$

like in the dry FBM.

(Obviously, even if this is the constitutive curve of our model, in a stress controlled experiment it is not possible to notice all the waves and all the k_{max} maxima because of the nature of our experiment. So for the work hardening case, we will jump after the flast maximum value or after the last inflection point to the asymptotic value while for the case of the catastrophic failure, after the maximum/inflection point, the model will fail).

The critical point $a_c(kmax = 1)$ is always a function of the probability density function used for the disorder and for the Weibull distribution is work hardening, the constitutive curve has k_{max} local maxima and at the critical value $a_c = 0.305$.

Phase 2 and 3:

The curve $k_c(a)$ separates two different regimes: for the parameter regime below the curve, avalanche distribution with an exponential law are obtained, while above this curve the avalanche distribution is characterized by a power law where

$$P(s) \sim s^{-\beta} \; \beta = 2.12 \pm 0.05$$

which is quite different from the power law obtained in the FBM (Hemmer Hansen). In the phase 2 it is possible to show that for $k_{max} > 1$, the constitutive curve of the model (obtained in the strain ensemble) is still caractherized by k_{max}, but the first maximum is smaller than the other ones. In the region 3 instead it is possible to show that the constitutive behaviour is not characterized by local maxima.

Each phase shows a common behaviour for $k_{max} \to \infty$, which is the appearance of a plateau whose length depends on the number of allowed failures: the bigger it is,the longer it is. For the work hardening case, this transient will not be noticed because we will pass directly to that part of the curve with a residual stiffness while for the case of the failure, the model will fail when the curve stress-strain will reach the maximum.

What happens in the case in which a residual stiffness is not allowed but the fibers that have failed $kmax$ times are not allowed to withstand further load (catastrophic failure)? The behaviour is quite different from the case of the work hardening and it depends at the same time on the kind of disorder we chose. When the disorder is quenched the statistics of the avalanche shows a power law whose exponent is about -5/2 like in the dry FBM. When

$kmax$ is bigger, obviously the number of the avalanches growth but the statistics of the avalanches themselves do not change at all. For the annealed the situation changes; if $a < a_c$ the results are similar to the dry FBM. In the region 2 the exponent of the power law is 2.12 ± 0.05 similar to the case with residual stiffness. Below $k_c(a)$ the exponents vary as function of the value we assign to k between the two mean field exponents α and β.

In the following we report the result of a numerical simulation, in which we will analyse the constitutive behaviour of one single realization, the avalanche behaviour of the system and the order parameter $\varphi = 1 - D_{tot}$, and the count of the avalanches vs time (i.e. vs a given value of the external force).

For a sample of 10000 fibers and with thresholds taken by a uniform p.d.f. and using a damage reduction parameter $a = 0.8$, we get the following plots:

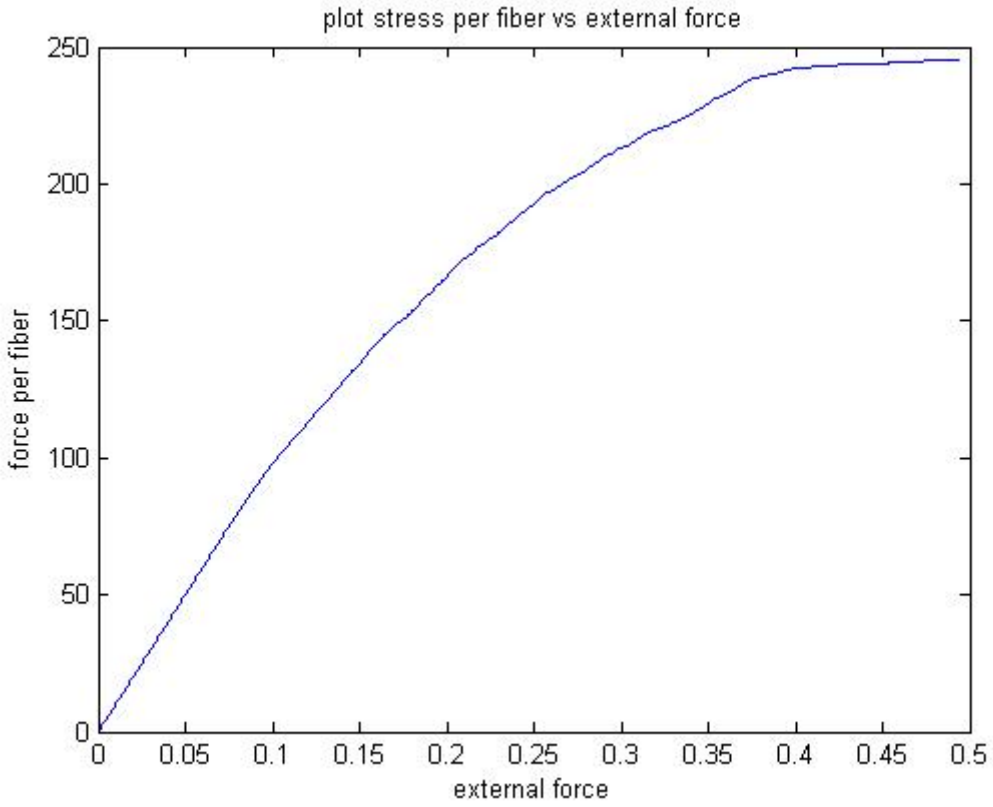
plot stress per fiber vs external force
force per fiber
external force
0
50
100
150
200
250
0
0.05
0.1
0.15
0.2
0.25
0.3
0.35
0.4
0.45
0.5

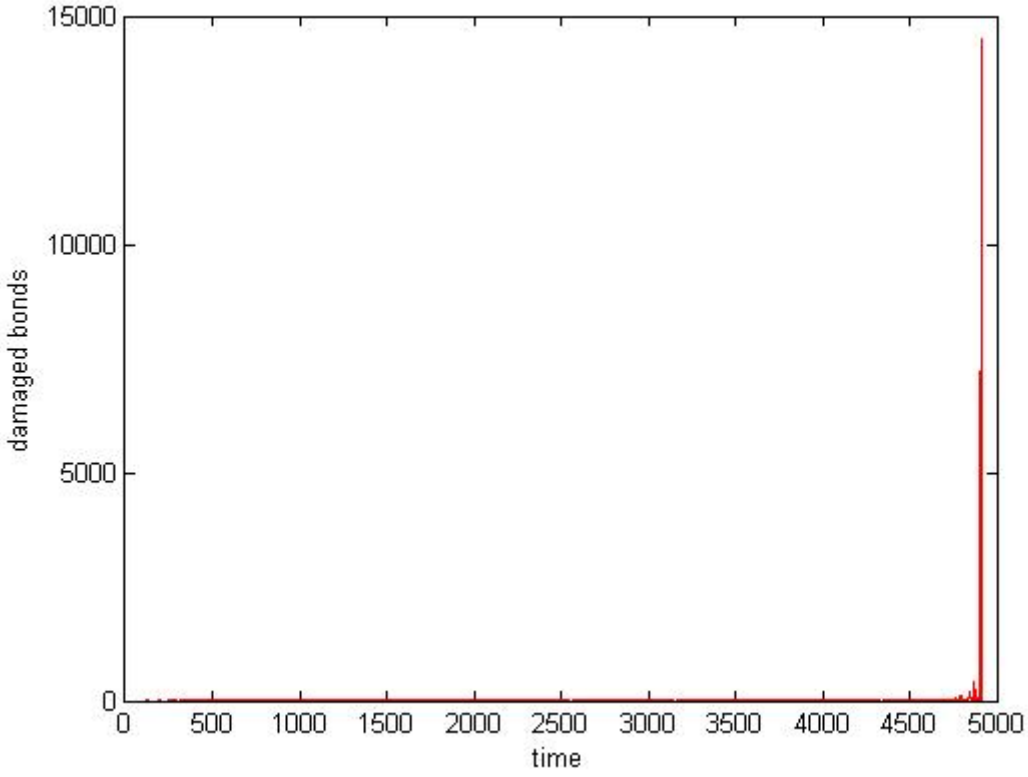
damaged bonds
time
0
5000
10000
15000
0
500
1000
1500
2000
2500
3000
3500
4000
4500
5000

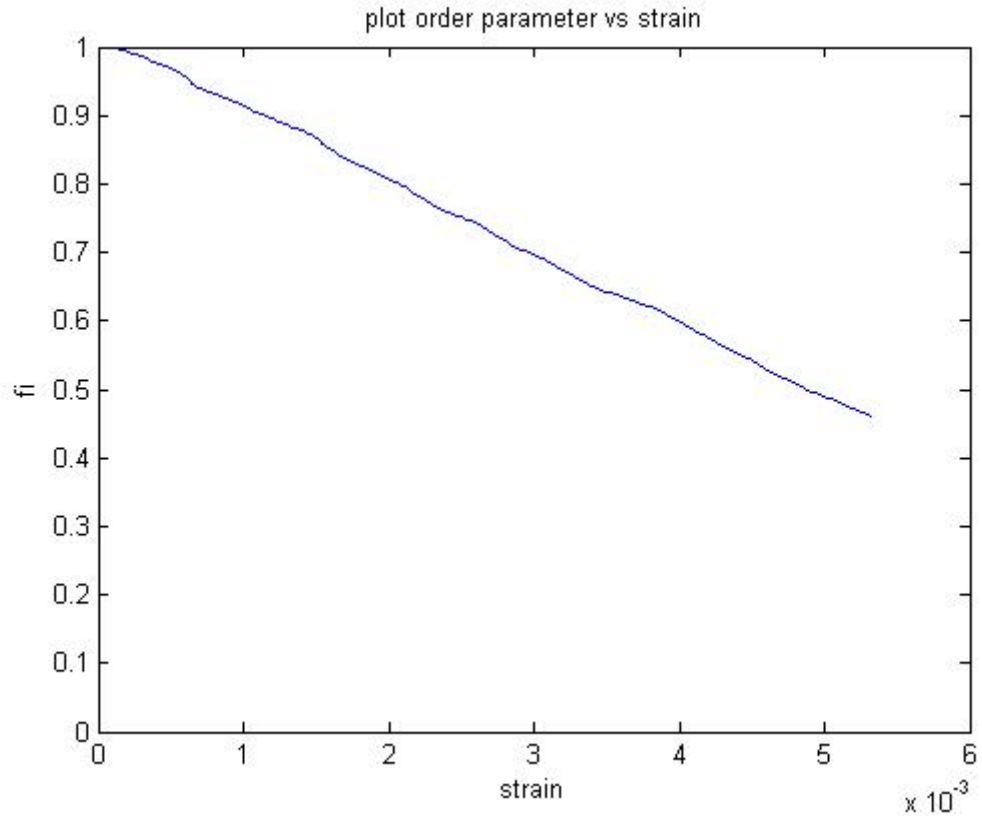
plot order parameter vs strain
fi
strain
x 10^-3
0
0.1
0.2
0.3
0.4
0.5
0.6
0.7
0.8
0.9
1
0
1
2
3
4
5
6

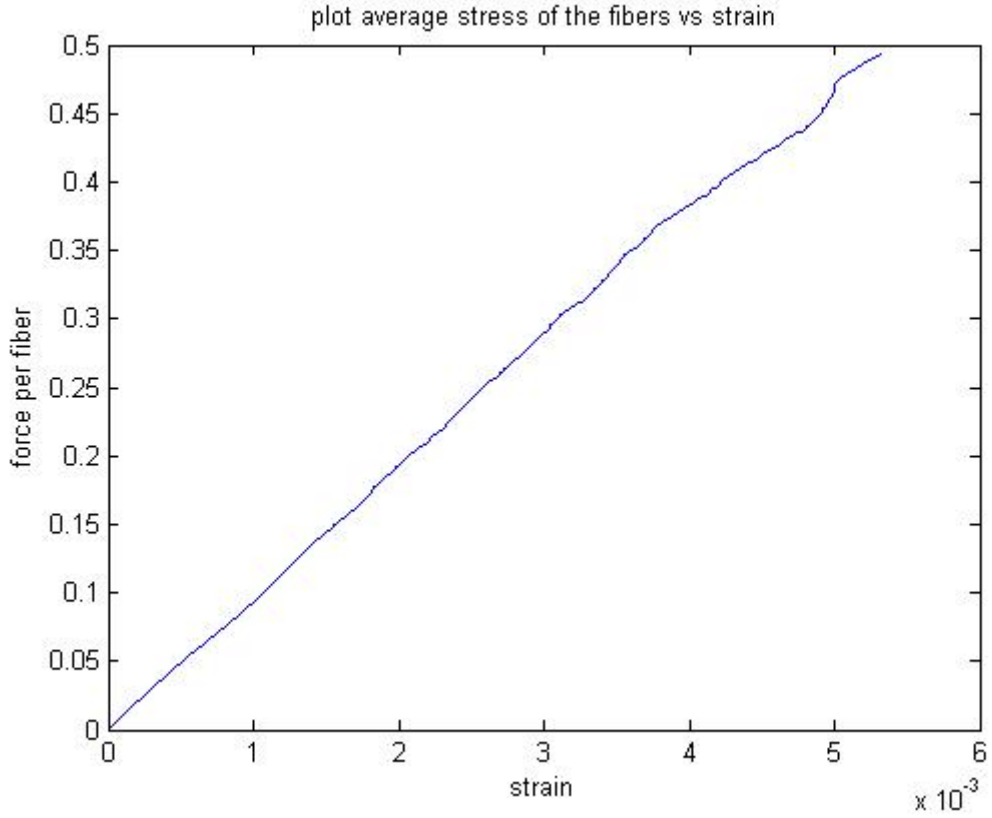
plot average stress of the fibers vs strain
force per fiber
strain
x 10^-3
0
0.05
0.1
0.15
0.2
0.25
0.3
0.35
0.4
0.45
0.5
0
1
2
3
4
5
6

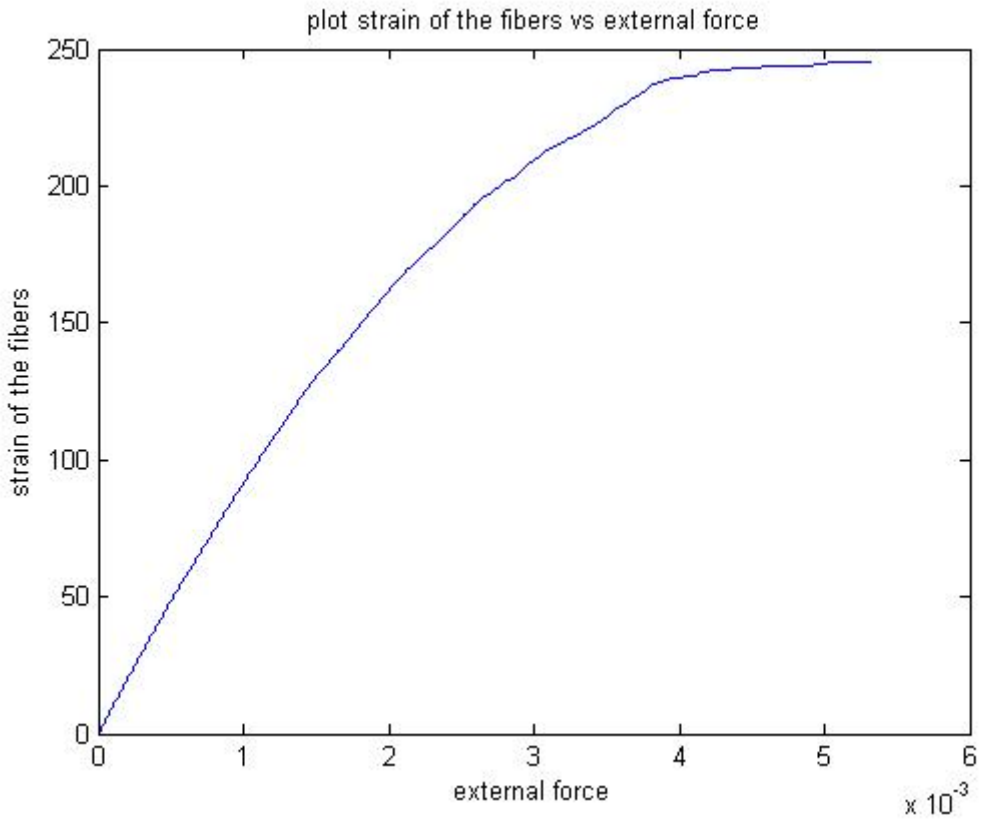

Figure 2.18: characteristic plots for the CFBM in a stress controlled experiment

As we notice by the plots, we can recognize a different curve from the one described in the case of the stress constant experiment. In fact the horizontal lines do not appear in the plot of the force per fiber vs strain but only some oblique lines are present. The reason of this depends on how we wrote the code: basically in a stress constant experiment we recognize a horizontal part in which we notice the appearance of the avalanches followed by a second oblique part in which nothing breaks (see fig 2.2 on the right). In our simulation this oblique line plus the horizontal line due to the avalanches (in black) is substituted by a unique oblique line (in red) obtained by interpolating the first point with whom the oblique line begins and the last point of the horizontal line. For this reason it is not possible to notice the so called "substeps". The following figure helps us to understand better the problem:

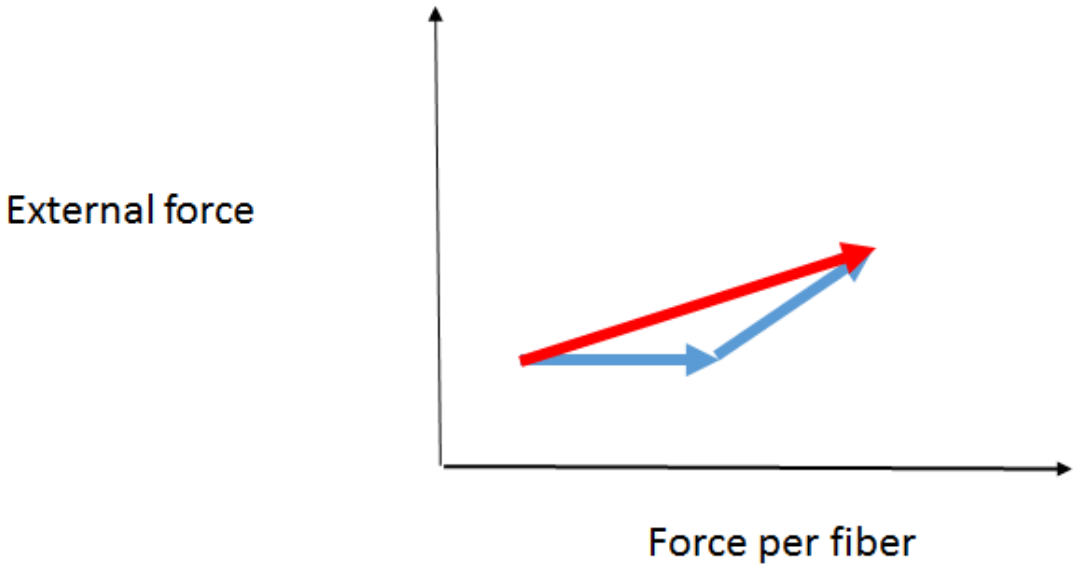

In black we observe the horizontal line in which an avalanche behaviour is present and the oblique line in which nothing breaks into the system: this is also the real constitutive curve of the system (in blue). In our simulation instead the first point and the last point are used to draw the variation of the stress per fiber vs the external force (in red). Basically the behaviour of the system is the same.

As regards the avalanche behaviour as we notice from the figure in red, a first phase is observed in which the magnitude of the avalanches is more or less the same. Close to the critical point instead we note avalanches of bigger magnitude till to the last one that leads us to the catastrophic failure of the whole model.

The avalanches are then distributed according to p.d.f. fitted quite well by a power law

$$P(s) \sim s^{-\tau}$$

where the exponent $\tau = 2.2451$ from the statistical analysis of the numerical simulations. Other simulations give us the same results with very little differences as regards the power law in good agreement with the theory.

The simulation was realized according to the algorithm previously described in the case of a stress constant experiment.

2.5.10 Close to the critical point

Another interesting property of the CFBM is about the exponent law close to a local maximum: it is possible to show (Hidalgo et al) that even if the exponent of the power law is given by β, if we try to measure this exponent close to a local maximum (that in the case of the dry FBM is the only maximum before the failure), the exponent is -1.5. So, it could be possible by experimental techniques to try to measure the sound pulses created by the failure of the fibers (which are related to the energy lost by the system because of the damage) and by this, to understand if we are close to a local maximum (to the failure of our model) or not. In fact the energy bursts that come out because of the breakings of the fibers are characterised by a

power law which has the same exponent of avalanche size distribution. This last sentence was proved first for the simple DFBM (Prahandi, Hemmere Hansen)

For the simple FBM in fact another way to write the avalanche distribution is

$$\frac{D(\Delta)}{N} = \frac{1}{N}\frac{\Delta^{\Delta-1}}{\Delta!}\int_0^{x_c}[1-\frac{xp(x)}{Q(x)}]p(x)[\frac{xp(x)}{Q(x)}]^{\Delta-1}\exp(-\Delta xp(x)/Q(x))dx$$

(2.105)

where $Q(x) = \int_x^\infty p(y)dy$ is the fraction of fibers exceeding x. If we consider a uniform distribution,

$$p(x) = \frac{1}{x_m - x_0}$$

(2.106)

The previous expression becomes

$$\frac{D(\Delta)}{N} = \frac{1}{x_m - x_0}\frac{\Delta^{\Delta-1}}{\Delta!}\int_{x_0}^{x_c}\frac{x_m-2x}{x}\left[\frac{x}{x_m-2x}e^{-x/(x_m-2x)}\right]^{\Delta}dx$$

(2.107)

So, introducing the parameter

$$\varepsilon = \frac{x_c - x_0}{x_m}$$

(2.108)

and the new integration variable

$$z = \frac{x_m - 2x}{\varepsilon(x_m - x)}$$

we obtain

$$\frac{D(\Delta)}{N} = \frac{2\Delta^{\Delta-1}e^{-\Delta}\varepsilon^2}{\Delta!\,(1+2\varepsilon)}\int_0^{4/(1+2\varepsilon)}\frac{z}{(1-\varepsilon z)(2-\varepsilon z)^2}e^{\Delta[\varepsilon z+\ln(1-\varepsilon z)]}\,dz$$

(2.109)

For small ε,

$$\varepsilon z + \ln(1-\varepsilon z) = -\frac{1}{2}\varepsilon^2 z^2 - \frac{1}{3}\varepsilon^3 z^3 - \cdots$$

that gives us

$$\frac{D(\Delta)}{N} \sim \frac{\Delta^{\Delta-1} e^{-\Delta} \varepsilon^2}{2\Delta!} \int_0^4 e^{-\Delta[\frac{1}{2}\varepsilon^2 z^2]}\, z dz = \frac{\Delta^{\Delta-2} e^{-\Delta}}{2\Delta!}(1 - e^{-8\varepsilon^2\Delta})$$

(2.110)

and using the Stirling approximation,

$$\Delta! = \Delta^{\Delta} \mathrm{e}^{-\Delta} \sqrt{2\pi\Delta}$$

we have

$$\frac{D(\Delta)}{N} \sim (8\pi)^{-\frac{1}{2}} \Delta^{-\frac{5}{2}} (1 - e^{-\Delta/\Delta_c})$$

(2.111)

with

$$\Delta_c = \frac{1}{8\varepsilon^2}$$

(2.112)

So, by these considerations, it is possible to write that

$$\frac{D(\Delta)}{N} = \begin{cases} (8/\pi)^{1/2} \varepsilon^2 \Delta^{-\frac{3}{2}} & for\ \Delta \ll \Delta_c \\ (8/\pi)^{1/2} \Delta^{-\frac{5}{2}} & for\ \Delta \gg \Delta_c \end{cases}$$

(2.113)

A very similar proof can be given for the CFBM but we suggest to consider the paper by Hidalgo et al for the calculations.

This behaviour gives us the sensation that the physics of the system changes drastically when we are close to the critical point of the failure, giving us hints of a possible failure. This could be quite important from an experimental viewpoint to understand when the FBM or the CFBM is close to the catastrophe. Does this behaviour exist for other systems in nature as well? As we will see the answer at the question is yes (Milanese et al., 2016): we are talking about the statistical central force model in static for which two kind of exponents for the power law were obtained: one for the whole simulation and one for the steady-plastic state; these exponents obviously depend on the boundary conditions applied but it is quite interesting to note how the nature follow the same scheme for so different systems.

Before finishing the Chapter, it could be necessary to point out a very important aspect regarding the study of the CFBM we previously made: this simple model of fibers was studied in traction only and not in compression. This could be a future work to develop by the thermodynamic study in order to understand how the system of fibers approaches the phenomenon of the “buckling”.

Chapter 3

About the Porous Media

"Each soil has had its own history. Like a river, a mountain, a forest, or any natural thing, its present condition is due to the influences of many things and events of the past."

Charles Kellogg, The Soils That Support Us, 1956

3.1 The Physics of porous media

3.1.1 Introduction

What is a porous medium? A common definition is "material containing pores or voids". The pores are typically filled with a fluid that can be a liquid or a gas and the skeletal material is obviously a solid. According to lines above, we can understand that the definition of porous medium is basically abstract, in the sense that a soil or a concrete can be considered like a porous medium; but at the same time an amount of sand with a concentration of water inside, both contained into a box can be considered a porous medium (Darcy in fact conduced his own experiment about the flux of water inside a porous medium by considering this kind of system at the end of '800). Even the foams are porous media although their solid skeleton is considered very fragile and quasi-fluid. However in the following pages we will deal simply with systems like soils or concrete. We will analyze the governing equations of this kind of systems (we will see basically two equations: one for the equilibrium of the solid and the other one for conservation of the mass of the fluid by using the theory of mixtures by De Boer) and then we will introduce a way to solve them.

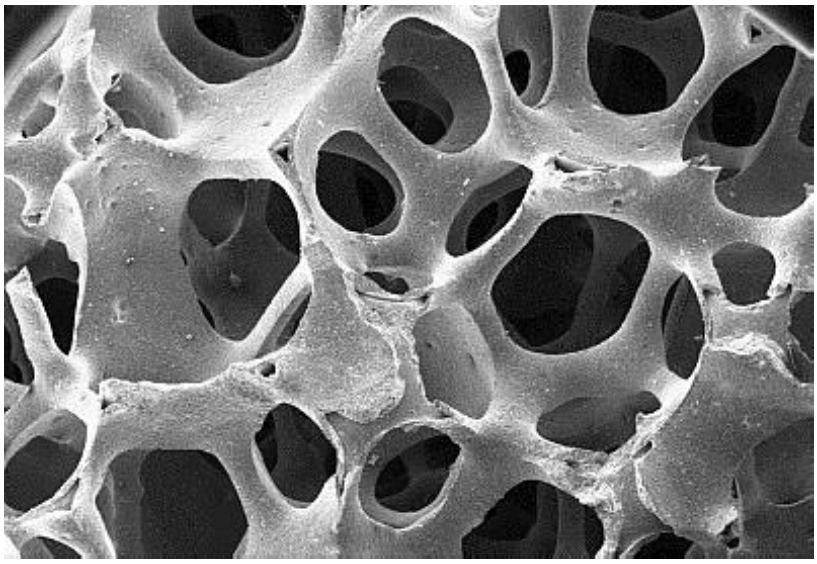

Figure 3.1: a possible skeletal material associated to the structure of a porous medium

Before going ahead, it is useful to make a clarification about the notation we will use: we will consider vector and matrixes with the unique symbol $\overrightarrow{\ }$. This is done to simplify the notation itself.

3.1.2 Porous media: governing equations

It is very difficult to describe the mechanics of a porous medium in a microscopic viewpoint for the reasons we just gave; so its mechanics is described on a macroscopic scale assuming that the porous medium is continuous everywhere, with air, water and solid grains forming like an overlapping continuum.

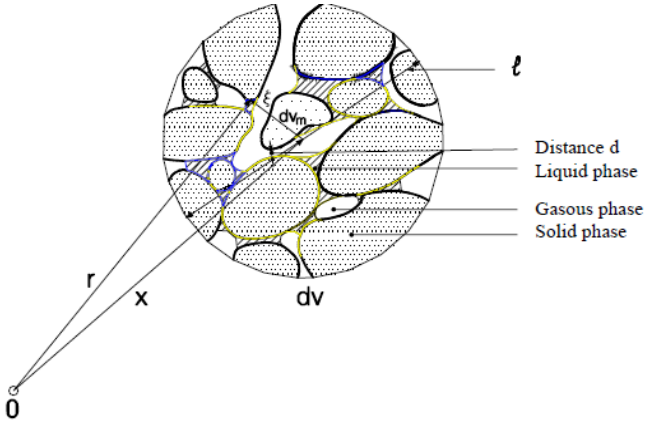

Figure 3.1: the structure of a porous medium in a mesoscopic scale

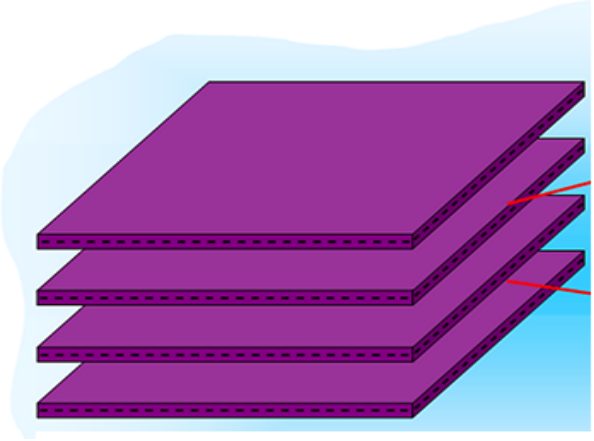

Figure 3.3: the structure of a porous medium by thinking it of overlapping layers

If the air pressure is nearly uniform over the domain, and the air flow is not significant, it may be assumed that the air pressure p_a in the unsaturated zones remains at atmospheric pressure or simply

$$p_a = 0$$

3.1.3 Description of the skeleton deformation

Let us consider a Cartesian coordinate system as reference for our displacements, velocities and deformations.

In continuum mechanics we can try to describe the motion of a single particle by using two different approaches: the Eulerian one and the Lagrangian one; in the first one we fix a particular point in space, x, y, z and we concentrate on what happens in that region of the space; on the other hand, in the Lagrangian one the situation is quite different in the sense that we fix a particular particle and we focus our attention on the variations of the observables on that particle.

So, for the finite deformation of the solid skeleton it is convenient to consider a Lagrangian viewpoint, even if we have no such big differences in small strain or displacements in the two approaches. However even if the deformation of the soil skeleton is small, the fluid in the pore structure can flow through long distances depending on the drained conditions. It could be preferable to use an Eulerian description to describe the fluid flow behavior.

In the following pages, we will describe both vectors and tensors by the same symbol $\longrightarrow$ in order to simplify the notation in the chapter, while the scalars will not be characterized by the arrow on their top.

So, the displacement vector $\vec{u}$ of a typical particle from its initial position $\vec{X}$ to its position $\vec{x}$ at the time t is

$$\vec{u} = \vec{x} - \vec{X} \tag{3.1}$$

For a particle with property E, its material derivative with respect the time in a Lagrangian viewpoint is

$$\frac{DE}{Dt} = \partial E(\vec{X}, t)/\partial t$$

(3.2)

while if we use the Eulerian point of view,

$$\frac{DE}{Dt} = \frac{\partial E(\vec{x}, t)}{\partial t} + \frac{\partial E(\vec{x}, t)}{\partial t}\dot{\vec{u}}$$

(3.3)

where $\dot{\vec{u}}$ is the velocity of the particle, i.e.

$$\dot{\vec{u}} = \frac{\partial \vec{x}(\vec{x}, t)}{\partial t}$$

(3.4)

Another important quantity we have to define is the *porosity* of the porous medium:

$$n = \frac{volume\ of\ voids}{total\ volume\ of\ soil}$$

(3.5)

If we define

$$nS_w = \frac{volume\ of\ water}{total\ volume\ \ of\ soil}$$

(3.6)

we can note that the actual relative velocity of water is $\dot{w}/nS_w$.

So the absolute velocity of water (with respect an inertial frame) is

$$\dot{\vec{U}} = \dot{\vec{u}} + \frac{\dot{\vec{w}}}{nS_w}$$

(3.7)

where $\dot{\vec{u}}$ is the velocity of the solid phase and $\dot{\vec{w}}$ the velocity of the water.

Porous media like soil, rock and concrete are composed by mass of solid grains separated by spaces or voids. As we said first, it is assumed that voids in a porous medium are filled with air or water or both. If only air is present the porous medium is defined like *dry*, while if only water is present the porous medium is called *saturated*. When both air and water are present, the porous medium is called *partially saturated*. For these three conditions, it is very important to define the following physical quantities:

$$S_w = \frac{volume\ of\ water}{volume\ of\ voids}$$

the degree of saturation of water

$$S_a \frac{volume\ of\ air}{volume\ of\ voids}$$

the degree of saturation of air;

Obviously their summation must be equal to the unit according to

$$S_w + S_a = 1$$

3.1.4 Effective stress in partially saturated soils

The concept of the effective stress was introduced by Terzaghi, that showed experimentally that the effective stress is able to control the deformations of the solid skeleton. For saturated soils, Terzaghi related the vector of the effective stress $\vec{\sigma}'$ to the total stress and the water pressure according to

$$\vec{\sigma} = \vec{\sigma}' - \vec{m}p_w$$

(3.8)

where $\vec{m}^T = [1,1,1,0,0,0]$.

The discovery of the principle of effective stress marks the beginning of the era of modern soil engineering and it is at the basis of the mathematical theory we are developing.

For saturated soils, this principle was confirmed with high accuracy, provided that the solid grain is small compared with that of the overall solid skeleton.

For partially saturated soils, the validity of the principle of effective stress has been questioned. However if we would like to extend it to the unsaturated zones, we could use the Bishop's relation which states

$$\vec{\sigma} = \vec{\sigma}' - \vec{m}p$$

(3.9)

where

$$p = \mathrm{X}p_w + (1 - \mathrm{X})p_a$$

(3.10)

where X is the Bishop's parameter, which was suggested like dependent on the degree of saturation of water. However it is possible to state that X is dependent on other factors like the soil structure and the process of wetting and drying. In the previous expression, we can consider

the pressure p like the pressure acting on the solid grains so that the physical meaning of the Bishop's relation is to relate the pressure on the solid grains to the pressure of water and air inside the medium. A typical approximation of the Bishop's parameter is

$$\mathrm{X}{\sim}S_w$$

so that

$$p = S_w p_w + S_a p_a \tag{3.11}$$

$$\vec{\sigma} = \vec{\sigma}' - \vec{m}(S_w p_w + S_a p_a) \tag{3.12}$$

In the following equations, we will not consider the vector notation for the symbols already introduced.

The previous equations can be further simplified by the assumption of the zero air pressure so that

$$p = S_w p_w$$

$$\vec{\sigma} = \vec{\sigma}' - \vec{m}(S_w p_w)$$

Now, if we would like to take into account the compressibility of the solid grains, the equation of the effective stress could be modified according to

$$\vec{\sigma} = \vec{\sigma}'' - \vec{m}\alpha p \tag{3.13}$$

where $\vec{\sigma}''$ is the real effective stress vector and α the coefficient of compressibility of the solid grains which is equal to 1 for most soils and goes from 0.4 to 0.6 for rocks or concrete (it is in these cases that it is important to take it into account).

3.1.5 Partial saturation and capillary pressure

There is much evidence that a liquid solid interface resists tensile forces because of the attraction between adjacent molecules in the surface. It is such interface tension that causes the phenomenon of capillarity. Capillarity enables a dry soil to draw water to elevations above the phreatic line and it also enables a draining soil mass to retain water above the phreatic line. The height of water column a soil can support, depends on the capillary pressure difference p_c, which is defined as

$$p_c = p_a - p_w$$

(3.14)

The value of the capillary forces is inversely proportional to the size of soil void at the air-water interface. Owing to the great difference in the particle size within sands and clays, there will be a great difference in the capillary tensions that may develop within two classes of soils, i.e. letting us achieve large capillary tensions for clays and very small ones for sands.

In the hypothesis of zero air pressure, obviously

$$p_c = -p_w$$

So, negative water pressures are thus maintained in the partially saturated soils through the mechanism of the capillary force and such negative pressures provide a cohesive effect in the partially saturated zones. By the Equations of the capillary pressure and of the pressure on the solid skeleton, we can write the effective stress like

$$\vec{\sigma}' = \vec{\sigma} - \vec{m} S_w p_c$$

(3.15)

Now, the capillary pressure is dependent on the size of the soil void; for a given granular material with specific void ratio, and under isothermal conditions, we can assume that there exists a unique function

$$p_c = p_c(S_w)$$

(3.16)

If water flows occurs, by similar arguments, we can state that there exists a unique function such that

$$\vec{k}_w = \vec{k}_w(S_w)$$

or

$$\vec{k}_w = \vec{k}_w(p_c)$$

Obviously the determination of these two last relations was the effect of extensive experimental studies.

3.1.6 Constitutive relations

In absence of significant rotations, the constitutive law relating the effective stress change $d\vec{\sigma}'$ to the total strain $d\varepsilon$ is

$$d\vec{\sigma}' = \vec{D}(d\vec{\varepsilon} - d\vec{\varepsilon}^0 - d\vec{\varepsilon}^p)$$

(3.17)

where $d\vec{\varepsilon}^0$ is the change of initial strain due to the non stress effects like temperature, creep or soil wetting. We will assume that these effects are not present.

Then $d\vec{\varepsilon}^p$ is the change of volumetric strain due to the uniform compression of the solid grains, that can be written like

$$d\vec{\varepsilon}^p = -\vec{m}\frac{dp}{3K_s}$$

(3.18)

where K_s is the average bulk modulus of the grains. So if we substitute this last equation in the constitutive law and we neglect the second contribute,

$$d\vec{\varepsilon}^p = \vec{D}(d\vec{\varepsilon} + \vec{m}\frac{dp}{3K_s})$$

(3.19)

It could be more convenient to write the constitutive law like

$$d\vec{\sigma}'' = \vec{D}d\vec{\varepsilon}$$

(3.20)

Forgetting the vector notation. Comparing the 3.17, 3.18 and 3.19

we arrive to

$$\alpha\vec{m} = \vec{m} - \frac{\vec{D}\vec{m}}{3K_s}$$

(3.21)

from which, pre multiplying by $\vec{m}^T$, we get

$$\alpha = 1 - \frac{\vec{m}^T\vec{D}\vec{m}}{9K_s}$$

(3.22)

If we are going to consider isotropic materials, the quantity $\vec{m}^T[D]\vec{m}$ is equal to $9K_t$ where K_t is the bulk modulus of the overall soil mixture. So for isotropic materials,

$$\alpha = 1 - \frac{K_t}{K_s}$$

(3.23)

3.1.7 Momentum equilibrium equation

We assume that the system moves with the solid phase and hence the convective acceleration applies only to the fluid. For a unit volume of the soil mixture, the overall equilibrium equation relates the total stress $\vec{\sigma}$ and the body force $\vec{b}$ to the acceleration of the soil skeleton and the relative acceleration of water in the form

$$\vec{L}^T \vec{\sigma} - \rho \vec{b} = \rho \ddot{\vec{u}} + \rho_w n S_w \frac{D}{Dt}\left(\frac{\dot{\vec{w}}}{nS_w}\right)$$

(3.24)

where

$$\vec{L} = \begin{pmatrix} \partial_x & 0 & 0 \\ 0 & \partial_y & 0 \\ 0 & 0 & \partial_z \\ \partial_y & \partial_x & 0 \\ 0 & \partial_z & \partial_y \\ \partial_z & 0 & \partial_x \end{pmatrix}$$

(3.25)

is the differential operator, ρ_w the density of the water and ρ the density of the soil mixture, which is written like

$$\rho = \rho_s(1 - n) + \rho_w n S_w$$

(3.26)

In which ρ_s is the density of the grain. The weight of the air is neglected.

In the next, we introduce the momentum equilibrium equation for water alone. In the case of water passing through a soil, the validity of the Darcy law is assumed, so that for a unit volume, the Darcy law can be generalized to

$$\vec{k}_w^{\ -1}\dot{\vec{w}} = -\vec{\nabla}p_w + p_w(\vec{b} - \frac{D\dot{\vec{U}}}{Dt})$$

(3.27)

where $[k_w]$ is the dynamic permeability matrix of the water. For the isotropic case it is convenient to replace by a single k_w value. In the above the left hand side represents the viscous drag force resisting to the water flow and $\dot{\vec{U}}$ is the actual velocity of water while its acceleration

$$\frac{D\dot{\vec{U}}}{Dt} = \ddot{\vec{u}} + \frac{D}{Dt}(-\frac{\dot{\vec{w}}}{nS_w})$$

(3.28)

3.1.8 Water flow continuity equation

For a unit of soil mixture, the *rate* of water inflow is given by

$$-\vec{\nabla}^T\dot{\vec{w}}$$

Now, there are five factors that contribute to the change of water stored in the unit volume of the solid-fluid ensemble:

a) Volumetric strain of the soil skeleton

$$\vec{m}^T\partial\vec{\varepsilon}/\partial t$$

b) Compressive volumetric strain of the grain due to the pressure changes

$$\frac{1-n}{K_s}\frac{\partial p}{\partial t}$$

c) Compressive volumetric strain of water

$$\frac{\vec{m}S_w}{K_w}\frac{\partial p_w}{\partial t}$$

with K_w bulk modulus of water

d) Increase of water storage due to the saturation changes

$$n\frac{\partial S_w}{\partial t} = n\frac{\partial S_w}{\partial p_w}\frac{\partial p_w}{\partial t} = C_s\frac{\partial p_w}{\partial t}$$

Where C_s is the specific moisture capacity which can be in general evaluated from the $S_w - p_w$ curves as $n\frac{\partial S_w}{\partial p_w}$

e) Compressive volumetric strain of the grain due to effective stress

$$-\frac{1}{3K_s}\vec{m}^T\frac{\partial\vec{\sigma}'}{\partial t} = -\frac{1}{3K_s}\vec{m}^T\vec{D}\frac{\partial\varepsilon}{\partial t} - \vec{m}^T\vec{D}\vec{m}\frac{1}{(3K_s)^2}\frac{\partial p}{\partial t}$$

So the final continuity equation can be written like

$$-\nabla^T \dot{\vec{w}} = n\frac{S_w}{K_w}\frac{\partial p_w}{\partial t} + C_s\frac{\partial p_w}{\partial t} + S_w\left[\vec{m}^T - \frac{\vec{m}^T\vec{D}}{3K_s}\right]\frac{\partial \varepsilon}{\partial t} + S_w[\frac{(1-n)}{K_s} - \vec{m}^T\vec{D}\vec{m}\frac{1}{(3K_s)^2}]\frac{\partial p}{\partial t}$$

(3.29)

Putting together all the contributes. Using the definitions of p and α,

$$-\nabla^T \dot{\vec{w}} = n\frac{S_w}{K_w}\frac{\partial p_w}{\partial t} + C_s\frac{\partial p_w}{\partial t} + S_w\alpha\vec{m}^T\frac{\partial \varepsilon}{\partial t} + S_w[\frac{(\alpha-n)}{K_s}(S_w + \frac{C_s}{n}p_w)]\frac{\partial p_w}{\partial t}$$

(3.30)

That is the general equation for the continuity of water flow through a partially saturated porous medium.

3.1.9 Summary of governing equations

The equations we provided are able to describe the physics of all kinds of porous media including rocks, concrete and soils. We will summarize them in the following:

1) *EQUILIBRIUM OF SOIL MIXTURE*

$$\vec{L}^T\vec{\sigma} - \rho\vec{b} = \rho\vec{u} + \rho_w n S_w\frac{D}{Dt}(\frac{\dot{\vec{w}}}{nS_w})$$

2) *EQUILIBRIUM OF WATER*

$$\overrightarrow{k_w}^{-1}\vec{w} = -\vec{\nabla}p_w + p_w[\vec{b} - \ddot{\vec{u}} - \frac{D}{Dt}\left(\frac{\dot{\vec{w}}}{nS_w}\right)]$$

3) *CONTINUITY OF WATER FLOW*

$$-\vec{\nabla}^T\dot{\vec{w}} = n\frac{S_w}{\overrightarrow{K_w}}\frac{\partial p_w}{\partial t} + C_s\frac{\partial p_w}{\partial t} + S_w\alpha\vec{m}^T\frac{\partial \vec{\varepsilon}}{\partial t} + S_w[\frac{(\alpha-n)}{K_s}(S_w + \frac{C_s}{n}p_w)]\frac{\partial p_w}{\partial t}$$

4) *REAL EFFECTIVE STRESS*

$$\vec{\sigma} = \vec{\sigma}'' - \vec{m}\alpha S_w p_w$$

5) *CONSTITUTIVE RELATION*

$$d\vec{\sigma}'' = \vec{D}d\vec{\varepsilon}$$

6) *INCREMENTAL STRAIN*

$$d\vec{\varepsilon} = \vec{L}d\vec{u}$$

7) *PARTIAL SATURATION RELATIONSHIPS*

$$S_w = S_w(p_w)$$
$$\overrightarrow{k_w} = \overrightarrow{k_w}(p_w)$$
$$C_s = n\frac{\partial S_w}{\partial p_w}$$

The above system of equations is the generalized Biot formulation for dynamic behavior of saturated/unsaturated porous media. It consists of elementary equations like the momentum equation and the continuity equation plus some constitutive and experimental equations, introduced to close the system and to have a number of unknowns equal to the number of equations

This system of equation can be solved with some boundary conditions:

a) Prescribed displacements

$\vec{u} = \overrightarrow{u_b}$ on Γ_u at $t > 0$

b) Prescribed tractions

$\vec{t} = \overrightarrow{t_b}$ on Γ_t at $t > 0$

c) Prescribed water flow

$\dot{\vec{w}} = \dot{\vec{w}}_b$ on Γ_w at $t > 0$

that can be written as

$$\vec{k}_w\left(-\vec{\nabla}p_w + \rho_w\left[\vec{b} - \ddot{\vec{u}} - \frac{D}{Dt}\left(\frac{\dot{\vec{w}}}{nS_w}\right)\right]\right) = \dot{\vec{w}}$$

d) Prescribed water pressure

$p_w = p_{wb}$ on Γ_{p_w} at $t > 0$

The initial condition are

$$\vec{u} = \vec{u}_0$$

$$\dot{\vec{u}} = \dot{\vec{u}}_0$$

$$p_w = p_{w0}$$

The differential equation system (1-7) is characterized by nine unknowns:
$u, w, p_w, \varepsilon, \sigma, \sigma'', S_w, k_w, C_s$.

Now, to solve this system of equations, which is non linear, can be quite expensive; for this reason we have to introduce some simplifications. We will analyze two of them: the partially saturated dynamic u-p formulation and the fully saturated dynamic $u - p$ formulation.

3.1.10 Partially saturated dynamic U-P formulation

If we suppose that the acceleration of water with respect the soil skeleton is not significant compared to the motion of the soil skeleton itself, the variable w can be eliminated by dropping the acceleration terms associated with w by the assumption that

$$\frac{D\vec{w}}{Dt} \ll \ddot{\vec{u}}$$

or

$$\frac{D}{Dt}\left(\frac{\dot{\vec{w}}}{nS_w}\right) \ll \vec{u}$$

The validity of this assumption was discussed by Zienkiewicz et al [40]. The equation system can now be reduced by eliminating $\dot{w}$ between the second and the third equations of the system itself. So in the end

$$\begin{cases} \vec{L}^T\vec{\sigma} - \rho\vec{b} = \rho\ddot{\vec{u}} \\ \nabla^T\left[\overrightarrow{k_w}\left(\nabla p_w - \rho_w\left(\vec{b} - \ddot{\vec{u}}\right)\right)\right] = \dfrac{S_w}{K_w}\dfrac{\partial p_w}{\partial t} + C_s\dfrac{\partial p_w}{\partial t} + S_w\alpha m^T\dfrac{\partial\vec{\varepsilon}}{\partial t} + S_w\left[\dfrac{(\alpha - n)}{K_s}\left(S_w + \dfrac{C_s}{n}p_w\right)\right]\dfrac{\partial p_w}{\partial t} \\ \vec{\sigma} = \vec{\sigma}'' - \vec{m}\alpha S_w p_w \\ d\vec{\sigma}'' = \vec{D}d\vec{\varepsilon} \\ d\vec{\varepsilon} = \vec{L}d\vec{u} \\ \begin{cases} S_w = S_w(p_w) \\ \overrightarrow{k_w} = \overrightarrow{k_w}(p_w) \\ C_s = n\dfrac{\partial S_w}{\partial p_w} \end{cases} \end{cases}$$

This is the dynamic $u-p$ formulation for partially saturated porous media where the displacements u and the water pressure p_w are taken like primary unknowns.

3.1.11 Fully saturated dynamic U-P formulation

When the medium is fully saturated, we have the following conditions:

$$S_w = 1$$

$$\overrightarrow{k_w} = const$$

$$C_s = 0$$

$$p = p_w$$

The above system of equations further simplifies:

$$\begin{cases} \vec{L}^T\vec{\sigma} - \rho\vec{b} = \rho\ddot{\vec{u}} \\ \vec{\nabla}^T\left[\overrightarrow{k_w}\left(\nabla p_w - \rho_w\left(\vec{b} - \ddot{\vec{u}}\right)\right)\right] = \alpha\vec{m}^T\dfrac{\partial\vec{\varepsilon}}{\partial t} + S_w\left[\dfrac{n}{k_w} + \dfrac{\alpha - n}{k_s}\right]\dfrac{\partial p_w}{\partial t} \\ \vec{\sigma} = \vec{\sigma}'' - \vec{m}\alpha p_w \\ d\vec{\sigma}'' = \vec{D}d\vec{\varepsilon} \\ d\vec{\varepsilon} = \vec{L}d\vec{u} \\ nothing\ more \end{cases}$$

We quote other further simplifications of the main differential equation system:

1) The partially saturated consolidation form

$$\frac{D}{Dt}\left(\frac{\dot{\vec{w}}}{nS_w}\right) \to 0$$

$$\ddot{\vec{u}} \to 0$$

(in which we assume the acceleration forces to be negligible)

2) The partially saturated dynamic undrained form:

$$\dot{\vec{w}} \to 0$$

$$\frac{D}{Dt}\left(\frac{\dot{\vec{w}}}{nS_w}\right) \to 0$$

Where the application of the load is so rapid or the permeability is so small that no important drainage occurs;

3) The fully saturated dynamic undrained form

Equal to the partially saturated dynamic undrained form with the conditions

$$S_w = 1$$

$$\vec{k}_w = const$$

$$C_s = 0$$

$$p = p_w$$

That simplify the system

4) The fully saturated consolidation form

equal to 1) with

$$S_w = 1$$

$$\vec{k}_w = const$$

$$C_s = 0$$

$$p = p_w$$

Obviously the choice of the approximation depends on the kind of problem we want to solve and on the kind of system we are dealing.

3.2 Discretization and solution of the governing equations

We have presented the governing equations for a porous medium and as we noticed, we are dealing with a coupled problem structure-fluid. The non linear equations we derived, are extremely difficult to solve from an analytic viewpoint even if in literature we can find some examples of solutions for simple systems. Furthermore, some attempts to solve these equations through the finite difference methods can be found. But in dealing with problems of complex geometry and arbitrary non linearity, the finite difference method is difficult to apply. For this reason the finite element method became so popular.

3.2.1 Finite element Discretization

Generally a boundary value problem can be represented as

$$\vec{A}(u) = \vec{C}\vec{u} + \vec{p} = \vec{0} \quad in\ \Omega$$

(3.31)

$$\vec{B}(u) = \vec{D}\vec{u} + \vec{q} = \vec{0} \quad in\ \Gamma$$

(3.32)

where $[C], [D]$ are differential operators, linear or non linear, $\vec{p}, \vec{q}$ are functions defined in the domain Ω and on the boundary Γ and u is the exact solution to the previous governing equations, subject to the boundary conditions.

For most practical problems the exact solution can be impossible to find, so some approximate methods are necessary. For instance it is possible to build an approximation $\vec{u}^*$ of the solution $\vec{u}$ using a series of shape functions with a set of unknown parameters. When the approximation $\vec{u}^*$ is substituted inside the previous equations, the equations themselves are not satisfied and the residual in the domain

$$\vec{R}_\Omega = \vec{A}(\vec{u}^*) = \vec{A}\vec{u}^* + \vec{p} \quad in\ \Omega$$

(3.33)

is supplemented by a boundary residual

$$\vec{R}_\Gamma = \vec{B}(\vec{u}^*) = \vec{A}\vec{u}^* + \vec{q} \quad in\ \Gamma$$

(3.34)

These residuals are different from zero but they can be made to zero in some "weighted" sense by writing

$$\int_\Omega \vec{W}^T \vec{R}_\Omega d\,\Omega + \int_\Gamma \vec{W}'^T \vec{R}_\Gamma d\,\Gamma = 0$$

(3.35)

or

$$\int_\Omega \vec{W}^T (\vec{C}\vec{u}^* + \vec{p}) d\,\Omega + \int_\Gamma \vec{W}'^T (\vec{D}\vec{u}^* + \vec{q}) d\,\Gamma = 0$$

(3.36)

where the functions $\vec{W}^T$ and $\vec{W}'^T$ can be chosen independently. The above method is the so called weighted residual method. We will not apply it to the saturated dynamic $u - p$ formulation.

Let us apply the equation 3.36 to the equilibrium equation of partially dynamic formulation and its boundary condition:

let us forget the vector notation for the symbol we already introduced. So

$$\int_\Omega \vec{W}^T (\vec{L}^T \vec{\sigma} - \rho\vec{b} - \rho\ddot{\vec{u}}) d\,\Omega + \int_\Gamma \vec{W}'^T (\vec{l}^T \vec{\sigma} - \vec{t}) d\,\Gamma = 0$$

(3.37)

Now, if we use the Green's theorem, the first term on the left hand side can be replaced by

$$\int_{\Omega} (\vec{L}\vec{W})^T \vec{\sigma} d\Omega + \oint_{\Gamma_u+\Gamma_t} \vec{W}^T \vec{l}^T \vec{\sigma}\, d\Gamma$$

(3.38)

Limiting the choice of the weighting function to

$$W = 0 \;\; on\, \Gamma_u$$

and

$$W' = -W \;\; on\, \Gamma_t$$

The equation 3.37 is reduced to

$$\int_{\Omega} (\vec{L}\vec{W})^T \vec{\sigma} d\Omega + \oint_{\Gamma_u+\Gamma_t} \vec{W}^T \rho \ddot{\vec{u}}\, d\Omega = \int_{\Omega} \vec{W}^T \rho \vec{b}\, d\Omega + \oint_{\Gamma_t} \vec{W}^T \vec{t} d\Gamma$$

(3.39)

The continuity equation of water can be rewritten by substituting the equation

$$d\vec{\varepsilon} = \vec{L} d\vec{u}$$

in

$$\nabla^T \left[\overrightarrow{k_w}\left(\nabla p_w - \rho_w(\vec{b} - \ddot{\vec{u}})\right)\right] = \frac{S_w}{K_w}\frac{\partial p_w}{\partial t} + C_s \frac{\partial p_w}{\partial t} + S_w \alpha m^T \frac{\partial \vec{\varepsilon}}{\partial t} + S_w \left[\frac{(\alpha - n)}{K_s}\left(S_w + \frac{C_s}{n} p_w\right)\right]\frac{\partial p_w}{\partial t}$$

as

$$\vec{\nabla}^T\left[\overrightarrow{k_w}\nabla p_w + \overrightarrow{k_w}\,\rho_w(\vec{b} - \ddot{\vec{u}})\right] + S_w \alpha \vec{m}^T \vec{L}\dot{\vec{u}} + \frac{1}{Q^*}\dot{p} = 0$$

(3.39 a)

if we define

$$\frac{1}{Q^*} = C_s + n\frac{S_w}{K_w} + S_w\frac{\alpha - n}{K_s}\ (S_w + \frac{C_s}{n}p_w)$$

(3.40)

From the assumptions

$$\frac{D\vec{w}}{Dt} \ll \ddot{\vec{u}}$$

or

$$\frac{D}{Dt}\left(\frac{\dot{\vec{w}}}{nS_w}\right) \ll \ddot{\vec{u}}$$

for the dynamic $u - p$ formulation, the boundary condition

$$\vec{k}_w\left(-\vec{\nabla}p_w + \rho_w\left[\vec{b} - \ddot{\vec{u}} - \frac{D}{Dt}\left(\frac{\dot{\vec{w}}}{nS_w}\right)\right]\right) = \dot{\vec{w}}$$

can be simplified as

$$\vec{k}_w\left(-\vec{\nabla}p_w + \rho_w(\vec{b} - \ddot{\vec{u}})\right) = \dot{\vec{w}} \quad on\ \Gamma_u$$

(3.41)

Again, the weighted residual method to the continuity equation of water flow (3.39 a) and the boundary condition (3.41), we can write

$$\int_\Omega \overrightarrow{W}^{*T}[\vec{\nabla}^T\left(-\overrightarrow{k_w}\left(\vec{\nabla}p_w - \rho_w(\vec{b} - \ddot{\vec{u}})\right)\right) + S_w\alpha\overrightarrow{m}^T\vec{L}\dot{\vec{u}} + \frac{1}{Q^*}\dot{p}\ d\Omega]$$
$$+ \int_{\Gamma_W} \overrightarrow{W}^{*T}[(-\overrightarrow{k_w}(\vec{\nabla}p_w - \rho_w(\vec{b} - \ddot{\vec{u}}) - \dot{\vec{w}})^T)n]\ d\Gamma = 0$$

(3.42)

where W^* and $\overline{W}^*$ are arbitrary weighting functions. It is assumed that the boundary condition of $p_w = \overline{p_w}$ on Γ_{pw} is satisfied by the choice of the approximation of p_w.

Applying the Green's theorem to the underlined terms of the above equation and limiting the choice of the weighting functions so that

$$W = 0 \ \ on \ \Gamma_p$$

and

$$W' = -W \ \ on \ \Gamma_w$$

The equation (3.42) is now rewritten like

$$\int_{\Omega} \vec{W}^{*T}[-(\vec{\nabla}\vec{W}^{*})^{T}\left(-\vec{k}_w\left(\vec{\nabla}p_w - \rho_w(\vec{b} - \ddot{\vec{u}})\right)\right) + \vec{W}^{*T}S_w\alpha\vec{m}^{T}\vec{L}\dot{\vec{u}} + \vec{W}^{*T}\frac{1}{Q^{*}}\dot{p}\ ]d\Omega + \int_{\Gamma_W} \vec{W}^{*T}\dot{\vec{w}}^{-T}n \ d\Gamma = 0$$

(3.43)

Following the standard procedure of the finite element method, the domain Ω is first divided into subdomains/elements, then the displacements and pore water pressure fields within an element are expressed in terms of a finite number of nodal values and interpolation (shape) functions

$$\vec{u}^{e} = \sum_{i=1}^{m} \vec{N}_{ui}^{e}\ \vec{u}_i^{e} = \vec{N}_u^{e}\vec{u}^{e}$$

(3.44)

and

$$p_w^{e} = \sum_{i=1}^{N} \vec{N}_{pj}^{e}\ p_{wj}^{e} = \vec{N}_p^{e}\vec{p}_w^{e}$$

(3.45)

where the superscript 'e' denotes the element under consideration and

$$\vec{u}_i^{e} = [u_{ix}, u_{iy}, u_{iz}]$$

(3.46)

is the displacement at the node i

$$\vec{\bar{u}}^e = [u_1^{e^T} \dots u_i^{e^T} \dots . u_m^{e^T}]^T$$

(3.47)

is the nodal displacement vector

$$p_{wj}^e$$

is the water pressure at node j

$$\vec{\bar{p}}_w^e = \left[p_{w1}^e \dots p_{wj}^e \dots p_{wn}^e\right]^T$$

(3.48)

is the nodal water pressure vector

m is the number of nodes per element for the shape function of the displacement

n is the number of nodes per element for the shape function of the water pressure

$$\vec{N}_u^e = [N_{u1}^e I \dots N_{ui}^e I \dots p_{wm}^e I]$$

(3.49)

is the shape function for the displacement (I_3 is a $3x3$ identity matrix)

$$\vec{N}_p^e = \left[N_{p1}^e \dots N_{pj}^e \dots N_{pn}^e\right]$$

(3.50)

is the shape function for the water pressure.

As the whole domain is concerned, the summation of all element contributions can be represented in terms of global shape functions as

$$\vec{u} = \vec{N}_u \vec{\bar{u}}$$

(3.51)

and

$$p_w = \vec{N}_p \overrightarrow{\overrightarrow{p_w}}$$

(3.52)

Many choices of elements are flexible, although generally isoparametric elements are chosen, in which the coordinates within an element are interpolated with the same shape function as in the displacement representation (3.51).

Now, we introduced all the vector quantities we need to keep on the description of the finite element method. For this reason, to make our writing simpler, we will omit it from this point ahead.

Substituting the approximations (3.51) and (3.52) for the displacement and water pressure into the equations (3.43) and (3.61) and taking the shape functions themselves as the weighting functions by the Galerkin method, we arrive to

$$\int_\Omega \left(\vec{L}\vec{N}_u\right)^T \vec{\sigma}\, d\Omega + \int_\Omega \vec{N}_u^T \rho \vec{N}_u \vec{u}\, d\Omega = \int_\Omega \vec{N}_u^T \rho \vec{b}\, d\Omega + \int_{\Gamma_t} \vec{N}_u^T \vec{t}\, d\Gamma$$

(3.53)

and

$$\begin{aligned}\int_\Omega \left(\vec{\nabla}\vec{N}_p\right)^T \vec{k}_w \vec{\nabla}\vec{N}_p p_w\, d\Omega \\ - \int_\Omega \left(\vec{\nabla}\vec{N}_p\right)^T \vec{k}_w \rho_w \vec{b}\, d\Omega \\ + \int_\Omega \left(\nabla\vec{N}_p\right)^T \vec{k}_w \rho_w \vec{N}_p \ddot{\vec{u}}\, d\Omega \\ + \int_\Omega \vec{N}_p^T S_w \alpha \vec{m}^T \vec{L}\vec{N}_u \dot{\vec{u}}\, d\Omega + \int_\Omega \vec{N}_p^T \frac{1}{Q^*} \vec{N}_p \dot{p}\, d\Omega + \int_{\Gamma_W} \vec{N}_p^T \dot{\vec{w}}^T n\, d\Gamma = 0\end{aligned}$$

(3.54)

with the representation of $\vec{\sigma}$ in equation (3.13) and ϱ in equation (3.26), (3.53 and 3.54) can be written as

$$\int_{\Omega} \vec{B}^T \vec{\sigma}'' d\Omega - \vec{\mathrm{Q}}\vec{p}_w + \vec{M}\ddot{\vec{u}} = \vec{f}^u$$

(3.55)

$$\vec{H}\vec{p}_w + \vec{G}\ddot{\vec{u}} + \vec{Q}^T\dot{\vec{u}} + \vec{S}\dot{\vec{p}}_w = \vec{f}^p$$

(3.56)

We will not use anymore the vector notation from now in order to simplify the notation.

In the previous formula

$$B = LN_u$$

is the strain operator

$$Q = \int_{\Omega} B^T S_w \alpha m N_p d\Omega$$

(3.57)

the coupling matrix

$$H = \int_{\Omega} \left(\nabla N_p\right)^T k_w \, \nabla N_p \, d\Omega$$

(3.58)

the permeability matrix

$$M = \int_{\Omega} N_p^T [\varrho_s(1-n) + \varrho_w n S_w \,] \, N_u \, d\Omega$$

(3.59)

the mass matrix

$$G = \int_{\Omega} \left(\nabla N_p\right)^T k_w \varrho_w N_u \; d\Omega$$

(3.60)

the dynamic seepage forcing matrix

$$S = \int_{\Omega} \left(N_p\right)^T \frac{1}{Q^*} N_p \; d\Omega$$

(3.61)

the compressibility matrix, with

$$f_u = \int_{\Omega} N_u^T [\varrho_s(1-n) + \varrho_w n S_w \,] \, b \, d\Omega + \int_{\Gamma_t} N_u^T t \, d\Gamma$$

(3.62)

$$f_p = \int_{\Omega} \left(\nabla N_p\right)^T k_w \varrho_w b \, d\Omega - \int_{\Gamma_t} N_p^T \dot{w}^T \, n \, d\Gamma$$

(3.63)

It is important to notice that the choice of the shape functions N_u and N_p must be of C_0 continuity.

Now, let us analyse the first term in (3.55): this term here represents the internal force and it is a function of displacement written as

$$\int_{\Omega} B^T \sigma'' d\Omega = \mathrm{P(u)}$$

(3.64)

For the isotropic linear elastic case, the constitutive relation can be replaced as

$$\sigma'' = D_e \varepsilon = D_e L u = D_e L N_u u = D_e B u$$

(3.65)

So the internal force term can be written as

$$\int_{\Omega} B^T \sigma'' d\Omega = \int_{\Omega} B^T D_e B u \, d\Omega = K_e u$$

(3.66)

In which we clearly recognize the elastic stiffness matrix, which is symmetric. However, in general problems characterized by a non linearity, the stiffness matrix can be a function of the displacements or of the strains: so function of the solution itself. The problem in these cases is non linear and only the tangential stiffness matrix can be written

$$K_T = \frac{\partial P(u)}{\partial u} = \int_{\Omega} B^T D_e B \, d\Omega$$

(3.67)

What about the effect of the dynamic seepage matrix? Its effect can be can be of importance only in the high frequency range where the $u - p$ formulation is no longer valid. Here we will assume that the dynamic seepage forcing term $G\ddot{u}$ is negligible and therefore omitted in the later discussions.

The resulting forms of the equations obtained can be summarized like:

1) *dynamic form*

$$\int_{\Omega} B^T \sigma'' d\Omega - \mathrm{Q} p_w + M\ddot{u} = f^u$$

$$H p_w + Q^T \dot{u} + S\dot{p}_w = f^p$$

2) *consolidation form*

$$\int_{\Omega} B^T \sigma'' d\Omega - \mathrm{Q} p_w = f^u$$

$$H p_w + Q^T \dot{u} + S\dot{p}_w = f^p$$

3) *dynamic undrained form*

$$\int_{\Omega} B^T \sigma'' d\Omega - \mathrm{Q} p_w + M\ddot{u} = f^u$$

$$Q^T \dot{u} + S\dot{p}_w = f^p$$

4) *static drained form*

$$\int_{\Omega} B^T \sigma'' d\Omega - \mathrm{Q} p_w = f^u$$

$$H p_w = f^p$$

For the fully saturated case, even if the equation system takes the same form as represented above, the matrixes are clearly different and this must be taken into account;

Resuming, we have:

Partially saturated

$$\begin{cases} Q = \int_{\Omega} B^T S_w \alpha m N_p d\Omega \\ M = \int_{\Omega} N_p^T [\varrho_s (1-n) + \varrho_w n S_w \,] \, N_u \, d\Omega \\ H = \int_{\Omega} (\nabla N_p)^T k_w \, \nabla N_p \, d\Omega \\ S = \int_{\Omega} (N_p)^T \frac{1}{Q^*} N_p \; d\Omega \\ f^u = N_u^T [\varrho_s (1-n) + \varrho_w n S_w \,] \, b \, d\Omega + \int_{\Gamma_t} N_u^T t \, d\Gamma \\ f_p = \int_{\Omega} N_u^T [\varrho_s (1-n) + \varrho_w n S_w \,] \, b \, d\Omega + \int_{\Gamma_t} N_u^T t \, d\Gamma \end{cases}$$

with

$$\begin{cases} k_w = k_w(p_w) \\ \frac{1}{Q^*} = C_s + n \frac{S_w}{K_w} + S_w \frac{\alpha - n}{K_s} \, (S_w + \frac{C_s}{n} p_w) \end{cases}$$

Fully saturated

$$\begin{cases} Q = \int_\Omega B^T S_w \alpha m N_p d\Omega \\ M = \int_\Omega N_p^T [\varrho_s(1-n) + \varrho_w n S_w \,] N_u \, d\Omega \\ H = \int_\Omega \left(\nabla N_p\right)^T k_w \, \nabla N_p \, d\Omega \\ S = \int_\Omega \left(N_p\right)^T \frac{1}{Q^*} N_p \; d\Omega \\ f^u = N_u^T [\varrho_s(1-n) + \varrho_w n \,] \, b \, d\Omega + \int_{\Gamma_t} N_u^T t \, d\Gamma \\ f_p = \int_\Omega N_u^T [\varrho_s(1-n) + \varrho_w n \,] \, b \, d\Omega + \int_{\Gamma_t} N_u^T t \, d\Gamma \end{cases}$$

with

$$\begin{cases} k_w = const \\ \frac{1}{Q^*} = \frac{n}{K_w} + \frac{\alpha - n}{K_s} \end{cases}$$

For the accuracy of the solution for these systems of equations, we quote Lewis et al., (1998).

In the next pages, we will discretize in time these last two systems of equation by using the GN22 Newmark algorithm.

3.2.2 Discretisation in time

If we write this system of equation at the time step $n+1$, we have

$$[\int_\Omega B^T \sigma'' d\Omega]_{n+1} - Q_{n+1} p_{n+1} + M_{n+1} \ddot{u}_{n+1} = {f^u}_{n+1}$$

$$H_{n+1} p_{n+1} + {Q_{n+1}}^T \dot{u}_{n+1} + S_{n+1} \dot{p}_{n+1} = {f^p}_{n+1}$$

that can be written in matrix form like:

$$\begin{pmatrix} M_{n+1} & 0 \\ 0 & 0 \end{pmatrix} \begin{pmatrix} \ddot{u}_{n+1} \\ \ddot{p}_{n+1} \end{pmatrix} + \begin{pmatrix} C_{n+1} & 0 \\ {H_{n+1}}^T & S_{n+1} \end{pmatrix} \begin{pmatrix} \dot{u}_{n+1} \\ \dot{p}_{n+1} \end{pmatrix} + \begin{pmatrix} K_{n+1} & -Q_{n+1} \\ {H_{n+1}}^T & S_{n+1} \end{pmatrix} \begin{pmatrix} u_{n+1} \\ p_{n+1} \end{pmatrix} = \begin{pmatrix} {f^u}_{n+1} \\ {f^p}_{n+1} \end{pmatrix}$$

where we added the damping matrix C for the solid part and where

$$p_{n+1} = p_w$$

Before analysing the algorithm of discretization in time for this system it is useful to understand how it is possible to discretize the same system without fluid inside.

3.3 The case of the solid without fluid

3.3.1 Equations

In order to compute the dynamical evolution of a simple elastic system without fluid, we need to use the Finite Element Method (FEM) to discretize in space and the Newmark method to discretize in time, the last one the most popular for dynamic analysis.

The system of differential equation we have to solve is, by switching off the fluid

$$\begin{cases} L^T\sigma - \rho b = \rho\ddot{u} + \mu\dot{u} \\ no\ equation\ for\ water \\ no\ equivalent\ stress \\ d\sigma = Dd\varepsilon \\ d\varepsilon = Ldu \\ no\ constitutive\ relations \end{cases}$$

where we have considered a linear viscous type resistance, resulting in a unit volume force like $\mu\dot{u}$. In the above, μ is a viscosity parameter which expresses a frictional resistance opposing to the motion. This may be due to the microstructure movements, air resistance etc. This kind of force is often related to the velocity in a non linear way, but for simplicity we will suppose that it will be $\mu\dot{u}$ with μ constant.

3.3.2 Discretization in time for the solid problem

So using the FEM, again switching of the fluid, the discretization in space gives us the following matrix equation

$$M\ddot{u} + C\dot{u} + Ku = f$$

(3.68)

where M is the mass matrix, C is the damping matrix and K the stiffness matrix while u is the vector of the displacements of the nodes of the structure, $\dot{u}$ the vector of the velocities and $\ddot{u}$ the vector of the accelerations. f instead is the vector of the nodal forces. The following step is to use a method to discretize in time the Equation (3.68). For this purpose we can use the method GN22 of the Newmark's family (Zienkiewicz, the finite element method, volume 1)

From Zienkiewicz, it is possible to write this vector and the velocity vector like a Taylor expansion:

$$u_{n+1} = u_n + \Delta t\dot{u}_n + \frac{1}{2}(1-\beta_2)\Delta t^2\ddot{u}_n + \frac{1}{2}(\beta_2)\Delta t^2\ddot{u}_{n+1}$$

(3.69)

$$\dot{u}_{n+1} = \dot{u}_n + \frac{1}{2}(1-\beta_1)\Delta t^2 \ddot{u}_n + \beta_1 \Delta t \quad \ddot{u}_{n+1}$$

(3.70)

where the two parameters $\beta_1 = \beta_2 = 0.5$.
These two equations together to the dynamic equation written for the station $n+1$,

$$M\ddot{u}_{n+1} + C\dot{u}_{n+1} + Ku_{n+1} = f_{n+1}$$

(3.71)

allow us the three unknowns u_{n+1}, $\dot{u}_{n+1}$, $\ddot{u}_{n+1}$ to be determined. If we express the (3.69) in terms of

u_{n+1} we have

$$\ddot{u}_{n+1} = \widehat{\ddot{u}_{n+1}} + \frac{2}{\beta_2 \Delta t^2} u_{n+1}$$

(3.72)

$$\dot{u}_{n+1} = \widehat{\dot{u}_{n+1}} + \frac{2\beta_1}{\beta_2 \Delta t} u_{n+1}$$

(3.73)

where

$$\widehat{\ddot{u}_{n+1}} = -\frac{2}{\beta_2 \Delta t^2} u_n - \frac{2}{\beta_2 \Delta t} \dot{u}_n - \frac{1-\beta_2}{\beta_2} \ddot{u}_n$$

(3.74)

$$\widehat{\ddot{u}_{n+1}} = -\frac{2\beta_1}{\beta_2 \Delta t} u_n - (1 - \frac{2\beta_1}{\beta_2})\dot{u}_n - (\frac{\beta_2 - \beta_1}{\beta_2})\Delta t \ddot{u}_n$$

(3.75)

These values are substituted into (3.71) and we get

$$u_{n+1} = -A^{-1}(f_{n+1} + C\widehat{\dot{u}_{n+1}} + M\widehat{\ddot{u}_{n+1}})$$

(3.76)

where

$$A = \frac{2}{\beta_2 \Delta t^2} M + \frac{2\beta_1}{\beta_2 \Delta t} C + K$$

(3.77)

We can compute then the accelerations by the (3.72) and (3.73).

Newmark's algorithm is used to solve a problem

$$M\ddot{u} + C\dot{u} + Ku = f$$

So, it is possible to apply it to the porous medium if we write the system

$$[\int_\Omega B^T \sigma'' d\Omega]_{n+1} - Q_{n+1} p_{n+1} + M_{n+1} \ddot{u}_{n+1} = {f^u}_{n+1}$$

$${H_{n+1} p_{n+1} + Q_{n+1}}^T \dot{u}_{n+1} + S_{n+1} \dot{p}_{n+1} = {f^p}_{n+1}$$

as

$$\begin{pmatrix} M_{n+1} & 0 \\ 0 & 0 \end{pmatrix}\begin{pmatrix} \ddot{u}_{n+1} \\ \ddot{p}_{n+1} \end{pmatrix} + \begin{pmatrix} C_{n+1} & 0 \\ {H_{n+1}}^T & S_{n+1} \end{pmatrix}\begin{pmatrix} \dot{u}_{n+1} \\ \dot{p}_{n+1} \end{pmatrix} + \begin{pmatrix} K_{n+1} & Q_{n+1} \\ {H_{n+1}}^T & S_{n+1} \end{pmatrix}\begin{pmatrix} u_{n+1} \\ p_{n+1} \end{pmatrix} = \begin{pmatrix} {f^u}_{n+1} \\ {f^p}_{n+1} \end{pmatrix}$$

(3.78)

where

$$Meq = \begin{pmatrix} M_{n+1} & 0 \\ 0 & 0 \end{pmatrix}$$

(3.79)

$$Ceq = \begin{pmatrix} C_{n+1} & 0 \\ {H_{n+1}}^T & S_{n+1} \end{pmatrix}$$

(3.80)

$$Keq = \begin{pmatrix} K_{n+1} & Q_{n+1} \\ {H_{n+1}}^T & S_{n+1} \end{pmatrix}$$

(3.81)

The following step is to assembly the mass matrix M, the stiffness matrix K and the damping matrix C. We will describe this step in Chapter 4.

Chapter 4

The statistical central force model

"Fracking ensures that the age of oil-and it's princely hydrocarbon cousin, the natural gas molecule-will not end because we have run out of fossil fuels. But it may end because burning these wonderful fuels puts the planet farther down a path we don't want to head down"

Russel Gold

In this chapter we will implement the method of the force central model applied for the dynamics. Milanese Schrefler and Molinari (2016) already applied it to a generic medium and to a porous medium in static. The following step is to apply it to the dynamics; the reason for which we apply it to the dynamics is that in many circumstances in the fracture processes, it is not possible to forget the dynamics effects on the structure: when a force changes in time not slowly in fact we need to consider the inertial and damping effects on the whole structure. Second, this tool was originally realized to give a response about the fracking in the soils. Obviously it is possible to extend it to other kind of processes, from the simple fracture in a material to the spalling into the concrete because of a thermal load from the external environment; but if we think about the phenomenon of the fracking, it is not possible not to take into account that in this process the dynamical effects come into play.

4.1 Analogies between RFM and FBM

4.1.1 Introduction

Why the necessity to extend the CFBM to a generic medium? In more realistic situations, the solid is not homogeneous and the disorder, in forms of microcracks or vacancies, strongly affects the nucleation process. Cracks for example may start from different defects and they can coalesce in contrast with the theories of Griffith.

The idea to apply this algorithm was born from a paper by Vespignani, Zapperi and Stanley on the so called Random Fuse Model (RFM). This particular kind of model is quite simple because of its scalar nature, given by the law

$$KV = I$$

(4.1)

where I is the current, V the potential and K the conductivity.

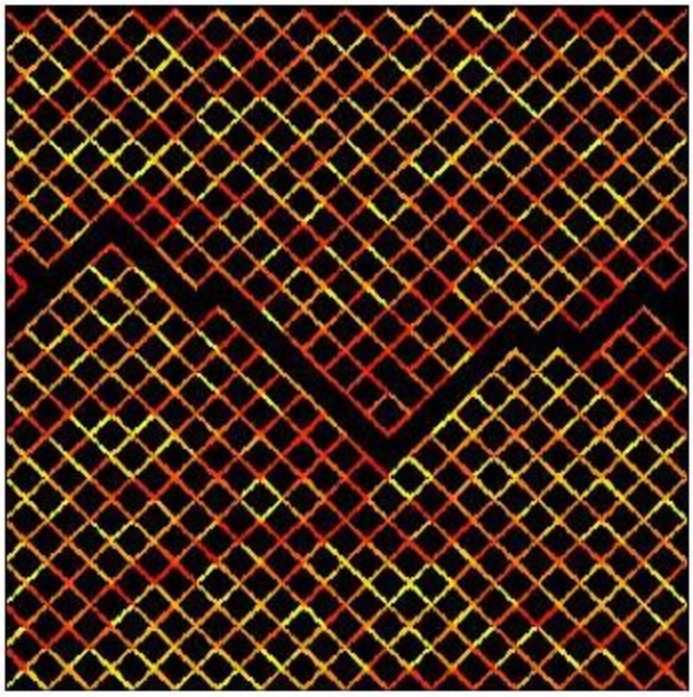

*Figure 4.1: a simple image of the RFM (*Zapperi et al.*, 1999)*

Let us describe briefly the RFM; consider a lattice whose dimensions are LxL. Our lattice is characterized by a number of bonds which are linked by a given network (fig 4.1). At each bond of the lattice, we associate a fuse in which the conductivity is $K_i = 1$. A potential V is applied to the system at the edges of the lattice: on one edge it is fixed while on the other edge it changes very slowly; so a global potential ΔV will act on the lattice and it will change in time allowing us to state that the system is loaded in static conditions. So a resultant current will cross the system and each bond; this current will be found by solving the so called Kirchoff equations for each node. If the current in a bond exceeds a threshold D_i, which is spread out according to a p.d.f. for each bond, the bond itself becomes an insulator ($K_i = 0$). The equilibrium is computed again into the system and because of the breaking of one bond, it is possible that other bonds will break, giving rise to an avalanche behavior. The process will stop when for a given ΔV imposed from the external environment, the system will be in equilibrium without further breakings. So in this kind of model, either the bonds are operational or are damaged.

Obviously the study of the RFM according to the introduction of the disorder is a direct application of the FBM to a different but similar physical problem and it is the extension to the 2D of a 1D problem represented by the dry FBM itself.

4.2 Extension of the CFBM to a Truss Lattice Model

4.2.1 Description of the model

So in this case we could bring the fibers of the "bundle" in a 2D lattice. Why to extend the CFBM to a truss lattice?

The dry FBM and one of its extension, the CFBM, are able to analyze the breakdown of a simple mono dimensional problem; for given value of the damage parameter a, it is possible to recover the constitutive behavior of some ceramic composites (Kun, Hermann, Hidalgo) but in this context it is not possible to pick up all the features of a 2D or 3D fracture process; for example in 2D in a real structure, pulled from two edges, we expect that because of the load, the structure damages in different points but we expect that a channel of fracture develops and growths into the system till bringing us to the final fracture; and this can happen without breaking each element of the system itself. So the extension to the 2D or to the 3D allows us to extend the fiber bundle model for it to be able to catch the fracture that was not able to do in 1D where the whole model arrived to a catastrophic breakdown.

So let us consider the figure below:

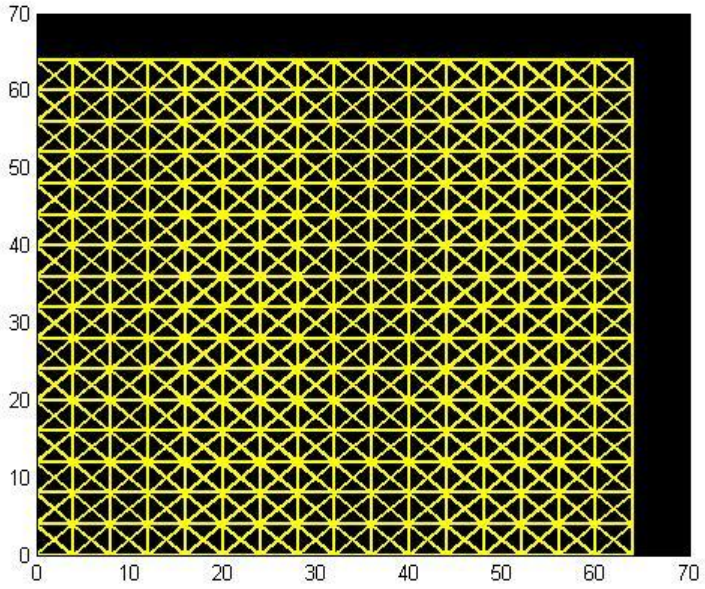

Figure 4.2: Image of the geometry of the truss lattice considered in the analysis

As we notice by the figure the extension in 2D of the FBM is made by a truss structure whose topology is described by the snapshot above.
We could load the system by forces placed on the nodes of the right edge, while the system is not able to move on the left one. However by using this load condition, we would not be able to observe the full stress strain curve of our system.
To each truss we assign a damage parameter a as it happened in the CFBM so that when its threshold, taken by a p.d.f., is reached, the Young modulus of the truss decreases to aE.
What's the physical meaning of our model? The lattice system represents a particular kind of material (for example, it could be Aluminum, Iron or a Composite) from a macroscopic viewpoint, while each truss is representative of the mesoscopic behavior of a part of the system itself, i.e. it is the representation of a small portion of material that may damage different times before arriving to the final breakdown (in order to reproduce the same mechanism of damage that we observe in the composites, chap. 3). As we already said, we assign each truss a Young Modulus which is 100 Mpa, so that our medium will be general at the moment. The system is homogeneous because the mesoscopic Young modulus is the same for each truss (we could obtain a composite structure if we gave a particular Young modulus to the horizontal trusses and a different one to the vertical ones).
The disorder is present in the system because each truss has a different threshold spread out according to a given distribution.
Why did we choose trusses to represent the medium from a mesoscopic viewpoint? That's why trusses are very simple systems, suffering only an axial force. They broke if they are stretched or pulled. So they are very simple to be used in a Finite Element Method and by knowing their thresholds for axial stresses, we are able to count the avalanches, as we'll see later. If we had used a 2D element as a membrane, for example, everything would have been more complex and we would have had to introduce a more complex method to count avalanches too. But this could be obviously a further extension or development of this model.
Simulations are performed over square lattices of side $L = 64\ mm$. The lattice is meshed according to three sizes $L = 16, 32$, and $64\ mm$, where *L* is the number of trusses aligned on the side direction. The size of vertical and horizontal bonds is $l_v = l_h = \frac{64}{L}\ mm$; the size of diagonal bonds is $l_d = \frac{64\sqrt{2}}{L} mm$. Trusses in the figure 4.2 above concurring to determine the global stiffness matrix $[K]$ have specific area values to reproduce the same behaviour of a four-node shell element. If we consider two squares into the truss structure in the figure 4.2, we get a 20-truss grid that can be divided into four 6-truss smaller grids, each of them sharing 2 trusses with the adjacent 6-truss grids. Equalizing the stiffness of the six-truss square grid to the stiffness of a four-node shell element it is possible to determine the following values for the truss area (J. G.VanMier, *Concrete Fracture: A Multiscale Approach* (CRC Press, Boca Raton, FL, 2012)),

$$A_1 = A_2 = \frac{3}{8} lt$$

(4.5)

$$A_3 = \frac{3\sqrt{2}}{8} lt$$

(4.6)

where A_1, A_2, and A_3 are the sectional areas for the horizontal, vertical, and diagonal trusses, respectively, that will be introduced into the local stiffness matrixes in order to build the general stiffness matrix. Obviously l is the length of the horizontal and vertical elements, and *t* is the

thickness. So, by this kind of work, it could be possible to obtain an equivalence between the biquadratic Lagrangian element with four nodes and thickness t, and a truss structure made by cells. That is possible if we consider the areas given by (4.5) and (4.6) coming out from the study of Van Mier. The figure below explains in a simple way how it is possible to discretize a bi-dimensional body Ω characterized by a load $q(x)$ on the boundary by truss element cells and bilinear lagrangian elements.

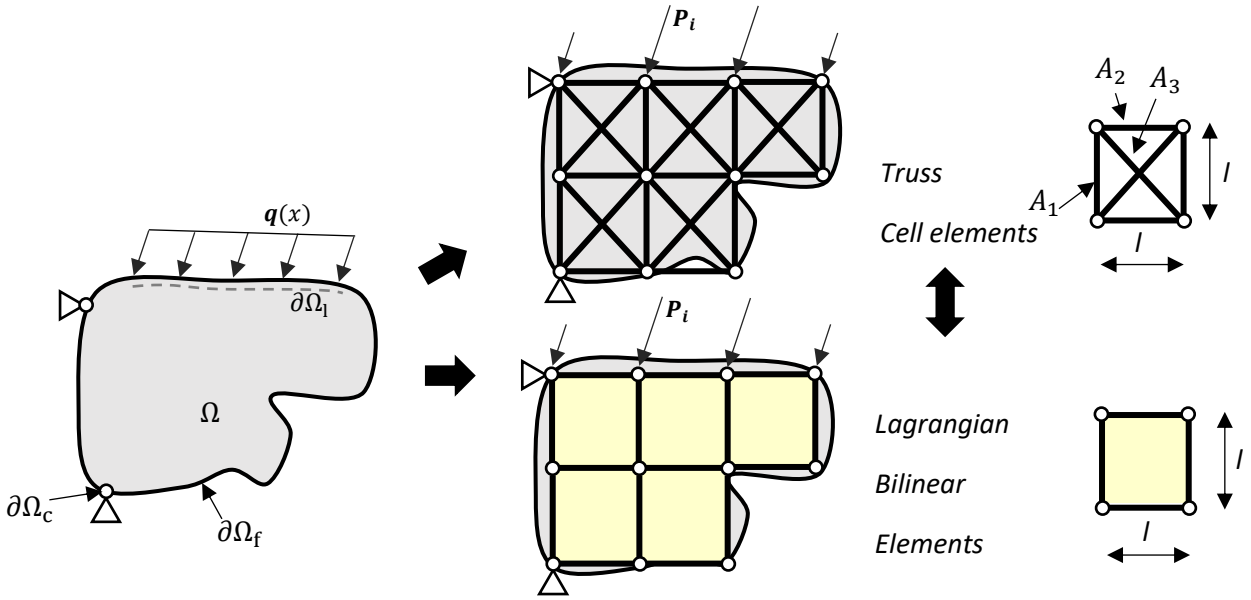

The equivalence we are talking about is energetic: what is possible to show is that this equivalence is valid for the load conditions in the figure below, for which we are able to obtain the same displacements than a bilinear lagrangian elements.

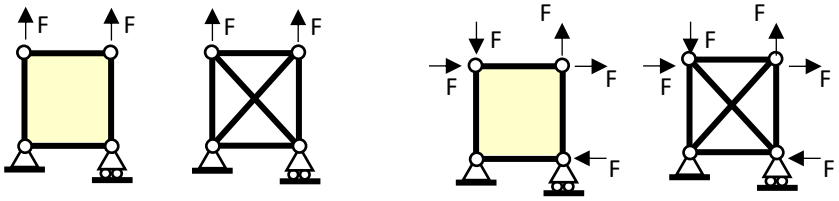

This means that if we load a bilinear lagrangian element with the same forces in the same points and we fasten it with the same boundary conditions above represented, we are able to get the same displacements on the nodes.
Instead for the following conditions of load, the equivalence is not satisfied:

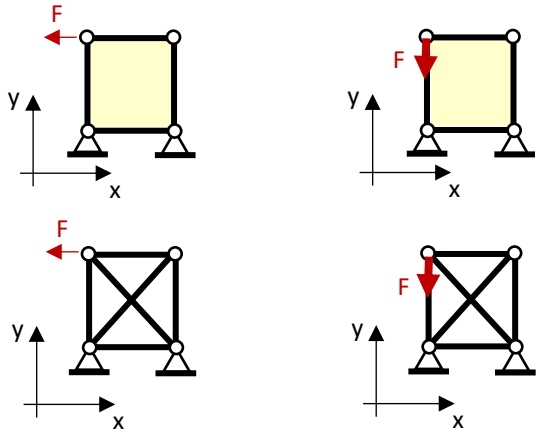

However it could be quite reasonable supposing that, by improving the quality of the mesh simply by increasing the number of the elements, the solution provided by Lagrangian bilinear elements and truss cell elements will coincide. In order to sustain this intuitive idea we performed some simple simulations by a commercial software in which with the same boundary conditions and the same applied load, we evaluated the solution coming out from the discretization by Lagrangian bilinear elements and we compared it with the truss cell one.

The results are given below:

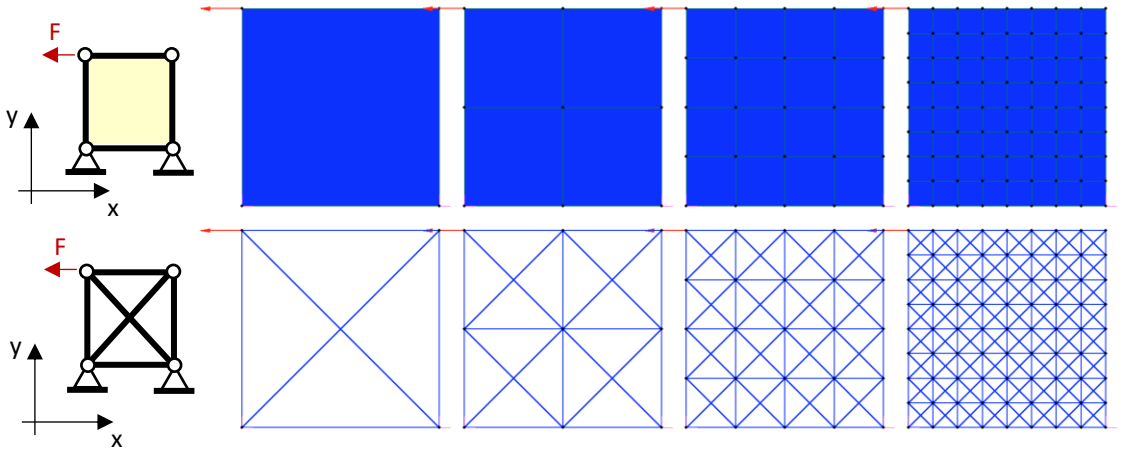

Disp x Bilinear element	Disp y Bilinear element	Disp x Truss element	Disp y Truss element	Comparison $\Delta x/\|x\|$	Comparison $\Delta y/\|y\|$	Number of divisions
-0.0923	-0.1343	-0.0874	-0.1278	5%	5%	8
-0.0685	-0.1015	-0.0574	-0.0867	16%	15%	4
-0.0461	-0.0706	-0.0337	-0.0529	27%	25%	2
-0.0406	-0.0497	-0.019	-0.0286	53%	42%	1

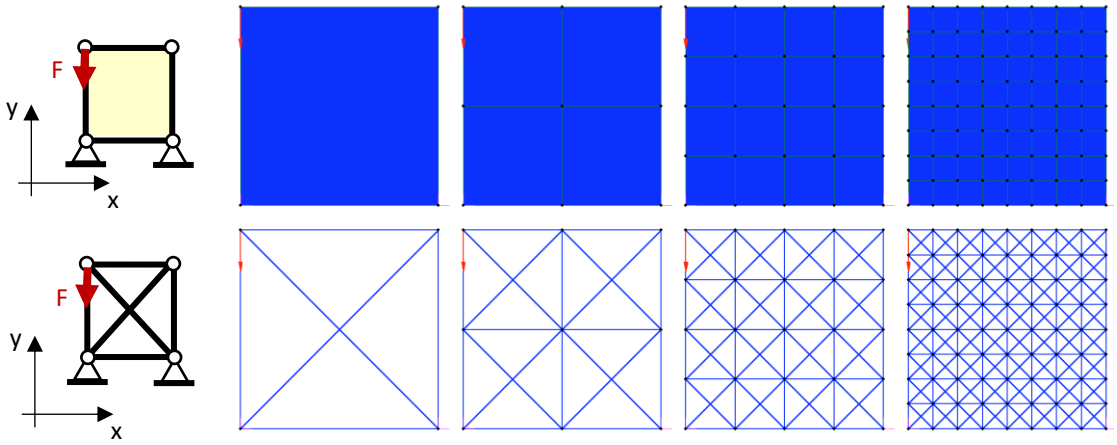

Disp x Bilinear element	Disp y Bilinear element	Disp x Truss element	Disp y Truss element	Comparison $\Delta x/\lvert x\rvert$	Comparison $\Delta y/\lvert y\rvert$	Number of divisions
-0.1907	-0.0923	-0.1802	-0.0874	6%	5%	8
-0.1486	-0.0685	-0.1298	-0.0574	13%	16%	4
-0.1031	-0.0461	-0.0871	-0.0337	16%	27%	2
-0.0802	-0.0406	-0.0571	-0.019	29%	53%	1

As we can notice, even in the cases in which the energetic equivalence in not proved (because of the previous load conditions), the bigger is the number of divisions/cells of truss elements, the closest is the solution provided by the bilinear Lagrangian elements and the truss elements themselves.

So it is reasonable to represent a body by truss cells and as we shown, by increasing the number of cells, from a math viewpoint the solution gets closer and closer to the one provided by bilinear elements. Furthermore, as we already explained, in our approach each single truss will represent a portion of material. For this reason the structure we are studying is not a real truss structure but a lattice model. This prevents us to study more complex phenomena that could happen inside the structure itself like buckling: in compression in fact trusses can damage or break because they represent simply the increasing of damage inside the volume they represent. It would not make sense to introduce more complex phenomena like buckling happening in real structures.

Now, our model is similar to the previous RFM. This means that we can assign to each truss a Young Modulus E, that in our simulations is 100 MPa, and a stress threshold spread according to a p.d.f. (an uniform one between 0 MPa and 1 Mpa). When the stress in a truss goes beyond the threshold, the Young Modulus becomes aE and the truss itself is damaged. A truss can damage only $kmax$ times so that in the simulation when $E < E_{kmax}$, $E = 0$.

4.2.2 Assembly of the Mass, stiffness and damping matrixes

Our truss structure is made by different bars moving into the plane $x - y$ according to the following picture already shown in Chapter 3:

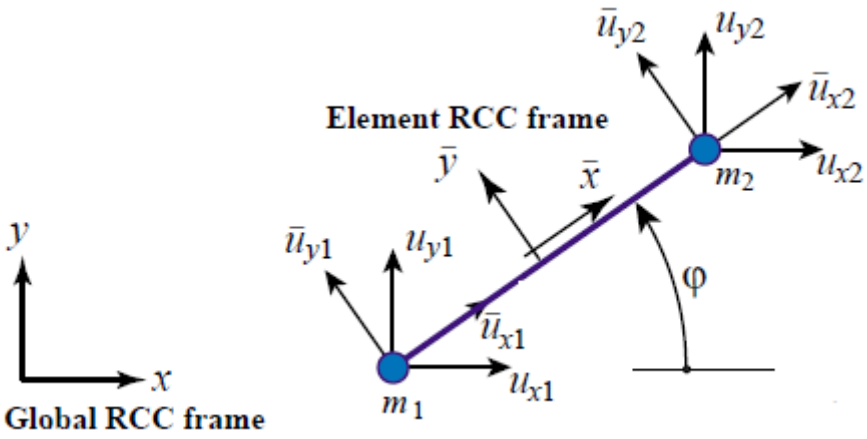

Figure 4.3: Local and global frames on a single truss

The figure 4.3 above shows an element of length $l = x_j - x_i$, with constant section A, Young modulus E and density ρ. Obviously, given the nature of our system, each node can move independently both in axial direction (causing a displacement u_i) and in orthogonal direction, with a displacement w_i so that, for a single element

$$\{u_i\}^T = \{u_i, w_i, u_j, w_j\}^T$$

(4.7)

The displacement of a generic point inside the element, P, can be expressed as function of the displacements of the nodes or as a function of the adimensional coordinate

$$\xi = \frac{x - x_i}{x_j - x_i}$$

(4.8)

If we use linear shape functions, shown in the figure below,

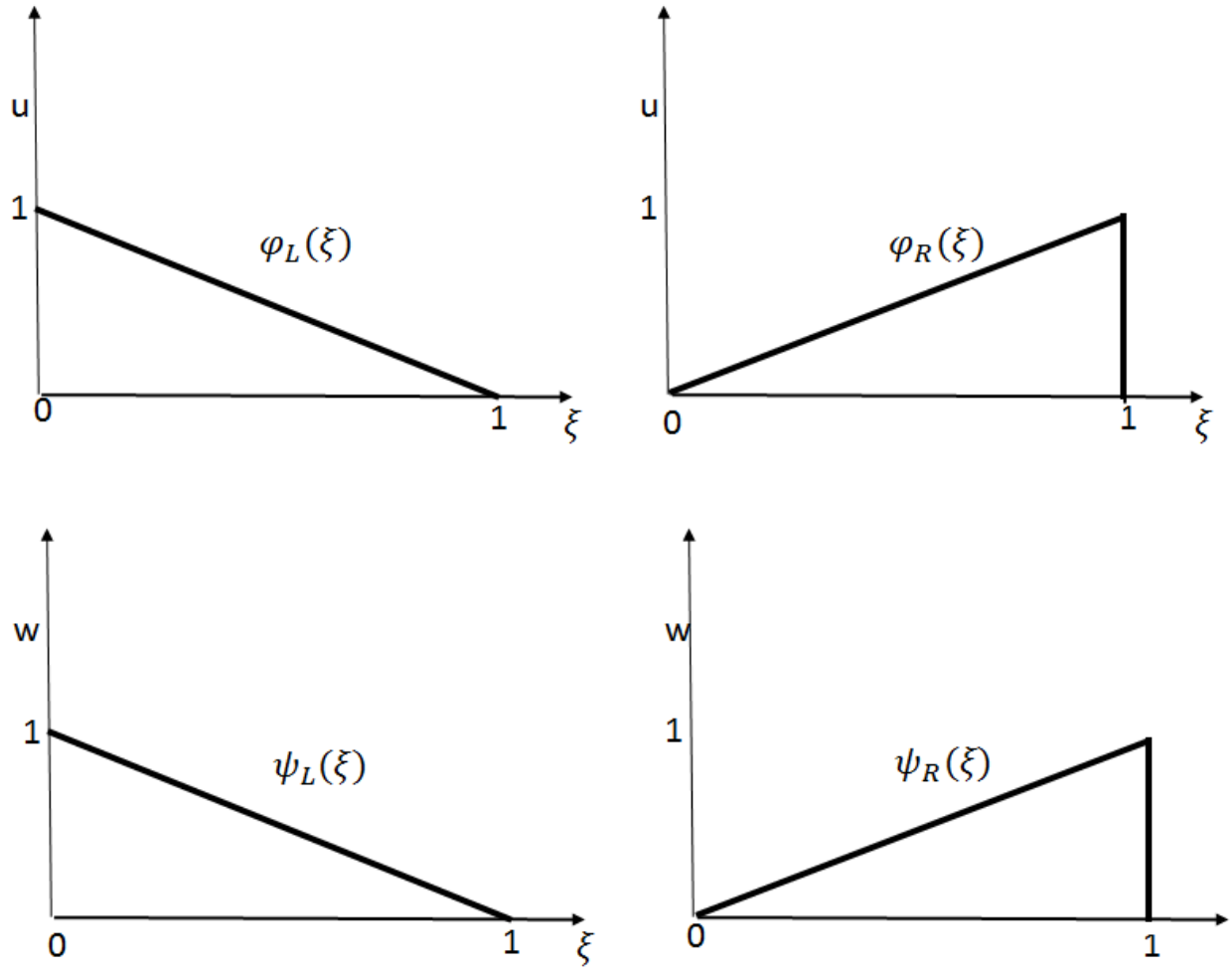

Figure 4.4: shape functions for the element truss

the axial displacement u and the orthogonal displacement w of each internal point become function of the nodal displacements according to:

$$u(\xi) = (1-\xi)u_i + \xi u_j$$

(4.9 a)

$$w(\xi) = (1-\xi)w_i + \xi w_j$$

(4.9 b)

So if we would like to compute the mass matrix of the truss element according to the variational approach, we can use the expression of the kinetic energy of the element:

$$T = 1/2 \int_0^l \varrho A(\dot{u}^2 + \dot{w}^2)dx = 1/2\, \varrho Al \left(\int_0^1 \dot{u}^2 d\xi + \int_0^1 \dot{w}^2 d\xi \right)$$

(4.10)

Using the expressions 4.9a and 4.9b and making the calculations we get

$$\int_0^1 \dot{u}^2 d\xi = \int_0^1 \left[(1-\xi)\dot{u}_i + \xi \dot{u}_j\right]^2 d\xi = \frac{1}{3}\dot{u_i}^2 + \dot{u}_i\dot{u}_j + \dot{u_j}^2$$

$$\int_0^1 \dot{w}^2 d\xi = \int_0^1 \left[(1-\xi)\dot{w}_i + \xi \dot{w}_j\right]^2 d\xi = \frac{1}{3}\dot{w_i}^2 + \dot{w}_i\dot{w}_j + \dot{w_j}^2$$

(4.11)

Now, let us gather the nodal displacements into the vector

$$\{u_E\}^T = \{u_i, w_i, u_j, w_j\}^T$$

and if we remind that the mass of the element is $m = \varrho A l$, the Eq (4.10) takes us to the definition of the following mass matrix of the element

$$[M_E] = m/6 \begin{pmatrix} 2 & 0 & 1 & 0 \\ 0 & 2 & 0 & 1 \\ 1 & 0 & 2 & 0 \\ 0 & 1 & 0 & 2 \end{pmatrix}$$

(4.12)

Let us compute now the stiffness matrix by using the expression of the potential energy of an infinitesimal element:

$$dV = \frac{1}{2} N\, du$$

(4.13)

where N is the axial stress and du an infinitesimal displacement. By using the expressions of the force and of the axial displacement,

$$N = EA\frac{\partial u}{\partial x}$$

(4.14)

and

$$du = \frac{\partial u}{\partial x} dx$$

(4.15)

we get the following expression for the elastic energy:

$$V = \frac{1}{2}\int_0^l EA\,(\partial u/\partial x)^2 dx \;= \frac{1}{2} EA/l \int_0^1 (\partial u/\partial \xi)^2\, d\xi$$

(4.16)

If we develop the calculations

$$\int_0^1 (\partial u/\partial \xi)^2 \, d\xi = \int_0^1 \left(u_j - u_i\right)^2 d\xi = \left(u_j - u_i\right)^2$$

(4.17)

and so we can get easily the stiffness matrix of the element:

$$[K_E] = EA/l \begin{pmatrix} 1 & 0 & -1 & 0 \\ 0 & 0 & 0 & 0 \\ -1 & 0 & 1 & 0 \\ 0 & 0 & 0 & 0 \end{pmatrix}$$

(4.18)

As regards the damping matrix [C], we use simply a linear combination of the mass and stiffness matrix according the so called Rayleigh's damping:

$$[C] = \alpha[C] + \beta[K]$$

(4.19)

where α and β are simply two scalar constant depending on the physical features of the material and that in our code will be taken equal to 0.5.

So the dynamic equations for the single element, taking into account possible axial forces or shear forces applied on the nodes, are:

$$[M_E]\{\ddot{q_E}\} + [C_E]\{\dot{q_E}\} + [K_E]\{q_E\} = \{F_E\}$$

(4.20)

where $\{F_E\} = \{N_i, T_i, N_j, T_j\}^T$

4.2.3 The global problem

We can try now to build the truss structure in the figure below to introduce a simple example of how it is possible to build the matrixes of the whole system. In the figure we have basically two different bars that we call A and B and three nodes, 1, 2, 3.

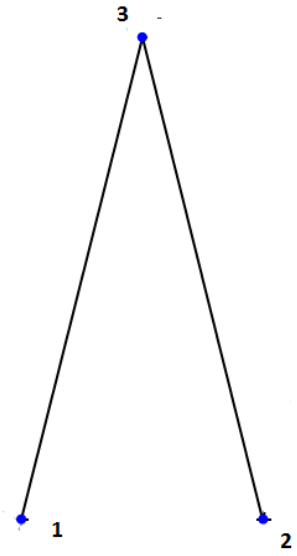

We can note that, because of the different orientation of the two bars, the axial displacement of the bar A corresponds to a shear displacement for the bar B, while an axial displacement for the bar B corresponds to a shear displacement for the bar A. This very simple example let us notice that the mass, stiffness and damping matrixes in local coordinates are not able to take into account of the real orientation of the bar in global RCC frame. So, in order to overcome this problem we are forced to describe the two degrees of freedom associated to each node by the displacements in global coordinates. For example the coordinate transformation from the global RCC frame to the local RCC frame for the first bar is given by:

$$\begin{Bmatrix} u_{1,A} \\ w_{1,A} \\ u_{2,,A} \\ w_{2,A} \end{Bmatrix} = \begin{Bmatrix} x_1 \cos\alpha + y_1 \sin\alpha \\ -x_1 \sin\alpha + y_1 \cos\alpha \\ x_2 \cos\alpha + y_2 \sin\alpha \\ -x_2 \sin\alpha + y_2 \cos\alpha \end{Bmatrix}$$

(4.21)

where (x_i, y_i) represents the displacements of the i-th node in the global frame. It is possible to show that the coordinate transformation of both bars can be written by the following matrix formulation:

$$\begin{Bmatrix} u_i \\ w_i \\ u_j \\ w_j \end{Bmatrix} = \begin{pmatrix} \cos\alpha_i & \sin\alpha_i & 0 & 0 \\ -\sin\alpha_i & \cos\alpha_i & 0 & 0 \\ 0 & 0 & \cos\alpha_i & -\sin\alpha_i \\ 0 & 0 & -\sin\alpha_i & \cos\alpha_i \end{pmatrix}$$

(4.22)

The previous formula can be rewritten like

$$\{q_E\} = [R]\{q\}$$

(4.23)

where $\{q_E\}$ is the vector of the local coordinates of the element, $\{q\}$ represents the vector of the absolute coordinates and $[R]$ the orthonormal rotation matrix between the two frames. The matrix $[R]$ allows us to transform the nodal forces F expressed in absolute coordinates, in axial and shear forces F_E in the frame of the element according to

$$\{F_E\} = [R]\{F\}$$

(4.24)

So, pre multiplying by $[R]^T$ the equation (4.20), we can get the equations in the global frame for each element:

$$[R^T][M_E][R]\{\ddot{q}\} + [R^T][C_E][R]\{\dot{q}\} + [R^T][K_E][R]\{q\} = [R^T][R]\{F\} = \{F\}$$

(4.25)

It is simple to verify that the mass matrixes in the global and in the local frame are equal, while the stiffness matrixes in the two frames are different; so

$$[M] = [R^T][M_E][R] = [M_E]$$

(4.26 a)

$$[K] = [R^T][K_E][R] \neq [K_E]$$

(4.26 b)

As regards the damping matrix $[C]$, this is a linear combination of the mass and stiffness matrixes; for this reason, by using the (4.26), we will have

$$[C] = [R^T][C_E][R] \neq [C_E]$$

(4.27)

After having changed all the matrixes in global coordinates, we can assembly the correspondent matrixes for the whole structure and we are able to write the motion equations

$$[M_{tot}]\{\ddot{q_{tot}}\} + [C_{tot}]\{\dot{q_{tot}}\} + [K_{tot}]\{q_{tot}\} = \{F_{tot}\}$$

(4.28)

In this way we are able now to compute the matrixes in global coordinates. If we use the two orthonormal matrixes

$$[R_A] = \frac{\sqrt{2}}{2}\begin{pmatrix} 1 & -1 & 0 & 0 \\ 1 & 1 & 0 & 0 \\ 0 & 0 & 1 & -1 \\ 0 & 0 & 1 & 1 \end{pmatrix}$$

(4.29)

$$[R_B] = \frac{\sqrt{2}}{2}\begin{pmatrix} 1 & 1 & 0 & 0 \\ -1 & 1 & 0 & 0 \\ 0 & 0 & 1 & 1 \\ 0 & 0 & -1 & 1 \end{pmatrix}$$

(4.30)

we compute the mass, stiffness and damping matrixes of each element

$$[K_A] = \frac{EA}{2L}\begin{pmatrix} 1 & -1 & -1 & 1 \\ -1 & 1 & 1 & -1 \\ -1 & 1 & 1 & -1 \\ 1 & -1 & -1 & 1 \end{pmatrix}$$

(4.31)

$$[K_B] = \frac{EA}{2L}\begin{pmatrix} 1 & 1 & -1 & -1 \\ 1 & 1 & -1 & -1 \\ -1 & -1 & 1 & 1 \\ -1 & -1 & 1 & 1 \end{pmatrix}$$

(4.32)

$$[M_A] = [M_B] = m/6\begin{pmatrix} 2 & 0 & 1 & 0 \\ 0 & 2 & 0 & 1 \\ 1 & 0 & 2 & 0 \\ 0 & 1 & 0 & 2 \end{pmatrix}$$

(4.33)

$$[C_A] = \alpha[M_A] + \beta[K_A]$$

(4.34)

$$[C_B] = \alpha[M_B] + \beta[K_B]$$

(4.35)

and then we build the global matrixes of the system:

$$[M_{tot}] = m/6\begin{pmatrix} 2 & 0 & 1 & 1 & 0 & 0 \\ 0 & 2 & 0 & 1 & 0 & 0 \\ 1 & 0 & 4 & 0 & 1 & 0 \\ 0 & 1 & 0 & 4 & 0 & 1 \\ 0 & 0 & 1 & 0 & 2 & 0 \\ 0 & 0 & 0 & 1 & 0 & 2 \end{pmatrix}$$

$$[K_{tot}] = \frac{EA}{2L}\begin{pmatrix} 1 & -1 & -1 & 1 & 0 & 0 \\ -1 & 1 & 1 & -1 & 0 & 0 \\ -1 & 1 & 2 & 0 & -1 & 1 \\ 1 & -1 & 0 & 2 & 1 & -1 \\ 0 & 0 & -1 & -1 & 1 & 1 \\ 0 & 0 & -1 & -1 & 1 & 1 \end{pmatrix}$$

$$[C_{tot}] = \alpha[M_{tot}] + \beta[K_{tot}]$$

The same approach will be used for assembling the mass, stiffness and damping matrixes for our truss lattice.

4.2.4 The damage algorithm

Till now we simply implemented a discretization in space for our system by using the FEM and the GN22 Newmark's method to get a discretization in time. The next step is to introduce the damage algorithm in our model. So let's consider the time interval from t to $t + dt$. In the hypothesis we introduced above, our system is absolutely linear so we do not need to apply the Newton Raphson method to get the solution u_{n+1}. This should be done if we introduced a not linear constitutive law for our material depending on the strain. We will clarify now this claim.

So, how the damage enter into the model? Basically, the method used is an extension of the CFBM as we already said before and so the algorithm works by introducing the concept of iteration and avalanche. This means that we fix for each truss a threshold in stress (that can remain constant or can be changed according to the quenched or annealed disorder) and we apply the load on the right edge of the structure while the left edge is fixed. So for a given external load f_n at a given time step n, one or more trusses will reach their thresholds in stress. For this reason, their Young modulus will be reduced by a factor $0 \leq a < 1$ and now it will be equal to $a^i E$ where

$0 \leq i - 1 < kmax$ is the number of damages already suffered by the truss. So, because of this damage process the global stiffness matrix and the damping matrix will change and the system cannot be anymore in equilibrium under the external load; let us introduce the following scheme of 4 trusses to better explain the way of reaching the equilibrium:

iteration	n.avalanche	Truss1	Truss2	Truss3	Truss4
1	3	1	0	1	1
2	2	1	0	0	1
3	1	0	1	0	0
4	0	0	0	0	0
$I = 3$	$S = 6$	$E_1 = a^2 E_1$	$E_2 = a^1 E_2$	$E_3 = a^1 E_3$	$E_4 = a^2 E_4$

So, for a given external load f_n we get some displacements, velocities and accelerations as solution of the numerical algorithm. However 3 trusses reach their thresholds and so their Young modulus is reduced. We are at the iteration number 1 and the number of avalanche S which is the number of damages into one iteration, is equal to 3.The equilibrium is not still achieved because under our external load the stiffness of the system has changed. So a further iteration is necessary storing the external load always equal to $f_n$and recomputing the equilibrium taking into account the new stiffness and damping of the system. Obviously some new displacements, velocities and accelerations will be achieved. Here the number of avalanche is equal to 2. The process goes ahead till at the $i-th$ iteration (in our example the fourth one) where the number of damaged trusses is equal to 0 and where we get the final values of $u_n, \dot{u}_n, \ddot{u}_n$. Only now it is possible to increase the external load passing to the following station which is f_{n+1}.

As we can note, the way of computing the equilibrium is identical to the case of the CFBM for the stress controlled experiment where we had a redistribution of the load lost by the damaged fiber on the other ones.

What about the behavior of the system in terms of linearity? Basically in our FEM model we are introducing a damage model in which the stiffness matrix (and so the damping matrix) changes. However the concept of damage we introduce is different from the theories of the deterministic damage, in which the damage D is a function of the strain of the model (Bazant); to this damage law $D = D(\varepsilon)$ we arrive by thermodynamic considerations. In this case the stiffness matrix (and the damping matrix as well) is also a function of the strain. In this deterministic case the problem is not linear and so we would need to iterate because the various matrixes are functions of the solution. In the extension of the CFBM to the 2D instead, the damage is a variable which depends obviously on the history of the external load but it is a stochastic variable as well, depending on thresholds picked up from the chosen p.d.f.

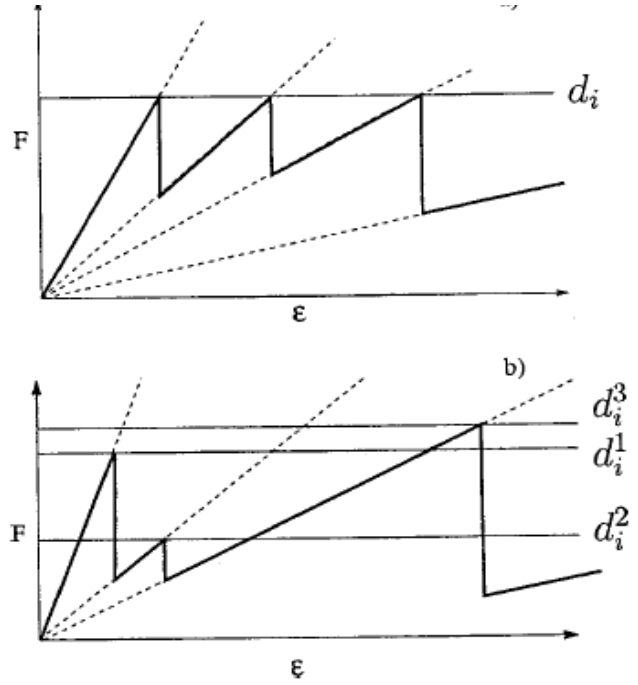

Figure 4.5: Annealed and quenched disorder for a single realization on a truss

As we notice from the pictures above in the case of the annealed and quenched disorder, for each truss the $\sigma - \varepsilon$ law is globally not linear, depending on the thresholds we meet. However locally, after we meet one threshold, the slope of the curve decreases and we notice a drop but till we meet another threshold, the curve $\sigma - \varepsilon$ is linear, passing always for the origin. This fact introduces some important aspects to the solution algorithm to compute the equilibrium.

This is the main difference between the two damage models. In fact when we impose a force or external displacements the system reaches a set of strains and so of stress. In this moment we can check for the threshold and eventually to change the Young modulus. If this happens we compute again the equilibrium for the system. But in the i.th iteration, when n trusses have damaged already and we try to reach the equilibrium with our boundary conditions already imposed checking if any truss damage, we get a path in which each truss has a $\sigma - \varepsilon$ law which is linear. For this reason during this path we do not need to iterate because the stiffness matrix is constant. The only iteration we need to consider is the iteration that allows us to verify if any trusses have suffered damage. The situation would be different if between a threshold and another one for the various trusses the $\sigma - \varepsilon$ law would have been not linear: not as the one of the picture above. In this case (for example for a quadratic law) in the path between two thresholds the stiffness would have been function of the solution. So a threshold iteration would have called a Newton Raphson iteration and the two kinds of iterations calling each other would have stopped when no more trusses have damaged and when the tolerance for the Newton Raphson algorithm would have been reached. This is not our case because of the constitutive law for single truss we introduced. So we do not need to use Newton Raphson's algorithm but only the threshold iteration algorithm. A CFBM iteration could call one Newton Raphson iteration and so on, only if between one threshold and another one, the $\sigma - \varepsilon$ law was not linear.

Now, one single truss can damage $kmax = 30$ times before breaking in our simulation and the damage parameter $a = 0.9$; if the initial Young modulus is the same for all the trusses (for the same reasons we explained into the FBM chapter), $E = 100\ MPa$, the Final value of the Young modulus to which a truss will considered completely broken will be $E = 0.9^{30}100 = 4.24\ MPa$. After this value, the stiffness of the broken truss will be removed by the global stiffness matrix. So its mass from the global mass matrix and its damping from the damping matrix (this last cancelation is a direct consequence of the Rayleigh's damping we chose to write the damping into the structure, which is simply a linear combination of the mass and stiffness matrixes).

4.3 The case of the porous medium

4.3.1 Extension of the model for a coupled problem

The problem for the porous medium (in the case of fully or partially saturated), is equivalent for the solid part. So the mass, stiffness and damping matrixes are equivalent. We need now to assembly the coupling matrix Q and the permeability matrix H.

In our Matlab code we choose to represent the fluid by continuous elements characterized by four nodes; we used these four nodes elements to build the permeability matrix H.

The coupling matrix Q instead is the link between the solid part and the fluid part: the elements of the matrix make up the link between the fluid field and the solid one: in fact it is possible to show (Milanese, Molinari, Schrefler) how a variation in pressure brings about a variation in the displacement field even in the absence of external forces. So in order to assembly the coupling matrix how can we represent the solid part by continuous elements if we already choose four nodes elements for the fluid part? The answer is quite simple: the elements must be chosen carefully in order to satisfy the inf-sup condition (also known as the Babuska-Brezzi condition) on the existence and uniqueness of the solution for mixed formulations. The condition is satisfied choosing a nine-node formulation for the displacements and a four-node formulation for the pressures. So this will be our chose in order to assembly the coupling matrix.
In the figure below we represent the three different choices to assembly the matrixes into the problem: a nine node truss element in green for the stiffness matrix for the solid part, a nine node continuous element for the solid part into the coupling matrix and a four node continuous element for the fluid part into the permeability and coupling matrix.

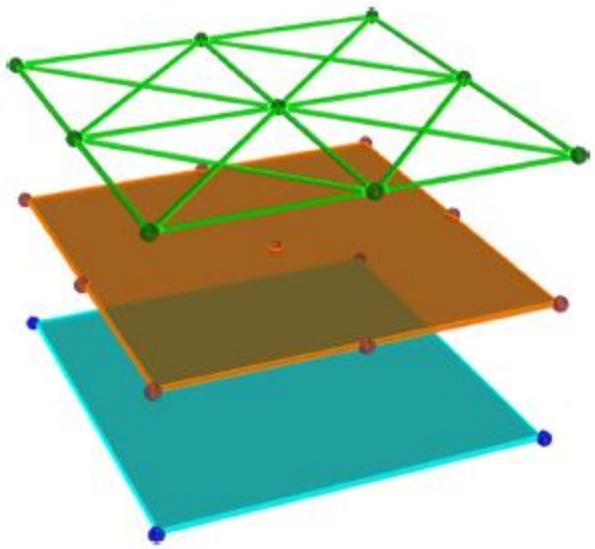

Figure 4.6: Representation of the solid part (truss structure), fluid part (four node element in blue) and coupling between the solid and the fluid part (nine node element in brown). Taken by Milanese et al., 2016

As regards the damage algorithm, we can say that it is equivalent to the damage algorithm of the solid. The damage will be calculated according to the same approach into the solid part but now also the fluid will be able to influence the solid part because of the coupled nature of the problem.

4.4 Results of the simulations

4.4.1 Static for a dry medium

We report the results of the simulations for a dry medium supposing that it is pulled from the four edges in static with the damage algorithm we introduce before. We will perform a “strain constant” experiment applying some displacements. This will allow us to look at the plateau of the constitutive behaviour. This configuration was already simulated by Milanese, Yilmaz, Molinari, Schrefler. We rewrote the code and we found that the results are the same.

Simulation 1: Static for dry medium

Mesh and BC for simulation 1

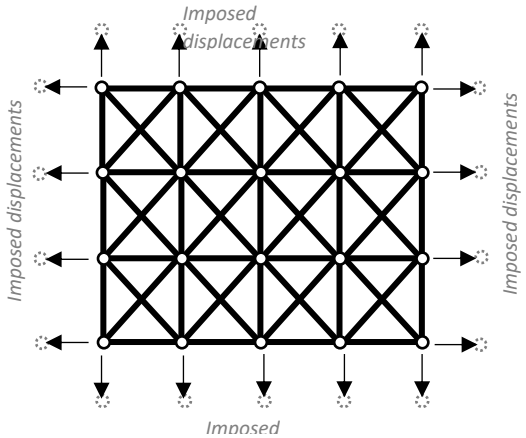

Young modulus *E* of the trusses	100 MPa
Displacement applied at each step on the nodes	1/5000 mm
Mesh	16 x 16
Length L	64 mm

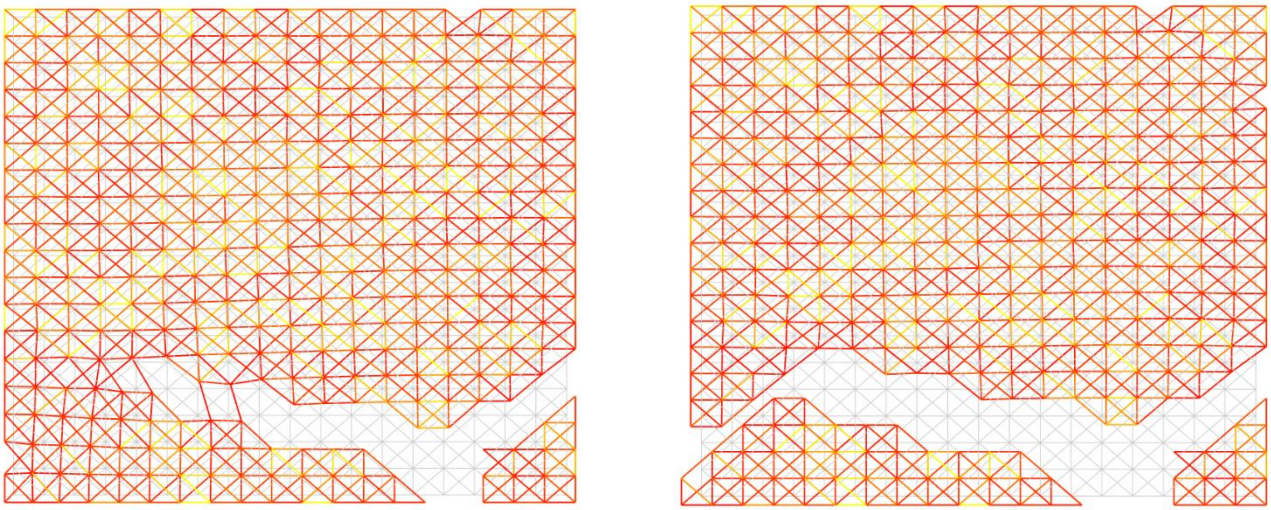

Development of the fracture in the mesh. We represent in yellow the trusses with high Young modulus and in red the trusses more damaged. One truss in the algorithm can be damaged up to 30 times before being considered broken in the simulation. The deformed configuration is plotted over the undeformed one.

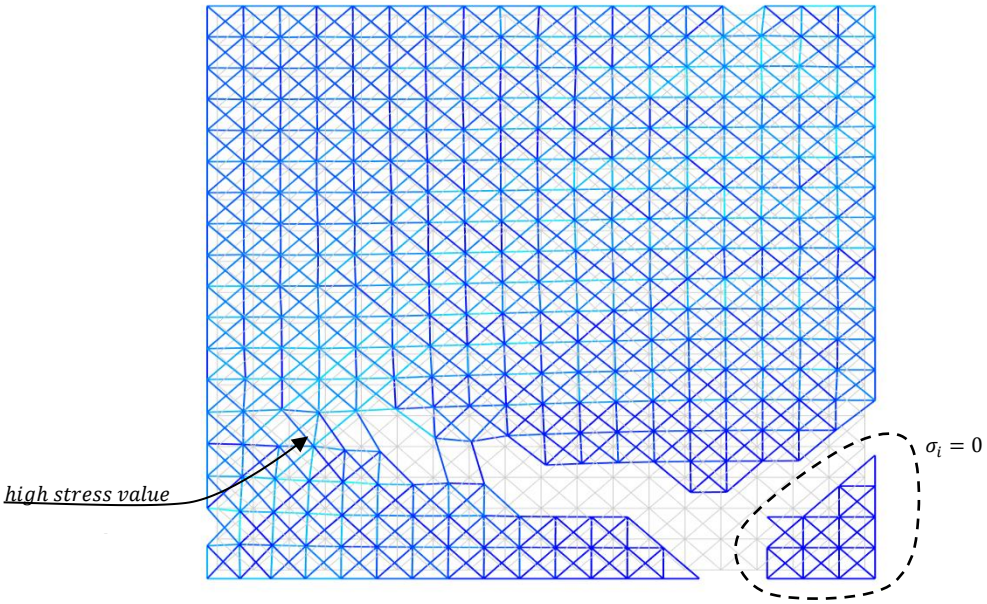

Development of the fracture in the mesh and undeformed configuration. In deep blue we represent the trusses with low stresses while in light blue the trusses with high Young modulus.

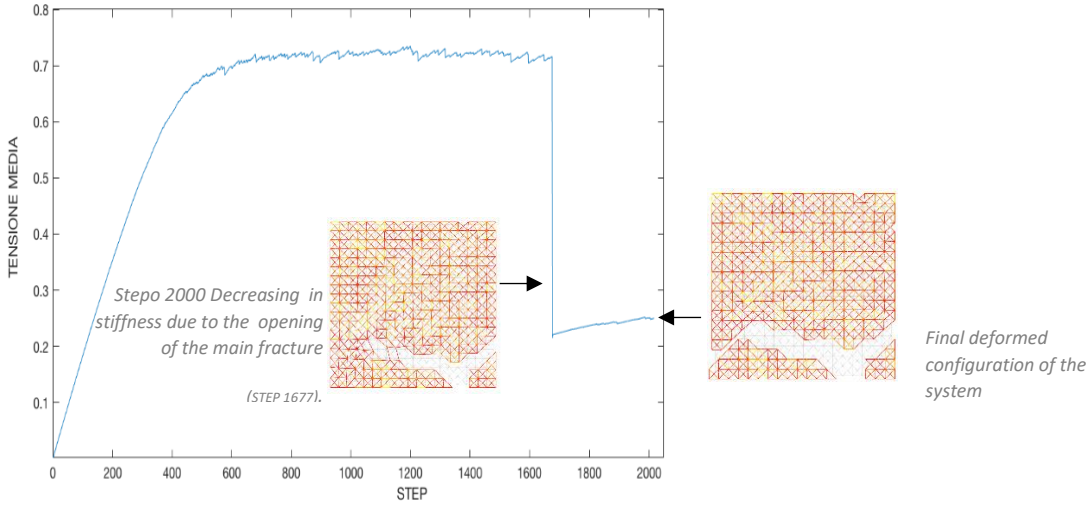

Average stress as function of the step .

At each time step in the simulation, we increased the displacement of a rate 1/5000. Let us consider the constitutive behaviour: in the first part of the curve we notice a linear behaviour, which is followed by a plastic part in which the medium begins to suffer a damage. The oscillations we have in the plateau of the plastic phase are due to the fact that the trusses begin to damage. At a certain point, we have a drop in the curve. This is due to the fact that a big failure event occurs, and this corresponds to the creation of the first part of the fracture. After this first drop, we keep on imposing displacements on the boundaries and even if other trusses damage, the average stress go back to increase. This process arrives up to the second "catastrophic" point in which we record another big failure event where another big amount of trusses break. In point of the curve stress-step, the channel of the fracture creates and the connectivity of the structure goes to 0.

The thing we notice is that the channel of the fracture does not create in a unique step but needs more steps to create; there is a certain *intermittency* in creating the channel: the channel is not created by a "fraying" of the truss fabric but by different openings of the fabric itself: the system needs more "catastrophic" events to create the channel of the fracture.

As we noticed by the figures, when the first opening creates between the step 1600 and 1800, we notice some trusses still attached and existing in the channel of the fracture. They are very damaged but not still broken. How could we read this situation from a physical viewpoint? A possible explanation could be that in this region the fracture channel is not opened yet and there are some residual stresses: this could be a cohesive method approach entrance in our method, in the sense that the Central Force Model predicts some residual stresses close to the point in which the fracture is going to open. Our model allows us to see this phenomenon according to another point of view.

4.4.2 Test case for dynamic: the consolidation

As regards the code in dynamics, it was validated by a comparison with ANSYS software as regards the problem of consolidation. As we know, in this phenomenon we load our system on one edge by a constant load fastening it on the opposite side. The phenomenon is analysed in dynamic so we are able to observe the transient. What happens in nature? Due to the coupled nature of the porous medium, in a first moment the load is taken by the water and it does not affect the structure; however after a certain time interval, depending basically on properties of the system, in particular by the permeability (i.e. the capability the water has to move inside the system), the water moves and the load is taken by the solid skeleton that suffers a lowering in the opposite direction of the load. So, the solid skeleton takes the load and after a transient everything reaches the stationarity condition. As regards the time required for the simulation, we decided to consider basically some steps, divided by a time of 0.1 sec. However, due to the large times we meet in this phenomenon, we were forced to increment the time interval dt about 1.5 times. So the time we will get in the x-axis of the plots we will show, will be related to the variable STEP according to

$$t_{i+1} = STEP_{i+1} dt\ 1.5^{i}\ step$$

The simulation was realized with a total of 43 steps. As regards the load applied on the structure, it acted on the top of it, on the nodes: till the step 10 it was growing linearly leaving from 0 N, After the step 10 it remained constant at a value of 0.1 N in each node. The structure was not free to move on the right, the left and the bottom while the pressure was put equal to 0 on the perimeter. We report the results of the test case:

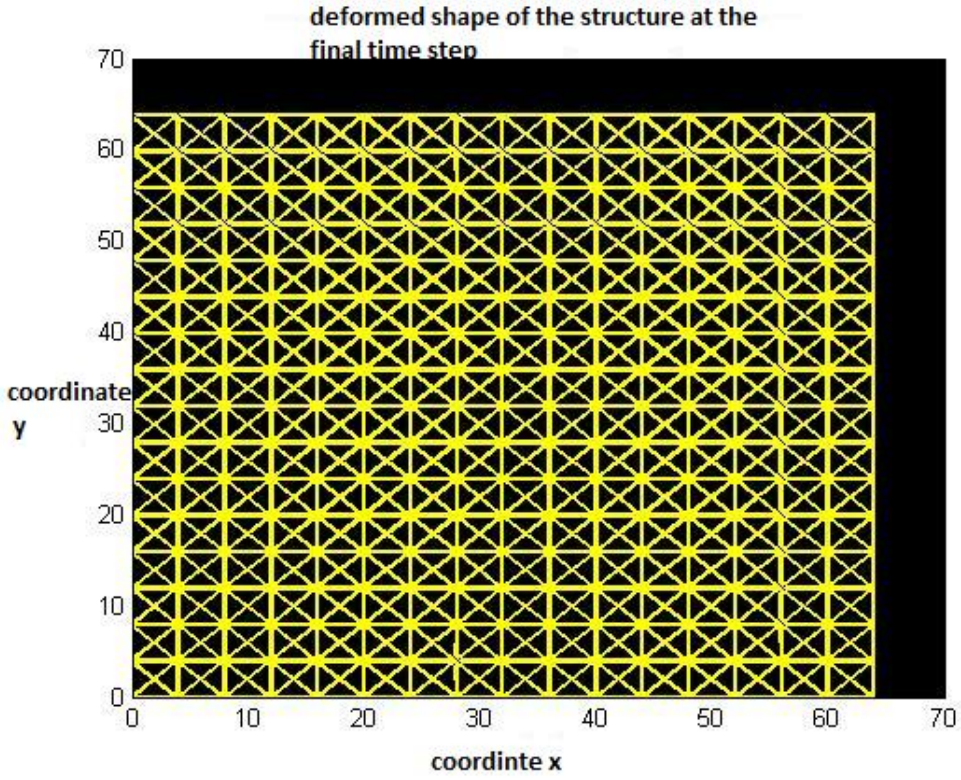

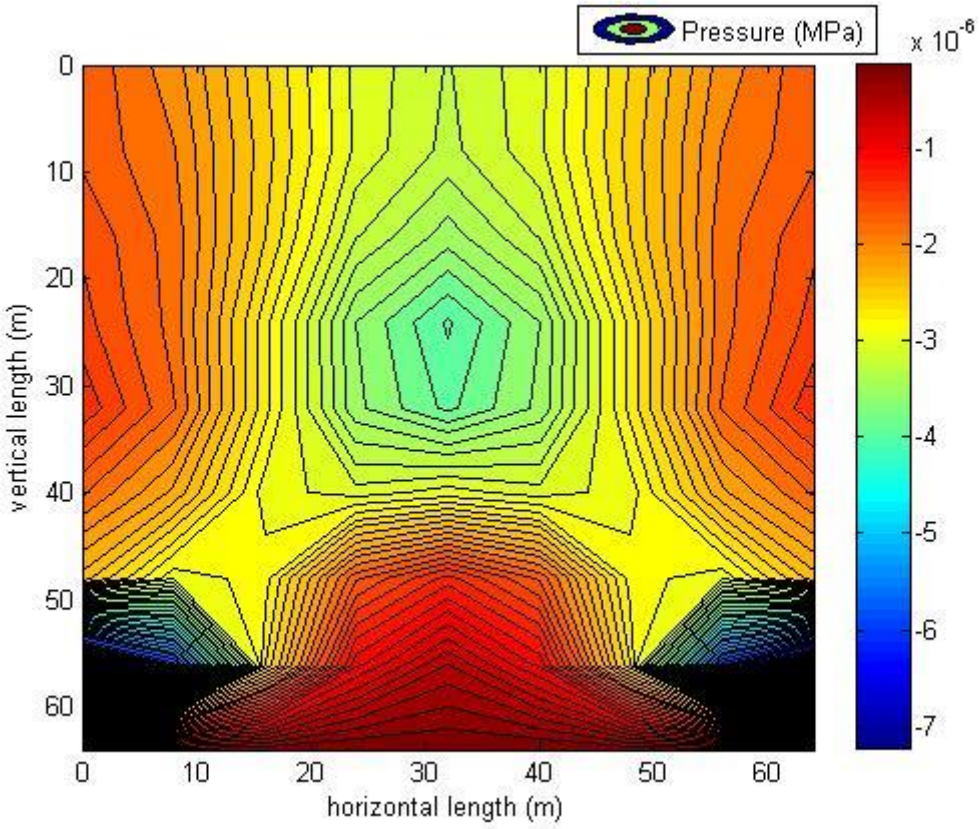

Figure 4.7: Representation of the deformed structure and of the distribution of the pressure of the water inside the medium due to the consolidation

So, as we notice at the time step 43 where all the displacements and pressures are constant and no more variables in time, the solid skeleton suffered a lowering of few millimetres (we can notice in the first picture the undeformed solid skeleton in blue) while the distribution of the pressure inside the medium is given by the second picture. We report some plots as regards the story of displacement and pressure in one point of the system: it is possible to recover the same trend of curves for each point of the system.

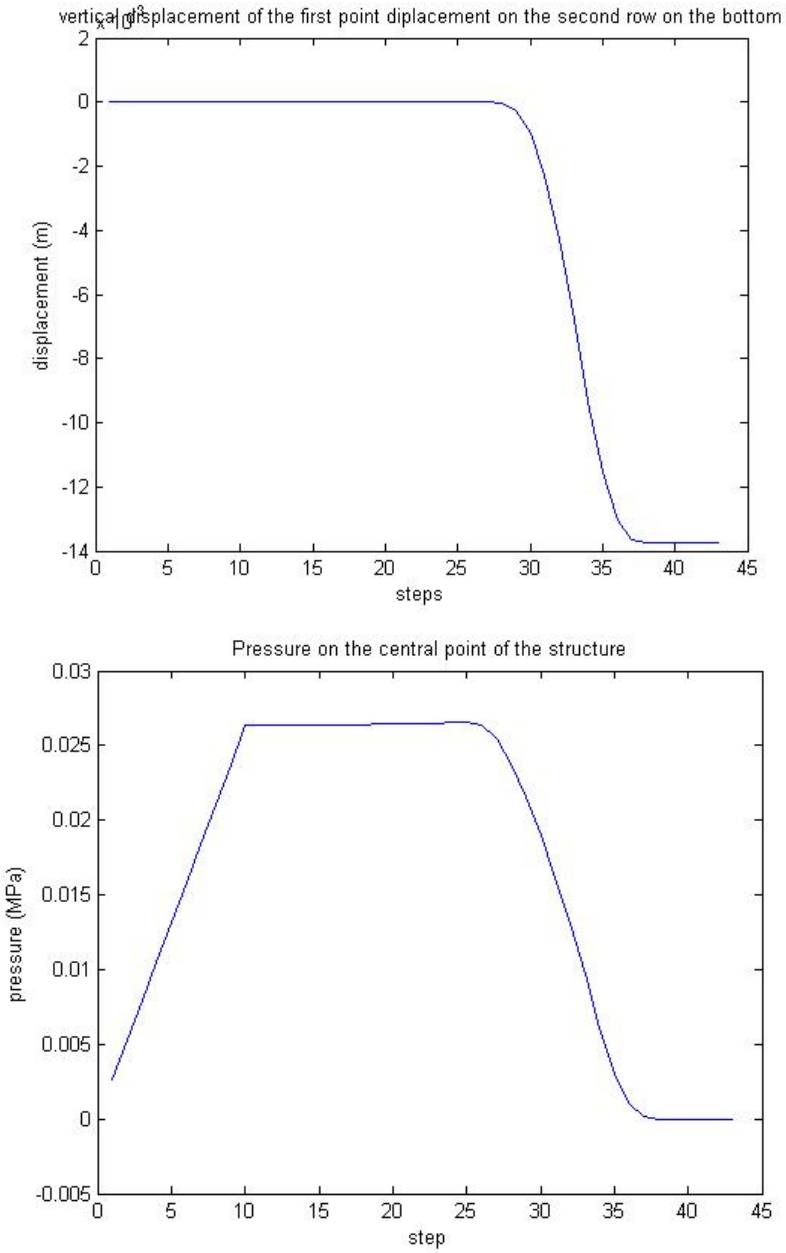

Figure 4.8: plots of the vertical displacements of one point of the structure and of the pressure in one point as function of time

The curves can change from point to point but it is interesting to notice that a stationary state is reached everywhere. So the phenomenon of consolidation is described by our code. The structure suffered on average a lowering of some millimetres and this mixed element numeric model was verified by comparing it with a benchmark case for the isothermal consolidation.

4.4.3 The dynamic of the porous medium

4.4.4 The problem of the Fracking

The truss lattice analysed in static belongs to the so called SDIDT systems: the acronym SDIDT stays for slowly driven interaction dominated threshold system that we will discuss in chapter 5, and that if some conditions are satisfied, falls into the set of SOC (Self Organised Criticality) systems.

As we know, in nature, earthquakes are the result of the movement of the faults. These movements however occur very slowly (about 1 cm per year): for this reason a good first model to describe this natural phenomenon is the code elaborated by Milaneseet al., (2017), in which they applied, in one of the cases treated, some shear and mixed boundary conditions. They worked in static and the assumption of the static is obviously satisfied because of the extremely slow movement of the faults. We will talk better about this problem in the next paragraph.

However what about the fracking? In fracking we pump water into a fracture of the land and we basically propagate the hole or the fracture by the pressure of the water. So if we would like to emulate the phenomenon of fracking inside the land in our statistical central force model, we would simply try to increase the flux in a point and to observe the creation of a hole or fracture. However the assumption of "static condition" could not be true anymore. Fracking is dynamic and the way in which we pump water inside the soil could be characterized by a frequency. So it is correct to give a description of fracking by our dynamic model.

What happens however in dynamics as regards the avalanche behaviour first analysed?

To answer this question, let us try to give a physical interpretation of the algorithm of the FBM. Basically, analysing back these two algorithms (which are the two faces of the same coin), we notice that when we apply some boundary conditions from the external world on the edges, the system tries to reach the equilibrium: and the way by it tries to reach it, is by the concept of iterations and avalanches. For example at iteration 1 the number of avalanche is n; at iteration 2 it will be m and so on till we arrive at the iteration i where the number of avalanche is 0. So the system has reached the *static equilibrium* for these boundary conditions. It could be possible now to associate an intrinsic time to our system, that we call "characteristic system time". How much is the amount of this time?

Basically this is the time required for having the complete relaxation of the system; so let us suppose to analyse the case of a constant load on the edges in dynamics: here when we apply a constant displacement on the four edges of the structure, as result of the load applied, some pressure waves begin to cross our system. These waves can interact among each other, can suffer reflections on the opposite edges and can be damped as well depending on the damping chosen into the system. These are in fact the result of our external forces acting on the system: the system breaks because of the passage of these waves, that create variations of stresses and they depend on the external boundary conditions we have just apply on the edge. Because of the damping we introduced into the dynamic equation, these pressure waves are forced to dissipate their energies till to "die". When they finish to cross the system, the system itself reaches the

equilibrium for the constant displacement applied from the external world; after that, the external load is increased; this is what happens in static (we analysed a static case in dynamics to notice the so called “transient”) and for this reason in static it is not important to estimate this time. The system in fact has always got its own time to relax and to do all the necessary iterations and avalanches to reach the equilibrium before the increment of the external load. And the time in which this happens is the damping time of the pressure waves that correspond from a physical viewpoint to the relaxation time the system needs to reach the equilibrium. We call this equilibrium like “static equilibrium”.

We report some plots to better understand the problem:

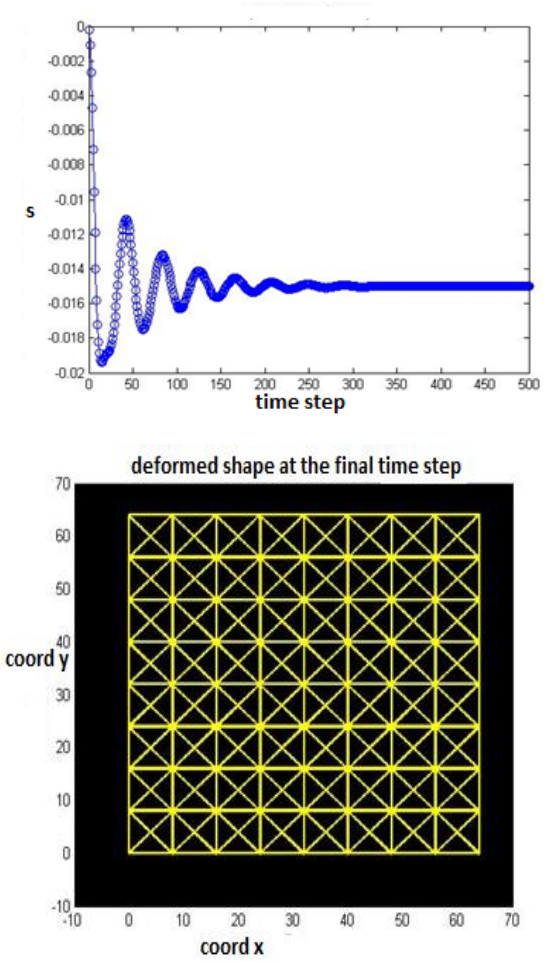

*Figure 4.9: Variation of the displacement **s** of the penultimate point on the bottom, in the right part of the structure as function of time because of the application of constant displacement at the four edges of the structure. As it is possible to notice, the damping is quite visible*

where the external displacements on the edges is equal to 2/5000 m (analysing the problem in the SI system) and the damping coefficients in the Rayleigh damping α and β are equal to 0.1. In the first picture we can visualize what we just explained some rows before; the complete damping due to the dissipation of the pressure waves into the system occurs after about 300 steps that correspond to 30 seconds (each step takes a time of 0.1 seconds).

4.4.5 Numerical results

We analyze now the numerical results in dynamic. Three sets of simulations will be considered; in the first one we will pull the medium from the four edges, emulating a strain constant experiment. We will apply a step in displacement in order to notice the differences with the simulation 1 we reported in the previous pages. In the second one we will increase the flux in the central point using a flux step and we will clamp the medium on the left and on the bottom, considering a condition of free flow on the nodes of the perimeter (0 Mpa). In the third one, with the same boundary conditions, we will apply a pressure on the central point always by a step function.

Simulation 2: Dynamic for a porous medium

Young modulus *E* of the trusses	100 MPa
Displacement step	10/5000
Mesh	64 x 64
Length L	64 mm
Δt	2 seconds
Boundary conditions	Pulled on the four edges

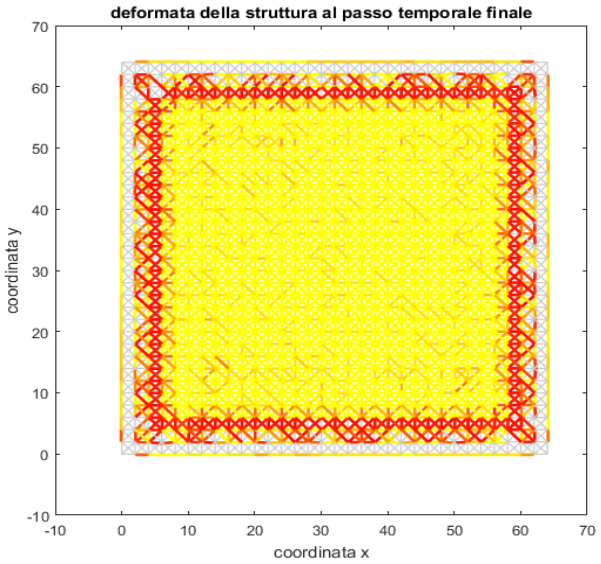

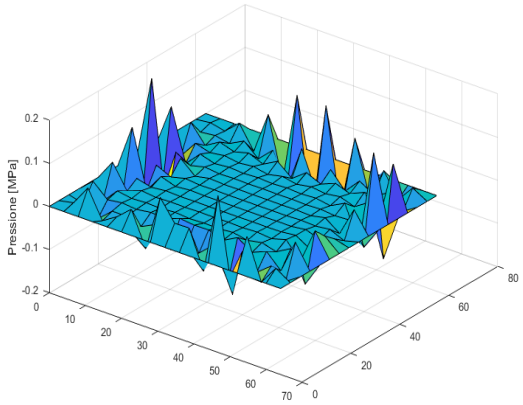

As we notice, by pulling from the four edges, the structure trivially breaks close to the edges themselves: it is not possible in this case to reproduce the effects of the static because of the "wall" induced by the inertia and the damping. Where the structure breaks on the edges we observe some rises in pressure.

Simulation 3: flux applied to the central point:

Young modulus *E* of the trusses	100 MPa
Flux on the centre of the mesh	$3 * 10^{-2}\ mm^3/s$
Mesh	64 x 64
Length L	64 mm
Δt	2 seconds
Boundary conditions	Pressure = 0 MPa on the four edges; clamped on the left and on the bottom

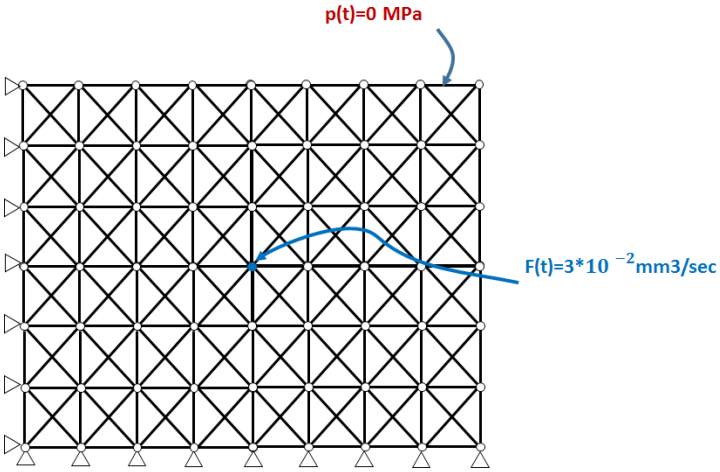

We report the values of damage now a series of graphics for different time steps: in the first ones we show on the top the damage in the structural part created by the increasing of the pressure (the level of damage increases from the yellow to the red); on the bottom the value of the pressure in the fluid part expressed in MPa according to the scale on the right side of the figure.

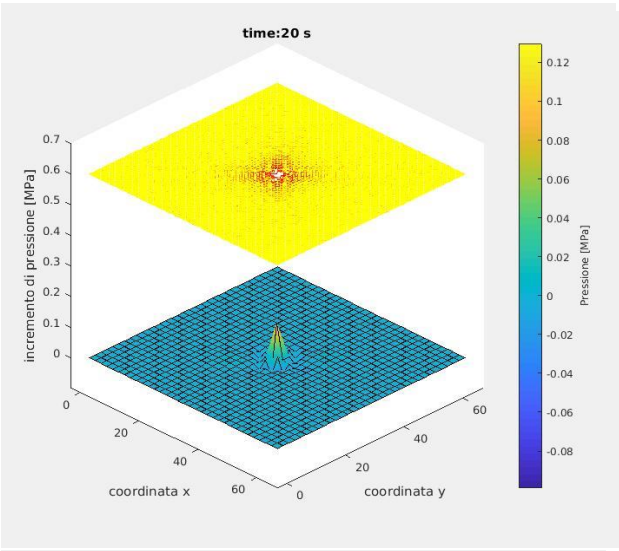
time:20 s
incremento di pressione [MPa]
coordinata x
coordinata y
Pressione [MPa]

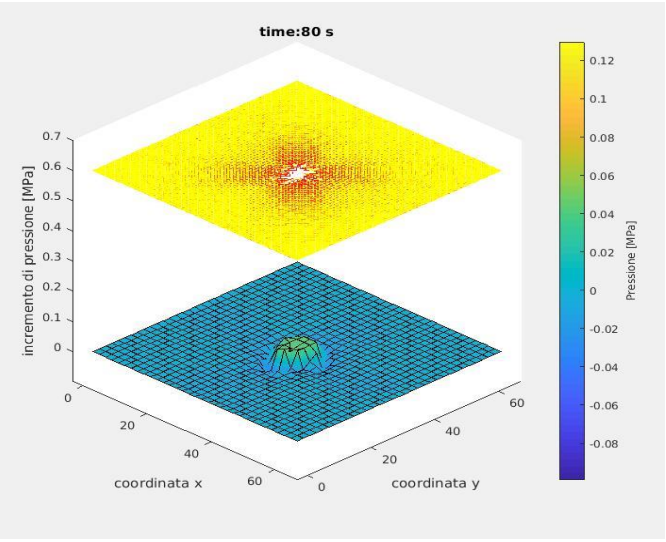
time:80 s
incremento di pressione [MPa]
coordinata x
coordinata y
Pressione [MPa]

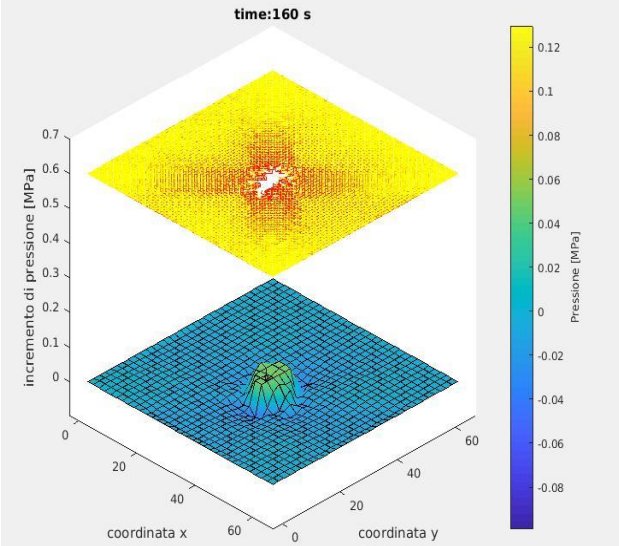
time:160 s
incremento di pressione [MPa]
coordinata x
coordinata y
Pressione [MPa]

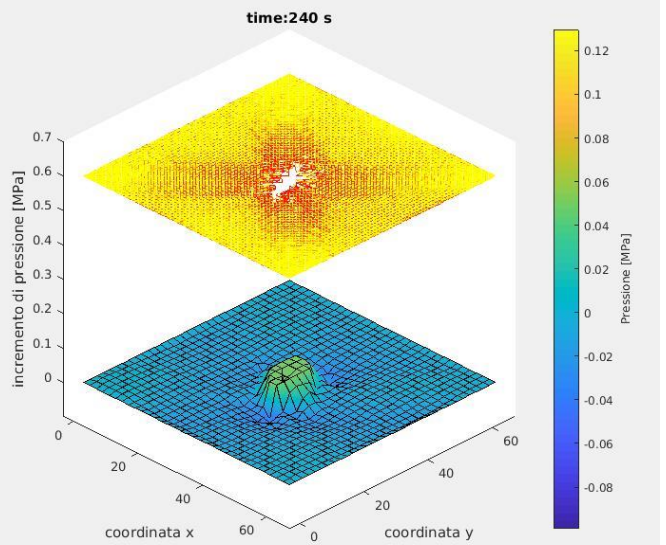
time:240 s
incremento di pressione [MPa]
coordinata x
coordinata y
Pressione [MPa]

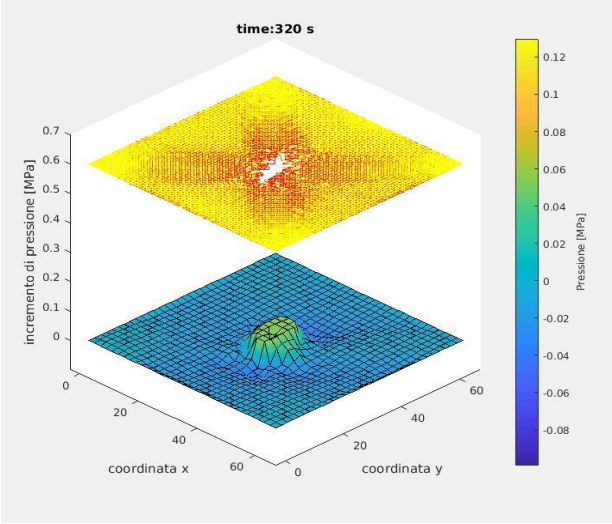
time:320 s
incremento di pressione [MPa]
coordinata x
coordinata y
Pressione [MPa]

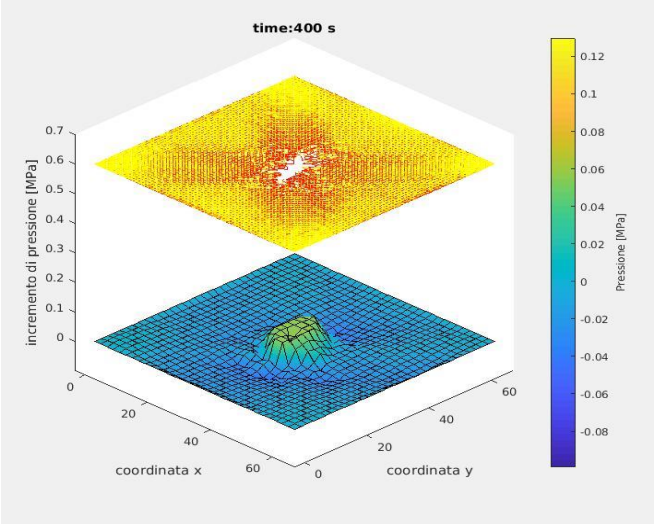
time:400 s
incremento di pressione [MPa]
coordinata x
coordinata y
Pressione [MPa]

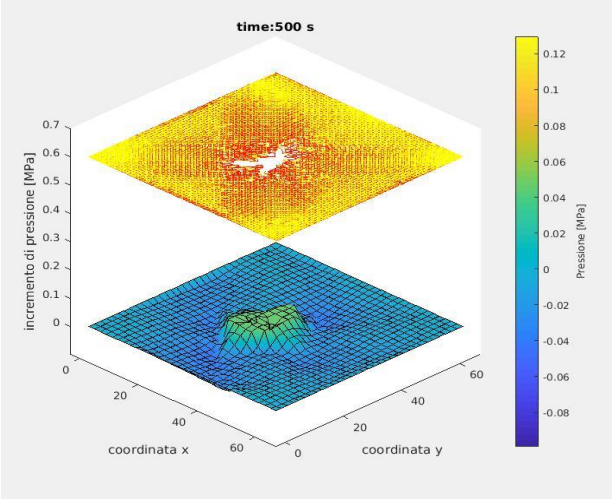
time:500 s
incremento di pressione [MPa]
coordinata x
coordinata y
Pressione [MPa]

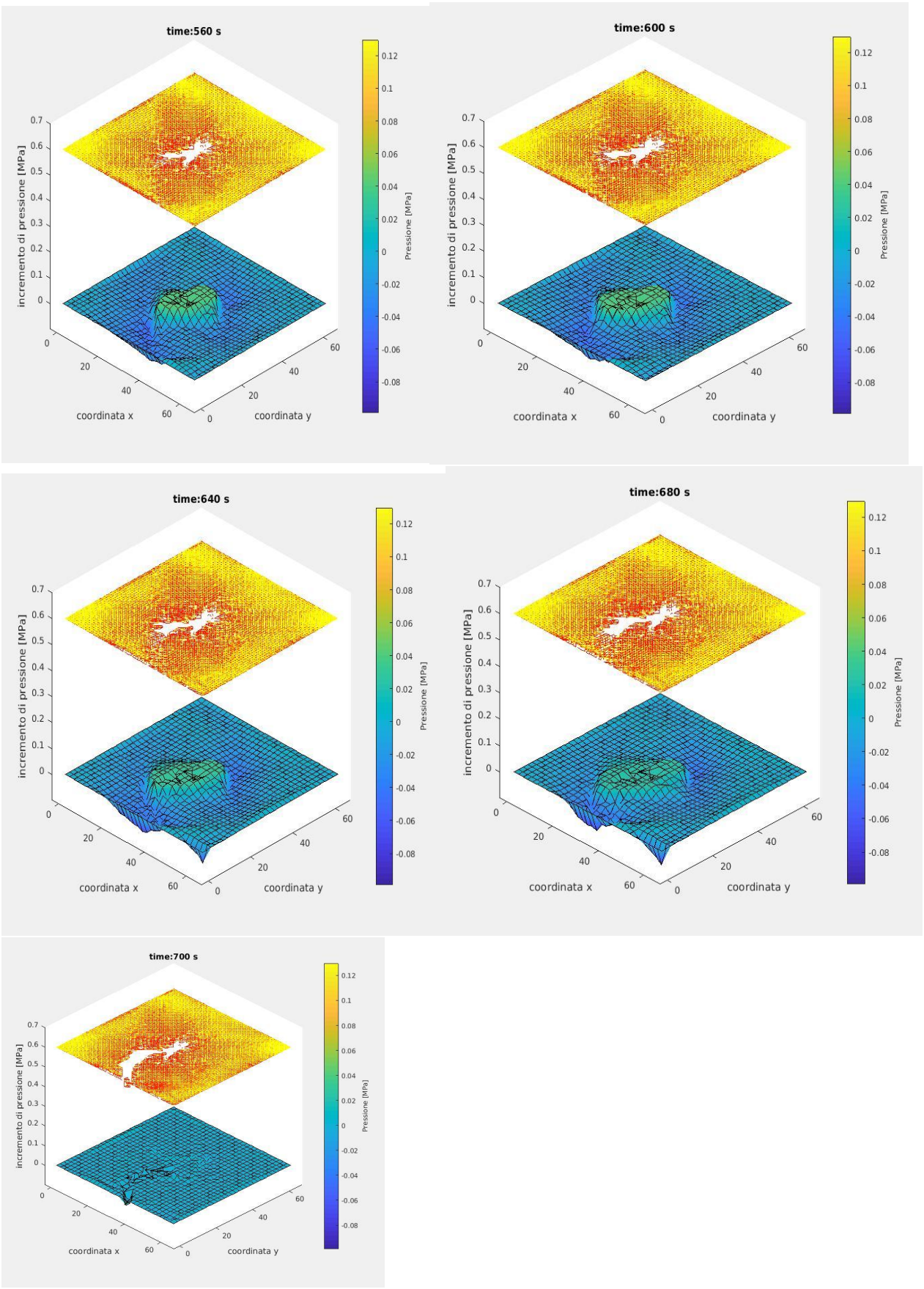

Figure 4.10: Damage (on the top) and pressure (on the bottom) into the system with a flux step applied in the central point of the mesh

In the remaining plots instead, we show the values of the stresses that the trusses of the structural part have to suffer (the stress is normalized with respect the maximum value of stress into the system and it increases going from the dark blue to the light blue)

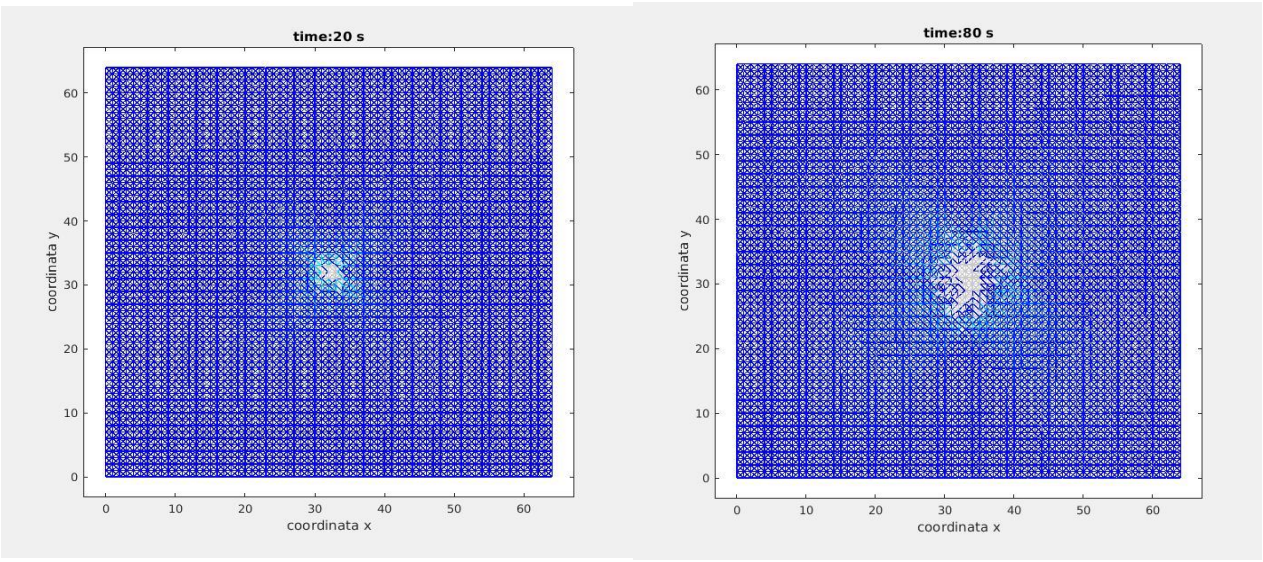

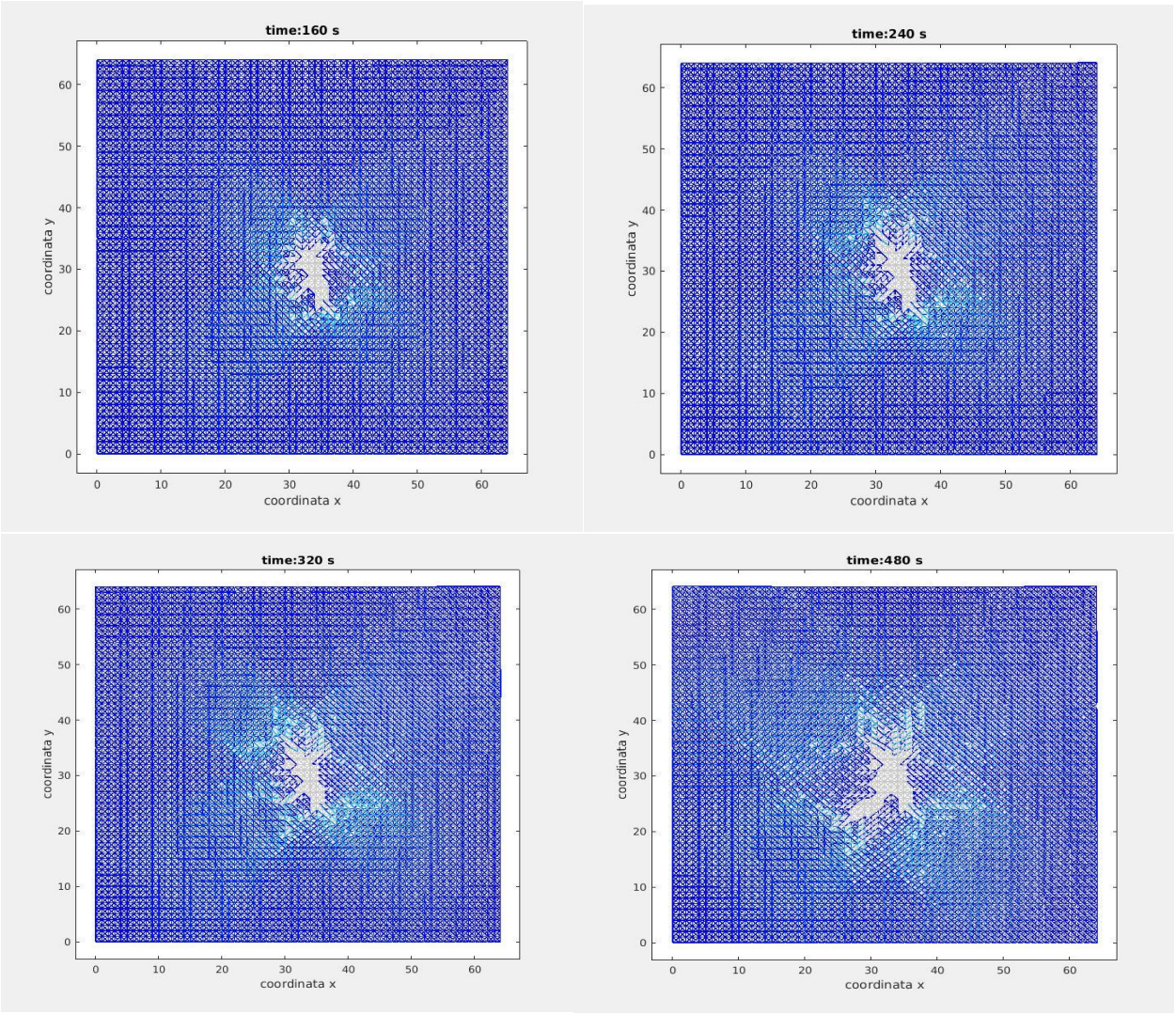
time:160 s
time:240 s
time:320 s
time:480 s
coordinata x
coordinata y
0
10
20
30
40
50
60

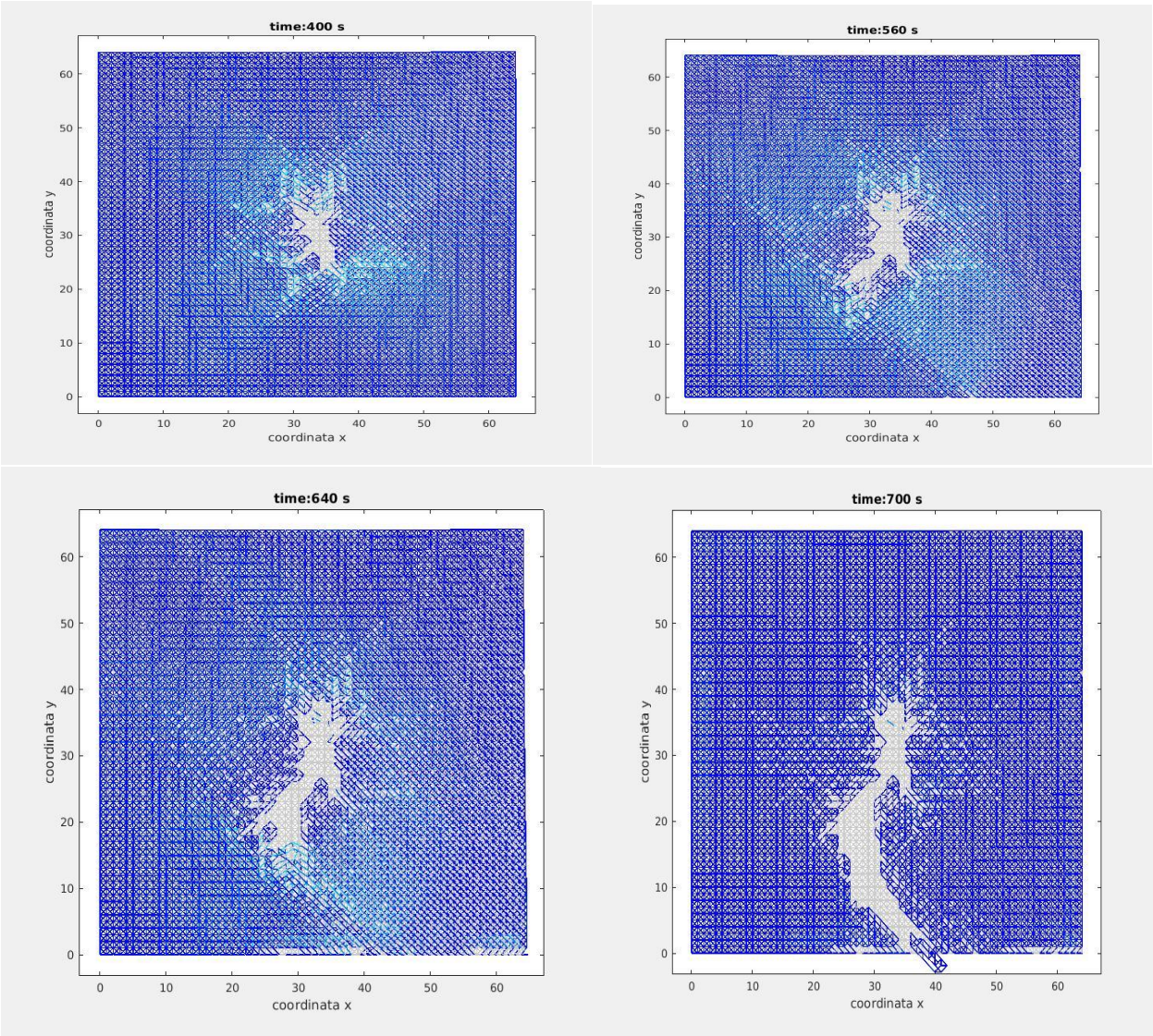

Figure 4.11: Stress of the trusses normalized with respect the maximum stress into the structural part of the system

Comments:

Let us try to give a physical explanation to the plots of the pressure we noticed above.

If we impose a constant flux in the central point of the mesh, the pressure increases on average in the system with respect the initial condition (pressure equal to 0 MPa) because we are pumping water. This is the general trend and associated to this we observe some drops in pressure close to the crack tip that creates in the solid part of the system. Why? Let us try to give an explanation about this.

The flow effect is transmitted to the solid through the pressure coupling term in the effective stress. The solid is loaded and upon rupture produces a sudden increase of the volumetric strain. This in turn produces a drop in pressure. Hence pressure *drop* upon rupture. Furthermore, the bigger is the variation of the stiffness (the damage), the bigger is the radius in which it will be possible to feel the change in the pressure inside the system.

In the next figure we show some points of the system in order to control the trend of the pressure in time and to evaluate its oscillations taking into account the development of the fracture.

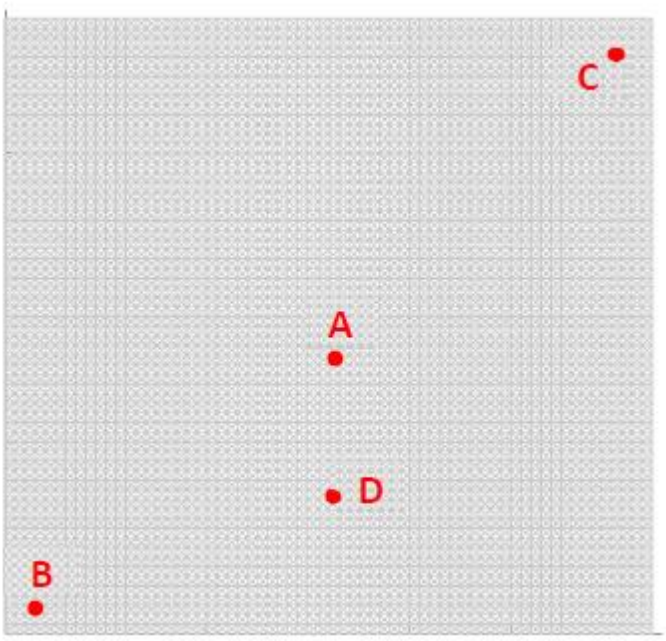

Figure 4.12: Points in the liquid part of the porous media selected for studying the trend in pressure

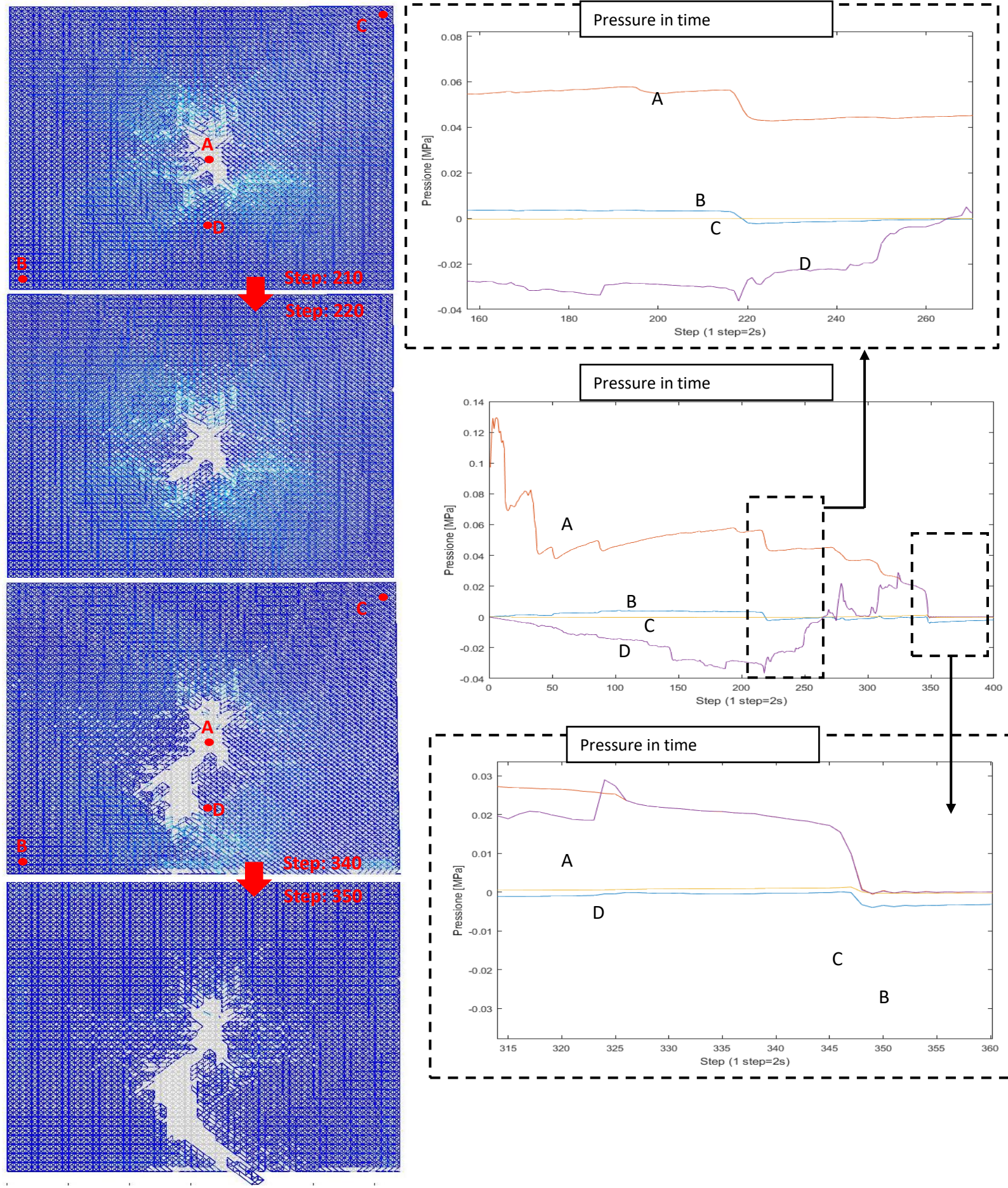

Figure 4.13: Pressure vs time in the points A, B, C, D.

As we notice the points B and C are almost unaffected by the pressure step while the drops are quite consistent on the points A and D (the point D represents the crack tip). In the end, when the fracture channel creates, the pressure assumes the same value in the four points because the water finds a "channel" to go out from the system. This is evident from the figures 4.10

Simulation 4: pressure applied to the central point:

Young modulus *E* of the trusses	100 MPa
Pressure on the centre of the mesh	$1\ MPa$
Mesh	64 x 64
Length L	64 mm
Δt	2 seconds
Boundary conditions	Pressure = 0 MPa on the four edges; clamped on the left and on the bottom

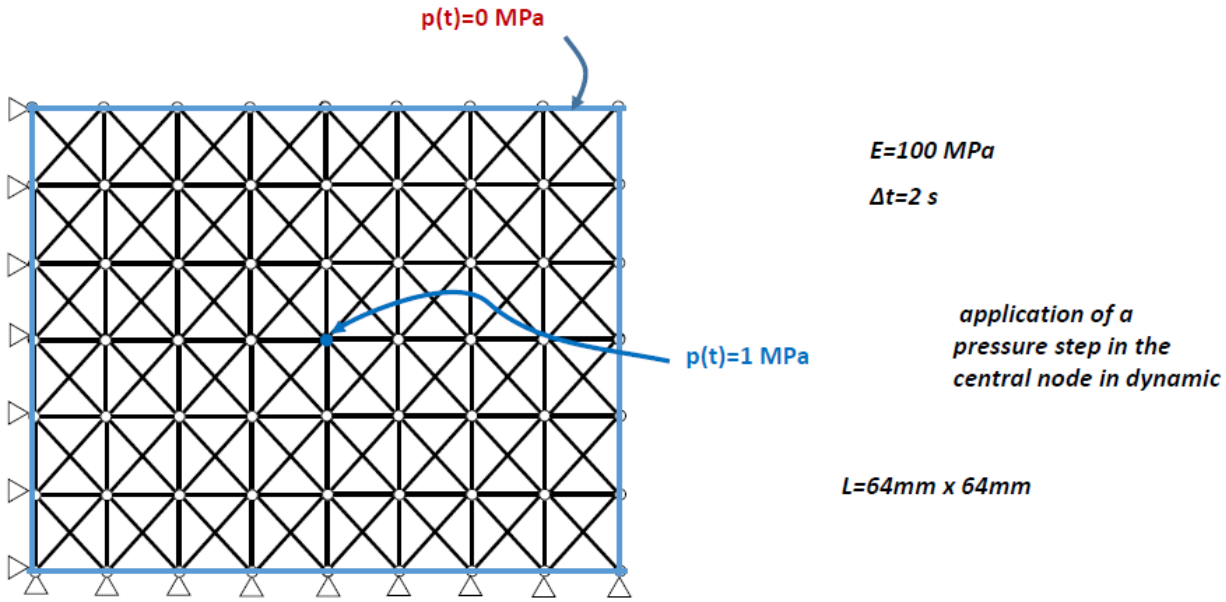

Because of the application of the pressure to the central node of the mesh, the solid skeleton damages and breaks and so the pressure increases into the system. We briefly report below the trends of the damages (yellow is not damage while red is close to the breaking point) and pressures expressed in MPa according to the scale on the right side of the figure .

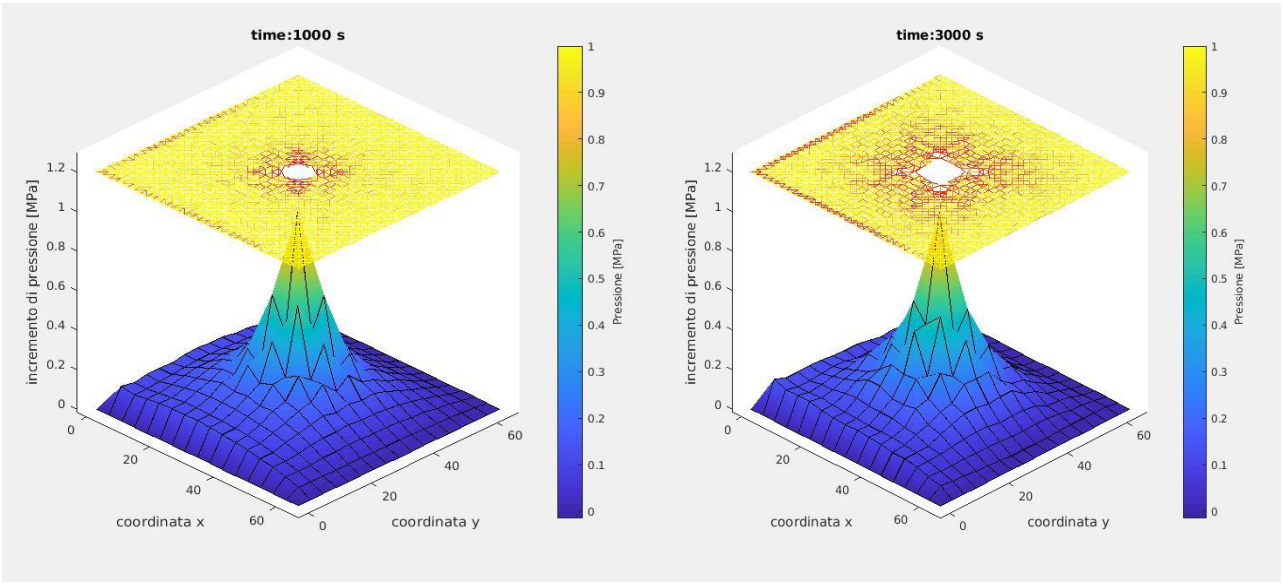
time:1000 s
incremento di pressione [MPa]
coordinata x
coordinata y
Pressione [MPa]
time:3000 s
incremento di pressione [MPa]
coordinata x
coordinata y
Pressione [MPa]

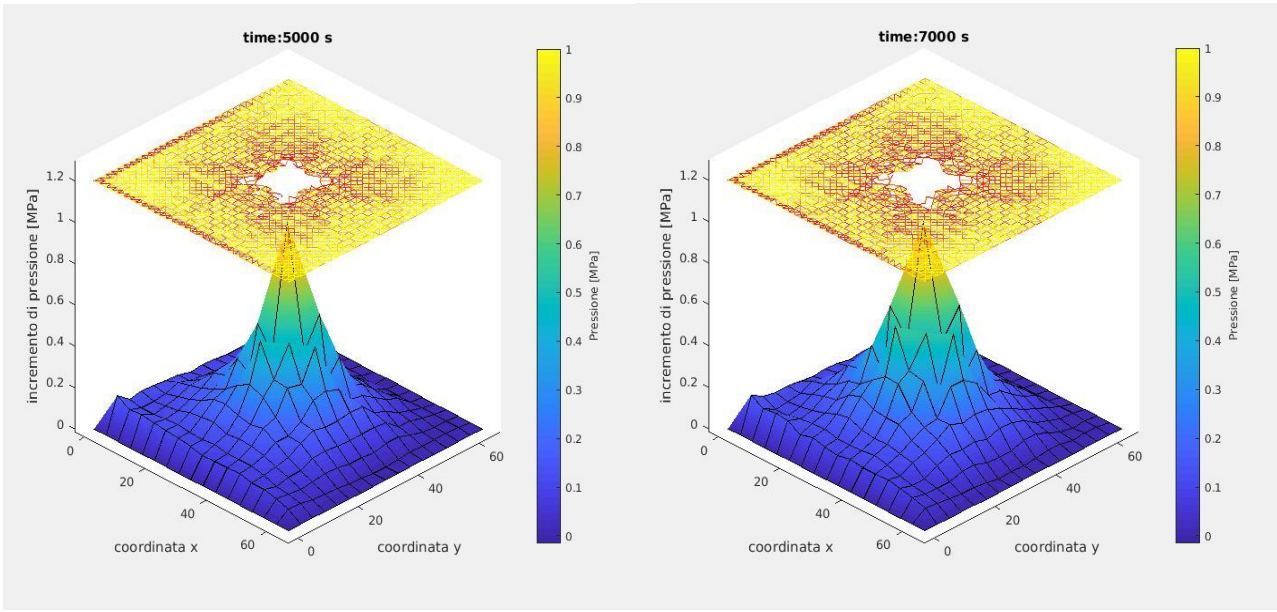
time:5000 s
incremento di pressione [MPa]
coordinata x
coordinata y
Pressione [MPa]
time:7000 s
incremento di pressione [MPa]
coordinata x
coordinata y
Pressione [MPa]

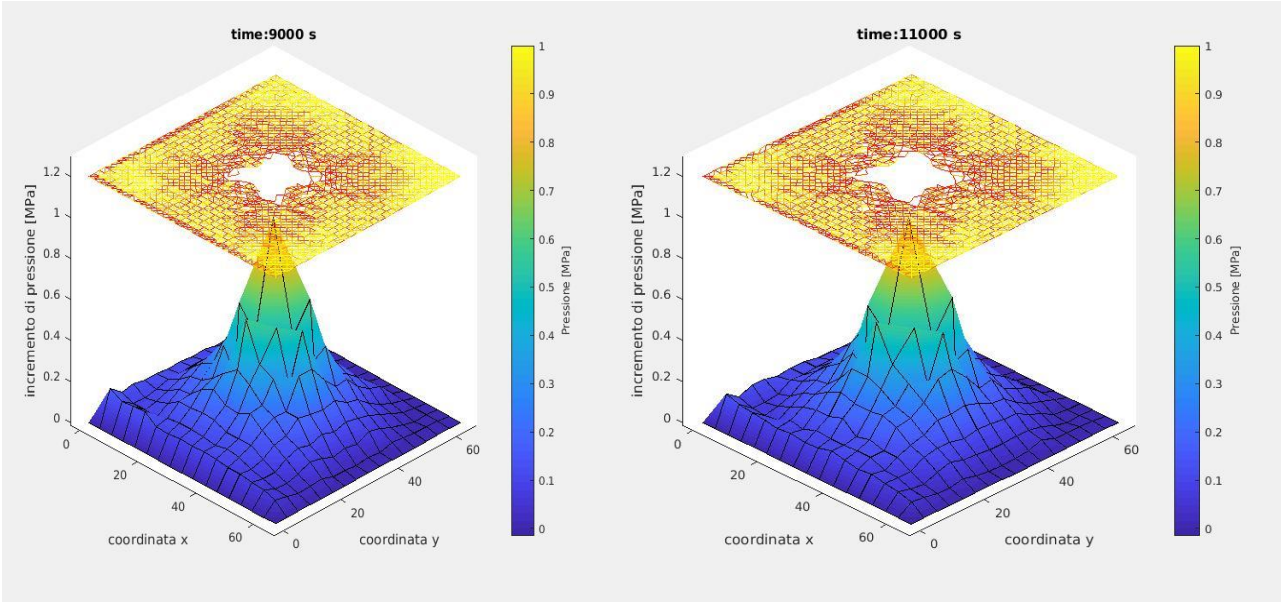
time:9000 s
incremento di pressione [MPa]
coordinata x
coordinata y
Pressione [MPa]
time:11000 s
incremento di pressione [MPa]
coordinata x
coordinata y
Pressione [MPa]

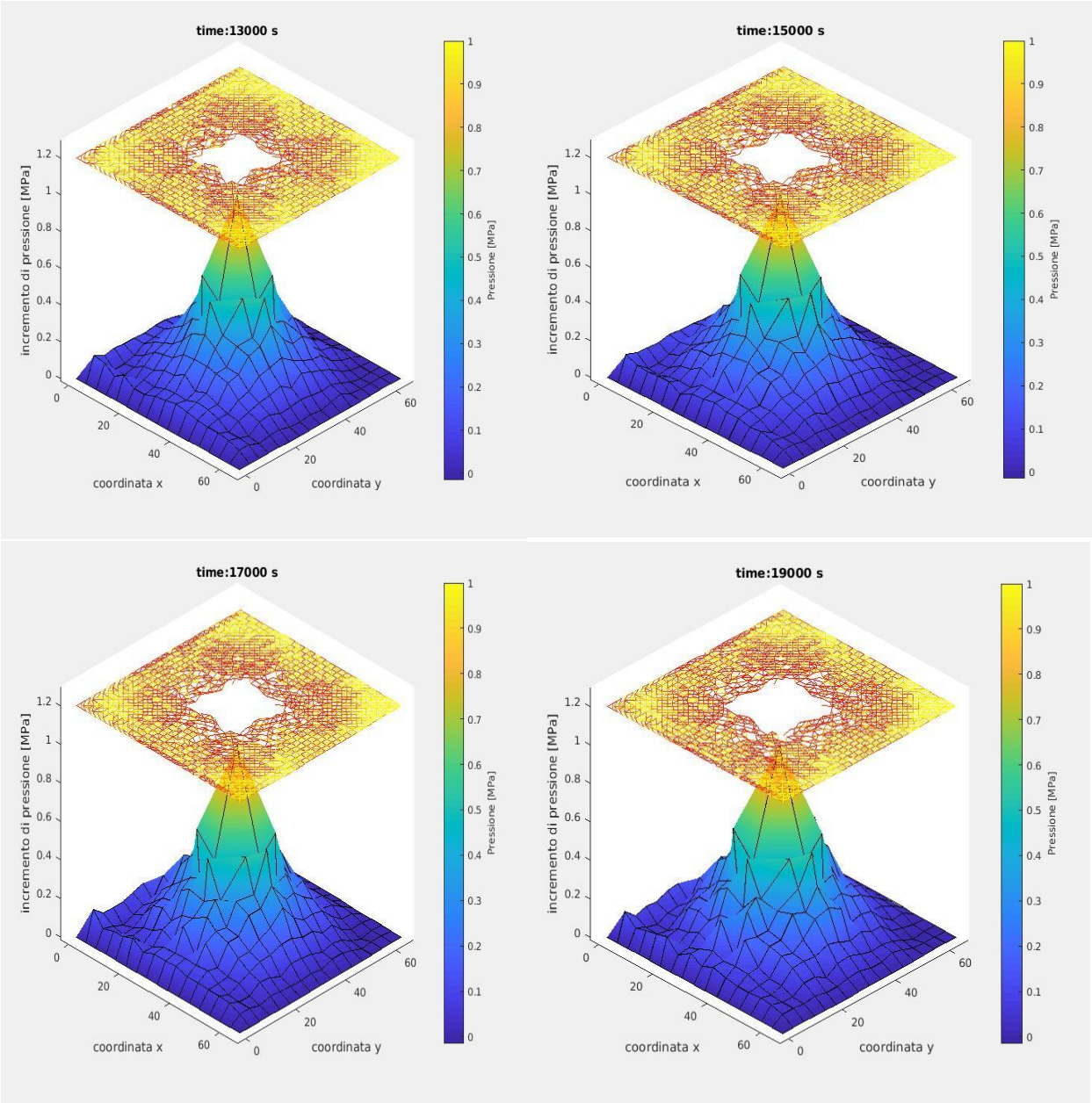

Comments:

In this case some rises are observed close to the crack tip. The explication is the following one: if a load, pressure , assigned displacement and an opening of the grid (advancing fracture) is applied suddenly the fluid takes initially almost all because its immediate response is as undrained and it is much less compressible than the solid skeleton: it discharges the solid. Then through the coupling (volumetric strain) with the fluid, the overpressure dissipates and the solid is reloaded Hence we have a pressure *rise* upon rupture.

These drops (for flux applied) and rises (for pressure applied) were already obtained by Milanese et al.,2017 in static and they do have an experimental evidence. This particular damage model is able to predict these oscillations that other models, like XFEM or cohesive models, are not able to. In our code, mixed to these drops or rises, we find also the inertial and damping effects. So in

dynamic we can have a complete description of the phenomenon that in static was not possible to pick up.

4.5 The average on all the possible realizations on a truss lattice

4.5.1 The idea of average

In chapter 2 we developed the theory of the statistical ensembles in order to get the average behavior of a bundle of fibers. In particular we showed that during a strain constant experiment, the average constitutive behavior can be written like

$$< \tau > = NE\{P_0(\varepsilon) + aP_1(\varepsilon) + \cdots + a^{kmax-1}P_{kmax-1}(\varepsilon)\}\varepsilon$$

where N is the total number of fibers into the bundle.

Obviously, we already explained the meaning of this expression: $< \tau >$ is the value of the stress on the bundle averaged among all the possible realizations of the disorder obtained by assigning different thresholds to the fibers of the bundle itself; ε is the strain acting on the bundle which is constant in the strain ensemble, while $P_0(\varepsilon), P_1(\varepsilon), \dots, P_{kmax-1}(\varepsilon)$ are the probability density functions we introduced in chapter 2.

We also talked about the variances and we showed that the variance $\Delta\left(\frac{n_i}{N}\right)$ expressing the fluctuation in finding the fraction of fibers damaged i times is:

$$\Delta\left(\frac{n_i}{N}\right) = \sqrt{\frac{P_i(1-P_i)}{N}}$$

So one important consequence of this equation is that for a large number of fibers N, all the fluctuations go to zero and there exists only one state of damage given by

$$D = \{P_0(\varepsilon), P_1(\varepsilon), \dots, P_{kmax}(\varepsilon)\}$$

We remind to the chapter 2 to recover all the conclusions about the statistical study of the CFBM.

Now, how can we apply our considerations to the truss lattice?

In the previous pages, we showed that Schrefler, Milanese and Molinari linked the average stress into the truss lattice to the average strain into the same structure and varying the boundary conditions they obtained a constitutive behaviour of the whole structure calculating average stress $\tau_{truss-lattice}$ and average strain $\varepsilon_{truss-lattice}$ point by point. Basically, applying some boundary conditions on the edges in static and varying them was equivalent to catch point by point the equivalent constitutive behaviour of the whole structure (i.e. the curve $\tau_{truss-lattice}, \varepsilon_{truss-lattice}$ for one single realization of the disorder). The physical meaning of this is that it is possible to get the macroscopic behaviour of the lattice by leaving from the microscopic one. Now we are going to do the same with the important difference that we are not considering one realization like in the simulation but the disorder will be already averaged into some $< \tau_{truss-single} > -\varepsilon$ curves

we will assign to the single trusses. After this we will compute the mean value of these $< \tau_{truss-single} >$ (that will be affected by a mistake because each $< \tau_{truss-single} >$ will have a mistake depending on its associated strain) and the mean value of the strains ε into the structure. The result is that we will get by points an average constitutive behaviour of the truss lattice varying $\varepsilon_{truss-lattice}$ ($\varepsilon_{truss-lattice}$ varies as consequence of the displacements applied on the boundaries) like in the previous pages for one single realization, with an important difference: the constitutive behaviour curve we will get, will be the real constitutive behaviour in the thermodynamic limit. There would not be differences if we decide to change the geometry of the truss structure because by increasing the number of truss from a physical viewpoint we reach in a good approximation the continuum. So the new curve $\tau_{truss-lattice} - \varepsilon_{truss-lattice}$ we get should be characterized by the same values for different geometries and because of the theorem of the variance its mistake would be equal to 0 for N big.

When we perform a stress/strain constant experiment on our truss lattice, obviously as result of the displacements applied on the edges, a set of strains on the trusses of our system will develop. These strains will be different one another and so the stresses for each truss. So, if we know that a particular strain ε acts on one truss of the truss lattice, by the study of the CFBM we also know that

$$< \tau >= E\{P_0(\varepsilon) + aP_1(\varepsilon) + \cdots + a^{kmax-1}P_{kmax-1}(\varepsilon)\}\varepsilon$$

(4.36)

will be the stress acting on that truss averaged among all the possible realization given by the disorder. Obviously now we are talking about the constitutive behaviour of one single truss: for this reason $N = 1$ in the last equation.

So, resuming, we can state that if we apply an imposed displacement on the lattice, each truss will have an expected Young modulus

$$< Y(\varepsilon) >= E\{P_0(\varepsilon) + aP_1(\varepsilon) + \cdots + a^{kmax-1}P_{kmax-1}(\varepsilon)\}$$

(4.37)

and an expected stress

$$< \tau(\varepsilon) > =< Y(\varepsilon) > \varepsilon$$

(4.38)

where ε changes for each truss of the truss structure.

But what about the mistake about the calculation of this last observable?

At this point we should remind that our original bundle is made now only by one truss and if we consider the mean stress for the single truss, by recovering the expression of chapter 2, we have

$$< \tau(\varepsilon) >= \lim_{N\to\infty} \sum_{i=0}^{k-1} E\varepsilon(a^i \frac{n_i}{N}) = \sum_{i=0}^{k-1} E\varepsilon(a^i P_i(\varepsilon))$$

(4.39)

where the terms $\frac{n_i}{N}$ for $N \to \infty$ represent from a physical viewpoint no more the fraction of fibers damaged i times but how many times our truss has damaged i times over N experiment for $N \to \infty$. In chapter 2 we began our calculations saying that the probabilities functions P_i represented the probability for a single fiber to damage $0,1,2, \dots, k$ times, and we built them according to this definition (Hermann, Kun, Hidalgo). Then we showed, by the theory of the ensembles that these functions also represent, in a bundle, the average fraction of fibers damaged $0,1,2, \dots k$ (Chapter 2). However, we are not able anymore to enjoy the fact that $N \to \infty$ and to erase the variance of this mean value in the thermodynamic limit. Here $N = 1$,so we expect a certain uncertainty about the stress on a truss. So our situation now is very similar to an experiment we are performing in which we pick up N different trusses pulling them to a given strain that we call ε. The variance of the stress of one single truss pulled at a strain ε is defined like:

$$Var\ (\tau(\varepsilon)) =< \tau(\varepsilon) >^2 - < \tau(\varepsilon)^2 >$$

(4.40)

So a single realization for τ is given by:

$$\tau = E\varepsilon D$$

(4.41)

where D is a random variable, basically the random variable damage associated to the truss. This variable damage in fact can assume the following spectrum of values $D = \{a^0, a^1, \dots \dots, a^{kmax}\}$.

In N experiments, the mean value of τ is

$$< \tau(\varepsilon) >= \sum_{i=0}^{k-1} E\varepsilon(a^i \frac{n_i}{N})$$

with $0 \leq i \leq kmax$.

So as we said before for N going to infinite, $\frac{n_i}{N}$ becomes the probability P_i and

$$< \tau(\varepsilon) >= \lim_{N\to\infty} \sum_{i=0}^{k-1} E\varepsilon(a^i \frac{n_i}{N}) = \sum_{i=0}^{k-1} E\varepsilon(a^i P_i(\varepsilon))$$

as seen in (4.39) .

This means that this last probability P_i can be seen now from a statistical viewpoint as the probability to get the value a^i of the variable damage D associated to the single truss at a strain ε. A single realization for τ^2 is

$$\tau^2 = (E\varepsilon)^2 a^j$$

or

$$\tau^2 = (E\varepsilon)^2 a^{2i}$$

(4.42)

with $2i = j$.

Now, if we perform N experiments, the mean value of τ^2 is

$$< \tau^2(\varepsilon) >= \sum_{i=0}^{k-1} E\varepsilon(a^{2i}\ \frac{n_{2i}}{N})$$

with $0 \leq 2i \leq kmax$, and for N going to infinite,

$$< \tau^2(\varepsilon) >= \sum_{i=0}^{k-1} E\varepsilon(a^{2i}\ P_{2i})$$

Basically we computed in Chapter 2 the variance of a bundle of fibers and we showed that in the thermodynamic limit, $N \to \infty$, this "mistake" on the stress went to 0. Now, in the case in which $N = 1$, so by a simple calculation

$$Var\ (\tau(\varepsilon)) = (E\varepsilon)^2 \left\{ \left(\sum_{i=0}^{k-1} a^i\ P_i(\varepsilon) \right)^2 - \sum_{i=0}^{k-1} a^{2i} P_{2i}(\varepsilon) \right\} \neq 0$$

(4.43)

In this way we are now able to compute the variance $Var\ (\tau(\varepsilon))$.

So for a given ε, each truss will have a mean value $< \tau(\varepsilon) >$ and a given variance that we can compute by supposing to realize N different experiment for each value of ε.

Now, let us indicate each truss of our truss structure with the index n. So the strain each truss will suffer into the structure will be ε_n and the average stress at that strain ε_n will be $< \tau_n(\varepsilon_n) >$ in the new notation.

So each truss suffers a strain ε_n , has got a $\tau_n(\varepsilon_n)$, which is obviously a random variable because of the disorder; but this random variable has got an average $< \tau_n(\varepsilon_n) >$ and a variance $Var\ (\tau(\varepsilon))$ as well.

Now before going ahead, let us resume some properties of the mean value and of the variance*:* if a and b are constant, X and Y two random variables and Z another random variable defined as $Z = X + Y$

Mean value

a) $< aX >= a\ < X >$

b) $< a + X > = a + < X >$

c) $< Z > = < X + Y > = < X > + < Y >$

d) $< aX + bY > = a < X > + b < Y >$

Variance:

e) $Var\ (aX) = a^2\ Var\ (X)$

f) $Var\ (a + X) = Var\ (X)$

g) Theorem of the variance:

If Z is a random variable defined like $Z = \sum_{i=1}^{n} a_i X_i$, then

$$Var(Y) = \sum_{i=1}^{n} a_i^2\ Var(X_i) + \sum_{i=1}^{n} \sum_{j \neq i} a_i a_j Cov(X_i, X_j)$$

We can observe that this last relation is valid both when the random variables are statistically independent and when they are dependent because of the appearance of the covariance.

Now, we have basically the function

$$\tau_{truss\ lattice} = \tau_{truss\ lattice}\big(\tau_1(\varepsilon_1),\ \tau_2(\varepsilon_2), \dots., \tau_N(\varepsilon_N)\big) \equiv \sum_{n=1}^{N} \frac{1}{N}\ \tau_n$$

(4.44)

which is the function that we compute for one single realization of our disorder. What is its mean value? By d), we have

$$< \tau_{truss\ lattice} > = < \sum_{i=1}^{N} \frac{1}{N}\ \tau_n > = \frac{1}{N}\ \sum_{n=1}^{N} < \tau_n >$$

(4.45)

In this way we computed the mean value associated to the constitutive behaviour of the truss lattice for a given N. This means from a statistical viewpoint that we are considering the average value $< \tau_{truss\ lattice} >$ among infinite curves $\tau_{truss\ lattice}$ given by the disorder.

Let's have an example to better understand this concept; in (4.45) we compute the average value among the mean values on all the possible realizations of each truss. And we showed this is equivalent to do infinite simulations of the same truss structure characterized by the same boundary conditions and computing the mean value among the infinite mean stresses obtained.

What about the variance of $< \tau_{truss-lattice} >$?

By the theorems about variance above shown, we have

$$Var(\tau_{truss-lattice}) = \frac{1}{N^2}\left(\sum_{n=1}^{N} Var\,(\tau_n\,) + \sum_{n=1}^{N}\sum_{m\neq n} Cov(\tau_n\,,\tau_m\,)\right)$$

(4.46)

Again, if we think of (4.45), this is the mean value among N terms, the N trusses: each of them has got a different value of strain and so a different value of mean stress; and each of them has got a different variance depending on ε. Furthermore it is possible that each truss is correlated with the other ones because of the avalanches that are the result of the presence of the truss structure.

We already computed $Var\,(\tau_n\,)$ in (4.40). What about the $Cov(\tau_n\,,\tau_m\,)$?

By definition,

$$Cov(\tau_n, \tau_m) = \mathbb{E}[\tau_n(\varepsilon_n)\,\tau_m(\varepsilon_m)] - \mathbb{E}[\tau_n(\varepsilon_n)]\mathbb{E}[\tau_m(\varepsilon_m)]$$

(4.47)

where the notation $\mathbb{E}(X)$ is the symbol used in statistic to indicate the mean value of a random variable X.
Now,

$$\mathbb{E}[\tau_n(\varepsilon_n)] =< \tau_n(\varepsilon_n) >$$

$$\mathbb{E}[\tau_m(\varepsilon_m)] =< \tau_m(\varepsilon_m) >$$

and we already computed these two mean values previously.

As regards $\mathbb{E}[\tau_n(\varepsilon_n)\cdot\tau_m(\varepsilon_m)]$, one single realization of the object $\tau_n(\varepsilon_n)\cdot\tau_m(\varepsilon_m)$ is given by

$$a^n E\varepsilon_n \cdot a^m E\varepsilon_m = a^{n+m} E^2 \varepsilon_n \varepsilon_m$$

(4.48)

and

$$\mathbb{E}[\tau_n(\varepsilon_n)\cdot\tau_m(\varepsilon_m)] = \sum_{i=0}^{k-1} a^{i,n} E\varepsilon_{i,n} \sum_{j=0}^{k-1} a^{j,m} E\varepsilon_{j,m}\; P(\tau_n(\varepsilon_n), \tau_m(\varepsilon_m))$$

(4.49)

where $P(\tau_n(\varepsilon_n), \tau_m(\varepsilon_m)$ is the joint probability associated to the two random variables $\tau_n(\varepsilon_n)\;\tau_m(\varepsilon_m)$. We do not have obviously this joint probability so let us assume that this last quantity is different from 0.

In the end we arrive to say that

$$Cov(\tau_n(\varepsilon_n), \tau_m(\varepsilon_m)) = E^2 \left[\sum_{i=0}^{k-1} a^{i,n} E\varepsilon_{i,n} \sum_{j=0}^{k-1} a^{j,m} E\varepsilon_{j,m} \; P(\tau_n(\varepsilon_n), \tau_m(\varepsilon_m)) - \varepsilon_n \sum_{i=0}^{k-1} a^{i,n} P_i(\varepsilon_n) \cdot \varepsilon_m \sum_{j=0}^{k-1} a^{j,m} P_j(\varepsilon_m) \right]$$

(4.50)

that can be generally different from 0.

However we can state from the theorem of the variance (4.49) that $Var(< \tau_{truss-lattice} >)$ goes to 0 for N (number of trusses into the structure) going to infinite. So by the theorem of the variance (e) we can state that the fluctuations around the average constitutive behaviour among all the possible realizations goes to 0 for big N. Basically this result is quite similar to the one found for the CFBM.

So, resuming: basically, because of the disorder spread into our truss structure because of the thresholds we assign, we will have infinite constitutive behaviour $\tau_{truss-lattice} - \varepsilon_{truss-lattice}$. We can also compute $< \tau_{truss-lattice} > - \varepsilon_{truss-lattice}$ which is, as we shown above, the average among infinite numerical experiments about our truss lattice. So, for N number of trusses fixed, we could think of a distribution of curves $\tau_{truss-lattice} - \varepsilon_{truss-lattice}$ with its mean value. The curves $\tau_{truss-lattice} - \varepsilon_{truss-lattice}$ are obtained by the numerical experiments while the curve $< \tau_{truss-lattice} > - \varepsilon_{truss-lattice}$ is their average. We showed that for big number of trusses, all the curves derived from the numerical experiments collapse into the curve

$$< \tau_{truss-lattice} > - \varepsilon_{truss-lattice}$$

because the variance goes to 0. This is exactly what happens in the CFBM as well. In the thermodynamic limit, the mistake associated at this curve goes to 0 and the last curve becomes **THE** constitutive behaviour of the structure, from which we can state in which point of the curve the model breaks, how it breaks (for big N there will be only one way in which the model will break: it will form an X.

A probabilistic law (depending on the threshold and so on the disorder) gets a deterministic law in the thermodynamic limit.

For small N we obtain always this "average" behaviour but the single realizations will be far away from this average because of the growth of the variance, like happened in the CFBM) and the damage law.

In this way it is possible by the statistics to determine from the microscopic behaviour of one element, the macroscopic behaviour of the whole structure and to get the statistic constitutive behaviour of a material, that for a large number of truss **IS** the constitutive behaviour. By the average curve $< \tau_{truss-lattice} > - \varepsilon_{truss-lattice}$ then it is possible to get a global damage law

$$D = 1 - E(\varepsilon_{av})/E_0$$

(4.51)

which is a function of the average constitutive behaviour. This damage law we are able to obtain now, is a function of the elastic properties of the material (E), it is a function of the way in which a single microscopic elements breaks (the damage parameters a and k_{max} that must be computed in an experimental viewpoint) and it contains already the disorder which is averaged according to the technique we introduced before. In the past we remind Mazars (1986) that was able to recover a damage law by thermodynamic considerations on the concrete in which the variable damage was expressed like:

$$D = \alpha_t D_t + \alpha_c D_c$$

(4.51)

where

$$D_t = F_t(\varepsilon)$$

(4.53)

with

$$F_t(\varepsilon) = 1 - \frac{(1 - A_i)}{\varepsilon} - \frac{A_i}{\exp(B_i(\varepsilon - K_0))}$$

(4.54)

$$i = t, c$$

In this relation $A_i$and B_i are coefficients that must be recovered by experimental measures while the weight coefficients α_t and α_c are chosen in this way:

In traction $\alpha_t = 1, \alpha_c = 0$ and $D = D_t$

In compression $\alpha_c = 1, \alpha_t = 0$ and $D = D_c$.

This is one of the many damage laws developed during the last years and as we can state it depends on the strain applied and on the properties of the material. For this reason to have built a new *global damage law* that contains both the elastic properties and the breaking properties of the micro-elements and the especially the disorder of the medium, is a great result for the statistical central force model.

So in order to get the average constitutive behaviour of the truss lattice model we need to know the average constitutive behaviour of one single truss.

A good benchmark would be to match our average constitutive model with the result of one simulation. For a truss lattice model, one truss had a Young Modulus $E = 100\ MPa$ and it could damage 30 times before breaking with a damage parameter equal to 0.9. So $a = 0.9$ and $k_{max} = 30$. The probability density function instead is a uniform distribution:

$$p(\sigma) = \frac{1}{s_2 - s_1}$$

where $s_1 = 0\ Mpa$ and $s_2 = 1\ Mpa$. So all the thresholds are picked up from this p.d.f.

The constitutive behaviour of one single truss, according to these hypothesis, will be represented in the following picture:

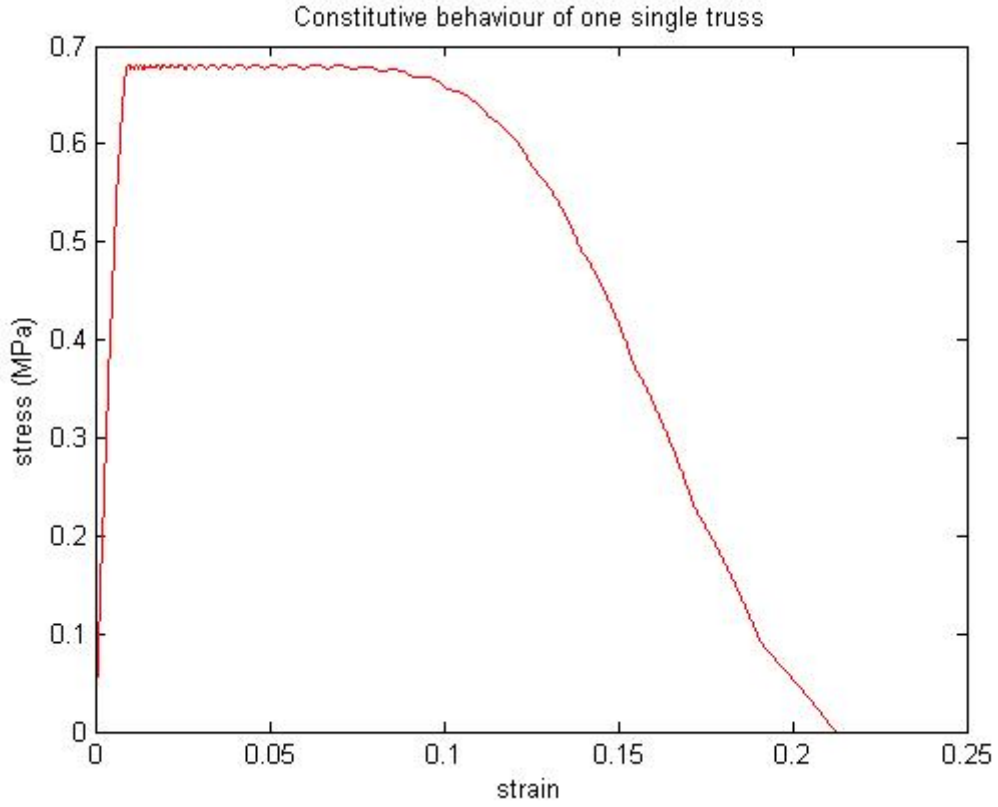

Figure 4.10: strain stress curve that we assign to each truss of our lattice as result of the theory of the ensembles

This constitutive law, obtained by a uniform probability density function, is quite complicated to insert into the code because of the presence of little waves on the plateau. Basically what we do is to assign this constitutive behaviour to each truss of our lattice model (without porous medium) and to apply some imposed displacements in static on the top, bottom, left and right edge: the same imposed displacements applied for the central force model in Milanese, Molinari and Schrefler. At the moment we do not consider the porous medium because our purpose is only to give the basic idea of the method. Obviously the stiffness matrix of the whole truss structure, will contain the Young modulus of each truss) that will be now a function of the strains obtained into the model for each truss according to the curve plotted above: so the model is clearly not linear and a Newton Raphson iterative algorithm must be applied.

4.5.2 Results of the simulations

Some simulations were performed for the system without water in static to show this concept.

A good benchmark about this is to consider the simple code written in static, without water and to compare the constitutive curves of the code obtained by the thresholds (Par 4.4.1.1) and the new code that uses a constitutive behaviour assigned to each truss (Par 4.5.1). If the theory is correct, by making N grow, all the possible realizations of the curves $\tau_{truss-lattice} - \varepsilon_{truss-lattice}$ we calculate by the first algorithm should collapse towards $< \tau_{truss-lattice} > - \varepsilon_{truss-lattice}$ that we compute by the Newton Raphson iterative algorithm because of the lowering of the variance around the mean value for $N \to \infty$. For N not so big instead, we should notice some differences among single realizations $\tau_{truss-lattice} - \varepsilon_{truss-lattice}$ (which are obtained by the first algorithm) and the mean value $< \tau_{truss-lattice} > - \varepsilon_{truss-lattice}$ (obtained by the second algorithm): that's why the variance is not close to 0.

We report some results very briefly.

Figure 4.14: Constitutive behaviour for the Statistical central force model with 272 trusses: in blue, green and red three different realizations given by the disorder. In Yellow the average among all the possible the constitutive behaviours

Figure 4.15: Constitutive behaviour for the Statistical central force model 1056 trusses: in blue, green and red three different realizations given by the disorder. In yellow the average among all the possible the constitutive behaviours

As we notice, the yellow curve stops at a certain point: in fact from the numerical code, the matrix becomes singular and it is not possible to invert it. So from a physical viewpoint, this numerical instability could be considered as the point in which in our truss lattice the fracture channel is born: that's why the yellow curve is the average among all the possible numerical experiments that can be considered by assigning different thresholds in stress to our trusses and so the point in which we record this instability is the average among all the possible breaking points.

The theory can be applied to the dynamic and to a porous medium as well. In fact the problem of the porous medium is simply a coupled problem and the stochastic part regards only the truss structure part.

Chapter 5

Self Organised Criticality

"An unlikely event is likely to happen because there are so many unlikely events that could happen."

Per Bak, How nature works

5.1 Complex systems

5.1.1 Generalities

The system we will be studying, made of trusses, can be considered like a complex system. So an overview about the complexity is necessary.

The study of the complex systems like an unified science has become recognized only in the few recent years and it is linked to many different disciplines, going from the human brain to the physiology, from the physics to the complex networks, from the "life" as we are used to call it, to the economy. For this reason we will try to give a generic definition of complex system.

What's basically a complex system? To answer this question, we must first understand the difference between the word complex and complicated. The dictionary claim of complex is "consisting of interconnecting or interwoven parts" and this comes from the Latin "cum-plexere". As regards the word complicated, this comes always from the Latin "cum-plicare" and this means like made of different parts that can be bended.

This important difference that we can recognize by studying the dictionary, says to us an important claim:

1) A complicated system can be studied by breaking it down in subsets and it can be understood by analysing the dynamics of each of them.
2) A complex system instead, is made by interwoven parts. So this particular structure hints us that its study should be done by considering it in its whole and by studying the interactions among its subsets/elements.

This difference between 1) and 2) is also at the basis of the struggling between two different approaches to the study of the physics: we are talking about Reductionism and Holism.

From a philosophical viewpoint, the Reductionism tries to understand the nature of complicated things by reducing them to the descriptions of its parts. This has been on the basis of the physics for many years in the past. Obviously this approach fails with complex systems: in fact, how is it possible that a system made by different subsets, interacting among them, shows a behaviour completely different with respect the single parts? (we can have an example of this phenomenon by observing the fly of a flock of birds: we know exactly the rule according to a single bird behaves, i.e. it follows the direction of its own neighbours but we are not able to understand why the whole flock moves in a given direction).

To answer this question maybe we should consider another important point of view in studying the different physics systems, which is given by the Holism: in it, we find the idea that the properties of the system cannot be determined or explained by its component parts alone, but they are rather explained in terms of the interactions among the parts. “The whole is more than the sum of the parts”. This summarizes the point of view of this philosophical stream. And this is also the basis of a new discipline, which is the complex system physics.

So this discipline, born in the last years, called *physics of the complex systems* is a new interdisciplinary field of science studying how parts of the system give rise to a collective behaviour of the system and how the system interacts with its environment.

Qualitatively, to understand the behaviour of a complex system, as we already said, we must understand not only the behaviour of the parts but how they act together to form the behaviour of the whole. It is because we cannot describe the whole without describing each part, and because each part must be described in relation to other parts, that complex systems are difficult to understand.
This is relevant to another definition of “complex”: “not easy to understand or analyse.”

These qualitative ideas about what a complex system is, can be made more quantitative. On the basis of the definition we gave about the complex systems, we can understand that we are basically surrounded by them: from the system “atmospheric weather” to the human brain; from the community of the ants to the fly of a flock of birds into the sky; and so on. The complex systems can be founded in every discipline that human beings developed in the centuries. However for many years, professional specialization has led science to progressive isolation of individual disciplines. How is it possible now that well-separated fields such as molecular biology and economics can suddenly become unified in a single discipline under the underlined concept of the complexity? How does the study of complex systems in general pertain to the detailed efforts devoted to the study of particular complex systems? In this regard one must be careful to acknowledge that there is always a dichotomy between universality and specificity.
A study of universal principles does not replace detailed description of particular complex systems. However, universal principles and tools guide and simplify our inquiries into the study of specifics. For the study of complex systems, universal simplifications are particularly important. Sometimes universal principles are intuitively appreciated without being explicitly stated. However, a careful articulation of such principles can enable us to approach particular systems with a systematic guidance that is often absent in the study of complex systems. A pictorial way of illustrating the

relationship of the field of complex systems to the many other fields of science is indicated in the Figure below. This figure shows the conventional view of science as progressively separating into disparate disciplines in order to gain knowledge about the ever larger complexity of systems. It also illustrates the view of the field of complex systems, which suggests that all complex systems have universal properties. Because each field develops tools for addressing the complexity of the systems in their domain, many of these tools can be adapted for more general use by recognizing their universal applicability. Hence the motivation for cross disciplinary fertilization in the study of complex systems.

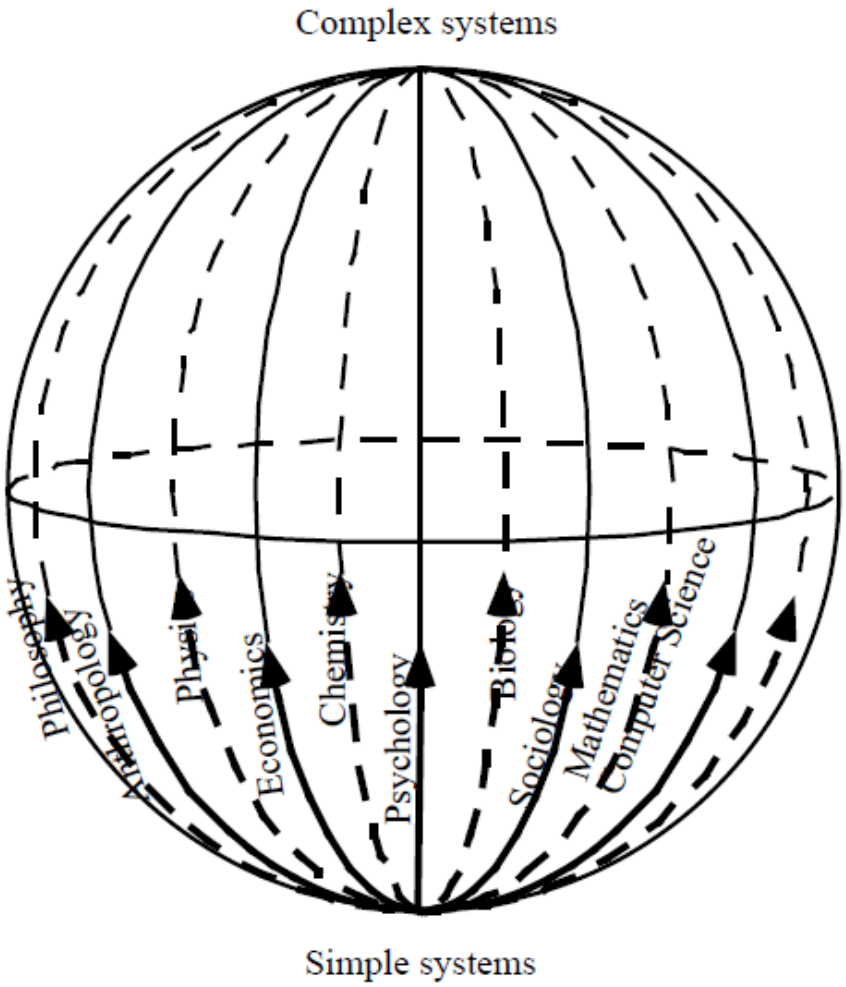

Figure 5.1: representation of the evolution of the world of complex systems (, Y.B. Yam, Dynamics of complex system, 1992)

Some interesting examples of complex systems we can find daily around us are given by: the Governments, the Body, the human life, the brain, the weather, a computer and a person. Instead, examples of simple systems are given by an oscillator, a pendulum and an orbiting planet.

5.1.2 Features of complex systems

Obviously after having given examples of complex system we must give a quantitative more precise definition of its properties and we need to describe them as well; we will make a list of the of the main features that characterize a complex system and assign them a measure that provide a first way of classification;

- Elements (and their number)
- Interactions (and their strength)
- Formation/Operation (and their time scales)
- Diversity/Variability
- Environment (and its demands)
- Activity(ies) (and its[their] objective[s])

For example let us consider the system life: its elements are the organisms that interact one another by non linear interaction like reproduction, competition, predation and communication. Its formation consists in evolution and the activity of each organism consists in the survival, reproduction, consumption and excretion. We could repeat the same considerations by considering human economies and societies, the physiology, the proteins and the neural networks by considering the following scheme:

SYSTEM	ELEMENT	INTERACTION	FORMATION	ACTIVITY
Proteins	Aminoacids	bonds	Protein folding	Enzymatic activity
Nervous system	Neurons	synapses	learning	Behaviour thought
Physiology	Cells	Chemical messengers	Developmental biology	movement
Life	Organisms	Reproduction Competition Predation communication	evolution	Survival Reproduction Consumption excretion
Human economies and societies	Human beings Technology	Communication Confrontation cooperation	Social evolution	Same as life? Exploration?
Truss lattice	Trusses	Bonds	------	To support the external load by “talking” one another

In the scheme above, in the last row we have inserted the truss lattice model we studied in the last chapter. This kind of system can be considered like complex; it is made of different sub elements, that we call trusses, that behave in the same way according to a constitutive behaviour fixed by thresholds. And at the same time they can “communicate” one another in order to reach the equilibrium because of imposed displacements from the external environment.

1.3 Emergence

In general there are two approaches to organize the properties of complex systems:

1) The first of these is the relationship among elements, parts and the whole. Since there is only one property of the complex system that we know for sure — that it is complex—the primary question we can ask about this relationship is how the complexity of the whole is related to the complexity of the parts. As we will see, this question is a compelling question for our understanding of complex systems.
   From the examples we have indicated above, it is apparent that parts of a complex system are often complex systems themselves. This is reasonable, because when the parts of a system are complex, it seems intuitive that a collection of them would also be complex. However, this is not the only possibility.
   Can we describe a system composed of simple parts where the collective behaviour is complex? This is an important possibility, called emergent complexity. Any complex system formed out of atoms is an example. The idea of emergent complexity is that the behaviours of many simple parts interact in such a way that the behaviour of the whole is complex. Elements are those parts of a complex system that may be considered simple when describing the behaviour of the whole.
   Can we describe a system composed of complex parts where the collective behaviour is simple? This is also possible, and it is called emergent simplicity. A useful example is a planet orbiting around a star. The behaviour of the planet is quite simple, even if the planet is the Earth, with many complex systems upon it. This example illustrates the possibility that the collective system has a behaviour at a different scale than its parts. On the smaller scale the system may behave in a complex way, but on the larger scale all the complex details may not be relevant.

Let us open a brief discussion about the truss lattice introduced in the previous chapter.
Does our system show emergent behaviour? If we analyse the simulations in static, we notice that for little meshes of the system the channel of the fracture comes out because of a fraying of the system: different trusses damage or break and in the end we notice the appearance of the "channel" which is the result of the "fraying" of the lattice. This behaviour disappears for big meshes, in which the channel of the fracture suddenly appears without fraying. It is like the trusses talk one another in order to decide where to make it appear into the model with their simple behaviour, represented by their constitutive law and by the mechanism of sharing the load that they are not able to withstand. From their simple behaviour a global property of the system comes out: the genesis of the fracture into the medium. This behaviour can be considered emergent (we can talk about simple emergence because a "channel of the fracture" comes out from the interaction among many elements) and it is more evident when the number of trusses growths, i.e. for big meshes (we underline the fact that in our code the algorithm is built in such a way that the "total mass" of the system is always the same and independent on the number of trusses used to mesh the system itself). It is not banal that the truss lattice breaks because of the sudden appearance of a channel instead of breaking because of the fraying of the system itself. For this reason we can describe this behaviour of the whole system like emergent. In static, if we suppose that our truss lattice describes a medium pulled in 4 different directions, we showed that there is a limit number of squares on the edges from which the emergent behaviour of the fracture appears. This number is 22. If we increase the number of square (more than 22) this

behaviour is more and more evident. What is the dimension of the discretization we should stop? To answer this question an experimental analysis would be important.

2) The second approach to the study of complex systems begins from an understanding of the relationship of systems to their descriptions. The central issue is defining quantitatively what we mean by complexity. What, after all, do we mean when we say that a system is complex? Better yet, what do we mean when we say that one system is more complex than another one? Is there a way to identify the complexity of one system and to compare it with the complexity of another system? To develop a quantitative understanding of complexity in physics tools of both statistical physics and computer science- information theory and computation-theory are used. According to this understanding, complexity is the amount of information necessary to describe a system. However, in order to arrive at a consistent definition, care must be taken to specify the level of detail provided in the description.

One of our targets is to understand how this concept of complexity is related to emergence—emergent complexity and emergent simplicity. Can we understand why information-based complexity is related to the description of elements, and how their behaviour gives rise to the collective complexity of the whole system?

So, resuming: the objectives of the field of complex systems are built on fundamental concepts—emergence, complexity—about which there are common misconceptions. Once understood, these concepts reveal the context in which universal properties of complex systems arise and specific universal phenomena, such as the evolution of biological systems, can be better understood.
A complex system is a system formed out of many components whose behaviour is emergent, that is, the behaviour of the system cannot be simply inferred from the behaviour of its components. The amount of information necessary to describe the behaviour of such a system is a measure of its complexity. In the following we will try to give some tools to describe from a quantitative viewpoint the complexity.

5.1.3 Complexity: how to measure it

A concept that is central to complex systems is a quantitative measure of how complex a system is. Loosely speaking, the complexity of a system is the amount of information needed in order to describe it. The complexity depends on the level of detail required in the description. A more formal definition can be understood in a simple way. If we have a system that could have many possible states, but we would like to specify which state it is actually in, then the number of binary digits (bits) we need to specify this particular state is related to the number of states that are possible. If we call the number of states Ω then the number of bits of information needed is

$$I = log_2 \Omega$$

To understand this we must realize that to specify which state the system is in, we must enumerate the states. Representing each state uniquely requires as many numbers as there are states. Thus the number of states of the representation must be the same as the number of states of the system. For a string of *N* bits there are 2*N* possible states and thus we must have

$$\Omega = 2^N$$

which implies that *N* is the same as *I* above. Even if we use a descriptive English text instead of numbers, there must be the same number of possible descriptions as there are states, and the information content must be the same. When the number of possible valid English sentences is properly accounted for, it turns out that the best estimate of the amount of information in English is about 1 bit per character. This means that the information content of this sentence is about 120 bits, and that of this book is about 3 106 bits.
For a microstate of a physical system, where we specify the positions and momenta of each of the particles, this can be recognized as proportional to the entropy of the system, which is defined as

$$S = K\ log\Omega$$

where $k\ = 1.381023\ Joule\ /\ ^\circ\ Kelvin$ is the Boltzmann constant which is relevant to our conventional choice of units . Using measured entropies we find that entropies of order 10 bits per atom are typical .The reason *k* is so small is that the quantities of matter we typically consider are in units of Avogadro's number (moles) and the number of bits per mole is 6.021023 times as large . Thus, the information in a piece of material is of order 1024 bits . There is one point about the equation above that may require some clarification. The positions and momenta of particles are real numbers whose specification might require infinitely many bits. Why isn't the information necessary to specify the microstate of a system infinite? The answer to this question comes from quantum physics, which is responsible for giving a unique value to the entropy and thus the information needed to specify a state of the system. It does this in two ways. First, it tells us that microscopic states are indistinguishable unless they differ by a discrete amount in position and momentum—a quantum difference given by Planck's constant *h*. Second, it indicates that particles like nuclei or atoms in their ground state are uniquely specified by this state, and are indistinguishable from each other. There is no additional information necessary to specify their internal structure. Under standard conditions, essentially all nuclei are in their lowest energy state. The relationship of entropy and information is not accidental , of course , but it is the source of much confusion . The confusion arises because the entropy of a physical system is largest when it is in equilibrium . This suggests that the most complex system is a system in equilibrium . This is counter to our usual understanding of complex systems . Equilibrium systems have no spatial structure and do not change over time . Complex systems have substantial internal structure and this structure changes over time .
The problem is that we have used the definition of the information necessary to specify the microscopic state (microstate) of the system rather than the macroscopic state (macrostate) of the system. We need to consider the information necessary to describe the macrostate of the system in order to define what we mean by complexity.
One of the important points to realize is that in order for the macrostate of the system to require a lot of information to describe it, there must be correlations in the microstate of the system. It is only when many microscopic atoms move in a coherent fashion that we can see this motion on a macroscopic scale.

5.2 “How nature works”
5.2.1 The power law and the origin of SOC

We said first that the science was split in a series of different disciplines (figure 5.1). Well, we can say that there are a number of empirical observations across the individual sciences that is impossible to understand by following the techniques developed within the specific scientific domains. These phenomena are the occurrence of some large catastrophic events, fractals, noise 1/f in a particular way. Why are they universal? In the following we will report some simple examples about these phenomena

EARTHQUAKES: as we already said, because of their composite nature, the complex systems can show catastrophic behaviour, in which one part of the system can affect the other ones. A typical example of this phenomenon is given by the cracks in the Earth crust. The scientists studying the physics of the earthquakes looked at the earthquakes themselves on a big timescale in order to get a law that could characterize the single one. For this reason it was possible to obtain a simple law, called Richter-Gutenberg law. Basically by this law, it turns out that every time there are 1000 earthquakes of magnitude 4 on the Richter scale, 100 earthquakes of magnitude 5, 10 of magnitude 6 and so on. In the figure we show this particular law, applied for a particular region of the Earth (the zone of New Madrid in USA) and in a restricted temporal period (between 1974 and 1983). The scale is obviously logarithmic, so the numbers on the vertical axes are 1,10,100.

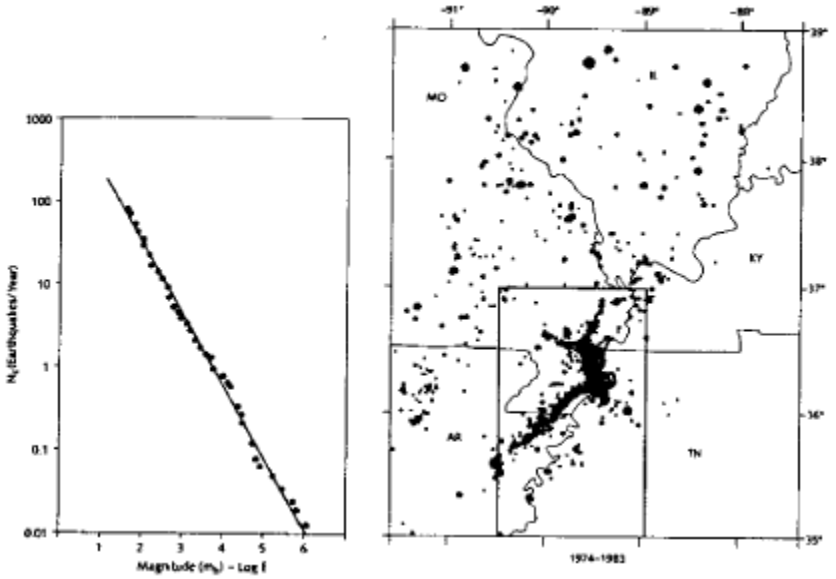

Figure 5.2: Gutenberg Richter law (on the left) and representation of points in which earthquakes occurred in New Madrid (How nature works, P.Bak)

In the figure on the right instead we report the specific points in the area in which we measured earthquakes (with the bigger dots representing the biggest ones).
This law is quite important because the dynamics of a complicated system as the crust of the Earth, with lakes, mountains, volcanos can be resumed by a simple power law; and this law also suggests that the large earthquakes, from a physical viewpoint do not play a special rule with respect the smallest ones, but they are basically the faces of the same coin.

MANDELBROT'S LAW: In Economics it is possible to find a version of the Gutenberg Richter law. Benoit Mandelbrot pointed out that the variation of the prices of the cotton, stocks and other commodities follows a very simple statistical law which is known as Levy's law. Mandelbrot collected data for the variation of the prices of the cotton for many years, month to month; then he counted how often the variation was between the 10 and 20 percent, how often between the 10 and 5 percent and so on. Just like for the Gutenberg Richter law in the region of New Madrid. In this case the distribution follows again a power law:

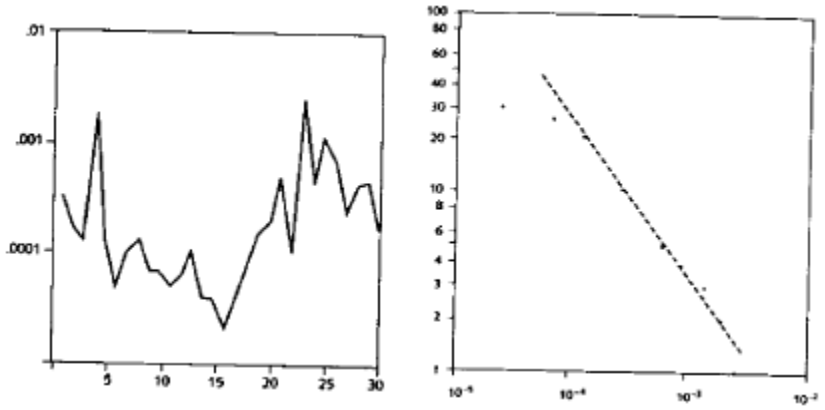

Figure 5.3: Mandelbrot's law (How nature works, P.Bak, 1992)

Mandelbrot studied different commodities and he found that they followed basically the same pattern.
The strange thing is that the economists have ignored for many years the works of Mandelbrot because the general picture they followed is that large and contingency events, like the crash of the 1929, are caused by abnormal circumstances. Basically the mistake made is to cut the data before of the analysis; obviously in this way it is not possible to build a general theory that could give like a general pattern of the phenomenon excluding some pieces of data.

EXTINCTIONS: In biological evolution, the professor Raup from University of Chicago, pointed out that the distribution of the extinction events could follow a power law. By using different data put together by the fossil records of thousands of marine species, he arrived to the following law:

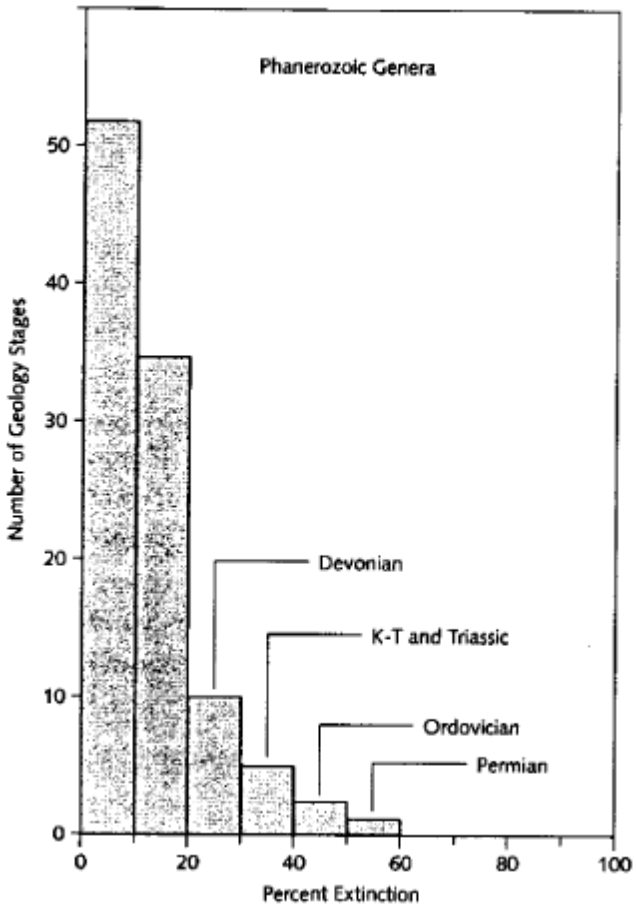

Figure 5.4: histogram of percent extinction vs number of geological stages ((How nature works, P.Bak, 1992)

In this simple histogram, it is possible to note that the events that lead to the extinction of a number of species on the earth crust between the 0 and the 10 percent, occurred many times, for more than 50 geological stages, while big extinction processes like the extinction in the Permian which made almost the 60 percent of the species on the Earth disappeared, occurred only one time. The technique used by Raup, was the same used by Mandelbrot and the same used for the Gutenberg Richter law. The same law, plotted as function of the time gives us:

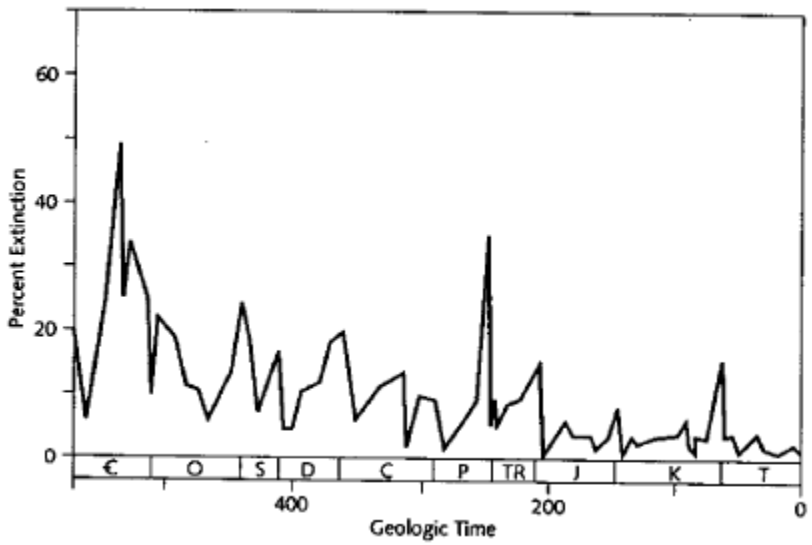

Figure 5.5: time vs percent of extinction ((How nature works, P.Bak, 1992)

What is important in these power law from a physical viewpoint? Although the large events occur with a well defined probability, this does not mean that the phenomenon could be considered like *periodical*. The fact that a large earthquake did not appear for a long time does not mean that it is due! The only thing we can assess is that these events will occur always with the same probability, given by a power law. The fact that the *regularity* must not be confused with the *periodicity* suggests that the same identical mechanism works at all the scales, from the extinction taking place every day, to the largest one, that caused the extinction of the 95 percent of the species on the Earth.

FRACTAL GEOMETRY: Mandelbrot coined the word fractal for geometrical structures which are present at all the length scales and was among the first to make the assumption that the nature is characterized by a fractal behaviour. Basically, if we consider a fractal and we increase one of its part, we can get the same starting structure again. In the figure below we report the Mandelbrot's fractal:

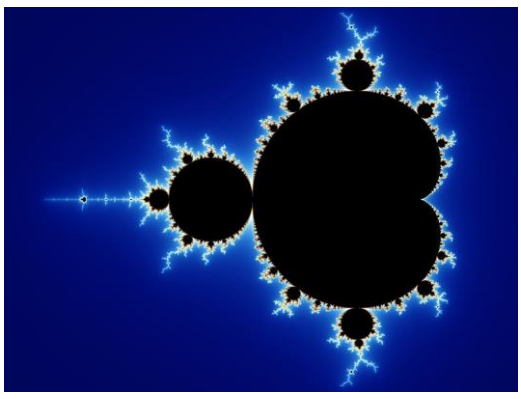

Figure 5.6: Mandelbrot's fractal ((How nature works, P.Bak, 1992)

The nature produces a great example of fractals. For example in a tree, each branch is more or less similar to the whole tree and every little branch is similar to its own branch and so on. The fractals

are present in the geomorphical profiles of the mountains or in the ice crystals, in the clouds and so on; the nature is full of these kind of objects. So how is it possible to build such kind of objects from a mathematical viewpoint? There is a substantial difference between an Euclidean object and a fractal which depends on the way in which we build them: a curve on the plane in fact is built by a function

$$f\big(x(t), y(t)\big) = 0$$

which describes the position of the point on the curve by varying the time t.
If we would like to build a fractal instead, we cannot use a curve but only an algorithm, i.e. a method that cannot be necessarily numerical and that must be repeated an infinite number of times. After a certain number of iteration the human eye is not able to see the difference anymore.
Each fractal is characterized by a "dimension". Let's consider for example the cost of the Norway

Figure 5.7: fractals in the coast of Norway ((How nature works, P.Bak, 1992)

which is characterized by a hierarchical structure of fjords within fjords and fjords within fjords of fjords. So the question we could formulate is: how long is a typical fjord? Two considerations: first, if we saw a part of a fjord or a part of a coastline, we would not be able to say how large it is if the picture would not show a ruler. Second: the length measured depends on the resolution of the ruler for the measurement. In fact a large ruler would give us a rougher estimate than a smaller ruler which would be able to take into account smaller length scales. So, one way to represent this is to measure how many boxes (in the figure above) or circles of size δ we need to cover the coast. Obviously, the smaller the box, the more boxes are needed to cover the coast. After having done

this, we repeat the whole process decreasing the dimension of the boxes till $\delta \to 0$. If we plot the logarithm of the length L measured by the boxes as a function of the logarithm of the sizes of the boxes, we have

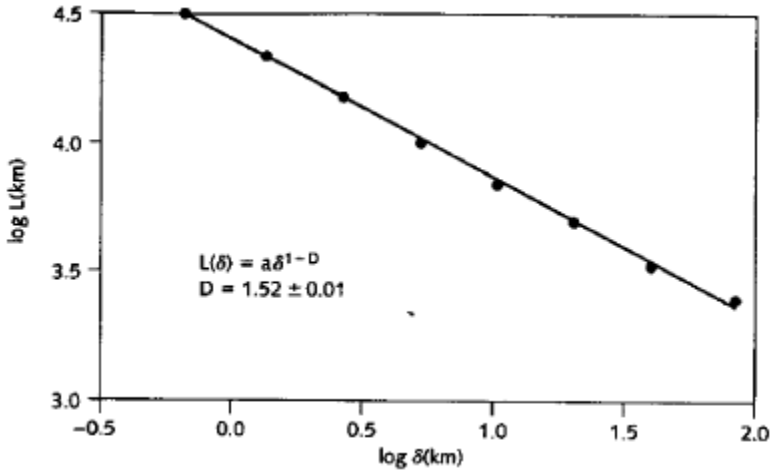

Figure 5.8: measure of the dimension of a fractal ((How nature works, P.Bak, 1992)

Still a power law, whose exponent is $\tau = 1.52$. This exponent is called *fractal dimension* of the coast and the fact that it is between 1 and 2 suggests the Norwegian coast is a complex fractal object whose dimension is between the dimension of a line on a plane and of a surface.
A lot of work was done for determining the geometrical properties of the fractals, like the fractal dimension we described above but the question about their origin still remained.

$1/f$ NOISE: The last phenomenon we describe is the so called $1/f$ noise; this was observed in different systems, like the flow of the river Nile, the light from a quasar and the highway traffic.

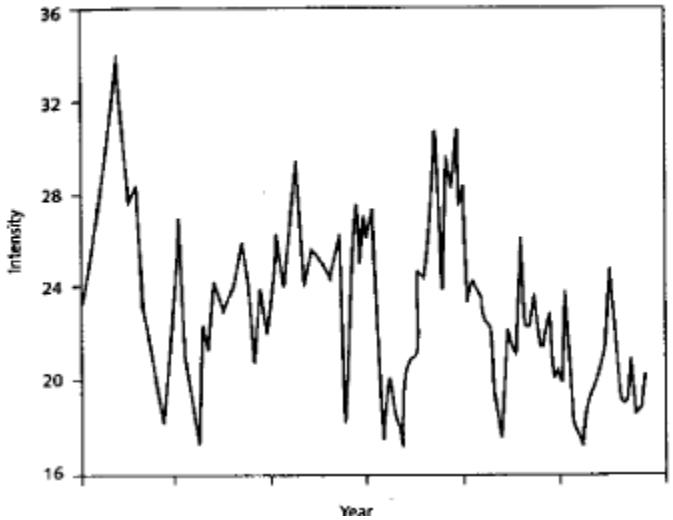

Figure 5.9: 1/f noise ((How nature works, P.Bak, 1992)

The figure above shows the light from a quasar measured in a period of 80 years. There are features of all sizes: rapid variations over minutes and slow variations over years. This kind of signal can be considered like the superposition of bumps of all sizes; so from a physical viewpoint it looks like a Norwegian coastline in time rather than in space. Equivalently, it can be considered a superposition of periodical signals of all frequencies; this means that there are features at all time scales. The strength or power of its frequency component is inversely proportional to f. For this reason it is called $1/f$ noise. This signal is so different from the white noise, in which there are no correlations between the value of the signal from one moment to the next.

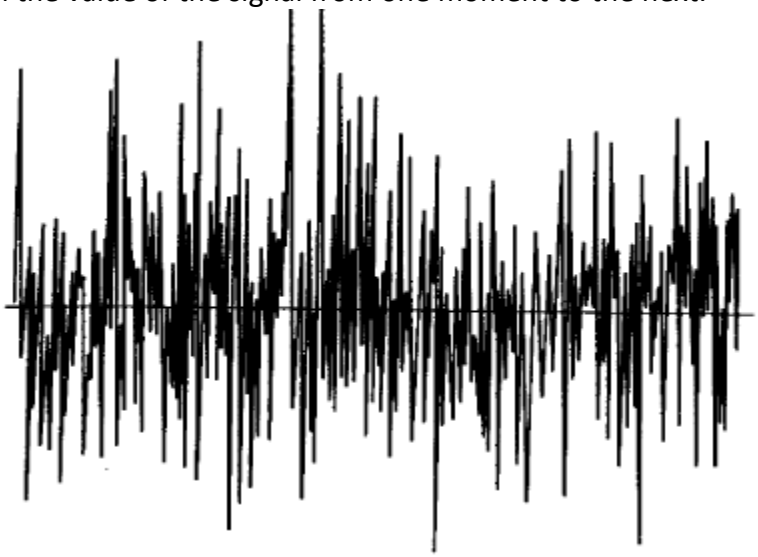

Figure 5.10: white noise ((How nature works, P.Bak, 1992)

In the figure above in fact it is possible to note that there are no slow fluctuations, i.e. large bumps.

So by all these examples, we can state basically that all these different systems, that are complex according to the description given at the beginning of the chapter, can be described by a power law, i.e:

$$N(s) = s^{-\tau}$$

s in this case depends on the system we are considering: it could be for example the energy released by an earthquake and N the number of earthquakes. s could be the length of a fjord and $N(s)$ the number of fjords with that particular length (Bak, how nature works). The same pattern always repeats for all our systems. Obviously the exponent τ is a characteristic of the system itself. The physical meaning that comes out from the power law is the so called *scale invariance*: the straight line that we found from an experimental viewpoint into the systems we described looks the same everywhere:
every little branch is similar to the tree, every little fjord is similar to the bigger one, every distribution of earthquakes recorded for a limited value of time is similar to the distribution recorded for million of years.
From a mathematical viewpoint it is possible to notice it by the structure of the power law: if we change the scale of the independent variable s by cs, we have:

$$N(cs) = cs^{-\tau} = c^{-\tau}s^{-\tau} = const \cdot s^{-\tau}$$

Thanks to this law, all the fractal objects/phenomena follow a distribution with a long tail where there is no a typical value around whom they spread. For the no fractal objects we see a different situation: the distribution of the values is a Gaussian and there is an average value well define with the large number of the objects around it.

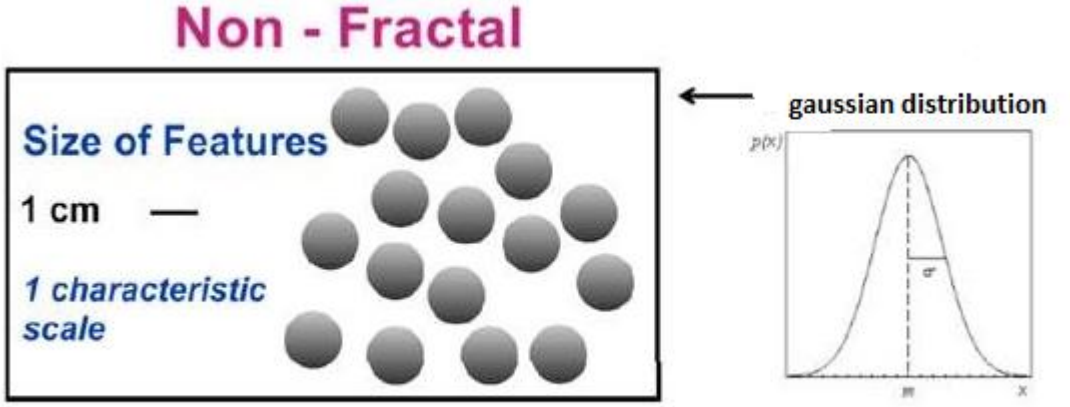

If we try to increase a smaller part of the Gaussian we do not get a Gaussian again. So the phenomena ruled by this law do not show invariance scale.
So, resuming: according to a naïve point of view, the nature should follow a pattern given by the Gaussian distribution; if this was true, there would exist a mean value (which would be the most likely one) and other values spread around it according to the variance of the Gaussian. So if we applied this picture to the complex systems in nature we would see probably one unique Norwegian fjord as regards the spatial structures (the concept can be applied to the channel of a fracture, to the distribution of the sand grains on a beach and so on), one unique earthquake characterized by a fixed magnitude and one unique degree of extinction. There would be recorded also little variations from the average value because of the mistakes expressed from a math viewpoint by the variance, but basically we would observe always the same pattern for each complex system. Furthermore the large events, so different and so far away from the average value would be a consequence of abnormal events and so they could be not considered in the statistical analysis (that's the reason for which the economists did not considered the Lavy's law for much time). This mean value would be also a "special" value for our system, the unique one. However the nature does not behave in this way; the statistical law followed is the power law, that shows scale invariance: this means that there are no fjords smaller than a particle or bigger than Norway. But between the two extremes there are the features of all the length scales and there is no a special value. Obviously our power law says to us that the number of bigger fjords is smaller than the number of smaller fjords in size. But it also says us that there is no a special mean value around all the dimensions of fjords spread; all the scale lengths appear and have the same importance.
That's the way in which complex systems work.
In the same way, the same thought can be applied for earthquakes and extinctions.
An important characteristic of the systems we analysed is that they exhibit the so called "punctuated" equilibrium: periods of stasis, in which nothing happens are interrupted by intermittent extinctions, earthquakes or changes of prices that we will call in our approach

"avalanches". Obviously this kind of picture must be applied to phenomena depending on the time (not for the spatial structures like fjords).
In all these examples, we described basically systems that are not in equilibrium. A complex system cannot be in balance." If an equilibrium system is disturbed slighthly, for example by pushing a grain of sand somewhere, nothing interesting happens. In general systems in equilibrium are not able to show any of the interesting behaviour discussed above like large catastrophes, $1/f$ noise and fractals (Bak, How nature works)". In the past a lot of scientists have assumed that large systems in Economy or Biology were in equilibrium, like the flat sand on a beach. If we are in a balance state obviously for little perturbations introduced into the system, the system itself reacts by a little answer: it is linear. Small freak events cannot have dramatic situations. Large fluctuations events can occur only if many random events pull in the same direction, which is highly unlikely. For this reason these large catastrophes are not considered form a statistical viewpoint. However an equilibrium theory is not able to explain the state of the systems we analysed. Why these systems are not in equilibrium? The answer depends on the scale length of the human lifetime; the changes are so small compared with human lifetime that the concept of equilibrium seems natural. As pointed by Gould and Eldrige for the system "life", this apparent equilibrium is only a period of tranquillity in which many species become extinct definitely and other ones do appear. This theory is known as theory of the *punctuated equilibrium.* "*Large intermittent bursts have no place in equilibrium systems but they appear in biology, geophysics, history". (*How nature works, Bak*)*

So, these phenomena we have described from an experimental viewpoint seem to have the same mathematical law: the power law. Can there be a Newton's law $F = ma$ for complex systems? Maybe the answer to this question is the quoted power law. The Self Organized Criticality (SOC) was born to give an interpretation to these phenomena.

5.2.2 The birth of SOC

A perceived idea to unify the above two aspects of fractality (in space and time) led Bak, Tchang and Wiesenfeld (BTW) to the so called postulate of SOC. Apparently they were guided by the observation of scaling in space and time (fractals and noise $1/f$) in equilibrium and non equilibrium systems. They believed basically that these two phenomena were correlated in some way, i.e. manifestations of the two sides of the same coin. According to BTW self organized systems drive themselves to a critical state in which we notice the invariance scale without the self tuning of an external parameter like happens for systems in Biology, Economy and History and the process of the self organization takes a lot of time, i.e. a very long transient before reaching the critical state.

So after having realized that complex systems exhibit this kind of characteristics BTW tried to build a simple model that could be able to fit the behaviour of self organised systems: the sandpile model; a sandpile exhibits punctuated equilibrium behaviour where periods of stasis are interrupted by periods of activity. The sand avalanches are caused by a domino effect in which a particular grain of sand pushes towards one or more grains causing different avalanches. These grains can interact with other grains in a chain reaction. We will now analyse from a quantitative viewpoint the behaviour of this model, which is the paradigm of all the SOC systems.

A final consideration is however due: the paper of BTW, (which is resumed for the main part into the considerations we gave above) led many readers to different perceptions of SOC i.e. what the SOC is. The result is shown in the picture:

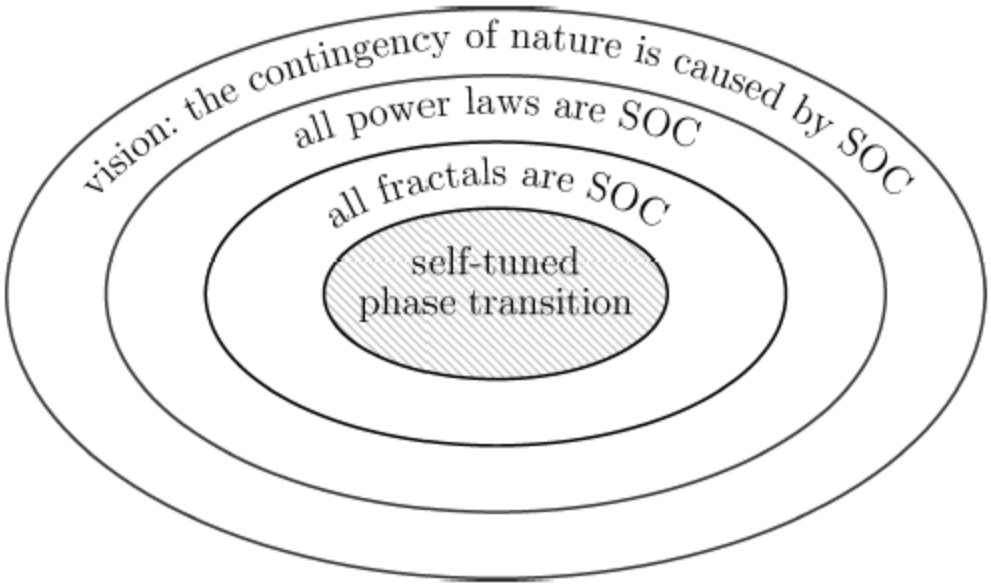

*Figure 5.11: big picture about perceptions of SOC (*Watkins et al., 2016*)*

The first idea is that self tuned phase transitions exist in nature and this is the core idea enunciated by BTW (above) in the SOC postulate as dynamical origin of the space-temporal fractals. In some contexts Milovanov and Iomin (2014) have shown that this idea can be further proved using their topological approach.

The second and the third perceptions are considered as wrong. Jensen (1998) and Sornette (2006) gave a particular interesting overview of power laws observed in nature which are caused by processes that are fundamentally different from SOC.

The fourth interpretation of SOC is like a "vision" and it is very interesting from a philosophical viewpoint: it comes out from the paper of the 1989 of BTW and it is quite speculative in its form. If this picture is correct for the real world we must accept the instability and catastrophes like unavoidable. Not only: large catastrophic events, like the extinction in Precambrian are caused by the same mechanisms than the smaller everyday events. They cannot be erased from our analysis. The contingency (considered like extraordinary and rare event) is caused by the self organized critical state reached by complex systems in punctuated equilibrium and they are not a consequence of large abnormal events "pushing all in the same directions".

We will discuss now the first perception in the following and we will give a basic introduction of the paradigm model of SOC: the sandpile model.

5.3 The SOC Models

There are different versions of SOC models. In less than 20 years more than two thousand papers have been published, and comprehensive reviews has not yet appeared.
A closer look at the literature reveals that the number of original models can be greatly reduced by noting that most of them are variations of prototype models. Using a "Draconian" approach, we can distinguish just two main families of SOC models. The first is represented by the stochastic SOC models such as the sandpile or forest-fire model, in which the self-organization process is the output of a stochastic dynamics. The second family groups together the so-called "extremal" or "quenched" models which are defined by a deterministic dynamics in a random environment. Examples of the latter family are the Invasion Percolation (IP) and the Bak-Sneppen model. The central Force Model we have described in the previous pages falls into this last kind of class. In the following we will describe the structure of the stochastic models using a Mean Field approach by Vespignani and Zapperi. We will deal with this kind of models only in order to have a clear example of what SOC is from a quantitative viewpoint, in order to understand the concept of critical state and self tuned phase transition.

5.3.1 The stochastic models: the sandpile

The sanpiles models are cellular automa with an integer or continuous variable z_i defined in a lattice d-dimensional. Each site is characterized by a threshold z_c which is generally fixed for each element of the system. How the system works? Basically a "grain" of energy is dropped randomly into the system and the different sites are able to store different grains till their threshold z_c. When the threshold is reached for a particular site i, it relaxes and the quantity of grains changes according to

$$z_i \rightarrow z_i - z_c$$

and the grains are transferred to the neighbours according to

$$z_j \rightarrow z_j - y_j$$

The relaxation of a site can induce to the relaxation of other sites that can induce to the relaxation of further sites and so on, following a domino reaction which is called avalanche. The dimension of an avalanche is the number of active sites.
For conservative systems the transferred energy is equal to the energy lost by a site on average, i.e.

$$\sum y_j = z_c$$

The only form of dissipation for these systems is by the drop of the grains from the boundaries of the systems that must be opened. It is worth to remind that during an avalanche the drop of the energy from the external world must stop until the system is again in equilibrium. This implies an infinite timescale separation between the external force and the internal dynamics of the system. So in these conditions, it is possible to show that the system reaches a critical state in which the law of distribution of the avalanches is given by

$$P(s) \sim s^{-\tau}$$

where s is the avalanche size.
In the original model introduced by BTW, $z_c = 2d$ and $y_j = 1$ but there are other interesting variations of this model like Manna's model (reference)
In the figure below we report the way of creating avalanches for the sandpile

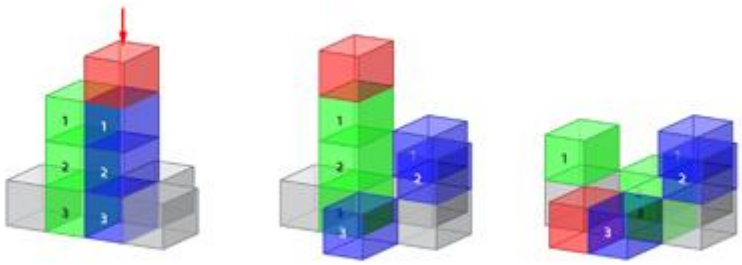

Figure 5.12: avalanches in the sandpile model

This critical state (we will see according to the Mean field approach why it is critical) is also stationary: in fact it is possible to show that the average density of the particles on the lattice (that for example in 2D would be $\delta = \sum_{i,j} z_{ij}/N$ with N the number of sites on the plane lattice) is constant in the critical state, in which we note the power law avalanche behaviour. This means that on average for a conservative systems, the number of particles dropped from the top into the system is equal to the number of particles that fall out from the boundaries. Why this model can be considered like an example of SOC? The answer is very simple: the model is driven by a slow external force (the adding of sand grains on the lattice); this is the only influence with the external environment. However the input we are giving to our system is like a "chance" that we give to the system in order to reach the critical state, which is always the same, and it is characterized by the same power laws, correlations etc. We are putting only the system in simple dynamic conditions, exchanging energy with it (from the top and from the boundaries) and we are not tuning any parameters for it to reach the critical state (as it happens for the phase transitions in water or ferro/para magnetism). In this sense we talk about criticality which is self organized: thanks to the little input we give to the system from the external world, the components of the system itself talk one another in order to reach the critical state without the tuning of any external control parameter! And if we repeat the experiment the critical state reached is always the same.

As we said before the avalanches are instantaneous with respect the external force. This rule is very simple to implement in a computer algorithm that allows to take into account two different timescales. This however corresponds to a non local interaction in which the evolution in time of each site depends on the configuration of the whole lattice. This is hard to describe and in order to do this we should fix a reference timescale and measure the driving rate on that scale. For this reason let's consider a generalized sandpile in which we introduce the probability h per unit of time that a particular site will receive a grain of sand. We can define the total energy flux $E = hL^d$ and we fix the typical driving timescale among avalanches like

$$\tau_d \sim 1/h$$

For $h \to 0$ we recover the slow driving limit. The system during an avalanche does not reach energy and in fact the timescale separation

$$\tau_d \to \infty$$

If we remove the timescale separation commonly accepted in the simulation, we are able to recover the locality into the model, that allows us to have a simple description of the model.

5.3.2 Mean field analysis of the sandpile

So the only way to study this system is by the laws of probability. For this reason the authors define the complete set $\sigma = \{\sigma_i\}$ of lattice variable that specifies the state of the system, where σ_i is the state in which a particular square of the lattice is. These values σ_i can take three different values or states: $\sigma_i = s$ for the stable sites in which the local energy $< z_{lim}$, $\sigma_i = c$ for the "critical" sites in which $z = z_{lim}$, and $\sigma_i = a$ for the active sites where $z > z_{lim}$. So the dynamical evolution of the system is determined by the transition probability $W(\sigma|\sigma')$ from the configuration σ' to the configuration σ. At a particular time step the state of a given site depends on the state of the same state at the previous step and from the states of the sites interacting with it. The most general form of the transition probability is given by:

$$W(\sigma|\sigma') = \prod_{i=1}^{n} w(\sigma_i|\sigma')$$

(5.1)

where $w(\sigma_i|\sigma')$ is the one transition probability, depending on the driving and reaction rates: it specifies the probability that a particular site is in the state σ_i if previously it was in a certain state and the other sites on the lattice were in other particular states. Everything is specified by the state system σ'. However in a non equilibrium system like this, it's very important to introduce the probability distribution $P(\sigma, t)$ to have a certain state σ at a time t. If we know this probability distribution, we are able to compute the average value of any function according to:

$$< A(t) >= \sum_{\sigma} A(\sigma) P(\sigma, t)$$

The evolution in time of this probability function is given by solving the Master Equation

$$\frac{\partial}{\partial t}P(\sigma,t)=\sum_{\sigma}W(\sigma|\sigma')P(\sigma',t)-W\left(\sigma'\middle|\sigma\ \ \right)P(\sigma,t)$$

(5.2)

The specific form of $W(\sigma|\sigma')$ determines the dynamics of the system and the steady state distribution. Tipically SOC systems show a stationary state in which all the averages are time independent. To this state corresponds a stationary distribution $P(\sigma)=P(\sigma,t\longrightarrow\infty)$. For equilibrium system, this has the form of Gibbs $P(\sigma)\approx\exp(-\beta H(\sigma))$ where $H(\sigma)$ is the Hamiltonian. For SOC system, as every not equilibrium system, there is no a general criterion and we are forced to solve the Master Equation in the stationary limit and to do this we have to use some approximate methods. Now, if we define the average densities ρ_a,ρ_c,ρ_s, active, critical and stable, (which are the number of certain sites over the total number of sites into the lattice), for homogeneous systems these densities can be written as

$$\rho_k=\sum_{\{\sigma\}}\delta(\sigma_j-k)P(\sigma,t)$$

(5.3)

If we substitute these densities in (5.2), we have

$$\frac{\partial}{\partial t}\rho_k(t)=\sum_{\{\sigma'\}}\sum_{\{\sigma\}}\delta\left(\sigma_j-k\right)\{\left(\prod_{i=1}^{n}w(\sigma_i|\sigma')\right)P(\sigma',t)-\left(\prod_{i=1}^{n}w\left(\sigma_i'\middle|\sigma\ \ \right)P(\sigma,t)\right)\}$$

(5.4)

that can be simplified by using the normalization equation for transition probability (Vespignani et al., 1998) giving:

$$\frac{\partial}{\partial t}\rho_k(t)=\sum_{\{\sigma'\}}w(k|\sigma')P(\sigma',t)-\rho_k(t)$$

(5.5)
where $k=a,s,c$ and $\sigma'=\{\sigma_i',\sigma_{i+e}'\}$ refers to a particular set of interacting sites that depends on the dynamics we consider into the system. For no local interactions σ' corresponds to the entire system. In this moment we introduce the Mean Field Approximation for the sandpile: the probability of each configuration σ, can be approximate to

$$P(\sigma)=\prod_{i}\prod\rho\sigma_i$$

(5.6)

The statistical meaning of this approximation is simple: we decide to approximate the probability of each configuration as the product of the probabilities of the single sites probabilities; so we decide to neglect all the possible statistical correlations among the sites.
Introducing the MF approximation in (5.4), we arrive to the following equation for the time evolution of the densities in the model:

$$\frac{\partial}{\partial t}\rho_k(t) = \sum_{\{\sigma'\}} w(k|\sigma') \prod_i \rho\sigma_i'(t) - \rho_k(t)$$

(5.7)

The next step is to develop the term $\sum_{\{\sigma'\}} w(k|\sigma') \prod_i \rho\sigma_i'(t) - \rho_k(t)$ for each density ρ_k and to take the stationarity limit of the three equations; this is possible to do from an analytic viewpoint and in the end we have the values of the three densities (active, critical and stable) for $t \to \infty$:

$$\rho_a = \frac{h}{\varepsilon} \qquad \rho_c = \frac{1}{g} \qquad \rho_s = \frac{g-1}{g}$$

with the condition $\rho_a + \rho_c + \rho_s = 1$. Here h is the probability per unit time that a square of the lattice receive a quantum of energy, ε is the dissipation parameter (it can be present to take into account the average energy dissipated in a elementary process but it's obviously present in conservative systems as well in order to consider the dissipation of the energy quantum from the boundaries and the fact that the system is finite) and g the number of sites involved in the dynamical relaxation process (For further details (Vespignani, Zapperi, *How self organized criticality works,1997*)).
Now, how it is possible to notice a stationary state is always reached: it comes out from our equations taking the limit $t \to \infty$. We must now discuss the critical behavior of the system: the balance between the conservation laws and dissipation is fundamental for the critical behavior of the system.
So in our model we can define two control parameters, which are h and ε: they are parameters that we can fix from the external world and are responsible of the exchange of energy between the system and the external world. The order parameter instead is linked to a scalar quantity that must underline the symmetry of the system. So we can chose $\rho_a = \frac{h}{\varepsilon}$. The model is critical just in the double limit $h, \varepsilon \to 0$ and $\rho_a \to 0$. (We will see in fact that the susceptibility of the system goes to infinite). However the critical point is a point in the space of phase and we are able to notice different regimes according to the different values of the two parameters h, ε as it is possible to notice in the figure below

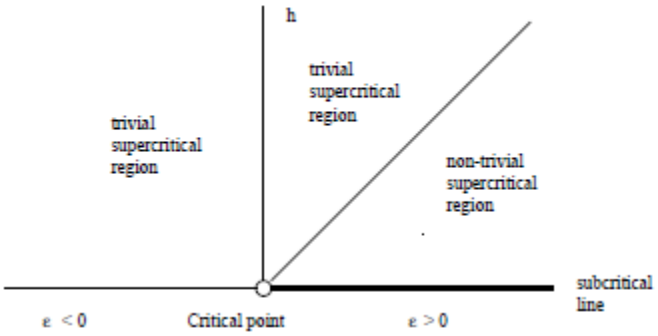

Figure 5.13: phase diagram for the sandpile model (Vespignani et al., 1998)

The model is supercritical when $h > 0$, $\varepsilon > h$ while it is subcritical when $h \to 0$, $\varepsilon > 0$.
An image of the critical, subcritical and supercritical state is reported below

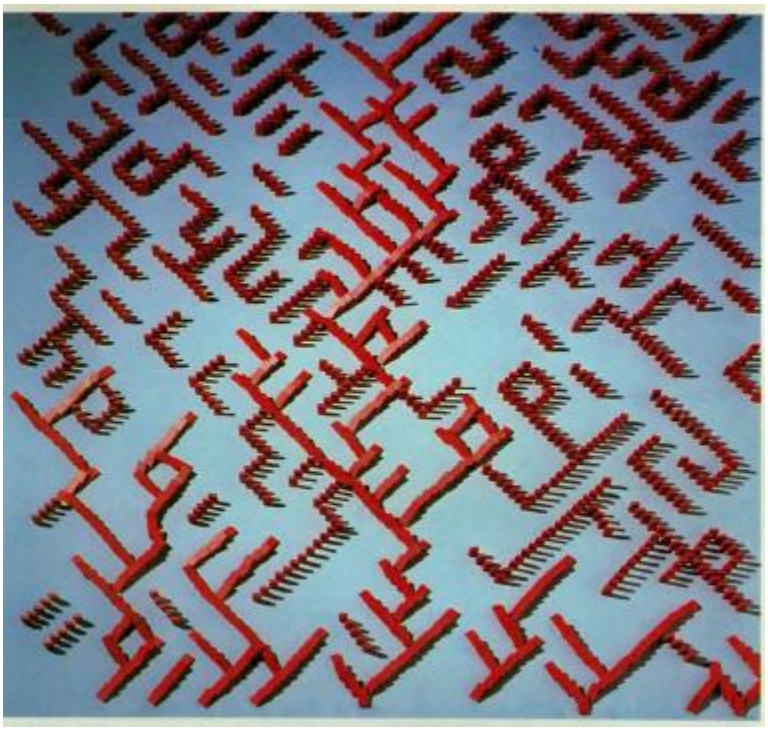

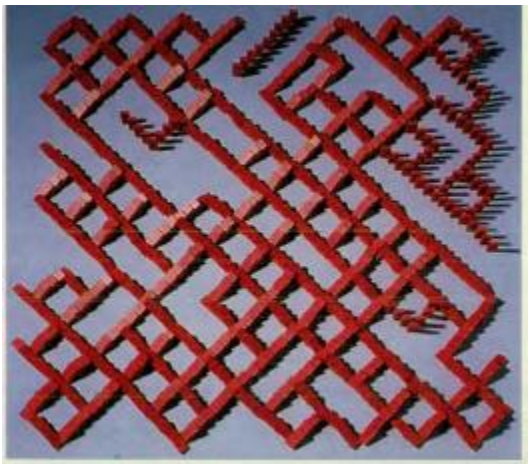

Figure 5.14: Critical, subcritical and supercritical regimes:
In the three pictures above we represented the sandpile model like a domino and we reported the critical subcritical and supercritical state.

This diagram (which is very similar to the diagram magnetic field-temperature) could be extended as well on the left by including $\varepsilon < 0$; however in this case we would have the birth of a trivial regions because we would have a sandpile in which a positive net amount of energy enters the system during the avalanche activity (negative dissipation). Furthermore another trivial region opens into the diagram and it is the region for which $h > \varepsilon$: this region makes no sense because $\rho_a$would be greater than 1. This means that the conservation rules play a crucial role: the two control parameter cannot be varied independently but they are linked because the global conservation law imposes that $\varepsilon > h$.
So let's begin to study the first region, the subcritical line.

5.3.2.1 The subcritical regime

As it is possible to note from phase diagram, the subcritical regime corresponds to a straight line; this is also the field of the numerical simulation because $h \to 0$ and the only parameter we can vary is the dissipation rate ε. Obviously the order parameter $\rho_a = 0$.
So before analysing the behaviour of the system in the subcritical regime it's important to study the propagation of a perturbation in the regime itself.
For small perturbations in the stationary state, we must introduce the response function or generalized susceptibility function:

$$\chi_{h,\varepsilon}(\mathrm{x} - \mathrm{x}'; \mathrm{t} - \mathrm{t}')$$

which is a function depending on the time and on the space and that describes the variation of the order parameter into the system according to:

$$d\rho_a = \chi_{h,\varepsilon}(\mathrm{x} - \mathrm{x}'; \mathrm{t} - \mathrm{t}')\Delta h \, d^d x' dt'$$

Integrating in the space and in the time we have the total variation of active sites into the system because of the perturbation:

$$\Delta\rho_a(x,t) = \iint \chi_{h,\varepsilon}(\mathrm{x}-\mathrm{x}';\mathrm{t}-\mathrm{t}')\Delta h\, d^d x' dt$$

Let's apply now a time dependent perturbation to the stationary state $h(x,t)$ and Let's suppose the system is homogeneous in space and time so that the averages on two points depend only on the time and space displacement.
Let's consider then an impulsive disturbance $\Delta h(x',t') = \delta(t)\delta^d(x)$; from a physical viewpoint we are adding a sand grain on the top of the stationary average driving field. Inserting this perturbation into $\Delta\rho_a$, by the properties of the Dirac's delta, we have

$$\Delta\rho_a(x,t) = \chi_{h,\varepsilon}(x,t)$$

expression that will be useful later.
The total susceptibility of the system can be computed by integrating in space and time the generalized susceptibility function:

$$\chi_{h,\varepsilon} = \int dt \int \chi_{h,\varepsilon}(x,t)\, d^d x$$

From a physical viewpoint it defines the total response of the system to an external perturbation. Instead, the total number of active sites is obtained integrating in space and time the density of the active sites, which is obviously a function of time and space $[1/sec * m\text{^}d]$

$$N_a = \int dt \int \Delta\rho_a(x,t)\, d^d x = \chi_{h,\varepsilon}$$

Now, If the external field is absent, i.e. $h \to 0$, the only active sites present into the system are due to the delta perturbation; so all the active sites are connected in time and space and so they form an avalanche whose average size is

$$< s >= N_a$$

This last statement is stated by the following expression

$$\chi_\varepsilon \equiv \lim_{h\to 0} \chi_{h,\varepsilon} = N_a =< s >$$

Let's consider now a different kind of perturbation $\Delta h(x',t') = \Delta h$ for $t' < t$ corresponding to a uniform driving in space and time. It is possible to show (Vespignani, Zapperi) that integrating for this kind of perturbation like we did for the Dirac's delta

$$\Delta\rho_a = \Delta h \chi_{h,\varepsilon}$$

So for an infinitesimal perturbation in the stationary state,

$$\chi_{h,\varepsilon} = \lim_{\Delta h\to 0} \frac{\Delta\rho_a}{\Delta h} = \frac{\partial\rho_a}{\partial h}$$

And again

$$N_a =< s >= \chi_\varepsilon = \lim_{h \to 0} \frac{\partial \rho_a}{\partial h}$$

following the same pattern applied before.
We are now ready to study the behavior of the system in the subcritical line. If we already know the expression of $\rho_a(h)$ in the stationary regime, a simple derivative gives us

$$\chi_\varepsilon = 1/\varepsilon$$

which goes to infinite for $\varepsilon \to 0$: this means that the system is in a subcritical regime for any ε different from 0 while for $\varepsilon = 0$ the susceptibility diverges and the response function becomes long ranged.
So close to the critical point the scaling behavior is characterized by the scaling law $\chi_\varepsilon \sim \varepsilon^{-\gamma}$ with $\gamma = 1$ and the correlation length diverges like $\xi \sim \varepsilon^{-\upsilon}$.
Since the energy is transferred locally and isotropically, the net energy current is given by $j \sim \frac{\partial \chi}{\partial r}$.
For local conservative models the energy current must satisfy on average the conservation law.

$$\int j d\sigma = cost$$

where $d\sigma$ is the $d-1$ dimensional surface element. This ensures that the energy that enters into the system in the stationary state is equal to the energy dissipated. For large r we have the solution

$$\chi \sim r^{2-d}$$

However in the presence of boundary or intrinsic dissipation, the system acquires a finite correlation length: in fact from a physical viewpoint the correlation length must go to 0 when the system size is reached. Obviously this affects also the susceptibility function: how can we express this from a mathematical viewpoint? If we denote by ξ always the value the correlation length would have in an infinite system at temperature , then the cut off takes place when $r > \xi$. As long as $\xi \ll r$ the value of χ_ε should be the same as that for the infinite system. We can express this by the general scaling form

$$\chi_\varepsilon \sim r^{2-d} \Gamma(r/\xi)$$

where $\Gamma(r/\epsilon)$ is a cut off function that behaves like

$\chi_\varepsilon \sim r^{2-d}$ for $\xi \ll r$

$\chi_\varepsilon \sim 0$ for $\xi \gg r$

Obviously the way the function $\Gamma(r/\xi)$ cuts the value of the susceptibility depends on its functional form. This is an example of finite size scaling. In general this phenomenon occurs for all the observables of our model if the dimension of the model itself is finite. (Generally, this behavior

of the observables is used in the numerical simulations in statistical physics in order to catch the exponents of the power laws that characterize the observables in an infinite system. This is done by a fit that involves systems of increasing size: the method is known as “finite size scaling method”).
So from a physical viewpoint this cut off, appears always in the scaling relations because of the finite size of the system. But as we will see it will not make sense to take the thermodynamic limit by applying the finite size scaling method to compute the exponent in an infinite system; in fact in this way we would obtain as result of the fits an infinite system in which the boundaries can be scaled out the system because their dimension is negligible with respect the core of the system; but the boundary is the only form that the system has to dissipate energy. As result: *“the boundary cannot be scaled out in the limit of large system as usually done in physical statics”*

By this we can calculate the zero field susceptibility

$$\chi_\varepsilon = \int \chi_\varepsilon(r) r^{d-1} dr \sim \xi^2$$

So by this we find the correlation exponent $\upsilon = 1/2$.
Now, in the conservative systems, when the size is increased, the effective dissipation rate depends on the size of the system. For this reason we can assume that

$$\varepsilon \sim L^{-\mu}$$

In fact the dissipation rate is given by the probability to find a border site into the system. So the exponent μ links the dissipation rate with the finite size of the system providing a general picture of locally dissipative and open boundary model. In the conservative systems, the characteristic length of an avalanche must go like $\xi \sim L$ to ensure dissipation through the boundaries. This implies that $\mu\upsilon = 1$ by which $\mu = 2$. Furthermore, if we know that

$$\chi_\varepsilon \sim < s >$$

for sure $\chi_\varepsilon \sim L^{\mu\gamma}$ and this gives us the scaling law

$$< s > \sim L^2 \quad for\ L \to \infty$$

Resuming, we found some of the mean field exponents by using the conservative laws:

$\gamma = 1$ $\mu = 2$ $\upsilon = 1/2$

As regards the other exponents, we should try to compute the exponent of the avalanche size distribution: following Grassberger and Latorre, the size distribution is characterized by a finite size scaling form according to:

$$P(s, \varepsilon) = s^{-\tau} G(s/s_c)$$

where $s_c \sim \varepsilon^{-1/\sigma}$ is the cutoff of the avalanche size.
In the same way

$$\rho_a(t) \sim s^{\eta} F(t/t_c)$$

where t_c defines the characteristic time which scales like $t_c \sim \varepsilon^{-\Delta}$ (why they scale like epsilon)???

The mean field analysis brings us to

$$\tau = \frac{3}{2} \qquad \sigma = \frac{1}{2} \qquad \eta = 0 \qquad \Delta = 1$$

(Vespignani et al., 1998)

Some considerations before finishing: it is important to remark that the numerical value of these exponents is the same as in other MF approaches, but their significance is different because they were derived with respect scaling fields.
Furthermore the degree of universality is overstated like in every MF approach: in particular the exponents do not depend on the dimension d and these exponents in low dimensions are in general wrong. The Mean field theories work better in high dimensions. However this approach was important to understand the method used to derive the exponents in a mean field approach and in order to understand the basic characteristic of a SOC system, that we will analyse later in detail by a resume.

5.3.2.2 The supercritical regime

The region of the supercritical regime is characterized by a finite density of the active sites, i.e. a non zero order parameter. Close to the critical point $h \ll 1 \quad \varepsilon \ll 1$ and $h < \varepsilon$.
The important information is that the external force varies not so slowly, so the concept of avalanche size could lose its own meaning: that's why different quantum of energy could drop on the lattice when an avalanche is still occurring into the system and This could bring to overlap different avalanches caused by different external forces. However in this part of the phase space this situation is avoided if the condition

$$h \ll t_c^{-1} \sim \varphi$$

is satisfied; this condition states that the external force varies very slowly with respect the characteristic time of the system to reach equilibrium with avalanches.
We remind to the paper of Vespignani and Zapperi, *How self-organized criticality works: A unified mean-field picture,* to better have details as regards this region.

What is important to notice in the end of these calculations is that if we exchange energy with the system by adding quantum energies on the top and we suppose that the fact that the system loses its energy from the boundaries is a way to dissipate energy, we have:

a) The system always reaches a stationary state; this is contained in the equations we analyzed. this can be subcritical or supercritical. The critical point is reached in the double limit $h \to 0 \;\; \varepsilon \to 0 \;\; \rho_a \to 0$. In this critical point the avalanche size is infinite (from a physical viewpoint this is obvious because we are erasing the dissipation way of the system putting $\varepsilon \to 0$. The system is not able anymore to dissipate energy and an infinite avalanche characterizes all the system even if a single grain of energy is added) and we approach this point by a so called second order phase transition. What is the characteristic of this kind of transition? They have the peculiar feature that in correspondence of a critical point, i.e. for a particular value of the control parameter, correlations become long-ranged (from a mathematical viewpoint they follow a power law) and the fluctuations occur on all length scales: the first statement means that "everyone speak with everyone" while the second one means that there is no a characteristic size and in order to satisfy the fact that the fluctuations occur at all length scales, the size distribution of the fluctuations show a power law dependence with no trivial exponent. Moreover the order parameter, an observable whose presence distinguishes the two phases vanishes in one phase while it is different from zero in the other one. Indeed the susceptibility, the physical quantity that measures the answer of the order parameter to the external impulse and fluctuations (by the linear response theorem) diverges with system size. And this is exactly the same kind of phenomenon we observe in the sandpile, different from a first order phase transition in which the correlations are not at all scale length and there is a characteristic size into the system (An example of 1st order phase transition is given in the system water; if we try to move from water to gas before the critical point, the water boils and it changes phase: but in this case there is only a characteristic length and in fact the boils have always the same shape and the same measure. The situation is different when we cross the two phases from the liquid to the gas in the critical point: here the system is cloudy if we try to observe it and in fact all the characteristic sizes are present into the system itself; the transition is of the second order).
b) The system is characterized by a finite size scaling: this is a consequence of the fact that the boundaries cannot be erased like it happens in statistical physical; here this happens because the dimension of the volume is big with respect the dimension of the boundary in the thermodynamic limit; so it is possible to not consider the boundaries; but in a SOC system the situation is different because the only way the system has to dissipate energy is by the boundaries; so they cannot be scaled out like in statistical physics in the thermodynamic limit because otherwise if we applied this approximation the system would not be able to dissipate! And the dissipation is fundamental to reach the critical state.
c) The system is critical and self organized because it always reaches a sub/super critical state. We do not do the fine tuning of any parameter like it happens for example in the Ising model to observe the criticality but we give to the system the opportunity to exchange energy with the external world, by storing it and by dissipating it from the boundaries. Then the system organizes itself to reach one of three regions above described, depending on the rates of energy exchange.

5.4 Necessary and sufficient conditions for SOC

The separation between the cause and the effect has been always problematic since the paper published by BTW in 1989. We will try to introduce now the necessary and sufficient conditions for these systems by using the paper by Watkins et al., 2016.

5.4.1 Necessary conditions

Some of the necessary conditions for SOC were listed before:

1) Non trivial scaling (finite size scaling, no dependence on a control parameter): as we noticed before in the traditional critical phenomena the control parameter can be tuned till to observe the critical point: this happens for example for temperature that can be set at a given value from the external world till observing the change of phase. This is not the case of SOC as we already said before. Indeed in the traditional critical systems, the phenomena observed and the measurements taken can approximate the infinite system in the thermodynamic limit by increasing the size of the system as the control parameter is tuned closer and closer to the critical point. This is not the case of SOC systems in which it is not possible to take a thermodynamic limit that would erase the boundaries and so the capability of dissipation of the system, with the result that all the observables that display any form of scaling or that are expected to be divergent in the thermodynamic limit, will depend on the size of the system with a cut off function.
2) Space temporal law correlations
3) Apparent self tuning to the critical point (of a possibly identified, underlying second order phase transition): this happened in the sandpile model, where the system reached a sub/super critical state alone and the phase transition to the critical point always occurred with the features of a second order transition.

5.4.2 Sufficient conditions

The sufficient conditions are considered basically like the key ingredient to have SOC, in the sense that if a system satisfies these conditions, for sure can be considered like a SOC system.
Resuming by the papers of BTW and all the works of 25 years of SOC, we have

4) Non linear interaction: this is allowed by the thresholds into the system
5) Avalanches (Intermittency that is expected in presence of thresholds + slowly driven external force)
6) Separation of time scales (in order to “count and sustain” the avalanches)

Together with the necessary conditions, we can state that “*a SOC is slowly driven, avalanching system, with no linear interactions that display non trivial power law correlations (cut off by the system size) as known from ordinary critical phenomena, but*

with internal self organized rather than external tuning of a control parameter (to a non trivial value)". Watkins et al., 2016.

Now the sufficient conditions 4), 5), 6) are the basic conditions which are satisfied by SDIDT systems (slowly driven, interaction dominated thresholds), with intermittency implied by the slow drive. The SDIDT is sufficient for the occurrence of SOC: this was conjectured by Jensen (Jensen, 1998). Another class of model that maintains the characteristics about we talked first but the slowly driven, are the IDT: these models, which are studied to these days, are in fact characterized by a finite drive. So now, the following Venn's diagram is able to make us understand what is actually the situation to define a SOC system:

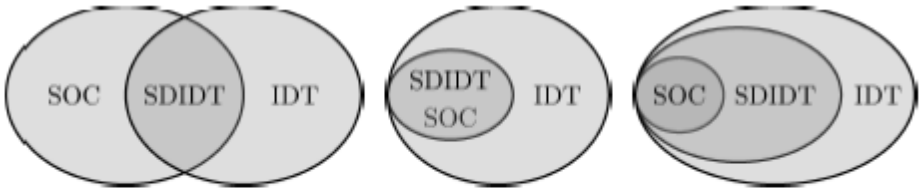

(a) SDIDT is a subset of IDT and of SOC. (b) Maybe all of SOC belongs to SDIDT. (c) Maybe SOC is a small subset of SDIDT.

*Figure 5.15: relations among SOC, SDIDT and IDT systems (*Watkins et al., 2016*)*

The relation between IDT and SDIDT is obvious; SDIDT are always a subset of IDT: in fact they have the same features of IDT plus the slowly driving. The relation between SDIDT and SOC is not so clear: according to the definitions 4) 5) and 6) and the identification given by Jensen, the systems SDIDT should exhibit a SOC behaviour: this is what Jensen stated and this is indicated in the figures a) and b). But to say that *all the SOC phenomena* are restricted to SDIDT like in figure b) is a very strong affirmation. This affirmation was proved only in one direction, i.e. all the systems SDIDT are SOC; but we do not know if there is SOC outside SDIDT! So we do not know what is correct between a) and b). b) would be correct if the conditions 4) 5) 6) would not be too narrow.
Indeed a study about the so called Forest Fire lack model (Pruessner and Jensen, 2002) could bring us to say that the conditions 4)-5)-6) are incomplete so only some SDIDT systems can show SOC! So maybe the figure c) could be the correct one where SOC is a subset of SDIDT.
All these considerations bring us to say that we are basically in a work in progress and that actually when we have a particular kind of system we can talk about "*hints of SOC".* In fact what we can state is only to understand if a system is SDIDT, but the only case in which the world of SOC coincides with the world of SDIDT is given in the figure b).

5.5 Are the FBM and the Central force model like SOC?

We are now ready to answer the main question: is the central force model a SOC model? In many papers, (Milanese et al., 2017) it was stated that in the central force model applied to the porous media we could find hints of SOC. Let's try to analyse the problem; as regards the sufficient conditions 4), 5), 6) we can assume they are fulfil satisfied in static; this could not be true in dynamic regarding the condition 6): so in dynamic, the Central Force Model does not respect the SDIDT conditions. Instead in static this is a SDIDT model at all. According to the picture b) that identifies SDIDT with SOC, we could state that the central force model is SOC; also the figure a) says to us the same because the central force model falls inside the SDIDT set, which is SOC. If the conditions 4) 5) 6) are incomplete instead, it could be possible that the central force model falls outside the SOC set even if it is a SDIDT model. So if we do not know exactly what picture is the correct one what we can say as told above, is "hints of SOC".
If we have a look to the necessary conditions instead what could we say? Obviously we know that if they are satisfied we are not sure the model is SOC (a condition can be necessary to have a phenomenon but no sufficient!) while if we know that they are not satisfied for sure the model is not SOC. So as regards the trivial scaling, we can state that our system has got a cut off as we can observe in the figure

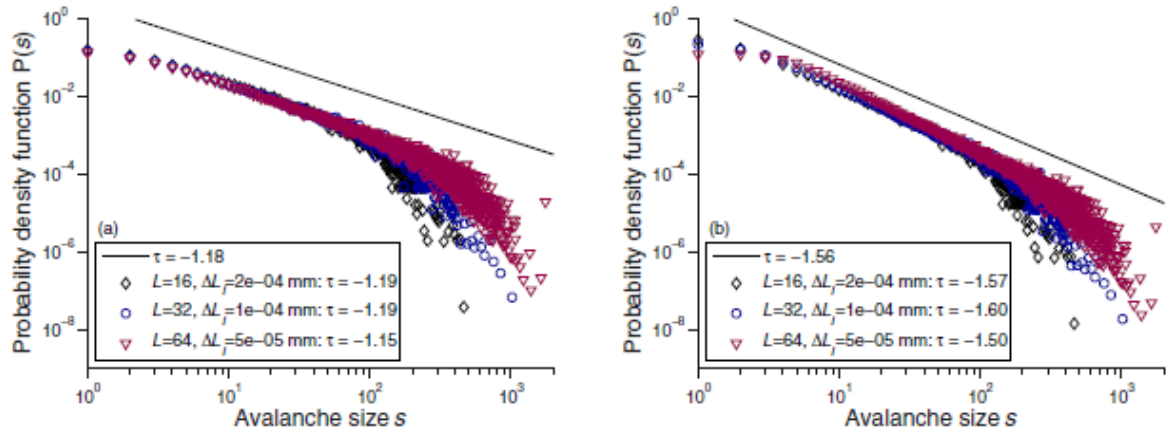

Figure 5.16: avalanches in the statistical central force model (Milanese et al., 2017)

where the model was pulled in the four directions and cut off scales with system size. Clearly the exponent of the cut off and the exponent of the probability density function depends on the boundary conditions.
There are then space temporal power law correlations: it is possible to notice this for the manner in which the channel of the fracture grows into the system: it does not grow at pieces like result of a progressive damaging or breakdown of the trusses, but it seems that since the moment in which we reach the stationary state, the trusses "talk one another" giving more importance to the channel that is growing with respect other micro channel that could come out from the damaging of the trusses. This could lead to think of possible long ranged correlations in space and time into the system.

As regards the phase transition of the second order the situation is controversial: if we perform a strain constant experiment or a stress constant experiment we will always have an avalanche behaviour. Obviously it would be better to study the system in a strain constant experiment

because we would be able to see the plateau of the constitutive behaviour. The difference with respect the FBM is that when the channel of the fracture is born the process stops: we can have a bigger avalanche or some bigger avalanches in the end but the order parameter of the system (that measures the ratio of “alive” trusses) does not go to 0 like in a second order transition where in the first phase is different from 0 and in the second one equal to 0 or vice versa.
The only quantity that goes to 0 is the connectivity that however is not an order parameter.
So in this case it is difficult to talk about a second order transition because it is difficult to talk about a phase transition in general, i.e. about the complete change in phase between a first phase (no broken) to a second phase (broken), like happened in the dry FBM of Abraimov for stress controlled experiment and in the CFBM always in the stress controlled case that we analysed from a numerical viewpoint.
So the third necessary condition is not satisfied and so the central force model is not expected to be SOC according to the picture above.
Furthermore in the best of our hypothesis, even if the necessary conditions were satisfied a problem would arise as regards the sufficient conditions: in fact they are true till the system breaks; at this point in fact we have no more avalanche behaviour, and separation of time scales (that would coincide); the systems SOC exchange energy with the external world; the sandpile dissipates it from the boundary while the central force model does it “breaking or damaging” a truss. But it is this way of dissipating energy which introduces a fundamental difference between sandpile and central force model: in the first one the thresholds are some limits in energy that each site on the lattice can withstand; when this threshold is reached the site relaxes and an avalanche leaves from it in the pattern we described above. However the threshold and the capability of the site to store energy remains always the same; the way that the system has to dissipate energy is from the boundaries. Nothing breaks in the sandpile. In the central force model instead when a threshold is reached, a truss damages decreasing its Young modulus. Then the avalanche leaves from it because the boundary condition (in strain/stress controlled experiment) must be satisfied, but the system has already dissipated an amount of energy by the damaging and it has stored only the amount of energy it was able to. This is the difference: in an avalanche the sandpile does not necessary lose energy; the Central force model (CFM) yes; in an avalanche the sandpile maintains its characteristics while the CFM changes its state of damage; and as we know the damage is an irreversible process and after some steps (a bit or much) the system will break. Not only: before the total breaking, the channel of the fracture will be born and so the process will stop. SOC systems are supposed to be brought by an *“attractor to the critical/stationary point and they remain there for all the life of the universe if they keep on exchanging energy with them”*
So this last consideration would distance the concept of SOC from the CFM.
For the CFBM we have the same situation: in the case of a stress controlled experiment, we could think of the maximum reached stress like a spinodal point that separates metastable states from unstable states like in the dry FBM; but when we reach the this point the model fails and the process stops.

Conclusions and future works

The present work showed an extension of a new technique, previously implemented by Milanese et al., in order to study the development and the nucleation of the fracture in a porous medium.

The innovative idea of the technique consists in representing the concept of disorder into the medium by the introduction of thresholds randomly spread according to a probability density function in the structural part, made by trusses.

As it was already discussed, the idea of using the concept of thresholds randomly spread into the system, was born by a way of studying the Random Fuse Model engaged by Stanley, Vespignani and Zapperi: the three physicists studied the “fracture” into this electrical model by considering the same algorithm built in the Fiber Bundle Model in order to reach the equilibrium.

For this reason, the natural extension of the work performed by the three scientists embeds to the world of the structural mechanics.

Basically, this PhD work developed in two different branches joining in the last part of chapter 4 when we talked about the constitutive behaviour of the truss lattice model that can be seen as the mean among all the possible realizations given by the disorder. The following picture clarifies the mental path which we developed:

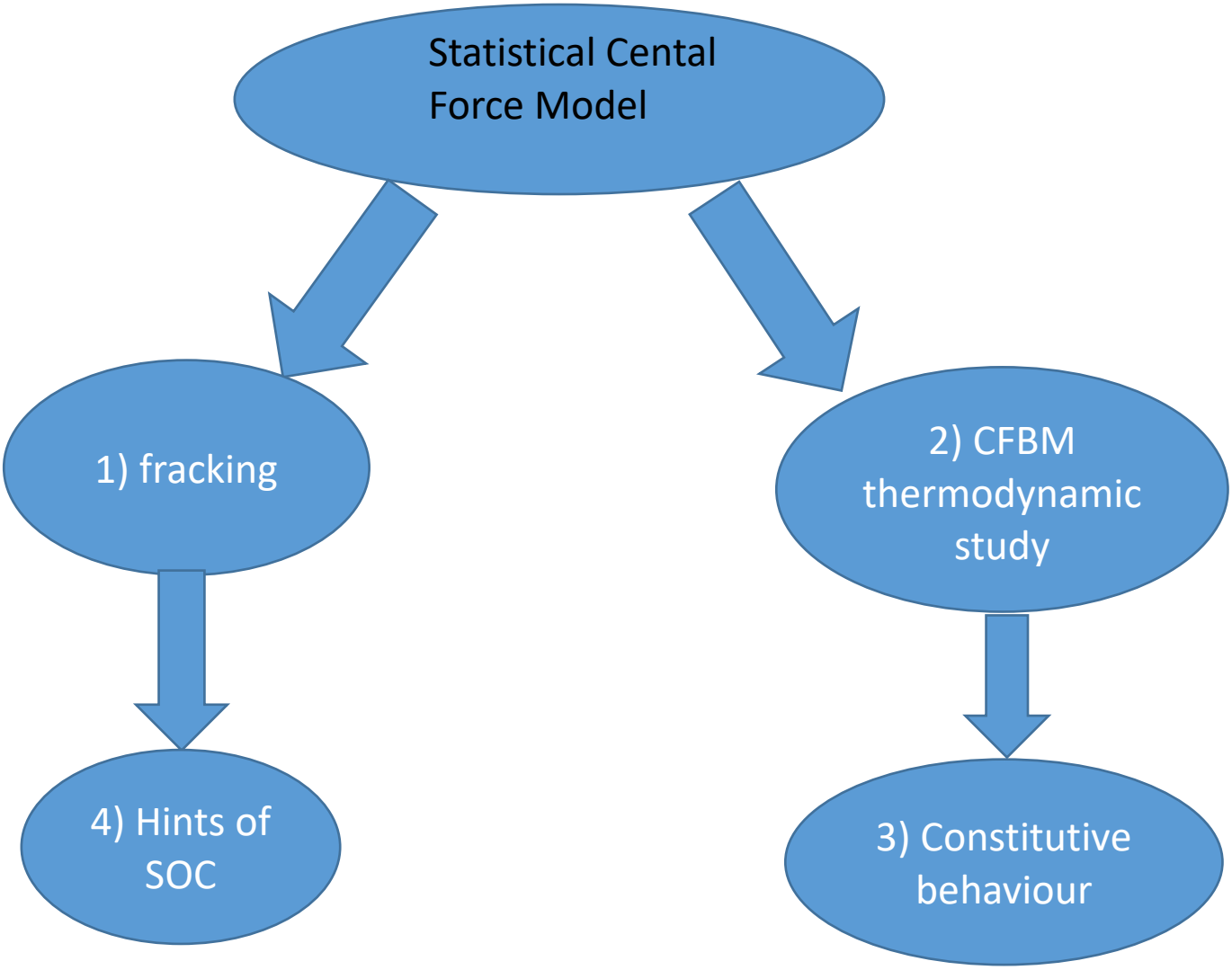

The starting point of the job is the study of the algorithm used by Stanley, Zapperi and Vespignani for the RFM. The application of this algorithm to the structural mechanics created the Statistical Central Force Model. The study of this last model was divided in two parts:

- from a theoretical viewpoint in Chapter 2 we addressed the study of the CFBM in an innovative viewpoint, by using the same approach by Pride and Touissaint for the DFBM. This new point of view allowed us to introduce the concept of entropy, internal energy, equivalent temperature and to study the CFBM during a strain constant experiment reproducing its constitutive behaviour to which we assigned a precise statistical meaning. This regards the right branch in the figure above.
- from a numerical viewpoint instead, we concentrated on the study of the hydraulic fracture. Previous works were realized by Milanese et al, 2016. The main problem in the simulations in their paper regarded the fact that the simulation were performed in static. Indeed, the fracking, a complex phenomenon in which the soil is filled by a liquid of some kind, cannot be considered as static but it occurs in dynamics. This was the main objective we reached during our simulation in Chapter 4 by which we reproduced the same results, from a qualitative viewpoint, for pressure rises and drops observed in the experimental tests during the fracking. We used the adjective qualitative because the material we used in our simulation is not real; the code needs to be validated and the present job only shows the potentiality of this kind of technique. This was the topic in the left branch in the figure above.

- The connection between the two branches is given by the achievement of a damage law to assign to our truss lattice for a dry medium by using the same constitutive behaviour we obtained for a bundle of fibers and applying it to a single fiber. The constitutive behaviour we got is assumed to be, by a statistical analysis, the mean value among all the possible realizations given by the disorder into the truss lattice.
- In chapter 5 in the end, we realized a research in order to understand if the Statistical Central Force Model can be included into the SOC systems. The answer for the dynamic is NO, while for the static we it is fair to talk about "hints" of SOC, as already mentioned in Milanese et al.

- Future works can be developed using the same technique

1) for a partially saturated porous medium and to develop a model in order to take into account that the permeability changes during the fracture. In our model the medium was totally saturated and the permeability was fixed in the beginning of the simulation. These would be the first and next improvements to get inside the Statistical Central Force Model to close it to reality.
2) It could be obvious to think about a 3D extension of the Statistical Central Force Model and to apply this extension to the static and the dynamic. It could be interesting to get the new statistical law of regarding the distribution of the avalanches. This should be different from the same distribution obtained for the system in 2D: as noticed in Statistical Physics, in fact, the exponents describing the observables change if the dimension is increased.
3) To extend the study of the Statistical Central Force Model in order to include inside another unknown into the system: by this, we could pass from a ***u-p*** system to a ***u-p-T*** system. Furthermore, a further complication to the problem could be introduced by considering water vapour into the system and the possibility that water changes its state: this could lead us to a triple couple problem among structure, liquid and air; in our model only the coupling between liquid and structure was analysed. By loading the system by a thermal load (a heat flux or a temperature gradient) it could be possible for example to simulate a particular kind of fracture very close to the explosion in concrete due to high temperatures, called spalling.
4) A Further extension of the model could be represented by the use of 2D elements in the structural part instead of trusses. In fact trusses were used because it is very simple to count avalanches and furthermore a strong equivalence exists between a truss structure and a 2D element structure. This process should lead us to results closest to the reality even if a study regarding the way of breaking of the 2D elements should be performed before going any further.
5) It would be interesting to investigate by the CFBM the mechanical behaviour of wood, which exhibits avalanche like behaviour.
6) From a theoretical viewpoint it would be interesting to extend the study of the CFBM to the stress ensemble and to use the same path we covered for the strain ensemble in CFBM for the statistical central force model, where the boundary conditions should be represented by the "nodal force ensemble" or the "strain edge ensemble". This study could make light regarding a possible phase transition into a 2D medium but, of course, it could be quite "painful" from an analytic viewpoint.

BIBLIOGRAPHY

1. Abaimov, S., Statistical Physics of non- thermal phase transitions. From foundations to applications. Springer
2. Ahmed, A. eXtended Finite Element Method (XFEM) - Modeling arbitrary discontinuities and Failure analysis. 196 (2009).
3. Bak, P., Tang, C. & Wiesenfeld, K. Self-organized criticality. *Phys. Rev. A* **38,** 364–374 (1988).
4. Bak, P., How nature works: the science of self organised criticality, Per Bak
5. Bar-Yam, Y. *Dynamics of Complex Systems (Studies in Nonlinearity) Variational Principles and the Numerical Solution of Scattering Problems*. *Computers in Physics* **12,** (1998).
6. Baxevanis, T. & Katsaounis, T. Scaling of the size and temporal occurrence of burst sequences in creep rupture of fiber bundles. *Eur. Phys. J. B* **61,** 153–157 (2008).
7. Bhattacharyya, P., Pradhan, S. & Chakrabarti, B. Phase transition in fiber bundle models with recursive dynamics. *Phys. Rev. E* **67,** 46122 (2003).
8. Belytschko, T., Liu, W.K., Moran, B., Elkhodary, K., *Non linear Finite elements for Continua and Structure*, Wiley, 2014
9. Hansen, A., Hemmer,P., Pradhan, S., The Fiber Bundle Model: Modeling Failure in Materials, Wiley, 2015
10. Hemmer, P. C., Hansen, A. & Pradhan, S. Rupture processes in fibre bundle models. *Lect. Notes Phys.* **705,** 27–55 (2006).
11. Hemmer, P. C. & Hansen, A. The Distribution of Simultaneous Fiber Failures in Fiber Bundles. *J. Appl. Mech.* **59,** 909 (1992).
12. Hidalgo, R. C., Kovacs, K., Pagonabarraga, I. & Kun, F. Universality class of fiber bundles with strong heterogeneities. *Epl* **81,** 54005 (2008).
13. Hidalgo, R. C., Kun, F. & Herrmann, H. J. Bursts in a fiber bundle model with continuous damage. *Phys. Rev. E* **64,** 66122 (2001).
14. Huang, K. Statistical Mechanics, 2nd Edition. *Statistical Mechanics* 512 (1987). doi:citeulike-article-id:712998
15. Garelli, M.,. Propagazione di cricche e impatti con la teoria della Peridinamica in Abaqus Laureando : Matteo Garelli Matricola n . 1041163. , Università degli studi di Padova(2015).
16. Klein, W., Gould, H. & Tobochnik, J. Phenomenological Theories of Nucleation. **V,** (2012).
17. Kloster, M., Hansen, A. & Hemmer, P. C. Burst avalanches in solvable models of fibrous materials. *Phys. Rev. E* **56,** 2615 (1997).
18. Krenk, S. *Non-linear modeling and analysis of solids and structures*. *Igarss 2014* (2009). doi:10.1007/s13398-014-0173-7.2

19. Kun, F., Raischel, F., Hidalgo, R. C. & Herrmann, H. J. Extensions of fiber bundle models. *Model. Crit. Catastrophic Phenom. Geosci. - A Stat. Phys. Approach* **705,** 57–92 (2007).
20. Kun, F., Zapperi, S., Herrmann, H. J., Sapienza, L. & Roma, P. a M. PHYSICAL JOURNAL B Damage in fiber bundle models. **279,** 269–279 (2000).
21. Kun, F., Zapperi, S. & Herrmann, H. J. Damage in Fiber Bundle Models. (1999). doi:10.1007/PL00011084
22. Latente, C., Ordine, P., Specie, P., Latente, C. & Il, A. Transizioni di fase 3.1. 1–34
23. Lewis, R. & Schrefler, B. *Finite Element Method in the Deformation and Consolidation of Porous Media*. *Osti.Gov* (1998). doi:10.1137/1031039
24. Madenci, E. Oterkus, E Peridynamics: Theory and its applications.. Springer, New York, 2014
25. Milanese, E., Yılmaz, O., Molinari, J. F. & Schrefler, B. A. Avalanches in dry and saturated disordered media at fracture in shear and mixed mode scenarios. *Mech. Res. Commun.* **80,** 58–68 (2017).
26. Pagonabarraga, I. & Mart, C. Avalanche dynamics of the continuous damage fiber bundle model. (2009).
27. Pradhan, S., Bhattacharyya, P. & Chakrabarti, B. K. Dynamic critical behavior of failure and plastic deformation in the random fiber bundle model. *Phys. Rev. E - Stat. Nonlinear, Soft Matter Phys.* **66,** (2002).
28. Pradhan, S., Hansen, A. & Chakrabarti, B. K. Failure processes in elastic fiber bundles. *Rev. Mod. Phys.* **82,** 499–555 (2010).
29. Pradhan, S., Hansen, A. & Hemmer, P. C. Crossover behavior in failure avalanches. *Phys. Rev. E - Stat. Nonlinear, Soft Matter Phys.* **74,** 1–9 (2006).
30. Pradhan, S., Hansen, A. & Hemmer, P. C. Crossover behavior in burst avalanches: Signature of imminent failure. *Phys. Rev. Lett.* **95,** 1–4 (2005).
31. Pride, S. R. & Toussaint, R. Thermodynamics of fiber bundles. *Phys. A Stat. Mech. its Appl.* **312,** 159–171 (2002).
32. Raether, F. Ceramic Matrix Composites – an Alternative for Challenging Construction Tasks. *Ceram. Appications* **1,** 45–49 (2013).
33. Raischel, F., Kun, F. & Herrmann, H. J. Continuous damage fiber bundle model for strongly disordered materials. *Phys. Rev. E - Stat. Nonlinear, Soft Matter Phys.* **77,** 1–10 (2008).
34. Roylance, D., Introduction to fracture mechanics, Department of Material Science and Engineering, 2001
35. Sabhapandit, S. Hysteresis and Avalanches in the Random Field Ising Model. *Physics (College. Park. Md).* 74 (2002).
36. Silling, S. A. & Lehoucq, R. B. Peridynamic theory of solid mechanics. Advances in Applied Mechanics. *Adv. Appl. Mech.* **44,** 73–168 (2010).

37. Silling, S. Defects and Interfaces in Peridynamics: A Multiscale Approach. *Sandia Natl. Lab. Report, SAND2014-19128C, Albuquerque, New Mex.* (2014).
38. Vespignani, A. & Zapperi, S. How self-organized criticality works: A unified mean-field picture. *Phys. Rev. E* **57,** 6345–6362 (1998).
39. Yaner Bam Yam, Dynamics of complex systems, Wesley, 1992
40. Watkins, N. W., Pruessner, G., Chapman, S. C., Crosby, N. B. & Jensen, H. J. 25 Years of Self-organized Criticality: Concepts and Controversies. *Space Sci. Rev.* **198,** 3–44 (2016).
41. Zapperi, S., Ray, P., Stanley, H. E. & Vespignani, a. Avalanches in breakdown and fracture processes. *Phys. Rev. E. Stat. Phys. Plasmas. Fluids. Relat. Interdiscip. Topics* **59,** 5049–5057 (1999).
42. Zapperi, S., Vespignani, A. & Stanley, E. H. Plasticity and avalanche behaviour in microfracturing phenomena. *Nature* **388,** 658–660 (1997).
43. Zienkiewicz, O. C. & Taylor, R. L. The finite element method - Solid mechanics, 1989.

44. Zienkiewicz, O. C. & Taylor, R. L., Zhu,J.Z. The Finite Element Method. Its Basis & fundamentals, 1982.